

PH.D. THESIS

Modeling and Adaptive Control of Magnetostrictive Actuators

by Ramakrishnan Venkataraman
Advisor: Professor P.S. Krishnaprasad

CDCSS Ph.D. 99-1
(ISR Ph.D. 99-1)



The Center for Dynamics and Control of Smart Structures (CDCSS) is a joint Harvard University, Boston University, University of Maryland center, supported by the Army Research Office under the ODDR&E MURI97 Program Grant No. DAAG55-97-1-0114 (through Harvard University). This document is a technical report in the CDCSS series originating at the University of Maryland.

Web site <http://www.isr.umd.edu/CDCSS/cdcss.html>

Abstract

Title of Dissertation: Modeling and Adaptive Control of
Magnetostrictive Actuators

Ramakrishnan Venkataraman, Doctor of Philosophy, 1999

Dissertation directed by: Professor P. S. Krishnaprasad
Department of Electrical Engineering

In this dissertation, we propose a model and formulate a control methodology for a thin magnetostrictive rod actuator. The goal is to obtain a bulk, low dimensional model that can be used for real-time control purposes. Previous and concurrent research in the modeling of magnetostrictive actuators and the related area of electrostrictive actuators have produced models that are of low order and reproduce their quasi-static response reasonably well. But the main interest in using these and other smart actuators is at a high frequency – for producing large displacements with mechanical rectification, producing sonar signals etc. The well known limitation of smart actuators that are based on electro-magneto-thermo-elastic behaviors of smart materials is the complex, input-rate dependent, hysteretic behavior of the latter.

The model proposed in this dissertation, is a bulk model and describes the behaviour of a magnetostrictive actuator by a system with 4 states. We develop

this model using phenomenological arguments following the work done by Jiles and Atherton for describing bulk ferromagnetic hysteresis. The model accounts for magnetic hysteresis; eddy current effects; magneto-elastic effects; inertial effects; and mechanical damping. We show rigorously that the system with the initial state at the origin has a periodic orbit as its Ω limit set. For the bulk ferromagnetic hysteresis model - a simplification of the magnetostrictive model, we show that all trajectories starting within a certain set approach this limit set.

It is envisioned that the model will help application engineers to do simulation studies of structures with magnetostrictive actuators. Towards this end, an algorithm is proposed to identify the various parameters in the model.

In control applications, one may require the actuator to follow a certain trajectory. The complex rate dependent behaviour of the actuator makes the design of a suitable control law a challenging one. As our system of equations do not model transient effects, they do not model the minor-loop closure property common to ferromagnetic materials. Therefore, the design of control laws making explicit use of the model (without modifications) is not possible. A major reason to use model free approaches to control design is that magnetostrictive actuators seem to have slight variations in their behavior with time. Therefore, we tried to use a direct adaptive control methodology that uses features of our model. The system is now looked at as a relative degree two linear system with set-valued input nonlinearity. Extensions of Eugene Ryan's work on universal tracking for a relative degree one linear system and Morse's work on stabilization for relative degree two linear systems were sought. Experimental verification of our method confirmed our intuition about the model structure. Though the tracking results were not very satisfactory due to the presence of sensor noise, the experimental

results, nevertheless validate our modeling effort.

Modeling and Adaptive Control of Magnetostrictive Actuators

by

Ramakrishnan Venkataraman

Dissertation submitted to the Faculty of the Graduate School of the
University of Maryland, College Park in partial fulfillment
of the requirements for the degree of
Doctor of Philosophy
1999

Advisory Committee:

Professor P. S. Krishnaprasad, Chairman/Advisor
Professor W. Levine
Professor S. Marcus
Professor S. Shamma
Professor S. Antman

© Copyright by
Ramakrishnan Venkataraman
1999

Acknowledgements

I would like to express my first words of gratitude to my advisor Professor P.S. Krishnaprasad. Without his guidance and support this dissertation would have never materialized. Apart from advising me on technical matters of this dissertation, he has also been a friend and supporter in difficult times. I wish to thank Professor S. Antman and the committee for taking the time and pains to review this dissertation. Due to their efforts, numerous bugs both typographical and otherwise were identified and subsequently corrected. I also wish to acknowledge and thank Professor Greg Walsh for lending me his DSP controller board and then spending hours with me, helping to configure the control system. Without his generosity, Chapter 5 would not have turned out as it did.

My friend Mr. Kidambi S. Kannan was a great source of knowledge when I started out with my modeling effort. I want to thank him and Mr. Tom Edison for their close companionship – and for being there whenever I needed their help. My sincere thanks to my colleagues at the Intelligent Servosystems laboratory - George Kantor, Andrew Newman, Tharmarajah Kugarajah, Herbert Struemper, Dimitris Tsakiris and Vikram Manikonda. Several times I have

tried their patience and they did not object. I have unabashedly approached the lab managers and they have always accommodated me without hesitation. The computer staff at the Institute for Systems Research - Amar Vadlamudi, Prasad Dharmasena, Kathy Penn to name a few, have been excellent in the maintenance and addition of new equipment. Because of the peculiar nature of my experimental work, I have had to approach them several times and they were always helpful. Without thanking Mr. Shyam Mehrotra and Mr. Robert Seibel of the Electrical engineering staff this dissertation would be incomplete. Shyam and Bob as I refer to them affectionately have always come to my aid when I was faced with the innumerable problems that come with doing experimental work.

I wish to acknowledge the financial support, provided by a grant from the National Science Foundation's Engineering Research Centers Program: NSFD CDR 8803012 and by the Army Research Office under the ODDR&E MURI97 Program Grant No. DAAG55-97-1-0114 to the Center for Dynamics and Control of Smart Structures (through Harvard University).

My wife Mary Thompson and my family have made great sacrifices to make it possible to pursue and finish this work. I hope that the result is worthy of their kindness.

Table of Contents

List of Figures	vii
1 Introduction	1
1.1 Origin of hysteresis	6
1.1.1 Ferromagnetic hysteresis	13
1.2 Constitutive description of hysteresis	21
1.3 Content of the dissertation	26
2 Bulk Ferromagnetic Hysteresis Model	33
2.1 Bulk Ferromagnetic Hysteresis Theory	34
2.1.1 Langevin Theory of Paramagnetism	34
2.1.2 Weiss Theory of Ferromagnetism	37
2.1.3 Bulk Ferromagnetic hysteresis model	38
2.2 Qualitative analysis of the model	45
2.2.1 Analysis of the Model for $t \in [0, \frac{5\pi}{2\omega}]$	69
2.2.2 Proof of Periodic behaviour of the Model for Sinusoidal Inputs	72
2.2.3 The Jiles-Atherton model	78
2.3 Extensions of the Main Result	79

3	Bulk Magnetostrictive Hysteresis Model	85
3.1	Thin magnetostrictive actuator model	86
3.2	Qualitative analysis of the magnetostrictive actuator model . . .	92
3.2.1	The uncoupled model with periodic perturbation	95
3.2.2	Analysis of the magnetostriction model	116
3.3	The magnetostrictive actuator in an electrical network	119
3.3.1	The magnetostrictive actuator in an electrical network . .	124
4	Parameter Estimation	129
4.1	Algorithm for parameter estimation from experimental data . . .	131
4.2	Experimental validation	140
5	Trajectory tracking controller design	155
5.1	Universal adaptive stabilization and tracking for relative degree one linear systems	156
5.1.1	Basic Idea	159
5.1.2	Extension to relative degree one, minimum phase, linear systems	164
5.2	λ tracking	167
5.2.1	Extensions to systems with input non-linearity	169
5.3	Relative degree two systems	174
5.3.1	Linear systems with input nonlinearity	177
5.3.2	Experimental results	180
6	Conclusions and Future Work	196
A	Banach Spaces	198

B Solutions of Ordinary Differential Equations	204
B.1 Existence of solutions	204
B.2 Extension of solutions	206
B.3 Uniqueness of solutions	208
B.4 Continuous dependence on parameters	209
C Stability of Periodic Solutions	211
C.1 Poincaré Map	212
D Perturbations of Linear Systems	214
E Principle of Least Squares	217
F Eddy Current Losses in a Magnetostrictive Actuator	219
Bibliography	223

List of Figures

1.1	Illustration of the <i>hysteresis</i> phenomenon.	2
1.2	Output of the hysteretic system of Figure 1.1 for 2 different inputs.	3
1.3	Illustration of the hysteresis phenomenon.	5
1.4	Free energy as a function of e for different T	8
1.5	Response function for $T < T_c$ (left) and $T \geq T_c$ (right).	9
1.6	Illustration of hysteresis between an external field and the order parameter.	10
1.7	Relationship between conjugate variables observed in various physical phenomena.	23
1.8	Hysteresis in engineering.	24
1.9	Experimental curves for a soft-iron ring [1].	31
1.10	The ETREMA MP 50/6 TERFENOL-D magnetostrictive actuator (Source: ETREMA Products Inc).	32
2.1	M vs H relationship for an ideal and a lossy ferromagnet.	39
2.2	Sample signals $u(\cdot)$ and $u_1(\cdot)$	60
2.3	Figure for the proof of Theorem 2.2.2	66

3.1	Schematic diagram of a thin magnetostrictive actuator in a resistive circuit.	92
3.2	Sample signals $u(\cdot)$ and $u_1(\cdot)$	112
3.3	Schematic diagram of a thin magnetostrictive actuator in a resistive circuit.	121
3.4	Schematic diagram of an magnetostrictive element as a part of an R-L-C network.	125
4.1	Schematic diagram of the circuit used for the identification of parameters.	130
4.2	The anhysteretic displacement curve for a thin magnetostrictive actuator.	135
4.3	Quasi-static strain vs applied magnetic field for an ETREMA FSZM 96-11B Terfenol-D rod (Courtesy ETREMA Products, Inc.). 141	
4.4	Displacement versus current data obtained from experiment. . .	149
4.5	Experimental results.	150
4.6	Simulation results for sinusoidal voltage inputs of frequencies 1 - 100 Hz.	151
4.7	Simulation results for sinusoidal voltage inputs of frequencies 200 - 500 Hz.	152
4.8	Experimental results.	153
4.9	Experimental results.	154
5.1	Equivalent realization for a linear system.	166

5.2	Adaptive λ -tracking for linear systems with input, output nonlinearity in the presence of noise.	170
5.3	Set valued input nonlinearity allowed by Ryan	173
5.4	Adaptive tracking controller idea for relative degree two, minimum phase systems with input non-linearity.	178
5.5	Set valued input nonlinearity for example 1.	179
5.6	Morse - Ryan controller applied to the system of example 1 . . .	186
5.7	The magnetostrictive actuator model.	187
5.8	ETREMA MP 50/6 Actuator characteristic at different driving frequencies.	187
5.9	Schematic diagram of the experimental setup.	188
5.10	Reference trajectory frequency approximately 1 Hz	189
5.11	Reference trajectory frequency approximately 10 Hz	190
5.12	Reference trajectory frequency approximately 50 Hz	191
5.13	Reference trajectory frequency approximately 200 Hz	192
5.14	Reference trajectory frequency approximately 500 Hz	193
5.15	Reference trajectory frequency approximately 750 Hz	194
5.16	Example system for discussion of root locus properties.	194
5.17	Root locus of example system.	195
5.18	Mechanical system model at high frequencies.	195
F.1	Derivation of V-I-x relationship for the thin magnetostrictive rod.	220
F.2	Representation of eddy current effects as a resistor in parallel with the primary coil.	221

Modeling and Adaptive Control of
Magnetostrictive Actuators
Ramakrishnan Venkataraman
February 11, 1999

This comment page is not part of the dissertation.

Typeset by L^AT_EX using the `dissertation` class by Pablo A. Straub, University of Maryland.

Chapter 1

Introduction

There is growing interest in the design and control of smart structures – systems with embedded sensors and actuators that provide enhanced ability to program a desired response from a system. Applications of interest include: (a) smart helicopter rotors with actuated flaps that alter the aerodynamic and vibrational properties of the rotor in conjunction with evolving flight conditions and aerodynamic loads; (b) smart fixed wings with actuators that alter airfoil shape to accommodate changing drag/lift conditions; (c) smart machine tools with actuators to compensate for structural vibrations under varying loads. In these and other examples, key technologies include actuators based on materials that respond to changing electric, magnetic, and thermal fields via piezoelectric, magnetostrictive and thermo-elasto-plastic interactions.

Typically such materials exhibit complex nonlinear and hysteretic responses (see Figure 1 for an example of a magnetostrictive material Terfenol-D used in a commercial actuator). Controlling such materials is thus a challenge. The present work is concerned with the development of a physics-based model for magnetostrictive material that captures hysteretic phenomena and can be sub-

ject to rigorous mathematical analysis towards control design.

In this dissertation, we propose a model for a thin magnetostrictive rod actuator that shows a hysteretic relationship between the current input and the displacement output. We first clarify the term *hysteresis* in the relationship between the input and output of a system or more generally two conjugate quantities that describe the state of a system. That is the focus of our attention for the rest of this section. In the next section, we study a theory explaining the probable origin of hysteresis between conjugate variables in a system. We also specialize this theory to the case of ferromagnetism and magnetostriction, and study its usefulness when faced with practical questions of real-time control of magnetostrictive actuators. In Section 1.2, we study alternative ways of modeling magnetostrictive actuators so that real-time control may be achievable.

Historically, Ewing first coined the term *hysteresis* (which means “to lag behind” in Greek) in his study of ferromagnetism [1]. To describe the phenomenon consider a system characterized by two scalar variables u and v . We assume u to be continuously dependent on time.

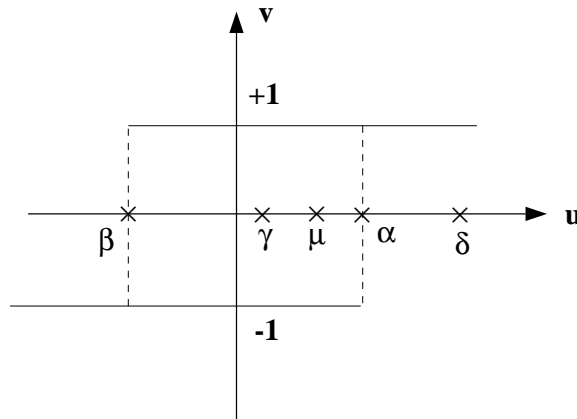


Figure 1.1: Illustration of the *hysteresis* phenomenon.

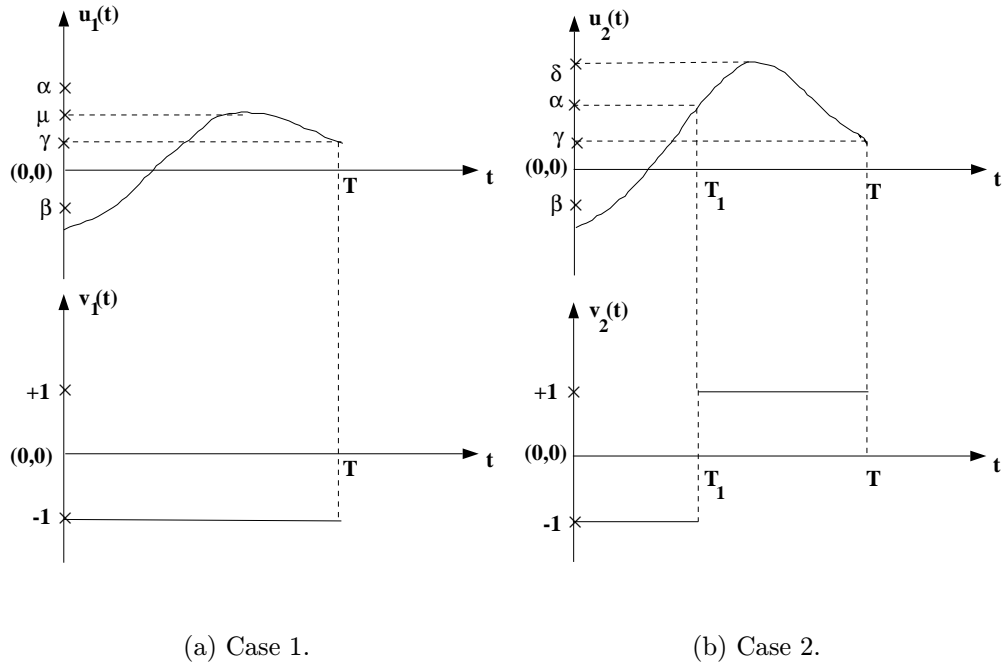


Figure 1.2: Output of the hysteretic system of Figure 1.1 for 2 different inputs.

Consider Figure 1.1. The relationship between u and v can be described by:

$$v = +1 \quad \text{if } u > \alpha, \quad (1-a)$$

$$v = -1 \quad \text{if } u < \beta, \quad (1-b)$$

$$v \quad \text{remains unchanged} \quad \text{if } \beta \leq u \leq \alpha \quad (1-c)$$

(1-a - 1-c) represent the *constitutive relationship* between u and v . By a constitutive relation between two variables u and v , we mean a mathematical relation that describes the behaviour of one of the variables as a function of the other variable and their history. This mathematical relation is not to be confused experimental data that show how one of the variables is influenced by the other.

This is because experimental data are typically obtained by applying some specific inputs and measuring the outputs, whereas a mathematical relationship is true for all inputs. Thus an experiment might suggest a certain constitutive relationship but that might be proved false by further experiment.

Suppose two input signals $u_i(t)$, $i = 1, 2$; $t \in [0, T]$ as shown in Figure 1.2 are applied to the system with $v_i(t = 0) = -1$, $i = 1, 2$. Then $v_1(t) = -1 \forall t \in [0, T]$. On the other hand, $v_2(t) = -1$ for $t \in [0, T_1]$ and $v_2(t) = 1$ for $t \in (T_1, T]$. This shows that the value of $v(T)$ depends on $v(0)$ and the input $u(\cdot)$ in the interval $[0, T]$. Such a relationship can be expressed as:

$$v(t) = \mathcal{R}_{\beta, \alpha}(v(t = 0), u(\cdot))(t) \quad t \in [0, T] \quad (2)$$

where $\mathcal{R}_{\beta, \alpha}$ is a map acting on $u(\cdot)$ defined on the interval $[0, t]$ and dependent on the initial condition $v(t = 0)$. The subscripts denote that the output *may* change value if the input reaches the threshold values α and β . Though the output even for a linear system can be expressed by an equation similar to (2), the difference is that the constitutive relationship between u and v given by (1-a - 1-c) is independent of time t . In other words, $v(T)$ only depends on the local maximum or minimum values achieved by $u(\cdot)$ in the interval $[0, T]$ and it does not matter when the maximum and minimum values are achieved. Such a dependence of the “output” variable on the history of the “input” variable is termed *hysteresis*.

There are several important details that we can make note of from the simple example above.

- The value of the output at time T depends only on the initial value of the output $v(0)$ and the local minimum and maximum values obtained by the

input $u(t)$ in the interval $t \in [0, T]$.

- To obtain the constitutive relationship between the variables u and v from experiment, one needs to apply all possible inputs $u(\cdot)$ and note the outputs $v(\cdot)$. In the above example, the output was linear as a function of the input $u_1(\cdot)$ while it showed hysteresis in response to input $u_2(\cdot)$.

More generally, the relation between the input and output variables (for inputs that will be described shortly) might be as shown in Figure 1.3. Assume that $u(\cdot)$ monotonically increases from a value $u(0) = \beta$ and to some value u_{max} and then decreases monotonically to $u(T) = \beta$. For $u_{max} = \alpha_i; i = 0, 1, 2$ the path followed by $(u, v)(t)$ for $t \in [0, T]$ is shown in Figure 1.3. In this case the paths followed by $(u, v)(\cdot)$ for increasing and decreasing values of $u(\cdot)$ are different no matter what u_{max} is.

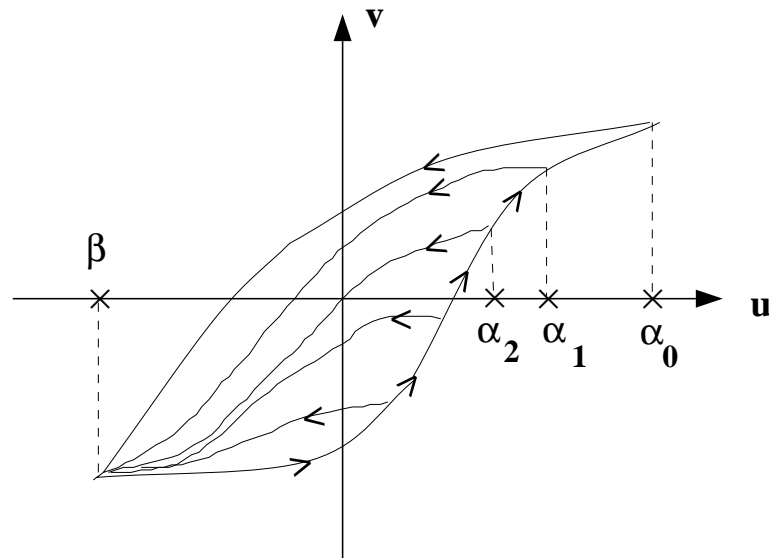


Figure 1.3: Illustration of the hysteresis phenomenon.

Hysteresis between independent and dependent variables is observed in sev-

eral physical and biological phenomena as well as in engineering, economics and so on. In physics we encounter it in plasticity, friction, ferromagnetism, ferroelectricity, superconductivity, magnetostriction, piezoelectricity and in shape memory effects among others. Thermostats and mechanical systems with dry friction [2] are examples in engineering where we see hysteresis. It is therefore natural to try to understand the common thread underlying the various occurrences of the hysteresis phenomenon. In the next section we present a well known theory that tries to explain a probable origin of hysteresis. Later in the same section, we specialize this theory to ferromagnetism. In the literature, this theory is known as *micromagnetics*.

It will become apparent in the next section that though the origin of hysteresis in ferromagnetism is plausibly explained by the theory of micromagnetics, its value is limited when our objective is to model the behaviour of a ferromagnet using macroscopic experimental data. For such an application a phenomenological approach is needed. This dissertation is concerned with the development of such a phenomenological theory for magnetostrictive actuators.

1.1 Origin of hysteresis

A probable origin of hysteresis in the input-output relationship of a system is

- multiple metastable states of a thermodynamic free energy functional and,
- energy dissipation in a system.

This statement can be understood by considering a simple example by Brokate and Sprekels [3]. Consider a system with an input variable $\tilde{\phi}$ and output variable e . Brokate and Sprekels refer to e as an *order parameter* perhaps because it

represents the state of the system at any instant along with the input variable $\tilde{\phi}$. It is a parameter as its value before the application of the input, influences the state $(e, \tilde{\phi})$ of the system after the input is applied. In the example considered earlier (equations (1-a) and (1-b)), the order parameter is v .

In the absence of an input, let the Helmholtz free energy density $F(\cdot, \cdot)$ be a function of an order parameter e and absolute temperature T . Then the equilibrium states of an isothermal system are given by the minima of the free energy density F with respect to e . Assuming $F(e, \cdot)$ to be differentiable with respect to e

$$\phi(e, T) \equiv \frac{\partial F}{\partial e}(e, T) = 0,$$

where the quantity ϕ describes the energetic response of the system with respect to a change of the order parameter. At equilibrium, the order parameter adjusts in such a way that ϕ vanishes. If the system is subjected to external influences, then an external field $\tilde{\phi}$ which is thermodynamically conjugate to the order parameter contributes the term $-\tilde{\phi}e$ to the free energy density. Then the total free energy density takes the form

$$F_{\tilde{\phi}}(e, T) = F(e, T) - \tilde{\phi}e.$$

The condition for equilibrium states is now $\frac{\partial F_{\tilde{\phi}}}{\partial e}(e, T) = 0$, that is,

$$\phi(e, T) = \tilde{\phi}.$$

This implies the order parameter adjusts in such a way that the external field is in balance with the internal response.

Suppose now that $F(e, T) = F_0(T) + \alpha_1(T - T_c)e^2 + \alpha_2e^4$. The shape of $F(\cdot, T)$ is depicted for different temperatures T in Figure 1.4. The response function ϕ is given by

$$\phi(e, T) = 2 \alpha_1 (T - T_c) e + 4 \alpha_2 e^3.$$

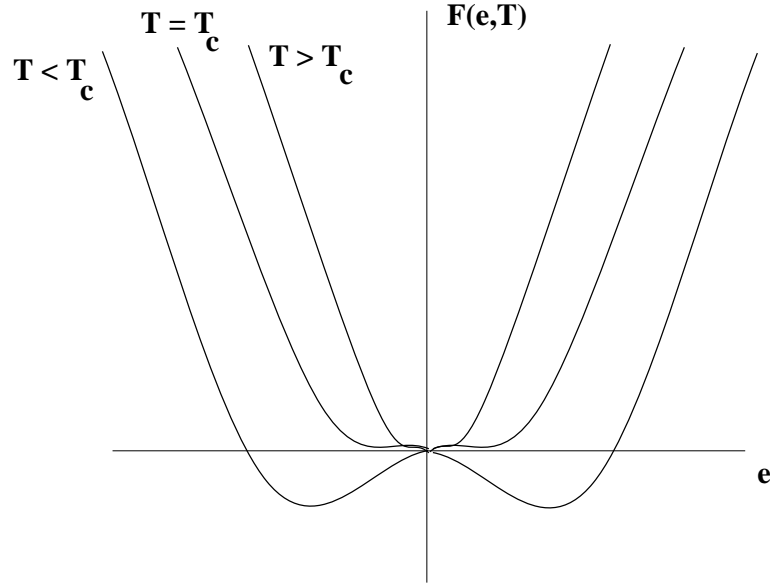


Figure 1.4: Free energy as a function of e for different T .

Therefore for vanishing external fields, the equilibrium value $e(T)$ of the order parameter associated with the temperature T , defined by the minima of $F(., T)$, is given by

$$e(T) = \begin{cases} 0 & \text{for } T \geq T_c \\ \pm e_0(T) & \text{for } T < T_c \end{cases} \quad \text{where } e_0(T) = \sqrt{\frac{\alpha_1}{2\alpha_2}(T_c - T)}.$$

Now we consider (e, ϕ) -curves for different values of T . For $T \geq T_c$, the function $e \mapsto \phi(e, T)$ is strictly increasing, while in the case $T < T_c$ the graph of this relation contains a downward sloping branch. A necessary condition for thermodynamic stability of equilibrium is the requirement $\frac{\partial^2 F}{\partial e^2} \geq 0$. Hence, the downward sloping branches represent unstable states which implies that thermodynamic processes following these branches cannot be realized by the system.

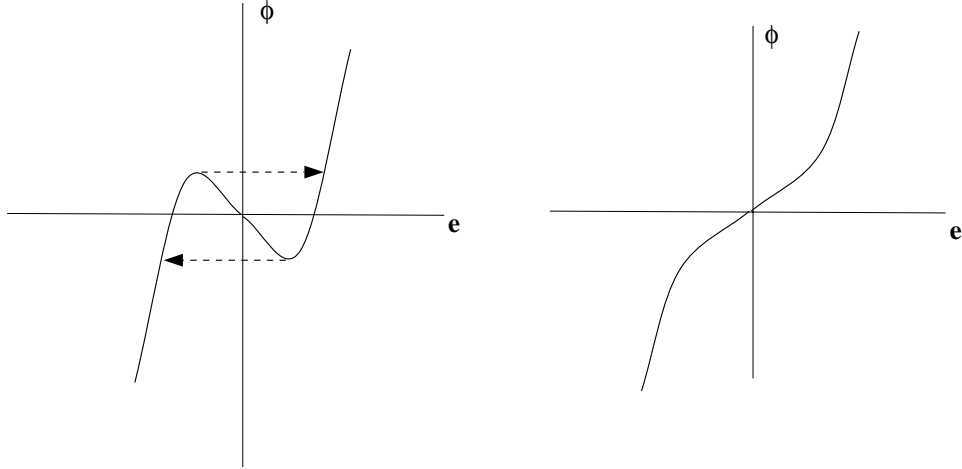


Figure 1.5: Response function for $T < T_c$ (left) and $T \geq T_c$ (right).

In the presence of an external field $\tilde{\phi}$, the first-order condition for minimum energy yields

$$\tilde{\phi} = 2\alpha_1(T - T_c)e + 4\alpha_2e^3.$$

We can obtain the optimal value of the parameter e by looking at the intersection of the curves $\phi = \tilde{\phi}$ and $\phi = 2\alpha_1(T - T_c)e + 4\alpha_2e^3$. For $T \geq T_c$, there is only one point of intersection, which corresponds to the absolute minimum of the energy function. For $T < T_c$, there can be two points of intersection if

$$|\tilde{\phi}| < \phi_c \equiv \frac{1}{\sqrt{\alpha_2}} \left(\frac{2\alpha_1}{3} (T_c - T) \right)^{\frac{3}{2}}.$$

- For a fixed $T (< T_c)$, if $\tilde{\phi} < -\phi_c$, then there is only one point of intersection on the left branch of the curve $\phi(e)$ which is the absolute minimum.
- If $\tilde{\phi} = -\phi$ then another point of intersection appears on the right branch of $\phi(e)$ which corresponds to a local minimum (a metastable state). The point of intersection with the left branch still corresponds to the absolute minimum.

- If $\tilde{\phi} = 0$ then both the points of intersection correspond to equal energies.
- If $0 < \tilde{\phi} < \phi_c$ then the intersection with the right branch represents the absolute minimum while the intersection with the left branch represents a metastable state.
- For $\tilde{\phi} > \phi_c$, there is only one intersection – that with the right branch.

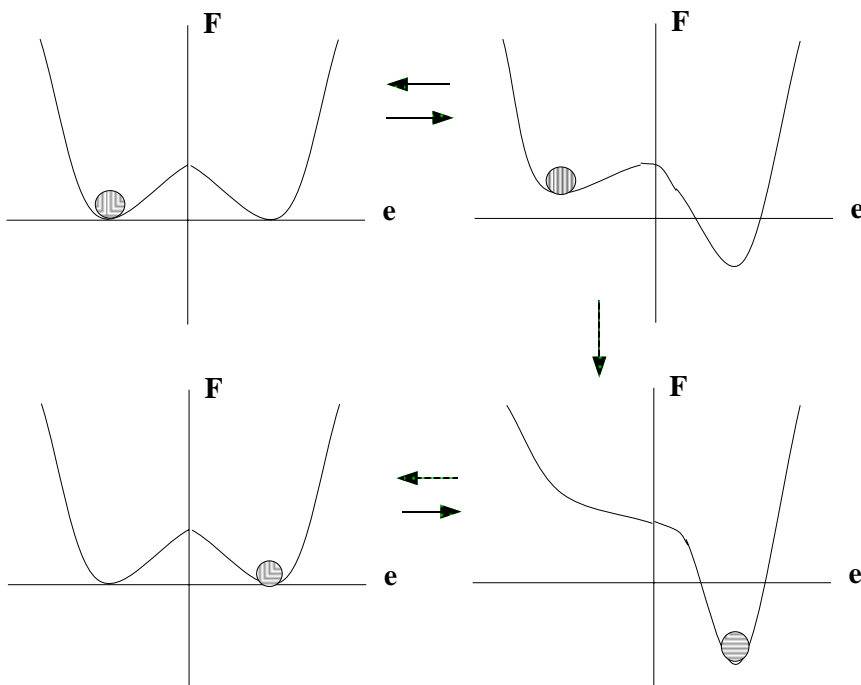


Figure 1.6: Illustration of hysteresis between an external field and the order parameter.

The points made above are illustrated in Figure 1.6. Suppose the system is slowly acted upon by an external field so that it reaches its equilibrium for each value of the external field. The system does this by dissipating energy, which is also an important feature of hysteretic systems. But we postpone the discussion of energy dissipation and only consider the relationship of the equilibrium states

with the external field at this time.

If the system is slowly acted upon by an external field $\tilde{\phi}$, starting from a value less than $-\phi_c$, then the system is in left branch until $\tilde{\phi} = \phi_c$. If $\tilde{\phi}$ is reduced to zero before it reaches the critical value ϕ_c , the system remains in the left branch as illustrated. But if $\tilde{\phi}$ is increased further beyond ϕ_c , then the system jumps to the minimum on the right branch. Now if $\tilde{\phi}$ is decreased from this value it stays on the right branch until $\tilde{\phi} = -\phi_c$. As $\tilde{\phi}$ decreases further it jumps to the left branch. If we look at the relationship between $\tilde{\phi}$ and e we note that it is *hysteretic*. Brokate and Sprekels refer to the change in the relationship between the conjugate quantities with changing temperature as a *phase transition*.

In the theory discussed above called the Landau theory, non-local spatial effects are completely ignored. By this we mean the following. Suppose the abstract system with order parameter e and input $\tilde{\phi}$ discussed above is a body occupying a region of space $\Omega \subset \mathbb{R}^3$. Since the free energy density was assumed to be in the form $F = F(e, T)$, its value at a spatial point \mathbf{x} in the domain Ω depends only on the values attained by e and T at that point. Then the order parameter is a function $e(\cdot) : \Omega \rightarrow \mathbb{R}; \mathbf{x} \mapsto e(\mathbf{x})$. It can be thought of as representing the phase inside the material body. It may also be a function of time t . As the order parameter is a function of \mathbf{x} , the total free energy must be a functional acting on a function space to which $e(\cdot)$ belongs.

In cases where two different phases of the material meet across an interface, the order parameter has a different value in the different phases. There is variation of $e(\cdot)$ across the interface and the interfacial energy cannot be neglected as the interface itself has a nonzero width. Suppose that a fixed constant temperature is maintained in the domain Ω which is an open, connected and

bounded subspace of \mathbb{R}^3 . Then a simple expression for the total free energy that incorporates local spatial effects is the *Ginsburg - Landau functional* [3],

$$\mathcal{F}[e] = \int_{\Omega} (F(e(\mathbf{x}), T) + \frac{1}{2} \gamma(e(\mathbf{x}), T) |\nabla e(\mathbf{x})|^2) d\mathbf{x}, \quad (3)$$

where γ is some positive function of e and T . The function F which may be regarded as the free energy density of the respective pure phases, has the same meaning as in the previous discussion and could have the same form considered there. The gradient term accounts for the influences of the points neighbouring the point $x \in \Omega$.

For equilibrium, the functional \mathcal{F} achieves a minimum value with respect to the variations of e and therefore e satisfies the *Euler-Lagrange* equation

$$\frac{\delta \mathcal{F}}{\delta e}[e](\mathbf{x}) = 0, \quad \forall \mathbf{x} \in \Omega, \quad (4)$$

where $\frac{\delta \mathcal{F}}{\delta e}[e]$ denotes the variational derivative of \mathcal{F} at e [3].

As mentioned before, the hysteresis is in the relationship between the order parameter at the equilibrium point of the system and the external field. For a system to reach the equilibrium point for a given external field it has to reach a local minimum of the energy function by dissipating energy. Sometimes the dynamics of reaching the equilibrium is ignored as authors focus on the equilibrium itself. Then in order to compute this equilibrium, they use gradient methods or Newton's method [4]. By this method, the system evolution in time can then be written as [3]

$$\frac{\partial e}{\partial t} = -\beta(e, T) \frac{\delta \mathcal{F}}{\delta e}$$

where $\beta(., T)$ is a positive function so that

$$\frac{d\mathcal{F}}{dt}[e(t)] \leq 0$$

In order to consider the full dynamics of the system, we have to use *Hamilton's principle* [5, 6],

$$\delta \int_{t_1}^{t_2} \mathcal{L} dt + \int_{t_1}^{t_2} \frac{\partial \mathcal{R}}{\partial \dot{q}} \cdot \delta q dt = 0$$

where \mathcal{L} is the Lagrangian function defined on the velocity phase space of the system, and \mathcal{R} is a *dissipation* function.

1.1.1 Ferromagnetic hysteresis

We noted in the previous discussion that a *non-convex* thermodynamic free energy function can cause hysteresis to appear in the relationship of conjugate quantities. We classified these quantities in an abstract form as *order parameters* and *external fields*. The order parameters and external fields for a few physical phase transitions are as in Table 1.1 [3]. At a particular temperature T less than the *Curie* temperature, a ferromagnetic material is known to be comprised of domains. Within each domain the magnetization vector \mathbf{M} has the same orientation. Thus the free energy functional has to take into account non-local effects.

Consider a rigid, homogeneous body occupying a region of space Ω which is open, bounded and a connected subset of \mathbb{R}^3 . The ferromagnetic body has a *magnetization field* \mathbf{M} defined on Ω . The magnetization field represents a volume density of macroscopic magnetic moment and this implies that \mathbf{M} induces a magnetic field \mathbf{H}_m at all points of space. If the magnetic field due to all external

Phase transition	Order parameter	External field
Ferromagnetic	Magnetization	Magnetic field
Ferroelectric	Polarization	Electric field
Martensitic	Strain	Stress

Table 1.1: Order parameters and external fields for experimentally observed phase transitions.

sources in the region Ω is $\mathbf{H}_{ext}(\mathbf{x})$ then the magnetic flux density in the region Ω is given by

$$\mathbf{B}(\mathbf{x}) = \mu_0 (\mathbf{H}_{ext}(\mathbf{x}) + \mathbf{H}_m(\mathbf{x}) + \mathbf{M}(\mathbf{x})) \quad (5)$$

$\mathbf{B}(\cdot)$, $\mathbf{H}_{ext}(\cdot)$, $\mathbf{H}_m(\cdot)$ in Ω have to obey Maxwell's equations of electromagnetism:

$$\nabla \cdot \mathbf{B}(\mathbf{x}) = 0 \quad (6-a)$$

$$\nabla \cdot \mathbf{H}_{ext}(\mathbf{x}) = 0 \quad (6-b)$$

$$\nabla \times (\mathbf{H}_{ext}(\mathbf{x}) + \mathbf{H}_m(\mathbf{x})) = 0 \quad (6-c)$$

$$\nabla \times \mathbf{H}_{ext}(\mathbf{x}) = 0 \quad (6-d)$$

We are assuming zero body current density in the ferromagnetic material in writing Equation (6-c). (6-b) and (6-d) are true because $\mathbf{H}_{ext}(\cdot)$ is due to all external sources and is independent of the magnetic body. (6-a - 6-d) imply

$$\nabla \cdot \mathbf{H}_m(\mathbf{x}) = -\nabla \cdot \mathbf{M}(\mathbf{x}) \quad (7)$$

We note that $\mathbf{H}_m(\cdot)$ is non-local because it has to satisfy the conditions

$$\mathbf{n} \cdot \mathbf{B}(\mathbf{x})|_{\pm}^{\pm} = 0, \quad (8\text{-a})$$

$$\mathbf{n} \times \mathbf{H}_m(\mathbf{x})|_{\pm}^{\pm} = 0 \quad (8\text{-b})$$

on the boundary $\partial\Omega$ of Ω . We assume that the surface current densities are zero. In (8-a - 8-b), \mathbf{n} is the unit normal taken positive in the outward sense with respect to a magnetized body; the symbol $|_{\pm}^{\pm}$ means that the value on the negative side of the surface is to be subtracted from the value on the positive side.

Given a magnetic moment distribution $\mathbf{M}(\cdot)$ within a body, the quantities $\mathbf{H}(\cdot)$ and $\mathbf{B}(\cdot)$ can be calculated by using Maxwell's equations as shown above. The theory of *Micromagnetics* seeks to answer the inverse question of determining the magnetic moment distribution at time $t = T$ if it is known at time $t = 0$ and the external field $\mathbf{H}_{ext}(\cdot)$ is specified for $t \in [0, T]$. The problem is set up as in the Landau theory with $\mathbf{M}(\cdot)$ as the order parameter function and $\mathbf{H}_{ext}(\cdot)$ as the external input function. An important assumption that is made in the theory of micromagnetics is that

$$|\mathbf{M}(\mathbf{x})| = M_s > 0 \quad \text{in } \Omega. \quad (9)$$

The free energy functional in this theory is given by [6]

$$E_{\mathbf{H}_{ext}}(\mathbf{M}) = \int_{\Omega} \left(\frac{1}{2} \alpha^2 |\nabla \mathbf{M}|^2 + \psi(\mathbf{M}) - \mathbf{H}_{ext} \cdot \mathbf{M} - \frac{1}{2} \mathbf{H}_m \cdot \mathbf{M} \right) d\mathbf{x}. \quad (10)$$

The summands are called the *exchange* energy, *anisotropy* energy, *interaction* (*Zeeman*) energy and *magnetostatic* energy. The exchange energy term models

the tendency of a specimen to exhibit large regions of uniform magnetization separated by very thin transition layers (domain walls) by penalizing spatial variations of \mathbf{M} . The anisotropy energy in which $\psi(\cdot)$ is a non-negative even function exhibiting crystallographic symmetry, models the existence of preferred directions of magnetization (*easy axes*), along which ψ is assumed to vanish. The interaction energy models the tendency of a specimen to have its magnetization aligned with the external field \mathbf{H}_{ext} . Finally, the magnetostatic energy is the energy associated with the magnetic field generated by \mathbf{M} [6, 7, 8].

The anisotropy and the interaction energies are purely determined by the magnetization at a point \mathbf{x} in the body; the exchange energy is due to local variations in the magnetization; and the magnetostatic energy has a non-local character depending on the distribution of magnetization on the body as a whole. The anisotropy and the interaction energy terms by themselves cause hysteresis in the magnetization field of a body as shown by Stoner and Wohlfarth [9]. The argument is very similar to the one we studied in the last section and is based on the non-convexity of the anisotropy energy function.

The equilibrium configuration of the magnetization field is found by minimizing $E_{\mathbf{H}_{ext}}$ given by (10) subject to the constraint (9). This leads to

$$\frac{\delta E_{\mathbf{H}_{ext}}}{\delta \mathbf{M}}(\mathbf{M})(\mathbf{x}) = \lambda(\mathbf{x}) \mathbf{M}(\mathbf{x}) \quad (11)$$

where $\lambda(\cdot)$ is a scalar valued function. The left hand side of the above equation has the following meaning. Suppose $\mathbf{M}(\mathbf{x}) = M_s \cdot (\alpha, \beta, \gamma)(\mathbf{x})$ where the vector (α, β, γ) is a vector of direction cosines of \mathbf{M} at point \mathbf{x} . If $\delta E_{\mathbf{H}_{ext}}(\mathbf{x})$ is the variation in $E_{\mathbf{H}_{ext}}(\mathbf{x})$ for a small variation $\delta \mathbf{M}(\mathbf{x}) = M_s \cdot \delta(\alpha, \beta, \gamma)(\mathbf{x})$ consistent with the constraint (9) and we can write $\delta E_{\mathbf{H}_{ext}}(\mathbf{x}) = \psi(\mathbf{x}) \cdot \delta \mathbf{M}(\mathbf{x})$ (only

retaining terms in the first degree in $\delta\mathbf{M}(\cdot)$ then $\frac{\delta E_{\mathbf{H}_{ext}}}{\delta\mathbf{M}}(\mathbf{M})(\mathbf{x}) = \psi(\mathbf{x})$.

Denoting

$$\mathbf{H}_{total}(\mathbf{x}) = \frac{\delta E_{\mathbf{H}_{ext}}}{\delta\mathbf{M}}(\mathbf{M})(\mathbf{x}), \quad (12)$$

we obtain from (11) and (12):

$$\mathbf{M}(\mathbf{x}) \times \mathbf{H}_{total}(\mathbf{x}) = 0. \quad (13)$$

To study the dynamics of the magnetization change without dissipation, we form the Lagrangian and use Hamilton's principle. This procedure leads to the equation [6]

$$\frac{d\mathbf{M}}{dt}(\mathbf{x}) = \lambda_1 \mathbf{M}(\mathbf{x}) \times \mathbf{H}_{total}(\mathbf{x}) \quad (14)$$

at every point \mathbf{x} in the body, where the *net magnetic field* \mathbf{H}_{total} is given by (12) and λ_1 is the gyroscopic constant.

Landau and Lifshitz (1935) in their original paper [10] argue that there is also a relativistic interaction between the moments in crystal which acts like a dissipative force. In other words, there is a dissipation of energy and magnetic moments tend to align with the external magnetic field. Therefore we must add another term to the right hand side of the above equation whose direction is perpendicular to both \mathbf{M} and $\mathbf{M} \times \mathbf{H}_{total}$.

$$\frac{d\mathbf{M}}{dt} = \lambda_1 \mathbf{M} \times \mathbf{H}_{total} + \lambda_2 \mathbf{M} \times (\mathbf{M} \times \mathbf{H}_{total}) \quad (15)$$

where $\lambda_2 \ll \lambda_1$. This equation is called the Landau–Lifshitz equation. Gilbert (1955) showed later [6] that the above equation can be obtained from a Lagrangian formulation and the use of a Rayleigh dissipation function

$$\mathcal{R} = \frac{1}{2} \int_{\Omega} \eta \left| \frac{d\mathbf{M}}{dt} \right|^2 d\mathbf{x} \quad (16)$$

where η is a constant for a given material (with no impurities).

The steady state equation relating \mathbf{H}_{total} and \mathbf{M} is given by

$$\mathbf{H}_{total}(\mathbf{x}) = \lambda(\mathbf{x}) \mathbf{M}(\mathbf{x}) \quad (17)$$

where $\lambda(\mathbf{x})$ is a scalar valued function.

In the last section on general hysteresis, it was noted that some authors prefer to study the equilibria by considering the process to be quasi-static and others study the full dynamic case. The former assume that the evolution equation to reach the equilibria to be of gradient type etc. However, it was shown by T. Shepherd that if the geometry of the system is kept in mind, then there is a natural algorithm to reach the equilibrium states for Hamiltonian systems [11]. It is interesting to note that for ferromagnetism, this approach leads to the Landau–Lifshitz equation. However there is still a difference in the sense that in Shepherd’s method the constant λ_2 is arbitrary, while for Landau and Lifshitz it signified a constant for the material.

For studying magnetostriction, we need to take into account strain energies, lattice structure and magnetoelastic energies in the free-energy formulation. As the magnetic body is now assumed to be deformable, let $p(\mathbf{x})$ denote the position of the point \mathbf{x} in the undeformed body after the body has undergone some deformation. In what follows, we use the tensorial notation with $\mathbf{x} = x_a$, $a = 1, 2, 3$; $p(\cdot) = p_i$; $\mathbf{M} = M_i$; $\mathbf{H} = H_i$; $i = 1, 2, 3$. The derivatives are denoted with two indices separated by a comma (for example $-H_{i,j} = \frac{\partial H_i}{\partial p_j}$), while second order tensors are denoted with two indices (for example – the stress

tensor is denoted t_{ij} . Repeated indices in the same term mean a summation (for example : $t_{ij,j} = \sum_{k=1}^3 t_{ik,k}$). Denote $p_{i,a} = \frac{\partial p_i}{\partial x_a}$. Thus by our notation $p_{i,a} p_{i,b} = \sum_{k=1}^3 p_{k,a} p_{k,b}$.

We now have two order parameters: the magnetization distribution $\mathbf{M}(\mathbf{x})$ and the strain distribution $\mathbf{C} = C_{ab}$; $a, b = 1, 2, 3$ defined by

$$C_{ab} = \frac{1}{2}(p_{i,a} p_{i,b} - \delta_{ab}) \quad (18)$$

where $\delta_{ab} = 1$ if $a = b$ and $\delta_{ab} = 0$ otherwise. The free energy functional for the magnetostriction case must remain unchanged if we rotate the co-ordinates axes. This implies that the energy functional must be a function of \mathbf{C} [8]. Denote the energy functional as $E_{\mathbf{H}_{ext}, \mathbf{T}}(\mathbf{M}, \mathbf{C})$ to emphasize its dependence on the external magnetic field and mechanical traction \mathbf{T} acting on the surface of the body $\partial\Omega$. Then it is given by [8, 10]

$$E_{\mathbf{H}_{ext}, \mathbf{T}}(\mathbf{M}, \mathbf{C}) = E_{\mathbf{H}_{ext}}(\mathbf{M}) + \mu_{abcd} C_{ab} C_{cd} + \gamma_{abcd} C_{ab} M_c M_d \quad a, b, c, d = 1, 2, 3, \quad (19)$$

where the first term on the right-hand-side is given by (10), the second term is the *elastic-strain energy* and the last term is the *magneto-elastic energy*. The constants μ_{abcd} , γ_{abcd} with $a, b, c, d = 1, 2, 3$ are non-negative.

Hamilton's principle for the dynamic case now yields two equations – one signifying magnetic equilibrium and the other mechanical equilibrium [8]. The dynamic magnetic equilibrium equation is the same as the Landau-Lifshitz equation (15), while the mechanical equilibrium equations are:

$$t_{ij,j} + M_j H_{i,j} + \rho f_i = \rho a_i \quad \text{in } \Omega \quad (20\text{-a})$$

$$t_{[ij]} = M_i H_j - M_j H_i \quad \text{in } \Omega \quad (20\text{-b})$$

$$t_{ij} n_j - \frac{1}{2} M_n^2 n_i = T_i \quad \text{in } \partial\Omega \quad (20\text{-c})$$

where $t_{ij} = \rho \frac{\partial E_{\mathbf{H}_{ext}, \mathbf{T}}}{\partial p_{i,a}} p_{i,a}$ is the stress field in the body, f_i is the i th component of a body force, $a_i = \ddot{p}_i$ is the i th component of the acceleration vector. $\mathbf{n} = (n_1, n_2, n_3)$ denotes the normal vector at a point the surface $\partial\Omega$ and $M_n = \mathbf{M} \cdot \mathbf{n}$. $t_{[ij]} = t_{ij} - t_{ji}$.

The term M_n arises in (20-c) because \mathbf{H} is discontinuous across the surface [8]. The tensor t_{ij} is not symmetric as shown by (20-b) because of the invariance of the free energy functional to rotation of the co-ordinate axes. The stress tensor t_{ij} is *not* the Cauchy or the Piola-Kirchoff stress tensors encountered in pure continuum mechanics (involving only strain energies). This is because the postulate of the Cauchy or the Piola-Kirchoff stress tensors (coming from the *stress hypothesis*) implies that they are purely short range effects – the *stress hypothesis* postulates the existence of a stress vector τ that acts across a hypothetical internal surface of a body and that completely quantifies the short-range forces exerted by the parts of the body on either side of the surface on one another across this surface. On the other hand, the stress tensor t_{ij} includes terms involving H_i (Equation (20-b)) which involve long range effects.

The above development of the theory has several subtle points that were not fully explored in this discussion because the main aim was to familiarize the reader with the subject matter. For a fuller description, we refer to Brown's classic [8].

1.2 Constitutive description of hysteresis

The problem of determining the magnetization and the strain for a body for a given external field \mathbf{H}_{ext} and surface traction \mathbf{T} amounts to solving the partial differential equations (15 - 20-b) along with constitutive equations relating the stress \mathbf{t} and the strain \mathbf{C} . Analytical solutions are impossible except for the simplest of geometries with restrictive assumptions on the magnitudes of the different energy quantities. Results on the qualitative analysis of the behaviour of the solutions are few and that too with simplifying assumptions of zero magnetostriction. If our aim is to control the behaviour of magnetostrictive actuators then we need to solve the PDE's in real time and plan the control action. This task is extremely difficult given the present technology. For example, even for a simple two dimensional body, the computation of the magnetization can become computationally expensive [12]. Thus we have to seek ways of simplifying the problem. In this context, problems relating to *model reduction* or the conversion of a set of partial differential equations (PDEs) to a set of ordinary differential equations (ODEs) are of interest.

Summarizing, one way of solving a real-time control problem for a magnetostrictive body would be to:

- write down the continuum equations satisfied by the state variables (or order parameters) and,
- reduce the number of equations to be solved by some means.

The former step implies that \mathbf{M} , \mathbf{H} , \mathbf{B} have to satisfy Maxwell's equations (5 - 6-d) and p_i , \mathbf{t} , \mathbf{C} have to satisfy the Euler-Lagrange equations (20-a - 20-c) inside the body. As we no longer start the discussion with a free energy functional,

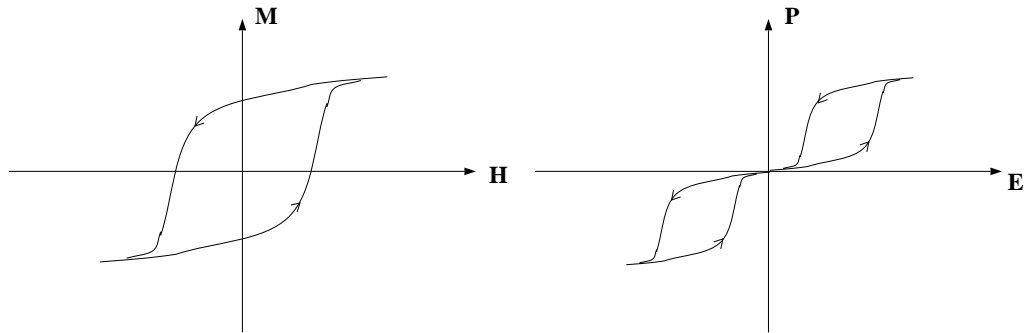
this step also requires the knowledge of constitutive relations between \mathbf{H} , \mathbf{t} and the order parameters \mathbf{M} , \mathbf{C} . The latter step is less well-defined and may involve only considering solutions that are near an operating point.

Alternatively, we could

- reduce the number of variables by only considering average or bulk variables,
- write down the equations satisfied by these quantities using physical principles.

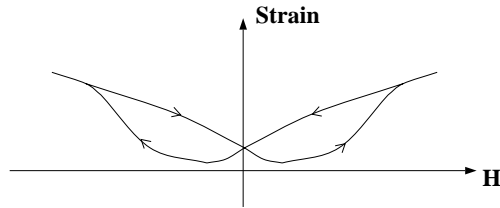
The first step now could be determined by the geometry of the body and the operating point. By its very nature, it is not well-defined and requires some experience and expertise on the part of the researcher. In the second step, we now use physical principles in the macroscopic form. For instance, we use Newton's laws of motions instead of Euler-Lagrange equations. Again to solve the equations, we need constitutive equations between conjugate variables. These equations could describe the hysteresis between conjugate variables as a functional relationship. In we use the second approach and describe hysteresis between conjugate variables in a constitutive fashion, then it is to be expected that the model will differ greatly depending on the phenomena where it is observed. Figure 1.7 shows sample curves that have been observed in experiments where one variable is varied periodically and the other is observed [1, 13, 14], while Figure 1.8 shows hysteresis due to backlash which is common in mechanisms with gears. We note that the figures only show the relationship between conjugate variables for one particular input. To obtain a mathematical equation (a constitutive relation) representing this relationship we need to apply all possible inputs and observe

the outputs.



(a) Ferromagnetism.

(b) Ferroelectricity.



(c) Magnetostriction.

Figure 1.7: Relationship between conjugate variables observed in various physical phenomena.

Some of the features of hysteresis observed in physical phenomena are listed below.

1. *Major-Loops.* Figures 1.7 and 1.8 show the path taken by the output (y-axis), while the input (x-axis) is increased and decreased sufficiently (until the output saturates). The forward and the backward paths constitute the major loops. For general continuous inputs, the value of the output is bounded by the corresponding major-loop output values. It must be

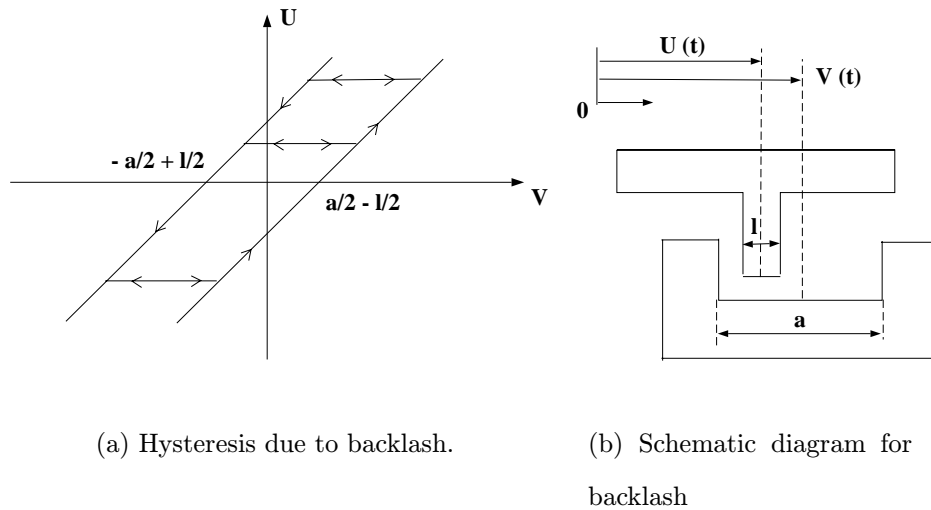


Figure 1.8: Hysteresis in engineering.

noted that hysteresis in superconduction does not show this feature.

2. *Causality*. The output depends only on the past values of the input.
3. *Monotonicity*. If the input is nondecreasing or nonincreasing, then so is the output.
4. *Order Preservation*. This implies that the forward paths are nonintersecting and so are the backward paths.
5. *Congruency*. If the initial value of the outputs of two systems differ by a constant, then for all input variations, the outputs of the two systems will differ by the same value. This property is not observed in ferromagnetic hysteresis. On the other hand hysteresis in superconduction shows this property [15].
6. *Minor-Loop Closure*. This important feature observed in ferro-magnetism

was known to 19th century researchers [1]. In Figure 1.9, the horizontal axis is the magnitude of the average magnetic field H in a soft-iron ring while the vertical axis is the magnitude of the average magnetic flux density B . The units are not important in this discussion. We can see the major loop in the (H, B) -plane that is obtained when H is increased from a large negative value $-H_{max}$ to a large positive value H_{max} and vice-versa. The trajectories for other general inputs can be seen inside the major loops. Suppose the input is decreased from H_{max} to H_1 and then increased to a value H_2 that is less than H_{max} . If the input is decreased again to H_1 then the corresponding value of the flux density is B_1 . In other words, the minor-loop inside the major loop closes on itself. From (H_1, B_1) , if the input is reduced to H_3 ; increased to $H_4 < H_{max}$; and then reduced to H_3 again, we see the same phenomenon.

We now make some brief remarks about a general theory of constitutive modeling of hysteresis. In this theory, no underlying physical phenomenon is considered and is purely a mathematical description of the relationship between two conjugate variables. The key aspect of this relationship is its hysteretic nature, and potentially this theory (with some modifications) could be applied to any of the phenomena in nature where hysteresis is observed. In practice, one has to carry out several experiments to identify a certain measure and this limits the great potential of this theory.

Krasnoselskii first introduced the concept of an hysteresis *operator* F [16, 17] between the input and output variables. A natural procedure is to consider F as a map from $C^0([0, T])$ to some Banach Space \mathcal{B} . One can then easily formulate the properties enumerated before, mathematically, as done in Vis-

intin’s monograph[17]. The operator space \mathcal{F} is then the set of all operators $F : C^0([0, T]) \rightarrow \mathcal{B}$ satisfying some ‘consistent’ subcollection of the properties enumerated above. By this we mean that none of the properties within the subcollection contradict any of the others within the same subcollection. This space \mathcal{F} can be endowed with many kinds of operator topologies [18], making it an infinite-dimensional space. One could require some cost functional to be minimised while identifying the operator F . Still, the problem is a very difficult one to solve, though there is some existence theory for some special operators[19].

A hysteresis operator that is widely used in magnetics community is the *Preisach* operator. Conceptually, it is an assemblage of elementary bi-stable hysterons that switch between -1 and $+1$ when u becomes greater than α with $v = -1$ or less than β when $v = +1$. Formally

$$\bar{v} = \int_0^\infty \int_0^\infty \omega(r, s) \mathcal{R}_{s-r, s+r}[v](t) ds dr$$

$\omega(r, s)$ is a density function, and initial values of the relays $\mathcal{R}_{s-r, s+r}[v]$ are defined by (2).

There has been considerable work done on the Preisach operator [15, 20], and on PDE’s involving the Preisach operator [3]. However, the identification problem of the density function is not easy and though the Preisach model shows slightly better predictive capability than the phenomenological *Jiles – Atherton* model [21], the computational cost is substantially higher [22].

1.3 Content of the dissertation

In this dissertation, we present a model for a thin rod magnetostrictive actuator. We show rigorously that the solution for this model exists and is unique when the

inputs are periodic in time and the initial states are at the origin. Furthermore, we show that this solution has an Ω limit set that is a periodic orbit. We also propose a method to obtain the parameters for this model. An application of this method to a commercial actuator is presented. Finally, we study the problem of trajectory tracking and propose a control law for this purpose. Experimental verification of this control law is also done.

The object of study in this dissertation is a thin magnetostrictive rod actuator that is available commercially. The cross-section of such an actuator is shown Figure 1.10 [23]. It comprises of the TERFENOL-D rod; non-linear springs to provide prestress; permanent magnets for biasing the actuator; a magnetic path; a push-rod; and outer casing. The deformation of the actuator in response to external stimulus (as a change in the applied magnetic field), results in the motion of the push-rod with respect to the outer casing. This motion can be utilized for actuation purposes.

If we are interested in control of this actuator, then not only do we have to worry about modeling the actuator itself, but also the associated components of the actuator correctly. This modeling procedure is fraught with uncertain knowledge of the system (that might change with temperature, age etc.). Therefore, it makes practical sense to use techniques in adaptive and robust control, that do not require a precise knowledge of the uncertainties, but only a rough knowledge of them in some sense. Hence, we treat the actuator itself along with the associated prestress, magnetic path, to be a mass-spring system with magneto-elastic coupling.

In the last section we noted that there are alternative ways of going about solving the real-time control problem. We also noted that the first method

leads to coupled PDE's that are extremely difficult to solve without detailed knowledge of the system. This method could potentially be useful in the design of new actuators or new magnetostrictive actuator materials themselves. But for real-time control, the second method of using bulk quantities as state variables is more practical, and is better suited to utilize techniques of modern control theory. Therefore in this dissertation we adopt this approach.

Suppose M denotes the average magnetization per unit volume, H denotes the average magnetic field per unit volume, and x denotes the displacement of the tip of the actuator. Let \dot{H} be the input variable.

In Chapter 2, we propose a model of ferromagnetic hysteresis using energy balance and the postulates of Jiles and Atherton. This model is a set of two differential equations describing the evolution of $H(\cdot)$ and $M(\cdot)$ as functions of time:

$$\dot{H} = u \tag{21-a}$$

$$\dot{M} = f(H, M, u) \tag{21-b}$$

The input u is a function of time t . For inputs $u(\cdot)$ that change sign in an interval of time $[a, b]$, the function f is discontinuous as a function of time and hence careful analysis is necessary to show even existence and uniqueness of solutions. It turns out that the model is only technically correct when the *states* H and M are periodic signals in time. Thus it would be incorrect to expect the model to give accurate predictions for general inputs $u(\cdot)$. For periodic inputs of time however, we show that the solution (with initial state at the origin) has an Ω limit set that is a periodic orbit.

In Chapter 3, we extend the ferromagnetic hysteresis model to a model of magnetostriction for a thin rod again using energy balance principles. The result is a set of three differential equations:

$$\dot{H} = u \tag{22-a}$$

$$\dot{M} = f(H, M, u, y) \tag{22-b}$$

$$m_{eff}\ddot{y} + c\dot{y} + dy = F + kM^2 \tag{22-c}$$

The displacement and velocity of the edge of the magnetostrictive rod y and \dot{y} are also state variables in addition to H and M . m_{eff} , c , d , k are constants. The inputs are u and F .

Equations (22-a) and (22-b) describe the evolution of the magnetic variables while (22-c) describes the evolution of the mechanical variables y and \dot{y} . As the function f depends on y and M appears in (22-c), the magnetic and mechanical evolution equations are *coupled*. Again by careful analysis we show that for periodic inputs the solution of this coupled set of equations (with initial state at the origin) has an Ω limit set that is a periodic orbit.

The finite resistivity of the magnetostrictive rods available commercially implies that eddy-currents circulate in the rod when the applied magnetic field is changed. This means that there is an energy loss and this loss has to be accounted for our energy balance equation. We go through this step and obtain a bulk model for a thin magnetostrictive rod that incorporates ferromagnetic hysteresis; elastic and magneto-elastic effects; inertial effects; losses due to mechanical motion; and eddy-current effects.

In Chapter 4, we address the problem of identification of the 12 parameters

that make up the model. By carefully grouping them and undertaking the identification of each group separately we show that the identification problem is reduced to solving three linear regression problems. We also go through an identification process for a commercial actuator and obtain the parameters particular to that actuator.

In Chapter 5, we address the problem of real-time trajectory tracking for a commercial actuator. The control law design is done by extending the work of Eugene Ryan [24] who proposed a universal adaptive tracking law for relative degree one systems with a set valued non-linearity (of a certain kind) at the input. We propose a control law that combines Ryan's work and that of Morse [25] who proposed a universal stabilizer for linear relative degree two systems. A proof of this control law was not carried out during the course of this dissertation because of time limitations. An implementation of the proposed controller was done on a TMS320C31 based DSP-board. The results of this experiment was not satisfactory due to the presence of rather large sensor noise. Nevertheless the fact that the closed-loop-system remained stable even for input frequencies of 500 Hz suggest that the model is correct in the frequency range of interest.

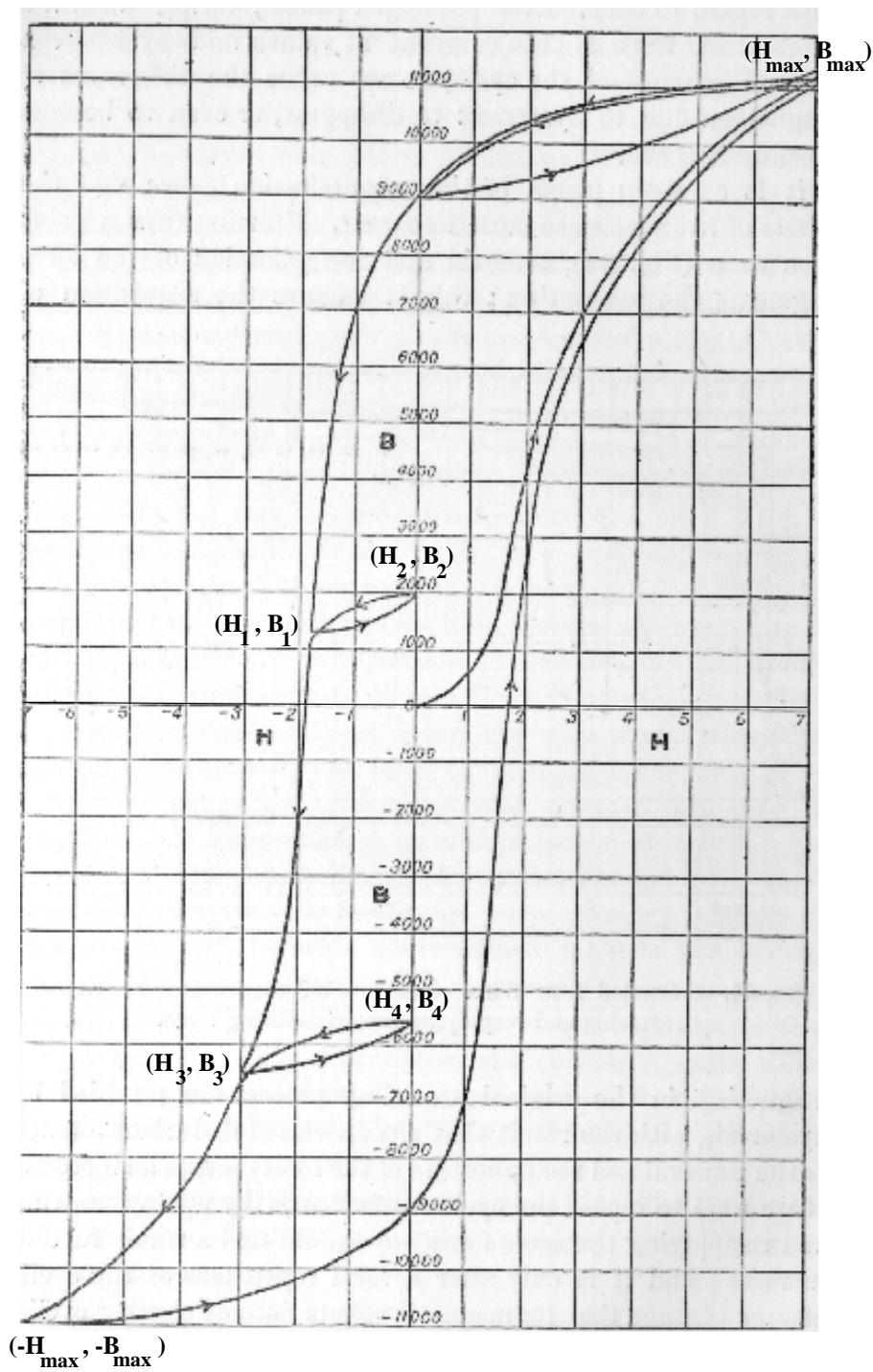


Figure 1.9: Experimental curves for a soft-iron ring [1].

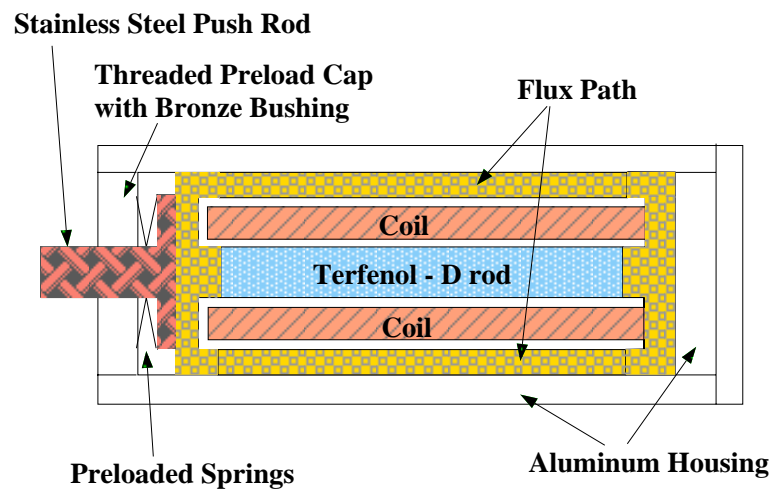


Figure 1.10: The ETREMA MP 50/6 TERFENOL-D magnetostrictive actuator
(Source: ETREMA Products Inc).

Chapter 2

Bulk Ferromagnetic Hysteresis Model

We have seen in Chapter 1 that hysteresis between the external field and the order parameter arises from two causes – metastability of the Helmholtz (free energy) functional and energy dissipation. In the case of ferromagnetism, metastability of the free energy functional arises due to the presence of easy axes for the magnetic moment. The energy dissipation is due to quantum-mechanical effects and is characterised by a constant in Equation (16). This constant is thus dependent on the ferromagnetic material. So theoretically, it seems plausible that it can be calculated from first principles. However, in practice, a ferromagnetic body may contain several defects due to impurity atoms, ions, missing ions at some lattice sites or lattice mismatch. The last reason is a result of the conditions under which a particular ferromagnetic body is grown. To account for the defects, one needs to add terms to both the Rayleigh dissipation function (analogous to kinetic friction) and to the energy functional to take note of pinning of domain walls (analogous to static friction).

Engineers using magnetostrictive actuators in applications are faced with the problem of determining the external magnetic field (using permanent magnets

or electromagnets) that must be applied to obtain a desired response from the actuator. From the previous discussion, we see that one needs to determine several facts about the given actuator like the nature and position of the defects in the actuator, the dissipation constants related to the interaction of the magnetic moments with themselves and with the defects, the easy directions for the anisotropy energy etc. To resolve these questions for each and every actuator and then the calculation of the magnetic moment distribution and the stresses in the actuator is impractical. This leads us to a model reduction problem, where we are faced with reducing the number of state variables in a given application.

For the case of magnetostrictive rod actuators with the length much larger than the diameter we have chosen to use another approach to obtaining low-order models for control purposes. This model is statistical in nature and based on Langévin and Weiss theories of paramagnetism and ferromagnetism.

2.1 Bulk Ferromagnetic Hysteresis Theory

2.1.1 Langevin Theory of Paramagnetism

The classical derivation of Curie's law was given by Langevin, using Boltzmann's statistics[26, 27]. In what follows, bold letters denote vectors like the magnetic field \mathbf{H} at a point in space, or the magnetization \mathbf{M} at a point in a magnetized body. The scalar quantities H, M etc. denote their magnitudes.

Consider a system of atomic magnetic moments \mathbf{m} and suppose that they do not interact with each other and are therefore free to point in any direction. If a magnetic field \mathbf{H} is applied to such a group of free moments, a couple acts on each moment, tending to rotate it into the direction of \mathbf{H} . This tendency

is opposed by the thermal agitation if the temperature is finite. The potential energy of a magnetic dipole in a magnetic field is given by

$$W_{para} = -\mathbf{m} \cdot \mathbf{H} = -m H \cos \theta, \quad (1)$$

where θ is the angle between the directions of \mathbf{m} and \mathbf{H} . The energy of thermal motion is of the magnitude of kT where k is Boltzmann's constant and T is the absolute temperature in Kelvins. Suppose $\cos \theta = 1$; $H = 10^6 \text{ A/m}$. The smallest possible magnetic moment is the Bohr magneton $M_B = 1.17 \times 10^{-29}$. Therefore $|W_{para}| = 1.17 \times 10^{-23}$. Now $kT = 1.38 \times 10^{-23} \times 300 = 4.1 \times 10^{-21} \text{ J}$, at room temperature. So thermal agitation is sufficient to make the angular distribution of the atomic moments almost random, resulting in only a very small magnetization parallel to the magnetic field.

The number of molecules having an energy in the range W_{para} to $W_{para} + dW_{para}$ is given by Boltzmann's statistics as

$$dn = n_0 e^{-\frac{W_{para}}{kT}} dW_{para}, \quad (2)$$

where n_0 is a constant chosen in such a way that integration of Equation (2) over all possible values of W_{para} shall be equal to the total number of molecules N . Using Equation (1) we get

$$\begin{aligned} dn &= n_0 e^{\frac{mH \cos \theta}{kT}} d(-mH \cos \theta) \\ &= n_0 e^{\frac{mH \cos \theta}{kT}} mH \sin \theta d\theta. \end{aligned} \quad (3)$$

The total number N of molecules must then be equal to Equation (3) integrated over all angles between 0 and π . The net magnetization of the sample is given

by the resultant of all magnetic moments along the direction of \mathbf{H} :

$$\begin{aligned}
M &= \int_0^\pi m \cos \theta \, dn \\
&= \frac{N \int_0^\pi m \cos \theta \, dn}{\int_0^\pi dn} \\
&= \frac{N \int_0^\pi m \cos \theta n_0 e^{\frac{mH \cos \theta}{kT}} m H \sin \theta \, d\theta}{\int_0^\pi n_0 e^{\frac{mH \cos \theta}{kT}} m H \sin \theta \, d\theta} \\
&= N m \left(\coth z - \frac{1}{z} \right) \\
&= M_s \mathcal{L}(z),
\end{aligned} \tag{4}$$

where

$$z = \frac{mH}{kT}. \tag{5}$$

$\mathcal{L}(z)$ is called the Langevin function. For a high enough value of the magnetic field H , nearly all the atomic moments are aligned in the direction of \mathbf{H} , and the value of $M \approx Nm = M_s$ – the saturation magnetization. For the sample calculation done before, $z = 2.8 \times 10^{-3}$. For $z \ll 1$, the Langevin function can be expanded as

$$L(z) = \frac{z}{3} - \frac{z^3}{45} + \dots$$

Neglecting higher-order terms,

$$M = \frac{Nm^2}{3kT} H. \tag{6}$$

This is Curie's law for paramagnetic materials.

2.1.2 Weiss Theory of Ferromagnetism

The magnetic field necessary to reach saturation according to Equation (4) may be estimated tentatively with $z = 7$. That is $H = \frac{7kT}{M_B} \approx 2.5 \times 10^9 A/m$. To magnetise a ferromagnetic substance to saturation, we only need $H \approx 1 A/m$ for Supermalloy and $5 \times 10^4 A/m$ for Alnico[26]. Usually it is between these values. Weiss reasoned that the atomic magnetic moments in a ferromagnetic substance interact strongly with one another and tend to align themselves parallel to each other. The interaction is such as to correspond to an applied field of the order of magnitude of $10^9 A/m$ for iron. The effect of an externally applied field is merely to change the direction of the spontaneous magnetization. Weiss first postulated this strong inner magnetic field and called it the “molecular field”. The molecular field was postulated to be

$$\mathbf{H}_m = \alpha \mathbf{M}. \quad (7)$$

If a magnetic field \mathbf{H} is applied parallel to the magnetization \mathbf{M} of the system, then the “effective” magnetic field at a point is given by equation.

$$\mathbf{H}_e = \mathbf{H} + \mathbf{H}_m.$$

An individual atomic moment now has the potential energy,

$$W_{\text{ferro}} = -\mathbf{m} \cdot \mathbf{H}_e = -m(H + \alpha M) \cos \theta.$$

Repeating the calculations done in the previous section according to Equations (2) - (4) we get

$$M(z) = M_s \mathcal{L}(z) = M_s \left(\coth z - \frac{1}{z} \right) \quad (8)$$

where M_s is the saturation magnetization and $\mathcal{L}(z)$ is the Langevin function. z in the above equation is given by

$$z = \frac{m(H + \alpha M)}{kT}. \quad (9)$$

Rewriting the above equation, we get

$$M = \frac{z k T}{m \alpha} - \frac{H}{\alpha} \quad (10)$$

Then the magnetization M is given by the simultaneous solution of Equations (8) and (10) for a given value of H . The ferromagnetic solid considered was lossless, and hence the same curve in the (H, M) -plane is traced during both the increasing and decreasing branches for a periodic H (Figure 2.1). This curve is called the “anhysteretic” curve. In the following sections we consider lossy solids, and the average magnetization is referred to as M while the magnetization given by Equation (8) is called M_{an} - the anhysteretic magnetization.

2.1.3 Bulk Ferromagnetic hysteresis model

In 1983, Jiles and Atherton[21] proposed a model for bulk ferromagnetic hysteresis. Their aim was to try and reproduce the bulk $B - H$ curves observed in ferromagnetic rods or toroids. The theory was based on the modification of the Weiss molecular field model in which the changes in magnetization due to the motion of domain walls under an applied field were accounted for. In effect, they postulate an expression for the dissipation of energy during domain wall motion. We have noted before that this quantity is a troublesome quantity to calculate from first principles because of the diversity of phenomena that contribute to it and from practical considerations having to do with estimating the number of

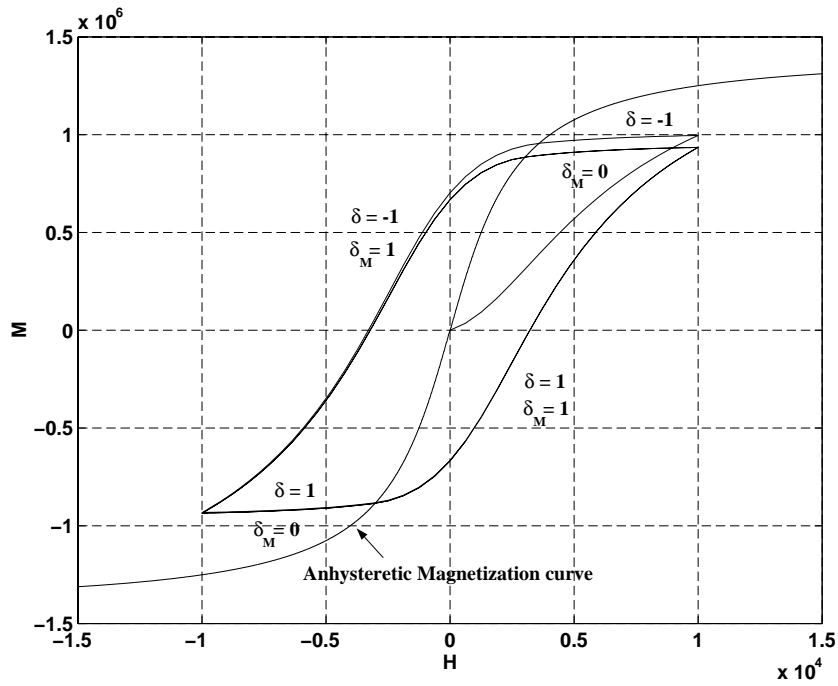


Figure 2.1: M vs H relationship for an ideal and a lossy ferromagnet.

defects in a particular ferromagnet etc. The contribution of Jiles and Atherton is to postulate a simple expression to account for the losses. This expression is very similar to the energy losses due to kinetic friction in that it says that the losses during the magnetization changes for a magnetic body is proportional to the change rate of change of magnetization.

Consider a thin ferromagnetic rod whose average magnetization is denoted by M . An external source (battery) produces a uniform magnetic field H in the body. This field H is purely due to the external source and is not the effective magnetic field in the body. A change in the field H brings about a corresponding change in the magnetization of the body in accordance with Maxwell's laws of electromagnetism. The work done by the external source δW_{bat} , is equal to the change in the internal energy of the material δW_{mag} and losses in the

magnetization process δL_{mag} :

$$\delta W_{bat} = \delta W_{mag} + \delta L_{mag}. \quad (11)$$

W.F. Brown [8] derives the work done by the battery in changing the magnetization per unit volume, in one cycle, to be given by

$$\delta W_{bat} = \oint \mu_0 H dM. \quad (12)$$

The relationship between the above energy expression and the usual expression of hysteresis energy loss per unit volume can be derived easily. The average magnetic flux density in the ferromagnetic body B is related to the magnetic field H and average magnetization M as :

$$B = \mu_0 (H + M). \quad (13)$$

As $\oint \mu_0 H dH$ and $\oint \mu_0 M dM$ are loop integrals of exact differentials and hence equal to zero, we have

$$\begin{aligned} \oint H dB &= \oint \mu_0 H dH + \oint \mu_0 H dM \\ &= \oint \mu_0 H dM \\ &= - \oint \mu_0 M dH \\ &= - \oint \mu_0 M dH - \alpha \oint \mu_0 M dM \\ &= - \oint \mu_0 M d(H + \alpha M) \\ &= - \oint M dB_e, \end{aligned} \quad (14)$$

where the constant α can take any value and

$$B_e = \mu_0 H_e = \mu_0 (H + \alpha M). \quad (15)$$

The Equation (14) is of interest because in Weiss's molecular field theory for ideal ferromagnetic rods (no losses), $M_{an} = M$ is a function of B_e and $\alpha > 0$ is the molecular field parameter. For an ideal ferromagnetic rod, M_{an} is given by the Langevin function [26, 27] – $M_{an} = M_s \mathcal{L}(z) = M_s (\coth z - \frac{1}{z})$ where M_s is the saturation magnetization. $z = \frac{H + \alpha M}{a}$ and a is a parameter that depends on the temperature of the specimen. Thus for an ideal ferromagnet, $\oint H dB$ and $\oint H dM$ are equal to zero as we expect them to be. Hence if H is a periodic function of time, then the same (anhysteretic) curve is traced for both the increasing and decreasing branches in the (H, M) -plane (Figure 2.1).

Using Equation (14), we obtain the expression for δW_{mag} from the ideal case:

$$\delta W_{mag} = - \oint M_{an} dB_e. \quad (16)$$

For a lossy ferromagnet, the expression for the magnetic hysteresis losses δL_{mag} is due to Jiles and Atherton. The motivation for this term (see Equation (19) below) is the observation that the hysteresis losses are due to irreversible domain wall motions in a ferromagnetic solid. They arise from various defects in the solids and are discussed in detail by Jiles and Atherton [28]. Here we provide a gist of their results. They consider the average magnetic moment per unit volume M to be comprised of an irreversible component M_{irr} and a reversible component M_{rev} . Furthermore, they claim M_{rev} to be related to the anhysteretic or ideal magnetization by,

$$M = M_{rev} + M_{irr}, \quad (17)$$

$$M_{rev} = c(M_{an} - M_{irr}), \quad (18)$$

where $0 < c < 1$ is a parameter that depends on the material. The energy loss due to the magnetization is only due to M_{irr} :

$$\delta L_{mag} = \oint k \delta (1 - c) dM_{irr}. \quad (19)$$

In the above equation, k is a nonnegative parameter, and δ is defined as,

$$\delta = \text{sign}(\dot{H}). \quad (20)$$

Furthermore, Jiles and Atherton make the assumption that if the actual magnetization is less than the anhysteretic value and the magnetic field strength H is lowered, then until the value of M becomes equal to the anhysteretic value M_{an} , the change in magnetization is reversible. That is,

$$\frac{dM_{irr}}{dH} = 0 \quad \text{if} \quad \begin{cases} \dot{H} < 0 \text{ and } M_{an}(H_e) - M(H) > 0 \\ \dot{H} > 0 \text{ and } M_{an}(H_e) - M(H) < 0 \end{cases} \quad (21)$$

At this point, we take stock of Equations (17 - 21). The reasoning behind Equation (18) is provided by Jiles and Atherton [28]. They use phenomenology-based arguments, the correctness of which is unclear. Basically, they explain the process of magnetization of a ferromagnetic body, as occurring in two stages. In one stage, the change in the magnetization is all reversible, whilst in the other it is a combination of reversible and irreversible changes. A similar qualitative explanation of the magnetization process can also be found in Bozorth [29] and Chikazumi [27]. The contribution of Jiles and Atherton is to quantify the same.

As will be seen later in the chapter, Equations (17 - 21) result in a model for magnetization that is numerically well-conditioned. Without Equation (21),

the incremental susceptibility at the reversal points $\frac{dM}{dH}$ can become negative. This can be checked by numerical simulations. Experimental observations suggest that the quasi-static incremental susceptibility is a non-negative quantity. Therefore we adopt the same assumptions as (a) they do not violate the laws of thermodynamics, (b) they make the quasi-static incremental susceptibility a non-negative quantity and (c) the extra structure makes the model numerically well conditioned. With these qualifying comments we proceed with the derivation of the state equations.

By Equations (17) and (18) we get

$$M = (1 - c) M_{irr} + c M_{an}. \quad (22)$$

Let

$$\delta_M = \begin{cases} 0 & : \dot{H} < 0 \text{ and } M_{an}(H_e) - M(H) > 0 \\ 0 & : \dot{H} > 0 \text{ and } M_{an}(H_e) - M(H) < 0 \\ 1 & : \text{otherwise.} \end{cases} \quad (23)$$

Then by Equations (21) and (22),

$$\frac{dM}{dH} = \delta_M (1 - c) \frac{dM_{irr}}{dH} + c \frac{dM_{an}}{dH}. \quad (24)$$

From Equations (11), (12), (14) and (19) and the expression for W_{mag} we get

$$\oint (M_{an} - M - k \delta (1 - c) \frac{dM_{irr}}{dB_e}) dB_e = 0.$$

Note that the above equation is valid only if $M(t)$ and $H(t)$ are periodic in the (H, M) -plane. In other words, the trajectory is a periodic orbit. We now make the *hypothesis* that the following equation is valid when we go from *any point on this periodic orbit to another point on the periodic orbit*.

$$\int (M_{an} - M - k \delta (1 - c) \frac{dM_{irr}}{dB_e}) dB_e = 0. \quad (25)$$

The above equation holds only on the periodic orbit. Therefore on the periodic orbit, the integrand must be equal to zero:

$$M_{an} - M - k \delta (1 - c) \frac{dM_{irr}}{dB_e} = 0. \quad (26)$$

Using Equations (24) and (26) we can show after some manipulations that

$$\frac{dM}{dH} = \frac{\frac{k \delta}{\mu_0} c \frac{dM_{an}}{dH} + \delta_M (M_{an} - M)}{\frac{k \delta}{\mu_0} - \delta_M (M_{an} - M) \alpha}. \quad (27)$$

Setting $k = 0$ gives us $\delta_M (M_{an} - M) \frac{dM}{dH} = -\frac{\delta_M (M_{an} - M)}{\alpha}$. As mentioned before, compatibility with the physical phenomenon demands that $\frac{dM}{dH} \geq 0$. α is a non-negative parameter and so for the above equation to make sense we must have

$$M_{an} - M = 0. \quad (28)$$

Thus $k = 0$ represents the lossless case. On the other hand, if $M_{an} - M = 0$, then for (26) to be true for all c , k must be equal to 0. Hence for the ferromagnetic hysteresis model,

$$k = 0 \iff M = M_{an}. \quad (29)$$

Rewriting Equation (27) so that we have $\frac{dM_{an}}{dH_e}$ in the numerator on the right hand side we get

$$\frac{dM}{dH} = \frac{\frac{k \delta}{\mu_0} c \frac{dM_{an}}{dH_e} + \delta_M (M_{an} - M)}{\frac{k \delta}{\mu_0} - \delta_M (M_{an} - M) \alpha - \frac{k \delta}{\mu_0} \alpha c \frac{dM_{an}}{dH_e}}. \quad (30)$$

This equation is different from the one obtained by Jiles and Atherton [21, 28]. We henceforth refer to it as the *bulk ferromagnetic hysteresis model* so as not to confuse it with the model in [28] that is popularly known as Jiles-Atherton model. For the sake of completeness we write down the other equations satisfied by the system:

$$M_{an}(H_e) = M_s \left(\coth \left(\frac{H_e}{a} \right) - \frac{a}{H_e} \right), \quad (31)$$

$$H_e = H + \alpha M, \quad (32)$$

$$\delta = \text{sign}(\dot{H}), \quad (33)$$

$$\delta_M = \begin{cases} 0: \dot{H} < 0 \text{ and } M_{an}(z) - M(H) > 0 \\ 0: \dot{H} > 0 \text{ and } M_{an}(z) - M(H) < 0 \\ 1: \text{otherwise.} \end{cases} \quad (34)$$

Equations (30 - 34) describe the bulk ferromagnetic hysteresis model. There are 5 non-negative parameters in this model namely a , α , M_s , c , k . Also $0 < c < 1$. Figure 2.1 shows the values taken by the discrete variables δ , δ_M at different sections of the hysteresis curve in the (H, M) -plane.

2.2 Qualitative analysis of the model

The model equations are only valid when the variables $M(t)$ and $H(t)$ are periodic signals of time. Therefore the solution of the model equations represent the physics of the system only when $M(t)$ and $H(t)$ form a periodic orbit in the (H, M) -plane. In simulations, the initial state of the system has to be on this orbit for the solution trajectory to represent the state of the system at any time t . But in practice, we do not know apriori what state the system is in. Then

can we use the above model? The answer in the affirmative is provided in this section. We show analytically that if the initial state is at the origin in the (H, M) -plane (which is usually not on the hysteresis loop), and apply a periodic input \dot{H} , then the solution *tends* asymptotically towards a periodic orbit in the (H, M) -plane.

First we prove an important property. Define state variables, $x_1 = H$, $x_2 = M$. Define

$$z = \frac{x_1 + \alpha x_2}{a}. \quad (35)$$

Denote $\mathcal{L}(z) = \coth(z) - \frac{1}{z}$ and $\frac{\partial \mathcal{L}}{\partial z}(z) = -\operatorname{cosech}^2(z) + \frac{1}{z^2}$. Then the state equations are:

$$\dot{x}_1 = u, \quad (36\text{-a})$$

$$\dot{x}_2 = g(x_1, x_2, x_3, x_4) u, \quad (36\text{-b})$$

where

$$x_3 = \operatorname{sign}(u), \quad (37\text{-a})$$

$$x_4 = \begin{cases} 0 & : x_3 < 0 \text{ and } \coth(z) - \frac{1}{z} - \frac{x_2}{M_s} > 0, \\ 0 & : x_3 > 0 \text{ and } \coth(z) - \frac{1}{z} - \frac{x_2}{M_s} < 0, \\ 1 & : \text{otherwise,} \end{cases} \quad (37\text{-b})$$

and

$$g(x_1, x_2, x_3, x_4) = \frac{\frac{k x_3}{\mu_0} \frac{c M_s}{a} \frac{\partial \mathcal{L}}{\partial z}(z) + x_4 M_s \left(\mathcal{L}(z) - \frac{x_2}{M_s} \right)}{\frac{k x_3}{\mu_0} - x_4 M_s \left(\mathcal{L}(z) - \frac{x_2}{M_s} \right) \alpha - \frac{k x_3}{\mu_0} \alpha \frac{c M_s}{a} \frac{\partial \mathcal{L}}{\partial z}(z)} \quad (38)$$

The system (36-a) - (38) has 2 continuous states: x_1 and x_2 . $u(\cdot)$ is the input. x_3 and x_4 are discrete variables that are functions of x_1, x_2 and u at any instant of time t . Therefore x_3 and x_4 are not discrete states. As the function g on the right hand side of Equation (36-b) depends on x_3 and x_4 , it is not continuous as a function of time. Therefore, the notion of solution to the system (36-a) - (72) is in the sense of Carathéodory (please refer to Appendix B for a discussion on this topic). A Carathéodory solution $(x_1, x_2)(t)$ to (36-a) - (72) for t defined on a real interval I , satisfies (36-a) - (72) for all $t \in I$ except on a set of Lebesgue measure zero. These points are those where g is discontinuous.

Theorem 2.2.1 *Consider the system of equations (36-a - 37-b). Let the initial condition $(x_1, x_2)(t = 0) = (x_{1_0}, x_{2_0})$ be on the anhysteretic curve:*

$$\begin{aligned} z_0 &= \frac{x_{1_0} + \alpha x_{2_0}}{a}, \\ x_{2_0} &= M_s \left(\coth(z_0) - \frac{1}{z_0} \right). \end{aligned} \quad (39)$$

Let the parameters satisfy

$$\frac{\alpha M_s}{3a} < 1, \quad (40)$$

$$0 < c < 1, \quad (41)$$

$$k > 0. \quad (42)$$

Let $u(\cdot)$ be a continuous function of t , with $u(t) > 0$ for $t \in [0, b)$ where $b > 0$ and $(x_1(t), x_2(t))$ denote the solution of (36-a) - (37-b). Then $(M_s \mathcal{L}(z(t)) - x_2(t)) > 0 \forall t \in (0, b)$. Else if $u(t) < 0$ for $t \in [0, b)$ where $b > 0$, then $(M_s \mathcal{L}(z(t)) - x_2(t)) < 0 \forall t \in (0, b)$.

Proof

We make a change of co-ordinates from (x_1, x_2) to (z, y) , where

$$\begin{aligned} z &= \frac{x_1 + \alpha x_2}{a}, \\ y &= M_s \mathcal{L}(z) - x_2. \end{aligned}$$

Denote $w = (z, y)$ and $x = (x_1, x_2)$. The domain of definition of the transformation $\psi : x \mapsto w$ is \mathbb{R}^2 . The Jacobian of the transform is given by

$$\frac{\partial \psi}{\partial x} = \begin{bmatrix} \frac{1}{a} & \frac{\alpha}{a} \\ \frac{M_s}{a} \frac{\partial \mathcal{L}}{\partial z}(z) & \frac{M_s \alpha}{a} \frac{\partial \mathcal{L}}{\partial z}(z) - 1 \end{bmatrix}.$$

The determinant of $\frac{\partial \psi}{\partial x}$ is

$$\det\left(\frac{\partial \psi}{\partial x}\right) = -\frac{1}{a} \quad \forall x \in \mathbb{R}^2.$$

Hence the results on existence, extension and uniqueness of solutions to the state equations in the transformed space carry over to the equations in the original state space.

Denote $\dot{w} = f(t, w, x_3, x_4)$. The initial conditions in the transformed co-ordinates are

$$w_0 = (z_0, y_0) = \left(\frac{x_{1_0} + \alpha x_{2_0}}{a}, M_s \mathcal{L}(z_0) - x_{2_0}\right).$$

The state equations in terms of w are:

$$\dot{z} = f_1(t, w) \tag{43-a}$$

$$\underline{\underline{\triangle}} \quad \frac{1 + \alpha \bar{g}(z, y, x_3, x_4)}{a} u, \tag{43-b}$$

$$= \frac{\frac{1}{a} \frac{kx_3}{\mu_0}}{\frac{kx_3}{\mu_0} - \alpha \left(x_4 y + \frac{kx_3}{\mu_0} \frac{cM_s}{a} \frac{\partial \mathcal{L}}{\partial z}(z)\right)} u, \tag{43-c}$$

$$\dot{y} = f_2(t, w) \quad (44\text{-a})$$

$$\triangleq \left(\frac{M_s}{a} \frac{\partial \mathcal{L}}{\partial z}(z) + \left(\frac{\alpha M_s}{a} \frac{\partial \mathcal{L}}{\partial z}(z) - 1 \right) \bar{g}(z, y, x_3, x_4) \right) u, \quad (44\text{-b})$$

$$= \frac{\frac{M_s}{a} \frac{kx_3(1-c)}{\mu_0} \frac{\partial \mathcal{L}}{\partial z}(z) - x_4 y}{\frac{kx_3}{\mu_0} - \alpha \left(x_4 y + \frac{kx_3}{\mu_0} \frac{cM_s}{a} \frac{\partial \mathcal{L}}{\partial z}(z) \right)} u. \quad (44\text{-c})$$

where

$$x_3 = \text{sign}(u), \quad (45\text{-a})$$

$$x_4 = \begin{cases} 0 & : x_3 < 0 \text{ and } y > 0, \\ 0 & : x_3 > 0 \text{ and } y < 0, \\ 1 & : \text{otherwise,} \end{cases} \quad (45\text{-b})$$

where

$$\bar{g}(z, y, x_3, x_4) = \frac{\frac{kx_3}{\mu_0} \frac{cM_s}{a} \frac{\partial \mathcal{L}}{\partial z}(z) + x_4 y}{\frac{kx_3}{\mu_0} - x_4 y \alpha - \frac{kx_3}{\mu_0} \alpha \frac{cM_s}{a} \frac{\partial \mathcal{L}}{\partial z}(z)}. \quad (46)$$

Let $D = \underbrace{(-\delta_1, b)}_t \times \underbrace{(-\infty, \infty)}_z \times \underbrace{\left(-\epsilon_1, \frac{k}{\mu_0} \frac{M_s(1-c)}{3a} + \epsilon_1\right)}_y$, where δ_1, ϵ_1 are

sufficiently small positive numbers.

As $u(t)$ is only defined for $t \geq 0$, we need to extend the domain of $u(\cdot)$ to $(-\delta_1, 0)$. This can be easily accomplished by defining $u(t) = 0$ for $t \in (-\delta_1, 0)$.

Then $f_1(t, w), f_2(t, w)$ exist on D which can be seen as follows.

1. In the time interval $(-\delta_1, 0)$, $u(t) = 0$ by definition. Therefore $x_3 = 0$ by (45-a) and $x_4 = 1$ by (45-b). This implies that $\bar{g}(z, y, 0, 1) = \frac{-y}{y}$. Defining $\bar{g}(z, 0, 0, 1) = -1$ makes $\bar{g}(z, y, 0, 1)$ continuous as a function of y . This also makes $f_1(t, w)$ and $f_2(t, w)$ well defined.

2. In the time interval $[0, b)$, $u(t) > 0$. Therefore $x_3 = 1$. Hence

$$\bar{g}(z, y, 1, x_4) = \frac{\frac{k}{\mu_0} \frac{cM_s}{a} \frac{\partial \mathcal{L}}{\partial z}(z) + x_4 y}{\frac{k}{\mu_0} - x_4 y \alpha - \frac{k}{\mu_0} \alpha \frac{cM_s}{a} \frac{\partial \mathcal{L}}{\partial z}(z)}.$$

We have to ensure that f is well defined $\forall (z, y) \in (-\infty, \infty)$

$$\times (-\epsilon_1, \frac{k}{\mu_0} \frac{M_s(1-c)}{3a} + \epsilon_1).$$

(a) $x_4 = 0$ implies $\bar{g}(z, y, 1, 0) = \frac{\frac{k}{\mu_0} \frac{cM_s}{a} \frac{\partial \mathcal{L}}{\partial z}(z)}{\frac{k}{\mu_0} - \frac{k}{\mu_0} \alpha \frac{cM_s}{a} \frac{\partial \mathcal{L}}{\partial z}(z)}$. By (40) and (41), the denominator of \bar{g} is always positive $\forall (z, y) \in (-\infty, \infty) \times (-\epsilon_1, \frac{k}{\mu_0} \frac{M_s(1-c)}{3a} + \epsilon_1)$. Hence $f_1(t, w)$ and $f_2(t, w)$ are well-defined.

(b) $x_4 = 1$ implies $\bar{g}(z, y, 1, 1) = \frac{\frac{k}{\mu_0} \frac{cM_s}{a} \frac{\partial \mathcal{L}}{\partial z}(z) + y}{\frac{k}{\mu_0} - y \alpha - \frac{k}{\mu_0} \alpha \frac{cM_s}{a} \frac{\partial \mathcal{L}}{\partial z}(z)}$. By (40), the denominator of \bar{g} is always positive $\forall (z, y) \in (-\infty, \infty) \times (-\epsilon_1, \frac{k}{\mu_0} \frac{M_s(1-c)}{3a} + \epsilon_1)$ if we choose ϵ_1 small enough. Hence $f_1(t, w)$ and $f_2(t, w)$ are well-defined.

• Existence of a solution

We first show existence of a solution at $t = 0$. To prove existence, we show that $f(\cdot, \cdot)$ satisfies Carathéodory's conditions.

1. We have already seen that $f(\cdot, \cdot)$ is well defined on D . We now check whether $f_1(t, w)$ and $f_2(t, w)$ are continuous functions of w for all $t \in (-\delta_1, b)$.

(a) For $t \in (-\delta_1, 0)$, $f_1(t, w)$, $f_2(t, w)$ are both zero and hence trivially continuous in w .

(b) At $t \geq 0$, $x_3 = 1$. To check whether $f_1(t, w)$, $f_2(t, w)$ are continuous with respect to w , we only need to check whether $\bar{g}_t(\cdot)$ is continuous as a function of w .

$$\bar{g}_t(w) = \frac{\frac{k}{\mu_0} \frac{cM_s}{a} \frac{\partial \mathcal{L}}{\partial z}(z) + x_4 y}{\frac{k}{\mu_0} - x_4 y \alpha - \frac{k}{\mu_0} \alpha \frac{cM_s}{a} \frac{\partial \mathcal{L}}{\partial z}(z)}.$$

In the above expression, the only term that could possibly be discontinuous as a function of w is

$$h(w) \triangleq x_4 y.$$

By (45-b), if $y \geq 0$, $x_4 = 1$ and if $y < 0$, $x_4 = 0$ (because $x_3 = 1$).

Therefore

$$\lim_{y \rightarrow 0^+} h(w) = \lim_{y \rightarrow 0^-} h(w) = 0.$$

Hence, $f(\cdot, \cdot)$ satisfies Carathéodory's first condition for $t \in (-\delta_1, b)$.

2. Next we need to check whether the function $f(t, w)$ is measurable in t for each w .

- (a) For $t \in (-\delta_1, 0)$, $u(t) = 0$. Therefore for each w , $f(\cdot, w)$ is a continuous function of time t trivially.
- (b) For $t \geq 0$, $u(t) > 0$. This implies by (45-a) that $x_3 = 1$. Hence for each w , x_4 is also fixed. Therefore for each w

$$f_1(t, w) = K_1(w) u(t),$$

$$f_2(t, w) = K_2(w) u(t),$$

where $K_1(\cdot)$, $K_2(\cdot)$ are functions of w , implying that $f(t, w)$ is a continuous function of t .

Hence, $f(\cdot, \cdot)$ satisfies Carathéodory's second condition for $t \in (-\delta_1, b)$.

3. For each $t \in (-\delta_1, b)$, $\bar{g}(\cdot)$ is continuous as a function of w . The denominator of $\bar{g}(\cdot)$ is bounded both above and below. The lower bound on $\bar{g}(\cdot)$ in D is

$$A = \frac{k}{\mu_0} \left(1 - \frac{\alpha M_s}{3a} \right) - \alpha \epsilon_1. \quad (47)$$

For all $(z, y) \in (-\infty, \infty) \times (-\epsilon_1, \frac{k}{\mu_0} \frac{M_s(1-c)}{3a} + \epsilon_1)$; $\frac{\partial \mathcal{L}}{\partial z}(z) \leq \frac{1}{3}$ implying

$$|\bar{g}(t, w)| \leq \frac{1}{A} \left(\frac{k}{\mu_0} \frac{M_s}{3a} + \epsilon_1 \right).$$

Thus $g(\cdot, \cdot)$ is uniformly bounded in D . By (43-b) and (44-b), $f(\cdot, \cdot)$ is also uniformly bounded in D . Hence $f(\cdot, \cdot)$ satisfies Carathéodory's third condition for $(t, w) \in D$.

Hence by Theorem B.1.1, for $(t_0, w_0) = (0, (0, 0))$, there exists a solution through (t_0, w_0) .

• **Extension of the solution** (We now extend the solution through (t_0, w_0) , so that it is defined for all $t \in [0, b)$.)

According to Theorem B.2.1, the solution can be extended until it reaches the boundary of D . As $f(t, z, y)$ is defined $\forall z$, we only need to ensure that $y(t)$ does not reach the boundary of the set $(-\epsilon_1, \frac{k M_s (1-c)}{3 \mu_0 a} + \epsilon_1]$. We show this by proving that $0 \leq y(t) \leq \frac{k M_s (1-c)}{3 \mu_0 a} \forall t \in [0, b)$. This implies that the solution can be extended to the boundary of the time t interval.

1. We know that $y(0) = 0$. We will show that $y(t) > 0 \forall t \in (0, b)$. As $\dot{y}(0_+) > 0$, $\exists b_1 > 0 \ni y(t) > 0 \forall t \in (0, b_1)$. If this were not true then we could form a sequence of time instants $t_k \rightarrow 0 \ni y(t_k) \leq 0$. Then

$$\lim_{t_k \rightarrow 0} \frac{y(t_k) - y(0)}{t_k - 0} = \lim_{t_k \rightarrow 0} \frac{y(t_k) - 0}{t_k} \leq 0$$

which contradicts $\dot{y}(0) > 0$.

Let b_1 denote the largest such time instant such that $y(t) > 0 \forall t \in (0, b_1)$.

Suppose $b_1 < b$. Then $y(b_1) = 0$ by continuity of $y(\cdot)$. At $t = b_1$, $x_3 = 1$ by (45-a) and $x_4 = 0$ by (45-b). Therefore

$$\begin{aligned} \dot{y}(b_1) &= \left(\frac{M_s}{a} \frac{\partial \mathcal{L}}{\partial z}(z) + \frac{\left(\frac{\alpha M_s}{a} \frac{\partial \mathcal{L}}{\partial z}(z) - 1 \right) \frac{k}{\mu_0} \frac{c M_s}{a} \frac{\partial \mathcal{L}}{\partial z}(z)}{\frac{k}{\mu_0} - \frac{k}{\mu_0} \alpha \frac{c M_s}{a} \frac{\partial \mathcal{L}}{\partial z}(z)} \right) u(b_1), \\ &= \left(\frac{M_s}{a} \frac{\partial \mathcal{L}}{\partial z}(z) - \frac{1 - \frac{\alpha M_s}{a} \frac{\partial \mathcal{L}}{\partial z}(z)}{\left(1 - \alpha \frac{c M_s}{a} \frac{\partial \mathcal{L}}{\partial z}(z) \right)} \frac{c M_s}{a} \frac{\partial \mathcal{L}}{\partial z}(z) \right) u(b_1). \end{aligned}$$

By (40) and (41)

$$\frac{1 - \frac{\alpha M_s}{a} \frac{\partial \mathcal{L}}{\partial z}(z)}{1 - c \frac{\alpha M_s}{a} \frac{\partial \mathcal{L}}{\partial z}(z)} < 1. \quad (48)$$

By (42) and (48)

$$\begin{aligned} \dot{y}(b_1) &> \left(\frac{M_s}{a} \frac{\partial \mathcal{L}}{\partial z}(z) - \frac{c M_s}{a} \frac{\partial \mathcal{L}}{\partial z}(z) \right) u(b_1), \\ &= \frac{M_s}{a} \frac{\partial \mathcal{L}}{\partial z}(z) (1 - c) u(b_1), \\ &> 0 \quad \text{by (41)}. \end{aligned}$$

Therefore for some $\epsilon > 0$ sufficiently small (with $\epsilon < b_1$),

$$\begin{aligned}
y(b_1 - \epsilon) &= y(b_1) - \epsilon \dot{y}(b_1) + o(\epsilon^2) \\
&= 0 - \epsilon \dot{y}(b_1) + o(\epsilon^2) \\
&< 0,
\end{aligned}$$

which is a contradiction of the fact that $y(t) > 0 \forall t \in (0, b_1)$.

Hence $y(t) > 0 \forall t \in (0, b)$.

2. We now verify that $y(t) \leq \frac{k}{\mu_0} \frac{M_s(1-c)}{3a}$.

As $u(t) > 0$ for $t \in (0, b)$, $x_3(t) = 1$ by (45-a). We proved that $y(t) > 0$ for $t \in (0, b)$ implying that $x_4(t) = 1$. By expanding the right-hand-sides of (43-b) and (44-b) with $x_3 = 1$ and $x_4 = 1$, we get

$$\dot{z}(t) = \frac{\frac{1}{a} \frac{k}{\mu_0}}{\frac{k}{\mu_0} - \alpha y - \frac{k}{\mu_0} \alpha \frac{c M_s}{a} \frac{\partial \mathcal{L}}{\partial z}(z)} u(t), \quad (49)$$

$$\dot{y}(t) = \frac{\frac{k}{\mu_0} \frac{(1-c) M_s}{a} \frac{\partial \mathcal{L}}{\partial z}(z) - y}{\frac{k}{\mu_0} - \alpha y - \frac{k}{\mu_0} \alpha \frac{c M_s}{a} \frac{\partial \mathcal{L}}{\partial z}(z)} u(t). \quad (50)$$

By substituting (49) into (50) we get

$$\begin{aligned}
y \dot{z} + \frac{1}{a} \frac{k}{\mu_0} \dot{y} &= \frac{k(1-c) M_s}{\mu_0 a} \frac{\partial \mathcal{L}}{\partial z}(z) \dot{z} \\
y \dot{z} + \frac{1}{a} \frac{k}{\mu_0} \frac{dy}{dz} \dot{z} &= \frac{k(1-c) M_s}{\mu_0 a} \frac{\partial \mathcal{L}}{\partial z}(z) \dot{z}.
\end{aligned} \quad (51)$$

Now $\bar{g}(z, y, 1, 1) > 0 \forall (z, y) \in (-\infty, \infty) \times (-\epsilon_1, \frac{k M_s(1-c)}{3 \mu_0 a})$ implying that $\dot{z} > 0 \forall (t, w) \in D$. Therefore (51) can be simplified to

$$y + \frac{1}{a} \frac{k}{\mu_0} \frac{dy}{dz} = \frac{k(1-c)M_s}{\mu_0 a} \frac{\partial \mathcal{L}}{\partial z}(z) \quad (52)$$

The maximum value of $y(\cdot)$ ($= y_{max}$) is when $\frac{dy}{dz} = 0$. Denote the corresponding value of z as $z_{y_{max}}$. Then (52) leads to

$$\begin{aligned} y_{max} &= \frac{k(1-c)M_s}{\mu_0} \frac{\partial \mathcal{L}}{\partial z}(z_{y_{max}}) \\ &\leq \frac{k(1-c)M_s}{\mu_0} \frac{1}{3a}. \end{aligned} \quad (53)$$

Therefore the solution can be extended in time to the boundary of $[0, b)$. In the course of continuing the solutions, we also proved that $(M_s \mathcal{L}(z(t)) - x_2(t)) > 0 \forall t \in (0, b)$.

• **Uniqueness**(We show the uniqueness of the solution.)

As $u(t) > 0$ for $t \geq 0$, $x_3 = 1$. As $y > 0$ for $t > 0$, $x_4 = 1$ for $t > 0$. We concentrate on this case below. At $t = 0$, $x_4 = 0$ and the Lipschitz constants obtained in the following analysis can again be used to show uniqueness.

A defined by (47) is a lower bound for the denominator of $f_1(t, w)$. With $w_1 = (z_1, y_1)$ and $w_2 = (z_2, y_2)$, we have

$$|f_1(t, w_1) - f_1(t, w_2)| \leq \frac{\frac{1}{a} \frac{k}{\mu_0}}{A^2} \left(\frac{k}{\mu_0} \frac{\alpha c M_s}{a} \left| \frac{\partial \mathcal{L}}{\partial z}(z_1) - \frac{\partial \mathcal{L}}{\partial z}(z_2) \right| + \alpha |y_1 - y_2| \right) u(t). \quad (54)$$

As $\frac{\partial \mathcal{L}}{\partial z}(z)$ is a smooth function of z , by Theorem B.3.1 \exists a non-negative constant $K \ni$

$$\left| \frac{\partial \mathcal{L}}{\partial z}(z_1) - \frac{\partial \mathcal{L}}{\partial z}(z_2) \right| \leq K |z_1 - z_2| \quad \forall z_1, z_2 \in (-\infty, \infty).$$

Hence

$$\begin{aligned}
|f_1(t, w_1) - f_1(t, w_2)| &\leq \frac{\frac{1}{a} \frac{k}{\mu_0}}{A^2} \left(\frac{k}{\mu_0} \frac{\alpha c M_s}{a} K |z_1 - z_2| + \alpha |y_1 - y_2| \right) u(t) \\
&\leq \frac{\frac{1}{a} \frac{k}{\mu_0}}{A^2} \left(\frac{k}{\mu_0} \frac{c \alpha M_s}{a} K \|w_1 - w_2\| + \alpha \|w_1 - w_2\| \right) \\
&\leq \frac{\frac{1}{a} \frac{k}{\mu_0}}{A^2} \left(\frac{k}{\mu_0} \frac{c \alpha M_s}{a} K + \alpha \right) \|w_1 - w_2\| u(t). \tag{55}
\end{aligned}$$

Now

$$\begin{aligned}
|f_2(t, w_1) - f_2(t, w_2)| &\leq \frac{u(t)}{A^2} \left(\left(\frac{k}{\mu_0} \right)^2 \frac{(1-c)M_s}{a} \left| \frac{\partial \mathcal{L}}{\partial z}(z_1) - \frac{\partial \mathcal{L}}{\partial z}(z_2) \right| \right. \\
&\quad \left. + \frac{k}{\mu_0} |y_1 - y_2| + \frac{k}{\mu_0} \frac{\alpha M_s}{a} \left| y_1 \frac{\partial \mathcal{L}}{\partial z}(z_2) - y_2 \frac{\partial \mathcal{L}}{\partial z}(z_1) \right| \right).
\end{aligned}$$

We can write

$$\begin{aligned}
y_1 \frac{\partial \mathcal{L}}{\partial z}(z_2) - y_2 \frac{\partial \mathcal{L}}{\partial z}(z_1) &= y_1 \frac{\partial \mathcal{L}}{\partial z}(z_2) - y_1 \frac{\partial \mathcal{L}}{\partial z}(z_1) - y_1 \frac{\partial \mathcal{L}}{\partial z}(z_1) - y_2 \frac{\partial \mathcal{L}}{\partial z}(z_1) \\
&= y_1 \left(\frac{\partial \mathcal{L}}{\partial z}(z_2) - \frac{\partial \mathcal{L}}{\partial z}(z_1) \right) + (y_1 - y_2) \frac{\partial \mathcal{L}}{\partial z}(z_1)
\end{aligned}$$

As $|y_1| \leq \frac{k(1-c)M_s}{\mu_0 3a}$ and $\frac{\partial \mathcal{L}}{\partial z}(z_1) \leq \frac{1}{3}$ for all $(t, z_1, y_1) \in D$.

$$\begin{aligned}
|f_2(t, w_1) - f_2(t, w_2)| &\leq \frac{u(t)}{A^2} \frac{k}{\mu_0} \left(\frac{k}{\mu_0} \frac{(1-c)M_s}{a} K |z_1 - z_2| + |y_1 - y_2| \right. \\
&\quad \left. + \frac{\alpha M_s}{a} \left(\frac{k(1-c)M_s}{\mu_0 3a} K |z_1 - z_2| + \frac{1}{3} |y_1 - y_2| \right) \right) \\
&= \left(\left(\frac{k}{\mu_0} \frac{(1-c)M_s}{a} K + \frac{\alpha M_s}{a} \frac{k(1-c)M_s}{\mu_0 3a} K \right) |z_1 - z_2| \right. \\
&\quad \left. + \left(1 + \frac{\alpha M_s}{3a} \right) |y_1 - y_2| \right) \frac{u(t)}{A^2} \frac{k}{\mu_0}
\end{aligned}$$

$$\begin{aligned}
&\leq \left(\left(\frac{k(1-c)M_s}{\mu_0 a} K + \frac{\alpha M_s k(1-c)M_s}{a \mu_0} \frac{M_s}{3a} K \right) \|w_1 - w_2\| \right. \\
&\quad \left. + \left(1 + \frac{\alpha M_s}{3a} \right) \|w_1 - w_2\| \right) \frac{u(t) k}{A^2 \mu_0} \\
&= \left(\frac{k(1-c)M_s}{\mu_0 a} K + \frac{\alpha M_s k(1-c)M_s}{a \mu_0} \frac{M_s}{3a} K \right. \\
&\quad \left. + 1 + \frac{\alpha M_s}{3a} \right) \|w_1 - w_2\| \frac{u(t) k}{A^2 \mu_0}
\end{aligned}$$

By (54) and (56)

$$\|f(t, w_1) - f(t, w_2)\| \leq B \|w_1 - w_2\| u(t) \quad (56)$$

where B is some positive constant. Hence by Theorem B.3.2, there exists atmost one solution in D .

For inputs $u(\cdot)$ with $u(t) < 0$ for $t \in (0, b)$, the same proof can be repeated to arrive at the conclusion that $(M_s \mathcal{L}(z(t)) - x_2(t)) < 0 \forall t \in (0, b)$.

□

The following corollary continues the ideas contained in Theorem 2.2.1

Corollary 2.2.1 *Suppose the parameters satisfy (40) - (42). If $u(t) > \epsilon >> 0$ for $t \in (0, b)$ then as $b \rightarrow \infty$, $x_2(t) \rightarrow M_s$.*

Proof

We again perform a change of co-ordinates $(x_1, x_2) \mapsto (z, y)$. By (43-b)

$$\begin{aligned}
\dot{z}(t) &= \frac{1 + \alpha \bar{g}(z, y, x_3, x_4)}{a} u \\
&> \frac{1}{a} u(t) \quad (57)
\end{aligned}$$

$$\begin{aligned}
&> \frac{\epsilon}{a} \quad (58)
\end{aligned}$$

where $\bar{g}(z, y, x_3, x_4)$ is given by (46) and x_3, x_4 are defined by (45-a) and (45-b) respectively. Inequality (58) shows that $z(\cdot) \rightarrow \infty$ as $b \rightarrow \infty$. Hence it is sufficient to study the behaviour of y as a function of z . It was shown in the proof of Theorem 2.2.1 that the evolution of y as a function of z satisfies

$$y + \frac{1}{a} \frac{k}{\mu_0} \frac{dy}{dz} = \frac{k(1-c)M_s}{\mu_0 a} \frac{\partial \mathcal{L}}{\partial z}(z) \quad (59)$$

The initial condition for the above differential equation is $y(z=0) = 0$. Define

$$v(z) = \frac{k(1-c)M_s}{\mu_0 a} \frac{\partial \mathcal{L}}{\partial z}(z)$$

Clearly $v(z) > 0 \forall z$. Employing Laplace transforms we have

$$Y(s) = \frac{V(s)}{\frac{k}{\mu_0} s + 1},$$

where the Laplace transform of $v(z)$, $y(z)$ are denoted as $V(s)$ and $Y(s)$ respectively. $V(s)$ exists because by definition of the Laplace transform

$$V(s) = \int_0^{\infty} v(z) \exp(-zs) dz,$$

and $v(z)$ is an integrable function of z (in fact, $\int_0^{\infty} v(z) dz = M_s$). By the Final-value theorem for Laplace Transforms [30],

$$\lim_{z \rightarrow \infty} y(z) = \lim_{s \rightarrow 0} sY(s).$$

Therefore,

$$\lim_{z \rightarrow \infty} y(z) = \lim_{s \rightarrow 0} \frac{sV(s)}{\frac{k}{\mu_0} s + 1}$$

Now (by another application of the Final value theorem for Laplace Transforms)

$$\begin{aligned}
\lim_{s \rightarrow 0} sV(s) &= \lim_{z \rightarrow \infty} v(z) \\
&= \lim_{z \rightarrow \infty} \frac{k(1-c)}{\mu_0} \frac{dM_{an}}{dz} \\
&= 0.
\end{aligned} \tag{60}$$

Hence,

$$\lim_{z \rightarrow \infty} y(z) = 0.$$

We conclude that $x_2(t) \rightarrow M_s$ as $t \rightarrow \infty$.

□

Suppose that an input $u(t) > 0$ for $t \in [0, b)$ has been applied to the system (36-a - 37-b). Let

$$x_0 = (x_{1_0}, x_{2_0}) = \lim_{t \rightarrow b} (x_1, x_2)(t). \tag{61}$$

x_0 is well-defined because of Theorem B.2.1. Define the set \mathcal{O}_1 as

$$\mathcal{O}_1 = \bigcup_{t \in (0, b)} x(t). \tag{62}$$

where $w(\cdot)$ is the solution of (36-a - 38). Define (Figure 2.2):

$$u(b) = \lim_{t \rightarrow b} u(t) \tag{63}$$

$$u_1(t) = -u(b - t) \quad \text{for } t \in [0, b]. \tag{64}$$

Let the initial condition be x_0 as defined in (61). Then the next theorem claims that there exists a time $0 < b_1 < b$ such that $x_2(b_1) = M_s \mathcal{L}(\frac{x_1(b_1) + \alpha x_2(b_1)}{a})$. In other words, the solution trajectory intersects with the anhyseretic curve in the (x_1, x_2) -plane at time $b_1 < b$.

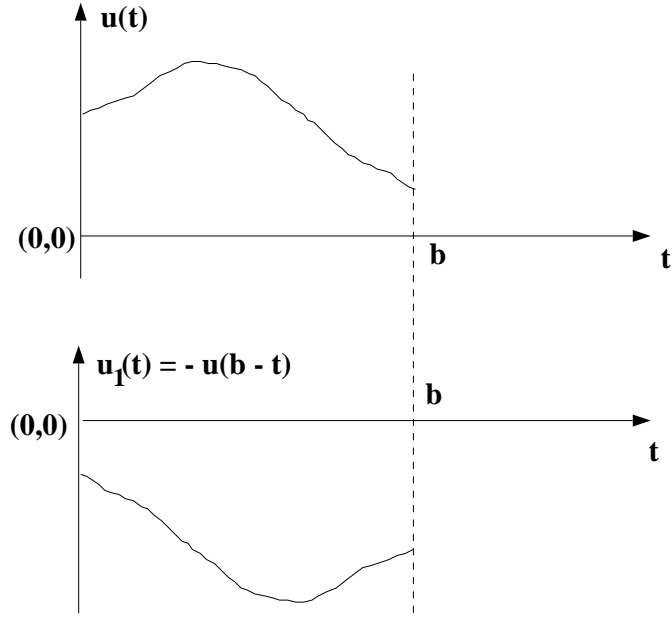


Figure 2.2: Sample signals $u(\cdot)$ and $u_1(\cdot)$.

Theorem 2.2.2 Consider the system of equations (36-a - 37-b). Let the initial condition $(x_1, x_2)(t = 0) = (x_{1_0}, x_{2_0})$ where (x_{1_0}, x_{2_0}) is defined by (61). Let the parameters satisfy (40 - 42). Let $u(t)$ be a continuous function of t with $u(t) > 0$ for $t \in [0, b)$, and $u_1(t)$ be defined by (63 - 64). If $u_1(t)$ is the input to the system (36-a - 37-b) for $t \in [0, b]$, then $\exists b_1 > 0$ such that $b_1 < b$ and $x_2(b_1) = M_s \mathcal{L}\left(\frac{x_1(b_1) + \alpha x_2(b_1)}{a}\right)$.

Proof

As before, we make a change of co-ordinates from (x_1, x_2) to (z, y) where

$$z = \frac{x_1 + \alpha x_2}{a},$$

$$y = M_s \mathcal{L}(z) - x_2.$$

The Jacobian of this transform is non-singular $\forall (x_1, x_2) \in \mathbb{R}^2$ and hence the

results on existence, extension and uniqueness of solutions to the state equations in the transformed space are applicable to the equations in the original state space. The state equations $\dot{w} = f(t, w)$ in terms of $w = (z, y)$ are given by (43-b - 45-b). The initial conditions in the transformed co-ordinates are

$$w_0 = (z_0, y_0) = \left(\frac{x_{10} + \alpha x_{20}}{a}, M_s \mathcal{L}(z_0) - x_{20} \right).$$

Let $D = \underbrace{(-\delta_1, b + \delta_1)}_t \times \underbrace{(-\infty, \infty)}_z \times \underbrace{\left(0, \frac{k}{\mu_0} \frac{M_s(1-c)}{3a} + \epsilon_1\right)}_y$, where δ_1, ϵ_1 are sufficiently small positive numbers.

We have to re-define $u_1(\cdot)$ so that it is well-defined over its domain $(-\delta_1, b + \delta_1)$. This can be easily accomplished by defining $u_1(t) = 0$ for $t \in (-\delta_1, 0) \cup (b, b + \delta_1)$. Then $f_1(t, w), f_2(t, w)$ exist on D which can be seen as follows.

1. In the time interval $(-\delta_1, 0) \cup (b, b + \delta_1)$, $u_1(t) = 0$ by definition. Therefore $x_3 = 0$ by (45-a) and $x_4 = 1$ by (45-b). This implies that $\bar{g}(z, y, 0, 1) = \frac{-y}{y}$. Defining $\bar{g}(z, 0, 0, 1) = -1$ makes $\bar{g}(z, y, 0, 1)$ continuous as a function of y . This also makes $f_1(t, w)$ and $f_2(t, w)$ well defined.
2. In the time interval $[0, b]$, $u_1(t) > 0$. Therefore $x_3 = -1$. Hence

$$\bar{g}(z, y, 1, x_4) = \frac{\frac{k}{\mu_0} \frac{cM_s}{a} \frac{\partial \mathcal{L}}{\partial z}(z) - x_4 y}{\frac{k}{\mu_0} + x_4 y \alpha - \frac{k}{\mu_0} \alpha \frac{cM_s}{a} \frac{\partial \mathcal{L}}{\partial z}(z)}.$$

We have to ensure that f is well defined $\forall (z, y) \in (-\infty, \infty) \times \left(0, \frac{k}{\mu_0} \frac{M_s(1-c)}{3a} + \epsilon_1\right)$.

- (a) $x_4 = 0$ implies $\bar{g}(z, y, -1, 0) = \frac{\frac{k}{\mu_0} \frac{cM_s}{a} \frac{\partial \mathcal{L}}{\partial z}(z)}{\frac{k}{\mu_0} - \frac{k}{\mu_0} \alpha \frac{cM_s}{a} \frac{\partial \mathcal{L}}{\partial z}(z)}$. By (40) and (41), the denominator of \bar{g} is always positive $\forall (z, y) \in (-\infty, \infty) \times \left(0, \frac{k}{\mu_0} \frac{M_s(1-c)}{3a}\right)$. Hence $f_1(t, w)$ and $f_2(t, w)$ are well-defined.

(b) $x_4 = 1$ implies $\bar{g}(z, y, -1, 1) = \frac{\frac{k}{\mu_0} \frac{cM_s}{a} \frac{\partial \mathcal{L}}{\partial z}(z) - y}{\frac{k}{\mu_0} + y\alpha - \frac{k}{\mu_0} \alpha \frac{cM_s}{a} \frac{\partial \mathcal{L}}{\partial z}(z)}$. By (40), the denominator of \bar{g} is always positive $\forall (z, y) \in (-\infty, \infty) \times (0, \frac{k}{\mu_0} \frac{M_s(1-c)}{3a} + \epsilon_1)$. Hence $f_1(t, w)$ and $f_2(t, w)$ are well-defined.

• **Existence of a solution**

We first show existence of a solution at $t = 0$. As in Theorem 2.2.1 to prove existence, we show that $f(\cdot, \cdot)$ satisfies Carathéodory's conditions.

1. We have already seen that $f(\cdot, \cdot)$ is well defined on D . We now check whether $f_1(t, w)$ and $f_2(t, w)$ are continuous functions of w for all $t \in (-\delta_1, b + \delta_1)$.

(a) For $t \in (-\delta_1, 0) \cup (b, b + \delta_1)$, $f_1(t, w)$, $f_2(t, w)$ are both zero and hence trivially continuous in w .

(b) At $t \in [0, b]$, $x_3 = -1$. To check whether $f_1(t, w)$, $f_2(t, w)$ are continuous with respect to w , we only need to check whether $\bar{g}(t, \cdot)$ is continuous as a function of w .

$$\bar{g}_t(w) = \frac{\frac{k}{\mu_0} \frac{cM_s}{a} \frac{\partial \mathcal{L}}{\partial z}(z) - x_4 y}{\frac{k}{\mu_0} + x_4 y \alpha - \frac{k}{\mu_0} \alpha \frac{cM_s}{a} \frac{\partial \mathcal{L}}{\partial z}(z)}.$$

In the above expression, the only term that could possibly be discontinuous as a function of w is

$$h(w) \triangleq x_4 y.$$

By (45-b), if $y \leq 0$, $x_4 = 1$ and if $y > 0$, $x_4 = 0$ (because $x_3 = -1$). Therefore

$$\lim_{y \rightarrow 0^+} h(w) = \lim_{y \rightarrow 0^-} h(w) = 0.$$

Hence, $f(\cdot, \cdot)$ satisfies Carathéodory's first condition for $t \in (-\delta_1, b + \delta_1)$.

2. Next we need to check whether the function $f(t, w)$ is measurable in t for each w .

(a) For $t \in (-\delta_1, 0) \cup (b, b + \delta_1)$, $u_1(t) = 0$. Therefore for each w , $f(\cdot, w)$ is a continuous function of time t trivially.

(b) For $t \in [0, b]$, $u_1(t) < 0$. This implies by (45-a) that $x_3 = -1$. Hence for each w , x_4 is also fixed. Therefore for each w

$$\begin{aligned} f_1(t, w) &= L_1(w) u_1(t), \\ f_2(t, w) &= L_2(w) u_1(t), \end{aligned}$$

where $L_1(\cdot)$, $L_2(\cdot)$ are only functions of w . This implies that $f(t, w)$ is a continuous function of t .

Hence, $f(\cdot, \cdot)$ satisfies Carathéodory's second condition for $t \in (-\delta_1, b + \delta_1)$.

3. For each $t \in (-\delta_1, b + \delta_1)$, $\bar{g}(\cdot)$ is continuous as a function of w . The denominator of $\bar{g}(\cdot)$ is bounded both above and below. The lower bound on $\bar{g}(\cdot)$ in D is

$$A = \frac{k}{\mu_0} \left(1 - \frac{c \alpha M_s}{3 a} \right).$$

For all $(z, y) \in (-\infty, \infty) \times (0, \frac{k}{\mu_0} \frac{M_s(1-c)}{3a} + \epsilon_1)$; $\frac{\partial \mathcal{L}}{\partial z}(z) \leq \frac{1}{3}$ implying

$$|\bar{g}(t, w)| \leq \frac{1}{A} \left(\frac{k}{\mu_0} \frac{c M_s}{3 a} \right) \sup_{t \in (-\delta_1, b)} u_1(t).$$

Thus $g(\cdot, \cdot)$ is uniformly bounded in D . By (43-b) and (44-b), $f(\cdot, \cdot)$ is also uniformly bounded in D . Hence $f(\cdot, \cdot)$ satisfies Carathéodory's third condition for $(t, w) \in D$.

Hence by Theorem B.1.1, for $(t_0, w_0) = (0, (z_0, y_0))$, there exists a solution through (t_0, w_0) .

• **Extension of the solution** (We now extend the solution through (t_0, w_0) , so that it is defined for all $t \in [0, b + \delta_1)$.)

According to Theorem B.2.1, the solution can be extended until it reaches the boundary of D . It obviously cannot reach the boundary of D in the z variable. We show that the solution reaches the boundary of D in the y variable.

As $y(0) > 0$, $\exists \tau > 0 \ni y(t) > 0 \forall t \in [0, \tau)$. Suppose such a τ does not exist. Then we can choose a sequence $t_k \rightarrow 0 \ni y(t_k) \leq 0$ implying that $y(0) \leq 0$ (by continuity of $(z, y)(\cdot)$ at $t = 0$) which is a contradiction. Define

$$b_1 = \sup \{ \tau \mid y(\tau) > 0 \text{ and } \tau \leq b \}. \quad (65)$$

Now one of two cases is possible:

- $b_1 < b$. This implies that at $t = b_1$, $y(b_1) = 0$. If this is not true and $y(b_1) > 0$, then we can choose $\epsilon > 0$ sufficiently small such that $y(b_1 + \epsilon) > 0$ contradicting (65).
- $b_1 = b$. We show that this is not possible.

If $b_1 = b$ then clearly the solution can be extended to $[0, b)$. As the map $\psi : (x_1, x_2) \mapsto (z, y)$ is a diffeomorphism, we consider the behaviour of the solution in terms of the variables $x = (x_1, x_2)$ for simplicity of analysis. Define the set \mathcal{O}_2 as

$$\mathcal{O}_2 = \bigcup_{t \in (0, b)} x(t).$$

Then we can make the following observations.

1. At time $t = b$

$$x_1(t = b) = 0. \quad (66)$$

2. The slope of the curves \mathcal{O}_1 and \mathcal{O}_2 in the (x_1, x_2) -plane is always positive (refer to Figure 2.3). The proof is as follows. By (36-a - 38)

$$\frac{dx_2}{dx_1}(x) = \frac{\frac{kx_3}{\mu_0} \frac{cM_s}{a} \frac{\partial \mathcal{L}}{\partial z}(z) + x_4 M_s \left(\mathcal{L}(z) - \frac{x_2}{M_s} \right)}{\frac{kx_3}{\mu_0} - x_4 M_s \left(\mathcal{L}(z) - \frac{x_2}{M_s} \right) \alpha - \frac{kx_3}{\mu_0} \alpha \frac{cM_s}{a} \frac{\partial \mathcal{L}}{\partial z}(z)}. \quad (67)$$

where $\mathcal{L}(z) = \coth(z) - \frac{1}{z}$ and $\frac{\partial \mathcal{L}}{\partial z}(z) = -\operatorname{cosech}^2(z) + \frac{1}{z^2}$. We have the following cases to consider:

- (a) $x_3 = 1$ and $x_4 = 0$.

By (40) the denominator is positive (proved in Theorem 2.2.1 and by (65)). The first part of the numerator of the right hand side of (67), is non-negative $\forall z$. Thus $\frac{dx_2}{dx_1}(x) > 0$ for this case.

- (b) $x_3 = 1$ and $x_4 = 1$.

The observations of the previous case hold in this case also. The second term is also non-negative by 37-b. Thus $\frac{dx_2}{dx_1}(x) > 0$ for this case also.

- (c) $x_3 = -1$. For this case, we can take a common factor of -1 in both the numerator and the denominator and reach the same conclusion as the previous two items.

Hence

$$\frac{dx_2}{dx_1}(x) > 0$$

for x belonging to the solution sets \mathcal{O}_1 and \mathcal{O}_2 .

3. For all $x \in \mathcal{O}_1$,

$$0 < \frac{\frac{cM_s}{a} \frac{\partial \mathcal{L}}{\partial z}(z)}{1 - \alpha \frac{cM_s}{a} \frac{\partial \mathcal{L}}{\partial z}(z)} < \frac{\frac{k}{\mu_0} \frac{cM_s}{a} \frac{\partial \mathcal{L}}{\partial z}(z) + M_s \left(\mathcal{L}(z) - \frac{x_2}{M_s} \right)}{\frac{k}{\mu_0} - M_s \left(\mathcal{L}(z) - \frac{x_2}{M_s} \right) \alpha - \frac{k}{\mu_0} \alpha \frac{cM_s}{a} \frac{\partial \mathcal{L}}{\partial z}(z)}.$$

The first inequality is due to the assertion of the previous item.

4. The point (x_{1_0}, x_{2_0}) belongs to both \mathcal{O}_1 and \mathcal{O}_2 .

5. The projection of both the sets \mathcal{O}_1 and \mathcal{O}_2 on the x_1 axis is the set $[0, x_{1_0}]$. This is a consequence of (36-a) and the definition of the input u_1 .

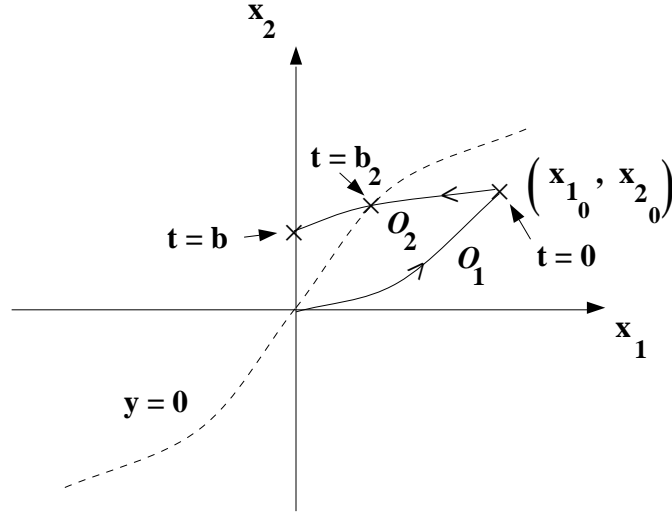


Figure 2.3: Figure for the proof of Theorem 2.2.2

Items 2–5 imply that the curve \mathcal{O}_2 lies above the curve \mathcal{O}_1 in the (x_1, x_2) -plane except at the point (x_{1_0}, x_{2_0}) (see Figure 2.3). Item 1 then implies

that the curve \mathcal{O}_2 intersects with the anhysteretic curve $y = 0$ in the first quadrant of the (x_1, x_2) -plane. This means that there exists a time $b_2 < b$ such that $y(t = b_2) = 0$ and $y(t) < 0$ for $t \in (b_2, b]$. Hence the hypothesis that $b_1 = b$ is not possible.

Thus we have shown that $\exists 0 < b_1 < b$ such that $y(b_1) = 0$.

- **Uniqueness**(We show the uniqueness of the solution.)

The state equations for the time interval $[0, b_1]$ are:

$$\dot{z}(t) = \frac{\frac{1}{a} \frac{k}{\mu_0}}{\frac{k}{\mu_0} - \alpha \frac{k}{\mu_0} \frac{cM_s}{a} \frac{\partial \mathcal{L}}{\partial z}(z)} u_1(t), \quad (68-a)$$

$$\dot{y}(t) = \frac{\frac{M_s}{a} \frac{k(1-c)}{\mu_0} \frac{\partial \mathcal{L}}{\partial z}(z)}{\frac{k}{\mu_0} - \alpha \frac{kx_3}{\mu_0} \frac{cM_s}{a} \frac{\partial \mathcal{L}}{\partial z}(z)} u_1(t). \quad (68-b)$$

We now show that the solution of (68-a) and (68-b) for $t \in [0, b_1]$ is unique. Denote $\dot{z} = f_1(t, w)$ and $\dot{y} = f_2(t, w)$ where $f_1(t, w)$ and $f_2(t, w)$ are defined by the right-hand-sides of (68-a) and (68-b) respectively. As $u(t) < 0$ for $t \geq 0$, $x_3 = -1$. As $y > 0$ for $t \in [0, b_1]$, $x_4 = 0$. With $w_1 = (z_1, y_1)$ and $w_2 = (z_2, y_2)$, we have

$$|f_1(t, w_1) - f_1(t, w_2)| \leq \frac{1}{a} \frac{k}{\mu_0} \left(\frac{k}{\mu_0} \frac{\alpha c M_s}{a} \left| \frac{\partial \mathcal{L}}{\partial z}(z_1) - \frac{\partial \mathcal{L}}{\partial z}(z_2) \right| + \alpha |y_1 - y_2| \right) u(t). \quad (69)$$

As $\frac{\partial \mathcal{L}}{\partial z}(z)$ is a smooth function of z , by Theorem B.3.1 \exists a non-negative constant $K \ni$

$$|f_1(t, w_1) - f_1(t, w_2)| \leq \frac{k}{A^2} \frac{k}{\mu_0} \frac{\alpha c M_s}{a} K |z_1 - z_2| u(t)$$

$$\leq \frac{\frac{k}{\mu_0}}{A^2} \frac{k}{\mu_0} \frac{c\alpha M_s}{a} K \|w_1 - w_2\| u(t) \quad (70)$$

Now

$$|f_2(t, w_1) - f_2(t, w_2)| \leq \frac{u(t)}{A^2} \left(\frac{k}{\mu_0}\right)^2 \frac{(1-c)M_s}{a} \left| \frac{\partial \mathcal{L}}{\partial z}(z_1) - \frac{\partial \mathcal{L}}{\partial z}(z_2) \right|.$$

Therefore

$$\begin{aligned} |f_2(t, w_1) - f_2(t, w_2)| &\leq \frac{u(t)}{A^2} \left(\frac{k}{\mu_0}\right)^2 \frac{(1-c)M_s}{a} K |z_1 - z_2| \\ &\leq \frac{u(t)}{A^2} \left(\frac{k}{\mu_0}\right)^2 \frac{(1-c)M_s}{a} K \|w_1 - w_2\| \end{aligned}$$

By (70) and (71)

$$\|f(t, w_1) - f(t, w_2)\| \leq B \|w_1 - w_2\| u(t) \quad (71)$$

where B is some positive constant. Hence by Theorem B.3.2, there exists atmost one solution in D .

□

We now study the system described by Equations (36-a - 37-b), together with the input given by

$$u(t) = U \cos(\omega t). \quad (72)$$

The periodic nature of the Ω limit set of the solution to the system of Equations (36-a - 37-b) and (72) is proved in 4 steps. Using Theorems 2.2.1 and 2.2.2 we show that:

1. Starting from $(x_1, x_2) = (0, 0)$, $x_2(t)$ increases for $t \in [0, \frac{\pi}{2\omega}]$, but lies below the anhysteretic magnetization curve.
2. For $t \in [\frac{\pi}{2\omega}, \frac{3\pi}{2\omega}]$, $x_2(t)$ first intersects the anhysteretic curve, then lies above it.
3. For $t \in [\frac{3\pi}{2\omega}, \frac{5\pi}{2\omega}]$, $x_2(t)$ first intersects the anhysteretic curve, then lies below it.

By repeating the analysis in Steps 2, 3, we can conclude that the solution trajectory of the system lies within the compact set $[-\frac{b}{\omega}, \frac{b}{\omega}] \times [-M_s, M_s]$.

4. We then look at $\{x_2(\frac{2n\pi}{\omega})\}$; $n = 0, 1, 2, \dots$. This sequence of points lie on the x_2 axis ($x_1 = 0$ line). We then show that the sequence has a unique accumulation point. This shows that the Ω limit set is a periodic orbit in the (x_1, x_2) -plane. Since x_3 and x_4 depend on x_1, x_2 , we conclude that the system of Equations (36-a - 72) with the origin as initial condition, have asymptotic periodic solutions.

2.2.1 Analysis of the Model for $t \in [0, \frac{5\pi}{2\omega}]$

Lemma 2.2.1 *Consider the system described by Equations (36-a - 37-b) with the input given by (72), and $(x_1(0), x_2(0)) = (0, 0)$. Suppose the parameters satisfy conditions (40) - (42). In the time interval $[0, \frac{\pi}{2\omega}]$, there exists a unique solution and it satisfies the condition $|x_2(t)| < M_s$.*

Proof

Choosing $b = \frac{\pi}{2\omega}$, we apply Theorem 2.2.1 as the initial condition is on the anhysteretic curve and $u(\cdot) > 0$ in the time interval $(0, \frac{\pi}{2\omega})$. The conclusion of Theorem 2.2.1 and 2.2.1 implies that $x_2(t) < M_s \forall t \in [0, \frac{\pi}{2\omega}]$.

□

By Theorem B.2.1 the trajectory reaches the boundary of the rectangle D in time. Hence

$$x\left(\frac{\pi}{2\omega}\right) = (x_1, x_2)\left(\frac{\pi}{2\omega}\right) \quad (73)$$

$$= \lim_{t \rightarrow \frac{\pi}{2\omega}} (x_1, x_2)(t). \quad (74)$$

is well-defined.

Lemma 2.2.2 *Consider the system described by Equations (36-a - 37-b) with the input given by (72), and $(x_1(0), x_2(0)) = (0, 0)$. Suppose the parameters satisfy conditions (40 - 42). In the time interval $[\frac{\pi}{2\omega}, \frac{3\pi}{2\omega}]$, there exists a unique solution and it satisfies the condition $|x_2(t)| < M_s$.*

Proof

Let $\tau = t - \frac{\pi}{2\omega}$ and $\epsilon = t$. Define $u_1(\tau) = U \cos(\omega t)$ for $t \in [\frac{\pi}{2\omega}, \frac{\pi}{\omega}]$, and $u(\epsilon) = U \cos(\omega t)$ for $t \in [0, \frac{\pi}{2\omega}]$. If the input $u_1(\tau)$ is applied to the system (36-a - 37-b) with initial condition $x(\tau = 0) = x(t = \frac{\pi}{2\omega})$ where $x(t = \frac{\pi}{2\omega})$ is given by (74), then the conditions of Theorem 2.2.2 are satisfied (with $u(\epsilon)$ taking the place of $u(t)$). This implies that there exists $0 < t_1^* < \frac{\pi}{2\omega}$ such that $x_2(\tau = t_1^*) = M_s \mathcal{L}\left(\frac{x_1(\tau=t_1^*) + \alpha x_2(\tau=t_1^*)}{a}\right)$.

Let $\mu = t - \frac{\pi}{2\omega} - t_1^*$. Now define $u(\mu) = U \cos(\omega(t))$, for $t \in [\frac{\pi}{2\omega} + t_1^*, \frac{3\pi}{2\omega}]$. Then with initial condition at $x(\mu = 0) = x(\tau = t_1^*)$, the conditions of Theorem 2.2.1 is satisfied. Then the conclusions of Theorem 2.2.1 and its corollary 2.2.1 imply that $x_2(t) < M_s \forall t \in [\frac{\pi}{2\omega}, \frac{3\pi}{2\omega}]$.

□

Again by Theorem B.2.1,

$$x(t = \frac{3\pi}{2\omega}) = (x_1, x_2)(\frac{3\pi}{2\omega}) \quad (75)$$

$$= \lim_{\mu \rightarrow \frac{\pi}{\omega} - t_1^*} (x_1, x_2)(\mu). \quad (76)$$

is well-defined.

Lemma 2.2.3 *Consider the system described by Equations (36-a - 37-b) with input given by (72), and $(x_1(0), x_2(0)) = (0, 0)$. Suppose the parameters satisfy Equations (40 - 40). the time interval $[\frac{3\pi}{2\omega}, \frac{5\pi}{2\omega}]$, there exists a unique solution and it satisfies the condition $|x_2(t)| < M_s$.*

Proof Let $\tau = t - \frac{3\pi}{2\omega}$ and $\epsilon = t - \frac{\pi}{2\omega} - t^*$. Define $u_1(\tau) = U \cos(\omega t)$ for $t \in [\frac{3\pi}{2\omega}, \frac{3\pi}{\omega} + \frac{\pi}{\omega} - t_1^*]$, and $u(\epsilon) = U \cos(\omega t)$ for $t \in [\frac{\pi}{2\omega} + t^*, \frac{\pi}{\omega}]$. If the input $u_1(\tau)$ is applied to the system (36-a - 37-b) with initial condition $x(\tau = 0) = x(t = \frac{3\pi}{2\omega})$ where $x(t = \frac{3\pi}{2\omega})$ is given by (76), then the conditions of Theorem 2.2.2 are satisfied (with $u(\epsilon)$ taking the place of $u(t)$). This implies that there exists $0 < t_2^* < \frac{\pi}{\omega} - t_1^*$ such that $x_2(\tau = t_2^*) = M_s \mathcal{L}(\frac{x_1(\tau=t_2^*) + \alpha x_2(\tau=t_2^*)}{a})$.

Let $\mu = t - \frac{3\pi}{2\omega} - t_2^*$. Now define $u(\mu) = U \cos(\omega(t))$, for $t \in [3\frac{\pi}{2\omega} + t_2^*, \frac{5\pi}{\omega}]$. Then with initial condition at $x(\mu = 0) = x(\tau = t_2^*)$, the conditions of Theorem 2.2.1 is satisfied. Then the conclusions of Theorem 2.2.1 and its corollary 2.2.1 imply that $x_2(t) < M_s \forall t \in [\frac{3\pi}{2\omega}, \frac{5\pi}{2\omega}]$.

□

2.2.2 Proof of Periodic behaviour of the Model for Sinusoidal Inputs

Let us first collect together some important properties of the bulk ferromagnetic hysteresis model.

Property 2.2.1 *Consider the system described by Equations (36-a - 37-b) with input given by (72). If the conditions (40 - 42) are satisfied and $x = (x_1, x_2) = (0, 0)$, then there exists a unique solution to the system.*

Proof

We have already shown that the solution exists and is unique for $t \in [0, \frac{5\pi}{2\omega}]$. By repeating the proofs in Lemmas 2.2.2 and 2.2.3 we can extend the existence and uniqueness of the solution $\forall t \geq 0$.

□

Property 2.2.2 *Consider the system described by Equations (36-a - 37-b) with input given by 72). Suppose (40 - 42) are satisfied and $x = (x_1, x_2) = (0, 0)$. Then along the solution trajectory $x(t) = (x_1, x_2)(t)$,*

$$\frac{dx_2}{dx_1}(x) > 0 \quad (77)$$

Proof

By (36-a - 38),

$$\frac{dx_2}{dx_1}(x) = \frac{\frac{kx_3}{\mu_0} \frac{cM_s}{a} \frac{\partial \mathcal{L}}{\partial z}(z) + x_4 M_s \left(\mathcal{L}(z) - \frac{x_2}{M_s} \right)}{\frac{kx_3}{\mu_0} - x_4 M_s \left(\mathcal{L}(z) - \frac{x_2}{M_s} \right) \alpha - \frac{kx_3}{\mu_0} \alpha \frac{cM_s}{a} \frac{\partial \mathcal{L}}{\partial z}(z)}. \quad (78)$$

where $\mathcal{L}(z) = \coth(z) - \frac{1}{z}$ and $\frac{\partial \mathcal{L}}{\partial z}(z) = -\operatorname{cosech}^2(z) + \frac{1}{z^2}$. We have the following cases to consider:

1. $x_3 = 1$ and $x_4 = 0$.

By (40) the denominator is positive (proved in Theorems 2.2.1 and 2.2.2).

The first part of the numerator of the right hand side of (78), is non-negative $\forall z$. Thus $\frac{dx_2}{dx_1}(x) > 0$ for this case.

2. $x_3 = 1$ and $x_4 = 1$.

The observations of the previous case hold in this case also. The second term is also non-negative by 37-b. Thus $\frac{dx_2}{dx_1}(x) > 0$ for this case also.

3. $x_3 = -1$. For this case, we can take a common factor of -1 in both the numerator and the denominator and reach the same conclusion as the previous two items.

Hence

$$\frac{dx_2}{dx_1}(x) > 0$$

for x belonging to the solution trajectory of (36-a - 38) for periodic inputs if the initial state is at the origin.

along the solution trajectory $x(t) = (x_1, x_2)(t)$.

□

Property 2.2.3 (Anti-symmetry) *Consider Equations (36-a - 37-b), with $u(t) \geq 0 \forall t \geq 0$. Suppose that (40 - 42) are satisfied. Let $y_u(t) = (y_1, y_2)(t, u)$ and $x_u(t) = (x_1, x_2)(t, u)$, denote two solutions with initial conditions $x(0), y(0)$ on the anhysteretic curve. If $y(0) = -x(0)$, then $y_u(t) = -x_{-u}(t)$.*

Proof

Though Theorem 2.2.1 only proved existence and uniqueness of a solution to (36-a - 37-b) for initial state at the origin, the same analysis can be done if the initial state is at any point on the anhysteretic curve. If $x(0), y(0)$ lie on the anhysteretic curve and $y(0) = -x(0)$, then the state equations satisfied by $-y$ and x is the same, and they have the same initial condition.

□

Property 2.2.4 *Consider the system (36-a - 37-b), with input given by (72). Suppose that (40- 42) are satisfied. Let \mathcal{O} be the set of all points on the (x_1, x_2) -plane forming the solution $x(t)$ with initial state at $(0, 0)$. In other words,*

$$\mathcal{O} = \bigcup_{t \geq 0} x(t)$$

If $u(t)$ does not change its sign $\forall t \in [a, b]$ and if $\tilde{x}(a), \check{x}(a) \in \mathcal{O}$ are two initial states of the system with $\tilde{x}_2(a) \geq \check{x}_2(a)$, then $\tilde{x}_2(t) \geq \check{x}_2(t) \forall t \in [a, b]$.

Proof

Suppose for some $t \in [a, b]$, $\tilde{x}_2(t) < \check{x}_2(t)$. Then by continuity of the solution trajectories, $\exists t^* \in (a, t), \exists \tilde{x}_2(t^*) = \check{x}_2(t^*)$. Now $\frac{d\tilde{x}_2}{dx_1}(t^*) = \frac{d\check{x}_2}{dx_1}(t^*)$ from Equation (78). Hence $\forall t \geq t^*$, $\tilde{x}_2(t) = \check{x}_2(t)$. This contradicts our initial assumption.

□

Property 2.2.5 *Consider the system given by Equations (36-a - 37-b), with input given by Equation (72). Suppose that (40 - 42) are satisfied. If $(x_1, x_2)(0) = (0, 0)$, then $|x_2(t)| \leq M_s \forall t \geq 0$. Thus the trajectory lies in the compact region $[-\frac{U}{\omega}, \frac{U}{\omega}] \times [-M_s, M_s]$ in the (x_1, x_2) - plane.*

Proof

By Lemmas 2.2.1 - 2.2.3, we have shown that

$$|x_2(t)| \leq M_s \quad \forall t \in [0, \frac{5\pi}{2\omega}].$$

By repeating the proofs of Lemmas 2.2.2, 2.2.3 for the time periods $[\frac{(2n+1)\pi}{2\omega}, \frac{(2n+3)\pi}{2\omega}]$, $[\frac{(2n+3)\pi}{2\omega}, \frac{(2n+5)\pi}{2\omega}]$ respectively for $n = 0, 1, 2, \dots$, we can conclude that

$$|x_2(t)| \leq M_s \quad \forall t \geq 0.$$

Trivially,

$$|x_1(t)| \leq \frac{U}{\omega} \quad \forall t \geq 0.$$

□

Theorem 2.2.3 *Consider the system given by Equations (36-a - 37-b), with input given by Equation (72). Suppose that the parameters satisfy (40 - 42).*

If $(x_1, x_2)(0) = (0, 0)$, then the Ω -limit set of the system is a periodic orbit of period $\frac{2\pi}{\omega}$.

Proof

Let $\theta = \omega t$, with $\theta + 2\pi$ identified with θ . Then the non-autonomous system given by Equations (36-a - 37-b) with input given by (72), can be transformed into an autonomous one with the auxiliary equation, $\dot{\theta} = \omega$. By Equation (36-a), the trajectory in the (x_1, x_2) - plane intersects transversally with the anhyseretic curve. This is because $\frac{dx_2}{dx_1}$ is well-defined and bounded at the points of intersection of the solution trajectory and the anhyseretic curve (this was seen in the proof of Theorem 2.2.2).

Thus there exists a sequence of intersections $\Pi_1 = p_k$ (Figure 2.2). This sequence has a convergent subsequence $\Gamma_1 = p_{n_k}$ because by Property(2.2.5), it lies in the compact set $[-M_s, M_s]$ on the x_2 axis. Let, $p_{n_k} \rightarrow p^*$. Let $\Pi_2 = p_k \setminus p_{n_k}$. If this sequence is finite, then we have nothing to prove. If however, this sequence is infinite, then it has a convergent subsequence, $\Gamma_2 = p_{m_k}$. If the limit point of this subsequence is also p^* , then again we have nothing to prove. In this case, we proceed further by extracting subsequences until we find one with the limit point $q^* \neq p^*$. Both the points $(0, q^*), (0, p^*)$ on the (x_1, x_2) -plane belong to the Ω limit set. Consider the trajectories with $\tilde{x}_2(0) = q^*$, and $\check{x}_2(0) = p^*$, and $q^* > p^*$. By Property 2.2.4, for $0 \leq t \leq \frac{\pi}{2\omega}$, $\tilde{x}_2(t) \geq \check{x}_2(t)$. Also for $\frac{\pi}{2\omega} \leq t \leq \frac{3\pi}{2\omega}$, $\tilde{x}_2(t) \geq \check{x}_2(t)$. and for $\frac{3\pi}{2\omega} \leq t \leq \frac{2\pi}{\omega}$, $\tilde{x}_2(t) \geq \check{x}_2(t)$. Hence for one period of the input sinusoid $\tilde{x}_2(t) \geq \check{x}_2(t)$. This is true for any period of the sinusoid and so we conclude that atleast one of the following statements must be true:

$$\begin{aligned} p^* &\notin \tilde{x}_2(t) \forall t \geq 0; \\ q^* &\notin \check{x}_2(t) \forall t \geq 0. \end{aligned}$$

That is, atleast one of the points q^*, p^* do not belong to the Ω limit set. Hence it is not possible that $p^* \neq q^*$. Thus the Ω -limit set of the system is a periodic orbit.

That the periods of the variables x_1 and θ on the Ω -limit set are $\frac{2\pi}{\omega}$ is obvious. The period of x_2 on the Ω -limit set is also $\frac{2\pi}{\omega}$ because $\text{sign}(\dot{x}_2) = \text{sign}(\dot{x}_1)$ or in other words $\frac{dx_2}{dx_1} > 0 \forall (x_1, x_2)$ on the Ω -limit set by Property 2.2.2.

□

Theorems 2.2.1 and 2.2.2 were the two main theorems used in proving the above theorem. As it is not necessary for the input $u(\cdot)$ to be co-sinusoidal for Theorems 2.2.1 and 2.2.2 to be valid, we can considerably strengthen the above theorem without any significant change in the proof. The main observation is that instead of (63 - 64) we could have

$$u(b) = \lim_{t \rightarrow b} u(t), \quad (79-a)$$

$$u_1(t) = -u(b - \phi(t)) \quad \text{for } t \in [0, b]. \quad (79-b)$$

where $\phi(\cdot) : [0, b] \rightarrow [0, b]$ is any continuous function.

Theorem 2.2.4 *Consider the system given by Equations (36-a - 37-b). Let the input $u(\cdot) : \mathbb{R} \rightarrow \mathbb{R}$ be a periodic and continuous function of time t with period T . Suppose that the parameters satisfy (40 - 42).*

If $(x_1, x_2)(0) = (0, 0)$, then the Ω -limit set of the system is a periodic orbit of period T .

Proof The proof is essentially same as that of Theorem 2.2.3.

□

Remarks:

1. If Theorem 2.2.1 is reproved for their set of equations, then by using the same method, we can show that the Ω limit set is a periodic orbit for the Jiles – Atherton model.
2. The important difference between the bulk ferromagnetic hysteresis model and the Jiles – Atherton model is that $k = 0$ *does not* represent the lossless case for the latter.

These remarks are explained further in the next subsection.

2.2.3 The Jiles-Atherton model

We now look at Jiles - Atherton model of ferromagnetic hysteresis and its variant as proposed by Deane [31, 32] and study their properties.

Jiles, Thoeke and Devine derive the equation for $\frac{dM}{dH}$ as shown below[33]. They use the following “molecular-field” expression instead of Equation (32):

$$H_e = H + \alpha M_{irr}. \quad (80)$$

Then Equations (26) and (22) give

$$\begin{aligned} M_{an} - M_{irr} &= \frac{\delta k}{\mu_0} \frac{dM_{irr}}{dH_e} \quad \text{ie.} \\ (M_{an} - M_{irr})(dH + \alpha dM_{irr}) &= \frac{\delta k}{\mu_0} dM_{irr} \quad \text{ie.} \\ \left(\frac{\delta k}{\mu_0} - \alpha (M_{an} - M_{irr}) \right) dM_{irr} &= (M_{an} - M_{irr}) dH \quad \text{ie.} \\ \frac{dM_{irr}}{dH} &= \frac{M_{an} - M_{irr}}{\frac{\delta k}{\mu_0} - \alpha (M_{an} - M_{irr})} \end{aligned} \quad (81)$$

Equation (81) can be found as Equation 6 in [33]. Now using Equation (18)

$$\begin{aligned} \frac{dM}{dH} &= \frac{dM_{rev}}{dH} + \frac{dM_{irr}}{dH} \\ &= c \frac{dM_{an}}{dH} + (1 - c) \frac{dM_{irr}}{dH} \\ &= c \frac{dM_{an}}{dH} + (1 - c) \frac{M_{an} - M_{irr}}{\frac{\delta k}{\mu_0} - \alpha (M_{an} - M_{irr})}. \end{aligned}$$

The above equation can be found as Equation (9) in [33]. Expressing the right hand side in terms of M using Equation (22) and using the condition on $\frac{dM_{irr}}{dH}$ as given by Equation (21) we obtain,

$$\begin{aligned}
\frac{dM}{dH} &= c \frac{dM_{an}}{dH} + \delta_M \frac{(1-c)(M_{an}-M)}{\frac{k\delta(1-c)}{\mu_0} - \alpha(M_{an}-M)} \\
&= c \frac{dM_{an}}{dH_e} + (1-c) \frac{\delta_M(M_{an}-M) \left(1 + \frac{\delta_M \alpha c}{1-c} \frac{dM_{an}}{dH_e}\right)}{\frac{k\delta(1-c)}{\mu_0} - \alpha(M_{an}-M)} \quad (82)
\end{aligned}$$

where δ_M is as defined before in Equation (23). The existence and uniqueness of the solution for the system

$$\dot{M} = \frac{dM}{dH} u,$$

where $u(t) = U \cos(\omega t)$, is similar to the previously shown result for the bulk ferromagnetic hysteresis model.

J. Deane([31, 32]) writes another equation for $\frac{dM}{dH}$.

$$\frac{dM}{dH} = c \frac{dM_{an}}{dH_e} + \delta_M \frac{(1-c)(M_{an}-M)}{\frac{k\delta(1-c)}{\mu_0} - \alpha(M_{an}-M)}. \quad (83)$$

Even with the above equation we can still show that the Ω limit set for sinusoidal inputs $u(t) = U \cos(\omega t)$, is periodic.

2.3 Extensions of the Main Result

In this section, we prove a result that looks like an asymptotic stability with phase result. Specifically, we show that the solution trajectory starting at any point on the $H = 0$ axis and $|M| < M_{\text{remnant}}$ where M_{remnant} is the remnant magnetization converges to a periodic trajectory.

But first we study the effects of initial states that are not $(0, 0)$. We prove next that the Ω limit set is still a periodic orbit when the initial state lies on the anhysteretic curve.

Theorem 2.3.1 *Consider the system given by Equations (36-a - 37-b), with a periodic input that is symmetric about $x_1 = 0$. Suppose that (40 - 42) are satisfied. If $(x_1, x_2)(0)$ satisfies*

$$x_2(0) = M_{an}(x_1(0) + \alpha x_2(0)).$$

then the Ω -limit set of the system is a periodic orbit.

Proof

As the initial state lies on the anhysteretic curve, the solution trajectory lies in a compact set in the (x_1, x_2) - plane. The proof of this statement is exactly similar to the proof of Property 2.2.5.

By Property 2.2.4, the increasing trajectories are either identical or do not intersect. The same is true for the decreasing trajectories. These two facts imply the statement of the theorem as shown by the proof of Theorem 2.2.3.

□

We now consider cases where the initial state does not belong to the anhysteretic curve. The most important cases are those when $x_1(0) = 0$ but $x_2(0) \neq 0$. Here it is possible that $x_2(t) > M_s$ for some time t . But we can still prove that the solution converges to a periodic orbit provided the parameters satisfy (40 - 42). This is because the solution trajectory still lies inside a compact set, though it is not the same as the set in Property 2.2.5. But we will only consider cases for which Property 2.2.5 still holds.

Lemma 2.3.1 *1. Consider the system given by Equations (36-a - 37-b), with a periodic input given by $u(t) = U \cos(\omega t)$. Suppose that (40 - 42) are satisfied. Let $x_1(0) = 0$; $p^* \geq x_2(0) \geq 0$, where p^* is the limit point*

obtained in the proof of Theorem 2.2.3. Then the Ω -limit set of the system is a periodic orbit.

2. Similarly, for $x_1(0) = 0$; $-p^* \leq x_2(0) \leq 0$, and $u(t) = -U \cos(\omega t)$, the Ω -limit set of the system is a periodic orbit.

Proof

1. We again show that the trajectory is bounded in the (x_1, x_2) -plane. $(0, p^*)$ belongs to the periodic orbit that is the Ω -limit set Ω_0 obtained in the proof of Theorem 2.2.3. Let (\hat{x}_1, \hat{x}_2) be the intersection of the anhyseretic curve and the set Ω_0 for $x_3 < 0$. Then the trajectory with initial condition $(x_1, x_2)(0, 0)$ such that $x_1(0) = 0$; $p^* \geq x_2(0) \geq 0$, for $t \in [0, \frac{\pi}{2\omega}]$ intersects the anhyseretic curve for some $t^* \ni 0 \leq t^* < \frac{\pi}{2\omega}$. It is obvious that the trajectory is bounded for the time period $[0, \frac{\pi}{2\omega}]$. We apply Theorem 2.3.1, to the trajectory with initial condition $(x_1, x_2)(t^*)$, we obtain the first assertion.
2. The second assertion is proved by repeating the above proof or by invoking anti-symmetry (Property 2.2.3).

□

Lemma 2.3.2 1. Consider the system given by Equations (36-a - 37-b), with a periodic input given by $u(t) = U \cos(\omega t)$. Suppose that (40 - 42) are satisfied. Let $x_1(0) = 0$; $-p^* \leq x_2(0) \leq 0$, where p^* is the limit point obtained in the proof of Theorem 2.2.3. Then the Ω -limit set of the system is a periodic orbit.

2. Similarly, for $x_1(0) = 0$; $p^* \geq x_2(0) \geq 0$, and input $u(t) = -U \cos(\omega t)$, the Ω -limit set of the system is a periodic orbit.

Proof

1. $(0, -p^*)$ lies on the Ω -limit set Ω_0 obtained in the proof of Theorem 2.2.3. Now the trajectory with initial condition $(x_1, x_2)(0, 0)$ such that $x_1(0) = 0$; $-p^* \leq x_2(0) \leq 0$, for $t \in [0, \frac{\pi}{2\omega}]$ is bounded below by the trajectory of the system with $(0, -p^*)$ as the initial state (Property 2.2.4). It is bounded above by the anhysteretic curve, as it is bounded above by the trajectory of the system with $(0, 0)$ as the initial state (Property 2.2.4). Thus it is bounded for $t \in [0, \frac{\pi}{2\omega}]$. For $t > \frac{\pi}{2\omega}$ the trajectory is bounded above by the anhysteretic curve, and below by Ω_0 . Hence there exists a time $t^* \in [\frac{\pi}{2\omega}, \frac{3\pi}{2\omega}]$, such that $(x_1, x_2)(t^*)$ lies on the anhysteretic curve. If we now apply Theorem 2.3.1 to the trajectory with initial condition $(x_1, x_2)(t^*)$, we have proved the first assertion.
2. The second assertion is proved by repeating the above proof or by invoking anti-symmetry (Property 2.2.3).

□

The above two lemmas leads us to the following theorem.

Theorem 2.3.2 *Consider the system with a periodic input given by $u(t) = \pm U \cos(\omega t)$,. Suppose that (40 - 42) are satisfied. Let $x_1(0) = 0$; $-p^* \leq x_2(0) \leq p^*$, where p^* is the limit point obtained in the proof of Theorem 2.2.3. Then the Ω -limit set of the system is a periodic orbit.*

Proof

This theorem is a consequence of the Lemmas 2.3.1 and 2.3.2.

□

The next theorem is the main result of this section.

Theorem 2.3.3 *Suppose the parameters satisfy (40 - 42) are satisfied.*

1. *Consider the system with a periodic input given by $u(t) = U \cos(\omega t)$,. Let $x_1(0) = 0$; $-p^* \leq x_2(0) \leq p^*$, where p^* is the limit point obtained in the proof of Theorem 2.2.3. Let $(x_1, x_2)(t)$ be the solution at any time t . Let $(p_1, p_2)(t)$ be the solution at any time t of the system with initial state $(0, -p^*)$. Then $|x_2(t) - p_2(t)| \rightarrow 0$, as $t \rightarrow \infty$.*
2. *Consider the system with a periodic input given by $u(t) = -U \cos(\omega t)$,. Let $x_1(0) = 0$; $-p^* \leq x_2(0) \leq p^*$, where p^* is the limit point obtained in the proof of Theorem 2.2.3. Let $(x_1, x_2)(t)$ be the solution at any time t . Let $(p_1, p_2)(t)$ be the solution at any time t of the system with initial state $(0, p^*)$. Then $|x_2(t) - p_2(t)| \rightarrow 0$, as $t \rightarrow \infty$.*

Proof

1. We have proved in Theorem 2.3.2 that the solution trajectory with initial state $(x_1, x_2)(0)$, where $x_1(0) = 0$; $-p^* \leq x_2(0) \leq p^*$, has an Ω -limit set Ω_1 . We had already obtained an Ω -limit set Ω_0 in the proof of Theorem 2.2.3. That they must be identical is obvious by the proof of Theorem 2.2.3 (otherwise Property 2.2.4 is violated). We know that $x_1(t) = p_1(t) \quad \forall t \geq 0$. From the previous two statements it is obvious that the claim must be true.

2. The proof of the second part can be easily proved by simply modifying the proof of the first part or by invoking anti-symmetry (Property 2.2.3).

□

Chapter 3

Bulk Magnetostrictive Hysteresis

Model

A change in the magnetization of a body in a magnetic field causes a deformation in it; this phenomenon is called magnetostriction. The deformation of a magnetic body in response to a change in its magnetization implies that the magnetic and elastic properties of the material are coupled. This phenomenon can be taken into account in the theory of micromagnetics by adding a *magnetoelastic* energy density term to the free energy as discussed in Chapter 1 (see (19)).

Motivated by this approach, we add similar terms to the energy balance equation (11) to account for the elastic nature of the actuator and the magneto-elastic coupling. We then analyze the resulting coupled equations representing magnetic and mechanical dynamic equilibrium for existence and uniqueness properties. We further prove that if the input signal is periodic in time and the initial state of the model is at the origin, then the Ω -limit set of the solution is a periodic orbit.

Eddy current losses and losses arising due to the resistance of the winding are also accounted for in our final model. Later in the chapter, we study the

behaviour of the magnetostrictive actuator as part of an electrical circuit with periodic forcing.

3.1 Thin magnetostrictive actuator model

We are interested in developing a low dimensional model for a magnetostrictive rod actuator. Hence the actuator along with the associated prestress and magnetic path to be a mass-spring system with magneto-elastic coupling. The magnetic hysteresis phenomenon is modeled as in Chapter 2. Ignoring eddy-current effects and lead resistance losses, the energy balance approach leads to coupled equations representing magnetic and mechanical dynamic equilibrium. As we show later, this model is only technically valid when the input signal is periodic. However, this is the case in many applications where one obtains rectified linear or rotary motion by applying a periodic input at a high frequency to these actuators. For instance, the hybrid motor [34, 35] developed during the author's Masters thesis produced a rotary motion using both piezoelectric and magnetostrictive actuators in a mechanical clamp and push arrangement.

Consider a thin magnetoelastic/magnetostrictive rod whose average magnetization is denoted by M . An external source (battery) produces a uniform magnetic field H in the body. This field H is purely due to the external source and is not the effective magnetic field in the body. A change in the field H brings about a corresponding change in the magnetization of the body in accordance with Maxwell's laws of electromagnetism. Because of its magnetostrictive nature, the change in H also produces an elastic effect.

We equate the work done by external sources (both magnetic and mechani-

cal), with the change in the free energy of the rod, change in kinetic energy, and losses in the magnetization process and the mechanical deformation:

$$\begin{aligned} \delta W_{bat} + \delta W_{mech} = & \underbrace{\delta W_{mag} + \delta W_{magel} + \delta W_{el}}_{\text{Change in internal energy}} \\ & + \underbrace{\delta L_{mag} + \delta L_{el}}_{\text{losses}} + \underbrace{\delta K}_{\text{Change in kinetic energy}} \end{aligned} \quad (1)$$

In Equation 1, δK is the work done in changing the kinetic energy of the system consisting of the magnetoelastic rod actuator, δW_{mag} is the change in the magnetic potential energy, δW_{magel} is the change in the magnetoelastic energy, δW_{el} is the change in the elastic energy, δL_{mag} are the losses due to the change in the magnetization, and δL_{el} are the losses due to the elastic deformation of the rod. The elastic energy is given by $W_{el} = \frac{1}{2} d x^2$, where x is the total strain multiplied the length of the actuator. As mentioned before, the magnetoelastic energy density in the continuum theory of micromagnetics is of the form strain multiplied by the square of the direction cosines of the magnetization vector. For our bulk magnetostriction investigation, we can similarly write down the following expression for the magnetoelastic energy W_{magel} :

$$W_{magel} = b M^2 x \mathcal{V}$$

where b is the magneto-elastic coupling constant and \mathcal{V} is the volume of the magnetostrictive rod. M is the average magnetic moment of the rod in the direction of the applied magnetic field which is along the axis of the rod. The expression for the magnetic hysteresis losses δL_{mag} is due to Jiles and Atherton as discussed in the previous chapter. The change in the magnetization dM is again assumed to be composed of a reversible component dM_{rev} and an irreversible

component dM_{irr} . The losses in the magnetization process is only due to the irreversible change in the magnetization:

$$\delta L_{mag} = \oint \mathcal{V} k \text{sign}(\dot{H}) (1 - c) dM_{irr}$$

where the integral is over one cycle of the input voltage/current which is assumed to be periodic. The losses due to mechanical damping are assumed to be $\delta L_{el} = \oint c_1 \dot{x} dx$. The change in the kinetic energy $\delta K = \oint m_{eff} \ddot{x} dx$. Therefore,

$$\begin{aligned} \delta W_{bat} + \delta W_{mech} &= \delta W_{mag} + \underbrace{\oint m_{eff} \ddot{x} dx}_{\delta K} \dots \\ &+ \underbrace{\mathcal{V} \oint b M^2 dx + \mathcal{V} \oint 2 b M x dM}_{\delta W_{magnet}} + \underbrace{\oint dx dx}_{\delta W_{el}} \\ &+ \underbrace{\mathcal{V} \oint k \text{sign}(\dot{H}) (1 - c) dM_{irr}}_{\delta L_{mag}} + \underbrace{\oint c_1 \dot{x} dx}_{\delta L_{el}} \end{aligned} \quad (2)$$

Now we obtain expressions for the left hand side of the above equation. For a thin cylindrical magnetostrictive actuator, with an average magnetic moment M , and an uniform magnetic field in the x direction H , the work done by the battery in changing the magnetization in one cycle, is given by [8]

$$\delta W_{bat} = \mathcal{V} \oint \mu_0 H dM.$$

Let an external force F in the x (axial) direction produce a uniform compressive stress σ within the actuator. Let the axial displacement of the edge of the actuator rod be x . Thus the mechanical work done by the external force in a cycle of magnetization is given by [8]

$$\delta W_{mech} = \oint F dx.$$

The total work done by the battery and the external force is

$$\delta W_{bat} + \delta W_{mech} = \mathcal{V} \oint \mu_0 H dM + \oint F dx.$$

We see that adding the integral of any perfect differential over a cycle does not change the value on the left hand side. Therefore

$$\delta W_{bat} + \delta W_{mech} = \mathcal{V} \left(\oint \mu_0 H dM + \oint \alpha M dM \right) + \oint F dx. \quad (3)$$

Equations 2 and 3 give

$$\begin{aligned} \oint (F - dx - c_1 \dot{x} - m_{eff} \ddot{x} - \mathcal{V} b M^2) dx + \mathcal{V} \mu_0 \oint (H + \alpha M - \frac{2bMx}{\mu_0}) dM \\ = \delta W_{mag} + \mathcal{V} \oint k \text{sign}(\dot{H}) (1 - c) dM_{irr}. \end{aligned} \quad (4)$$

Define the effective field to be

$$H_e = H + \alpha M - \frac{2bMx}{\mu_0}.$$

As the integration is over one cycle of magnetization

$$\oint H_e dM = - \oint M dH_e.$$

It was observed in Chapter 2, that if M is a function of H_e then there are no losses in one cycle. This is the situation for a paramagnetic material where $M = M_{an}$ is given by Langévin's expression as a function of H_e . Hence for the lossless case, the magnetic potential energy is given by

$$\delta W_{mag} = -\mathcal{V} \oint M_{an} dH_e.$$

Thus Equation 4 can be rewritten as

$$\mathcal{V} \mu_0 \oint (M_{an} - M - \frac{k \text{sign}(\dot{H}) (1 - c)}{\mu_0} \frac{dM_{irr}}{dH_e}) dH_e + \oint (F - dx - c_1 \dot{x} - m_{eff} \ddot{x} - b M^2 \mathcal{V}) dx = 0$$

Note that the above equation is valid only if H , M , x , \dot{x} are periodic functions of time. In other words, the trajectory of $(H, M, x, \dot{x})(t)$ in \mathbb{R}^4 is a periodic orbit. We now make the *hypothesis* that the following equation is valid when we go from one point to another point on this periodic orbit:

$$\mathcal{V} \mu_0 \int (M_{an} - M - \frac{k \text{sign}(\dot{H}) (1 - c)}{\mu_0} \frac{dM_{irr}}{dH_e}) dH_e + \int (F - dx - c_1 \dot{x} - m_{eff} \ddot{x} - b M^2 \mathcal{V}) dx = 0. \quad (5)$$

The above equation is assumed to hold only for the periodic orbit. Since dx and dH_e are independent variations arising from independent control of the external prestress and applied magnetic field respectively, the integrands must be equal to zero:

$$M_{an} - M - \frac{k \text{sign}(\dot{H}) (1 - c)}{\mu_0} \frac{dM_{irr}}{dH_e} = 0, \quad (6)$$

$$m_{eff} \ddot{x} + c_1 \dot{x} + dx + b M^2 \mathcal{V} = F. \quad (7)$$

Jiles and Atherton relate the irreversible and the reversible magnetizations as follows [28] (refer to the discussion on the subject in Chapter 2):

$$M = M_{rev} + M_{irr}, \quad (8)$$

$$M_{rev} = c(M_{an} - M_{irr}), \quad (9)$$

$$\frac{dM}{dH} = \delta_M (1 - c) \frac{dM_{irr}}{dH} + c \frac{dM_{an}}{dH}, \quad (10)$$

where δ_M is defined by

$$\delta_M = \begin{cases} 0 & : \dot{H} < 0 \text{ and } M_{an}(H_e) - M(H) > 0, \\ 0 & : \dot{H} > 0 \text{ and } M_{an}(H_e) - M(H) < 0, \\ 1 & : \text{otherwise.} \end{cases} \quad (11)$$

Using the relations (8) - (11), the Equations (6) and (7) for the magnetostriction model can be written as:

$$\frac{dM}{dt} = \frac{\frac{k\delta}{\mu_0} c \frac{dM_{an}}{dH_e} + \delta_M (M_{an} - M)}{\frac{k\delta}{\mu_0} - \left(\delta_M (M_{an} - M) + \frac{k\delta}{\mu_0} c \frac{dM_{an}}{dH_e} \right) \left(\alpha - \frac{2bx}{\mu_0} \right)} \frac{dH}{dt}, \quad (12)$$

$$m_{eff} \ddot{x} + c_1 \dot{x} + dx + bM^2 \mathcal{V} = F. \quad (13)$$

A magnetostrictive material has finite resistivity, and therefore there are eddy currents circulating within the rod. Using Maxwell's equations, we can derive the following simple expression for the power losses due to eddy currents [34] (Appendix F).

$$P_{eddy} = \frac{V^2 l_m}{N^2 8\pi\rho} \frac{B^2 + A^2}{B^2 - A^2}$$

where A , B are the inner and the outer radii of the rod, l_m is its length, N_m is the number of turns of coil on the rod, and V is the voltage across the coil of the inductor. Hence the eddy current losses can be represented equivalently as a resistor in parallel with the hysteretic inductor. This idea is quite well known and a discussion can be found in [27] or [34]. From the above expression for the power lost, the value of the resistor is,

$$R_{eddy} = \frac{N^2 8\pi\rho}{l_m} \frac{B^2 - A^2}{B^2 + A^2}$$

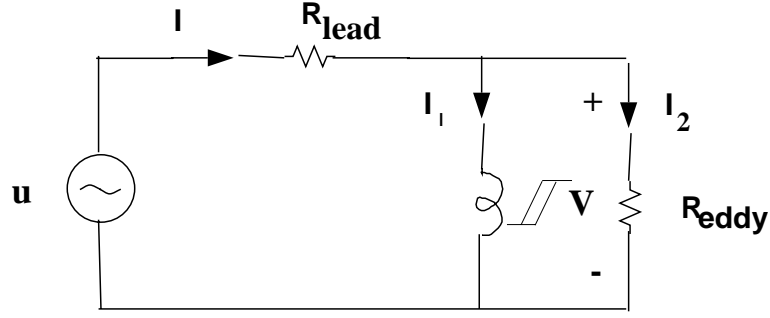


Figure 3.1: Schematic diagram of a thin magnetostrictive actuator in a resistive circuit.

The actual work done by the battery in changing the magnetization and to replenish the losses due to the eddy currents in one cycle is now given by

$$\delta\bar{W}_{bat} = \delta W_{bat} + \oint P_{eddy} dt + \oint I^2 R_{lead} dt \quad (14)$$

$$= -\mathcal{V} \oint \mu_0 M dH_e + \oint P_{eddy} dt + \oint I^2 R_{lead} dt \quad (15)$$

where R_{lead} accounts for the resistance of the winding and leads which contribute to the total energy loss. I is the total current input from the power source to the magnetostrictive actuator. Figure 3.1 shows a schematic of the full model. The hysteretic inductor stands for the magnetostrictive actuator model.

3.2 Qualitative analysis of the magnetostrictive actuator model

In this section, we study the magnetostriction model given by Equations (13) and (12). That is we do not take eddy current losses into consideration.

Equation (13) can be cast in the standard form of a ODE (refer to Appendix

B), if we identify x and \dot{x} as state variables. Equation (12) is already in the standard form and we can identify H and M as state variables also. Thus in an abstract notation with $w = (H, M, x, \dot{x})$ we can write the magnetostrictive model equations as

$$\dot{w} = f(w, F, \dot{H}), \quad (16)$$

where F is the external mechanical force acting on the rod. Both F and \dot{H} are viewed as inputs to the system. It is very important to note that the model equations (12) - (13) are only valid when all the state variables are periodic in time. What we mean is that the solution trajectory of the equations represent the physics of the system when it forms a periodic orbit in \mathbb{R}^4 space. This implies that for correct simulations, the initial state has to be chosen on this periodic orbit. But, usually in practice we do not know apriori what state the system is in. It is shown analytically that even if the initial state is at the origin in the $M - H$ plane (which is usually not on the hysteresis loop), and a periodic input \dot{H} is applied, the solution trajectory *tends* asymptotically towards a periodic solution. The problem statement is as follows. For simplicity, we consider F to be a constant (and hence trivially periodic) function of time. For periodic F that are not constant the same methods developed in this section can be used. The input \dot{H} is assumed to be periodic in time. Then we wish to prove that the Ω limit set of the solution trajectory $w(t)$ for the magnetostrictive model (12) - (13) is a periodic function of time. The proof proceeds in the following steps:

1. We study the effect of the coupling by replacing x in Equation (12) and M in Equation (13) by periodic functions $g(\cdot)$ and $h(\cdot)$ respectively. Their period is the same as the input \dot{H} . We show that the solution trajectories

tend to periodic orbits for both the magnetic ($\bar{x}(\cdot)$) and mechanical ($\bar{y}(\cdot)$) equations under these conditions.

2. As both the forcing functions and their response are periodic functions of time, we can restrict our attention to one period. Define the sets $B = \{\phi \in \mathcal{C}([0, T], \mathbb{R}) : |\phi| \leq \beta_1; |\phi(t) - \phi(\bar{t})| \leq M_1 |t - \bar{t}| \forall t, \bar{t} \in [0, T]\}$, $D = \{\psi \in \mathcal{C}([0, T], \mathbb{R}) : |\psi| \leq \beta_2; |\psi(t) - \psi(\bar{t})| \leq M_2 |t - \bar{t}| \forall t, \bar{t} \in [0, T]\}$, where $\beta_1, \beta_2, M_1, M_2$ are positive constants. Let $\mathcal{P}_1, \mathcal{P}_2 : \mathcal{C}([0, T], \mathbb{R}^2) \rightarrow \mathcal{C}([0, T], \mathbb{R})$ denote the projection operators defined by $\mathcal{P}_1(f, g) = f$ and $\mathcal{P}_2(f, g) = g$.

We then consider the mappings $\mathcal{G} : B \rightarrow \mathcal{C}([0, T], \mathbb{R}^2); g(\cdot) \mapsto \bar{x}(\cdot)$ and $\mathcal{H} : D \rightarrow \mathcal{C}([0, T], \mathbb{R}^2); h(\cdot) \mapsto \bar{y}(\cdot)$, and show them to be continuous.

3. We show that there exist positive constants $\beta_1, \beta_2, M_1, M_2$ such that $\mathcal{P}_2 \circ \mathcal{G} : B \rightarrow D$ and $\mathcal{P}_1 \circ \mathcal{H} : D \rightarrow B$.
4. Define the mapping Ψ as follows. $\Psi : B \times D \rightarrow B \times D; \Psi(\phi, \psi) = (\mathcal{P}_1 \circ \mathcal{H}(\psi), \mathcal{P}_2 \circ \mathcal{G}(\phi))$.

We show that the set $B \times D$ is a compact and convex set. By item 2, Ψ is a continuous map. Then by the Schauder fixed point theorem (see Appendix) there exists a fixed point for the mapping Ψ . This fixed point is the periodic orbit of the coupled system.

Before we analyze the magnetostriction model, we first prove a lemma which will be used in the analysis. First define

$$C_1 = \sup_z \left| \frac{\partial^2 \mathcal{L}}{\partial z^2} \right|. \quad (17)$$

C_1 is bounded as $\mathcal{L}(z)$ is a smooth function of z . The value of C_1 is approximately 0.106 (which we obtained numerically using the software Mathematica).

Lemma 3.2.1 *Suppose the parameters satisfy*

$$\frac{\alpha M_s}{3a} < 1. \quad (18)$$

Then there exists $G > 0$ such that $\forall \lambda$ with $|\lambda| \leq G$

$$\frac{\frac{(\alpha+\lambda)M_s}{3a} + C_1 \frac{2\lambda M_s}{a} \frac{(\alpha+\lambda)M_s}{a}}{1 - \frac{2\lambda M_s}{3a}} + \frac{(\alpha+\lambda)M_s}{\frac{k}{\mu_0}} \frac{2\lambda M_s}{3a} < 1, \quad (19)$$

$$\frac{2\lambda M_s}{3a} < 1 \quad (20)$$

Proof

Let

$$\nu(x) = \frac{M_s(\alpha + x)}{3a} \left(\frac{1 + \frac{6C_1 x M_s}{a}}{1 - \frac{2x M_s}{3a}} + \frac{2x M_s}{\frac{k}{\mu_0}} \right).$$

with $x \in \mathcal{D} = \{x : \frac{2x M_s}{3a} < 1\}$. Then $f(0) = \frac{\alpha M_s}{3a} < 1$. As $f(\cdot)$ is continuous as a function of x for $x \in \mathcal{D}$, $\exists G > 0$ such that $\forall x \in \mathcal{D}$ with $|x| \leq G$

$$f(x) < 1.$$

□

3.2.1 The uncoupled model with periodic perturbation

Define state variables

$$x_1 = H,$$

$$x_2 = M,$$

$$y_1 = x,$$

$$y_2 = \dot{x}.$$

Let

$$z = \frac{x_1 + \left(\alpha - \frac{2bg(t)}{\mu_0}\right) x_2}{a}.$$

Then the state equations are:

$$\dot{x}_1 = u, \tag{21}$$

$$\dot{x}_2 = \left(\frac{\frac{kx_3}{\mu_0} \frac{cM_s}{a} \frac{\partial \mathcal{L}}{\partial z}(z) + x_4 M_s \left(\mathcal{L}(z) - \frac{x_2}{M_s} \right)}{\frac{kx_3}{\mu_0} - x_4 M_s \left(\mathcal{L}(z) - \frac{x_2}{M_s} \right) \tilde{\alpha} - \frac{kx_3}{\mu_0} \tilde{\alpha} \frac{cM_s}{a} \frac{\partial \mathcal{L}}{\partial z}(z)} \right) u, \tag{22}$$

$$x_3 = \text{sign}(u), \tag{23}$$

$$x_4 = \begin{cases} 0 & : x_3 < 0 \text{ and } \mathcal{L}(z) > 0, \\ 0 & : x_3 > 0 \text{ and } \mathcal{L}(z) < 0, \\ 1 & : \text{otherwise,} \end{cases} \tag{24}$$

$$\dot{y} = Ay - \frac{b\mathcal{V}}{m_{eff}} h^2(t), \tag{25}$$

where $\mathcal{L}(z) = \coth(z) - \frac{1}{z}$; $\frac{\partial \mathcal{L}}{\partial z}(z) = -\text{cosech}^2(z) + \frac{1}{z^2}$; $\tilde{\alpha} = \alpha - \frac{2bg(t)}{\mu_0}$; $y = \begin{bmatrix} y_1 & y_2 \end{bmatrix}^T$; $A = \begin{bmatrix} 0 & 1 \\ -\frac{d}{m_{eff}} & -\frac{c_1}{m_{eff}} \end{bmatrix}$ and $g(\cdot)$, $h(\cdot)$ are $\frac{2\pi}{\omega}$ periodic functions of time. F is assumed to be zero for this discussion. The input is given by,

$$u(t) = U \cos(\omega t). \quad (26)$$

The initial state is $(x_1, x_2, y_1, y_2)(t = 0) = (0, 0, 0, 0)$. x_3, x_4 are functions of x_1, x_2 and u and therefore are not state variables.

Analysis of the uncoupled magnetic system

The proof of existence and uniqueness of trajectories for the system (21 - 24) is very similar to what was done in Chapter 2.

Theorem 3.2.1 *Consider the system of equations (21 - 24). Suppose $g(\cdot)$ be a known continuously differentiable function of t , with*

$$\left| \frac{2b g(\cdot)}{\mu_0} \right| \leq G \quad (27)$$

where $G > 0$ is sufficiently small. Let the initial condition $(x_1, x_2)(t = 0) = (x_{1_0}, x_{2_0})$ satisfy

$$\begin{aligned} \zeta_0 &= \frac{x_{1_0} + (\alpha + G) x_{2_0}}{a}, \\ x_{2_0} &= M_s \left(\coth(\zeta_0) - \frac{1}{\zeta_0} \right). \end{aligned} \quad (28)$$

Let the parameters satisfy

$$\frac{2GM_s}{3a} < 1 \quad (29)$$

$$\frac{\frac{(\alpha+G)M_s}{3a} + C_1 \frac{2GM_s}{1 - \frac{2GM_s}{3a}} \frac{(\alpha+G)M_s}{a}}{\mu_0} + \frac{(\alpha+G)M_s}{\mu_0} \frac{2GM_s}{3a} < 1, \quad (30)$$

$$0 < c < 1, \quad (31)$$

$$k > 0. \quad (32)$$

Let $u(\cdot)$ be a continuous function of t , with $u(t) > 0$ for $t \in [0, T)$ where $T > 0$ and $(x_1(t), x_2(t))$ denote the solution of (21) - (24). Let $\zeta(t) = \frac{x_1(t) + (\alpha + G)x_2(t)}{a}$. Then $(M_s \mathcal{L}(\zeta(t)) - x_2(t)) > 0 \forall t \in (0, T)$. Else if $u(t) < 0$ for $t \in [0, T)$ where $T > 0$, then $(M_s \mathcal{L}(\zeta(t)) - x_2(t)) < 0 \forall t \in (0, T)$.

Remarks :

It will be seen during the course of the proof that (29 - 30) are sufficient conditions on G for the proof to hold. It will also be seen that a necessary condition on G is that

$$\frac{c(\alpha + G) M_s}{3a} < 1 \tag{33}$$

which is obviously true if (29 - 31) are true.

Proof

We make a change of co-ordinates from (x_1, x_2) to (ζ, y) , where

$$\begin{aligned} \zeta &= \frac{x_1 + (\alpha + G)x_2}{a}, \\ y &= M_s \mathcal{L}(\zeta) - x_2. \end{aligned}$$

Denote $w = (\zeta, y)$ and $x = (x_1, x_2)$. The domain of definition of the transformation $\psi : x \mapsto w$ is \mathbb{R}^2 . The Jacobian of the transform is given by

$$\frac{\partial \psi}{\partial x} = \begin{bmatrix} \frac{1}{a} & \frac{\alpha + G}{a} \\ \frac{M_s}{a} \frac{\partial \mathcal{L}}{\partial z}(\zeta) & \frac{M_s(\alpha + G)}{a} \frac{\partial \mathcal{L}}{\partial z}(\zeta) - 1 \end{bmatrix}.$$

The determinant of $\frac{\partial \psi}{\partial x}$ is

$$\det\left(\frac{\partial \psi}{\partial x}\right) = -\frac{1}{a} \forall x \in \mathbb{R}^2.$$

Hence the results on existence, extension and uniqueness of solutions to the state equations in the transformed space carry over to the equations in the original state space.

Denote $\dot{w} = f(t, w, x_3, x_4)$. The initial conditions in the transformed co-ordinates are

$$w_0 = (\zeta_0, y_0) = \left(\frac{x_{1_0} + (\alpha + G) x_{2_0}}{a}, M_s \mathcal{L}(\zeta_0) - x_{2_0} \right).$$

Denote $\bar{\alpha} = \alpha + G$. The state equations in terms of w are:

$$\dot{\zeta} = f_1(t, w) \tag{34}$$

$$= \frac{1 + (\alpha + G) \bar{g}(t, \zeta, y, x_3, x_4)}{a} u, \tag{35}$$

$$\dot{y} = f_2(t, w) \tag{36}$$

$$= \left(\frac{M_s}{a} \frac{\partial \mathcal{L}}{\partial z}(\zeta) + \left(\frac{(\alpha + G) M_s}{a} \frac{\partial \mathcal{L}}{\partial z}(\zeta) - 1 \right) \bar{g}(\zeta, y, x_3, x_4) \right) u, \tag{37}$$

$$x_3 = \text{sign}(u), \tag{38}$$

$$x_4 = \begin{cases} 0 & : x_3 < 0 \text{ and } y_1 > 0, \\ 0 & : x_3 > 0 \text{ and } y_1 < 0, \\ 1 & : \text{otherwise,} \end{cases} \tag{39}$$

where

$$z(t) = \frac{x_1(t) + \tilde{\alpha}(t) x_2(t)}{a}, \tag{40}$$

$$y_1(t) = M_s \mathcal{L}(z(t)) - x_2(t), \tag{41}$$

and

$$\bar{g}(t, \zeta, y, x_3, x_4) = \frac{\frac{k x_3}{\mu_0} \frac{c M_s}{a} \frac{\partial \mathcal{L}}{\partial z}(z) + x_4 y_1}{\frac{k x_3}{\mu_0} - x_4 y_1 \tilde{\alpha}(t) - \frac{k x_3}{\mu_0} \tilde{\alpha}(t) \frac{c M_s}{a} \frac{\partial \mathcal{L}}{\partial z}(z)}. \tag{42}$$

Note that if $\zeta(t)$, $y(t)$ and $g(t)$ are known at any instant of time t , then both $z(t)$ and $y_1(t)$ are known. Explicitly, at each time t the inverse transforms are:

$$x_2(t) = M_s \mathcal{L}(\zeta(t)) - y(t) \quad (43)$$

$$x_1(t) = a\zeta(t) - (\alpha + G) M_s \mathcal{L}(\zeta(t)) + (G + g(t)) y(t) \quad (44)$$

$$z(t) = \zeta(t) - (G + g(t)) M_s \mathcal{L}(\zeta(t)) + (G + g(t)) y(t) \quad (45)$$

$$y_1(t) = M_s (\mathcal{L}(z(t)) - \mathcal{L}(\zeta(t))) + y(t) \quad (46)$$

As $g(t)$ is continuously differentiable function of time, $z(t, \zeta, y)$ and $y_1(t, \zeta, y)$ are continuously differentiable functions of (t, ζ, y) . A very important point is that at any instant of time $t \geq 0$

$$y(t) \geq y_1(t). \quad (47)$$

By (35) and (25), we have

$$\begin{aligned} \dot{\zeta} &= \frac{\frac{kx_3}{\mu_0} + (\bar{\alpha} - \tilde{\alpha}) \left(x_4 y_1 + \frac{kx_3}{\mu_0} \frac{cM_s}{a} \frac{\partial \mathcal{L}}{\partial z}(z) \right)}{\frac{kx_3}{\mu_0} - \tilde{\alpha} \left(x_4 y_1 + \frac{kx_3}{\mu_0} \frac{cM_s}{a} \frac{\partial \mathcal{L}}{\partial z}(z) \right)} u, \\ \dot{y} &= \frac{\frac{M_s}{a} \frac{kx_3}{\mu_0} \left(\frac{\partial \mathcal{L}}{\partial z}(\zeta) - c \frac{\partial \mathcal{L}}{\partial z}(z) \right) + (\bar{\alpha} - \tilde{\alpha}) \frac{M_s}{a} \frac{\partial \mathcal{L}}{\partial z}(\zeta) \left(x_4 y_1 + \frac{kx_3}{\mu_0} \frac{cM_s}{a} \frac{\partial \mathcal{L}}{\partial z}(z) \right) - x_4 y_1}{\frac{kx_3}{\mu_0} - \tilde{\alpha} \left(x_4 y_1 + \frac{kx_3}{\mu_0} \frac{cM_s}{a} \frac{\partial \mathcal{L}}{\partial z}(z) \right)} u. \end{aligned}$$

Let

$$D = \underbrace{(-\delta_1, T)}_t \times \underbrace{(-\infty, \infty)}_\zeta \times \underbrace{\left(-\epsilon_1, \frac{\frac{k}{\mu_0} \frac{M_s(1-c)}{3a} + \frac{k}{\mu_0} \frac{M_s}{3a} \frac{2GM_s}{3a} (c + 9C_1)}{1 - \frac{2GM_s}{3a}} + \frac{2GM_s^2}{3a} + \epsilon_1 \right)}_y,$$

where δ_1, ϵ_1 are sufficiently small positive numbers.

As $u(t)$ is only defined for $t \geq 0$, we need to extend the domain of $u(\cdot)$ to $(-\delta_1, 0)$. This can be easily accomplished by defining $u(t) = 0$ for $t \in (-\delta_1, 0)$.

Then $f_1(t, w)$, $f_2(t, w)$ exist on D which can be seen as follows.

1. Note that z is well-defined given a point (t, w) in D . In the time interval $(-\delta_1, 0)$, $u(t) = 0$ by definition. Therefore $x_3 = 0$ by (38) and $x_4 = 1$ by (39). This implies that $\bar{g}(t, \zeta, y, 0, 1) = \frac{-y_1}{y_1}$. Defining $\bar{g}(t, \zeta, 0, 0, 1) = -1$ makes $\bar{g}(t, \zeta, y, 0, 1)$ continuous as a function of y_1 (which is a continuous function of (t, ζ, y)). This also makes $f_1(t, w)$ and $f_2(t, w)$ well defined.
2. In the time interval $[0, T)$, $u(t) > 0$. Therefore $x_3 = 1$. Hence

$$\bar{g}(\zeta, y, 1, x_4) = \frac{\frac{k}{\mu_0} \frac{c M_s}{a} \frac{\partial \mathcal{L}}{\partial z}(z) + x_4 y_1}{\frac{k}{\mu_0} - x_4 y_1 \tilde{\alpha} - \frac{k}{\mu_0} \tilde{\alpha} \frac{c M_s}{a} \frac{\partial \mathcal{L}}{\partial z}(z)}.$$

We have to ensure that f is well defined $\forall (t, w) \in D$. This can be established by examining \bar{g} .

- (a) $x_4 = 0$ implies $\bar{g}(\zeta, y, 1, 0) = \frac{\frac{k}{\mu_0} \frac{c M_s}{a} \frac{\partial \mathcal{L}}{\partial z}(z)}{\frac{k}{\mu_0} - \frac{k}{\mu_0} \tilde{\alpha} \frac{c M_s}{a} \frac{\partial \mathcal{L}}{\partial z}(z)}$. By (40) and (41), the denominator of \bar{g} is always positive $\forall (t, w) \in D$. This is because

$$\begin{aligned} \text{Den. of } \bar{g} &\geq \frac{k}{\mu_0} \left(1 - \tilde{\alpha} \frac{c M_s}{3 a} \right) \\ &\geq \frac{k}{\mu_0} \left(1 - (\alpha + G) \frac{c M_s}{3 a} \right) \\ &> \frac{k}{\mu_0} \left(1 - (\alpha + G) \frac{M_s}{3 a} \right) \\ &> 0. \end{aligned}$$

by (30) because

$$\begin{aligned} 1 &> \frac{\frac{(\alpha+G) M_s}{3 a} + C_1 \frac{2GM_s}{a} \frac{(\alpha+G) M_s}{a}}{1 - \frac{2GM_s}{a}} + \frac{(\alpha + G) M_s}{\frac{k}{\mu_0}} \frac{2GM_s}{3 a} \\ &> \frac{(\alpha + G) M_s}{3 a}. \end{aligned} \tag{48}$$

Hence $f_1(t, w)$ and $f_2(t, w)$ are well-defined.

(b) $x_4 = 1$ implies $\bar{g}(\zeta, y, 1, 1) = \frac{\frac{k}{\mu_0} \frac{c M_s}{a} \frac{\partial \mathcal{L}}{\partial z}(z) + y_1}{\frac{k}{\mu_0} - y_1 \tilde{\alpha} - \frac{k}{\mu_0} \tilde{\alpha} \frac{c M_s}{a} \frac{\partial \mathcal{L}}{\partial z}(z)}$. As $y(t) \geq y_1$ we replace the y_1 in the denominator by y and then show it to be positive.

$$\text{Den. of } \bar{g} \geq \frac{k}{\mu_0} \left(1 - (\alpha + G) \frac{c M_s}{3a} \right) - (\alpha + G) y_{max} - (\alpha + G) \epsilon_1$$

where

$$y_{max} = \frac{\frac{k}{\mu_0} \frac{M_s(1-c)}{3a} + \frac{k}{\mu_0} \frac{M_s}{3a} \frac{2GM_s}{3a} (c + 9C_1)}{1 - \frac{2GM_s}{3a}} + \frac{2GM_s^2}{3a}. \quad (49)$$

As $y_{max} + \epsilon_1$ is the maximum value taken by y in the domain D

$$\begin{aligned} \text{Den. of } \bar{g} \geq \frac{k}{\mu_0} \left(1 - \frac{\frac{(\alpha+G)M_s}{3a} + C_1 \frac{2GM_s}{a} \frac{(\alpha+G)M_s}{a}}{1 - \frac{2GM_s}{3a}} + \frac{(\alpha+G)M_s}{\frac{k}{\mu_0}} \frac{2GM_s}{3a} \right) \\ - (\alpha + G) \epsilon_1, \end{aligned}$$

which is positive by (30) if we choose ϵ_1 small enough.

Hence $f_1(t, w)$ and $f_2(t, w)$ are well-defined $\forall (t, w) \in D$.

• Existence of a solution

We first show existence of a solution at $t = 0$. To prove existence, we show that $f(\cdot, \cdot)$ satisfies Carathéodory's conditions.

1. We have already seen that $f(\cdot, \cdot)$ is well defined on D . We now check whether $f_1(t, w)$ and $f_2(t, w)$ are continuous functions of w for all $t \in (-\delta_1, b)$.

(a) For $t \in (-\delta_1, 0)$, $f_1(t, w)$, $f_2(t, w)$ are both zero and hence trivially continuous in w .

- (b) At $t \geq 0$, $x_3 = 1$. To check whether $f_1(t, w)$, $f_2(t, w)$ are continuous with respect to w , we only need to check whether $\bar{g}_t(\cdot)$ is continuous as a function of w .

$$\bar{g}_t(w) = \frac{\frac{k}{\mu_0} \frac{cM_s}{a} \frac{\partial \mathcal{L}}{\partial z}(z) + x_4 y_1}{\frac{k}{\mu_0} - x_4 y_1 \tilde{\alpha}(t) - \frac{k}{\mu_0} \tilde{\alpha}(t) \frac{cM_s}{a} \frac{\partial \mathcal{L}}{\partial z}(z)}.$$

z is well defined given (t, w) and is a continuous function of (t, w) . Hence we can restrict our attention to $\bar{g}_t(w)$ above as a function of z . In the above expression, the only term that could possibly be discontinuous as a function of w is

$$h(w) \triangleq x_4 y_1.$$

As $y_1(\cdot, \cdot)$ is a continuous function of (t, w) in D we only need to check the behaviour of $h(w)$ as y_1 varies. By (39), if $y_1 \geq 0$, $x_4 = 1$ and if $y_1 < 0$, $x_4 = 0$ (because $x_3 = 1$). Therefore

$$\lim_{y_1 \rightarrow 0^+} h(w) = \lim_{y_1 \rightarrow 0^-} h(w) = 0.$$

Hence, $f(\cdot, \cdot)$ satisfies Carathéodory's first condition for $t \in (-\delta_1, T)$.

2. Next we need to check whether the function $f(t, w)$ is measurable in t for each w .

- (a) For $t \in (-\delta_1, 0)$, $u(t) = 0$. Therefore for each w , $f(\cdot, w)$ is a continuous function of time t trivially.
- (b) For $t \geq 0$, $u(t) > 0$. This implies by (38) that $x_3 = 1$. Hence for each (t, w) , z and hence x_4 is fixed.

The numerators and denominators of $f_1(t, \cdot)$ and $f_2(t, \cdot)$ are both continuous functions of t and are well-defined $\forall (t, w) \in D$ which we saw before. Hence $f(t, \cdot)$ is a measurable function of t for each w .

Hence, $f(\cdot, \cdot)$ satisfies Carathéodory's second condition for $t \in (-\delta_1, T)$.

3. For each $t \in (-\delta_1, T)$, $\bar{g}(\cdot)$ is continuous as a function of w . The denominator of $\bar{g}(\cdot, \cdot)$ is bounded both above and below. The lower bound on the denominator of $\bar{g}(\cdot, \cdot)$ in D is

$$A = \frac{k}{\mu_0} \left(1 - \frac{(\alpha + G) M_s}{3a} - (\alpha + G) y_{max} \right) - (\alpha + G) \epsilon_1. \quad (50)$$

Therefore

$$|\bar{g}(t, w)| \leq \frac{1}{A} \left(\frac{k}{\mu_0} \frac{c M_s}{3a} + y_{max} + \epsilon_1 \right) \triangleq B.$$

Thus $g(\cdot, \cdot)$ is uniformly bounded in D . As $u(\cdot)$ is continuous as a function of t , $f(\cdot, \cdot)$ is also uniformly bounded in D because by (35) and (25)

$$|f_1(t, w)| \leq \frac{1 + (\alpha + G) B}{a} \sup_{t \in [0, T]} u(t) \quad (51)$$

$$|f_2(t, w)| \leq \left(\frac{M_s}{3a} + \left(\frac{(\alpha + G) M_s}{3a} - 1 \right) B \right) \sup_{t \in [0, T]} u(t) \quad (52)$$

By taking the upper-bound on $\|f(\cdot, \cdot)\|$ to be the larger of the values on the right hand sides of (51) and (52), we see that $f(\cdot, \cdot)$ satisfies Carathéodory's third condition for $(t, w) \in D$.

Hence by Theorem B.1.1, for $(t_0, w_0) = (0, (0, 0))$, there exists a solution through (t_0, w_0) .

• **Extension of the solution** (We now extend the solution through (t_0, w_0) , so that it is defined for all $t \in [0, T)$.)

According to Theorem B.2.1, the solution can be extended until it reaches the boundary of D . As $f(t, \zeta, y)$ is defined $\forall \zeta$, we only need to ensure that $y(t)$ does not reach the boundary of the set $(-\epsilon_1, y_{max} + \epsilon_1]$. We show this by proving that $0 \leq y(t) \leq y_{max} \forall t \in [0, T)$. This implies that the solution can be extended to the boundary of the time t interval.

1. We know that $y(t=0) = 0$. We will show that $y(t) > 0 \forall t \in (0, T)$. As $y_1(t=0) \leq y(t=0) = 0$ and $x_3(t=0) = 1$, we must have $x_4(t=0) = 0$. Therefore,

$$\dot{y}(t=0) = \frac{\frac{M_s}{a} \frac{k}{\mu_0} \left(\frac{\partial \mathcal{L}}{\partial z}(\zeta) - c \frac{\partial \mathcal{L}}{\partial z}(z) \right) + (\bar{\alpha} - \tilde{\alpha}(0)) \frac{M_s}{a} \frac{\partial \mathcal{L}}{\partial z}(\zeta) \frac{k}{\mu_0} \frac{c M_s}{a} \frac{\partial \mathcal{L}}{\partial z}(z)}{\frac{k}{\mu_0} - \tilde{\alpha}(0) \frac{k}{\mu_0} \frac{c M_s}{a} \frac{\partial \mathcal{L}}{\partial z}(z)} u(t=0) \quad (53)$$

Before showing $\dot{y}(0) > 0$ we prove a fact that is very important. We know that $\frac{\partial \mathcal{L}}{\partial z}(z)(1-c) > 0 \forall z$. We show that if G is small enough then $(\frac{\partial \mathcal{L}}{\partial z}(\zeta) - c \frac{\partial \mathcal{L}}{\partial z}(z)) > 0$ also ($\forall t$):

$$\begin{aligned} \frac{\partial \mathcal{L}}{\partial z}(\zeta) - c \frac{\partial \mathcal{L}}{\partial z}(z) &= \frac{\partial \mathcal{L}}{\partial z}(\zeta) - \frac{\partial \mathcal{L}}{\partial z}(z) + \frac{\partial \mathcal{L}}{\partial z}(z)(1-c) \\ &= \frac{\partial^2 \mathcal{L}}{\partial z^2}(\zeta) \frac{(\bar{\alpha} - \tilde{\alpha}(t))x_2}{a} + o((\bar{\alpha} - \tilde{\alpha}(t))^2) + \frac{\partial \mathcal{L}}{\partial z}(z)(1-c) \\ &= \frac{\partial^2 \mathcal{L}}{\partial z^2}(\zeta) \frac{(G + g(t))x_2}{a} + o((\bar{\alpha} - \tilde{\alpha}(t))^2) + \frac{\partial \mathcal{L}}{\partial z}(z)(1-c), \end{aligned}$$

where $o(\epsilon^2)$ includes terms of order higher than ϵ and satisfies $\lim_{\epsilon \rightarrow 0} \frac{o(\epsilon^2)}{\epsilon} = 0$. As y is bounded in D , x_2 is also bounded because the inverse transform

$(\zeta, y) \mapsto x_2$ is given by (43). As $\frac{\partial \mathcal{L}}{\partial z}(z)(1-c) > 0 \forall z, \exists G$ small enough so that

$$\frac{\partial \mathcal{L}}{\partial z}(\zeta) - c \frac{\partial \mathcal{L}}{\partial z}(z) > 0 \quad \forall (t, \zeta, y) \in D. \quad (54)$$

With the above inequality in hand, we can easily show $\dot{y}(t=0) > 0$. The denominator of $\dot{y}(t=0)$ is positive (which was seen before when we checked whether \bar{g} was well-defined), and the terms in the numerator are also positive by (54). Therefore $\dot{y}(t=0) > 0$.

As $\dot{y}(0) > 0, \exists T_1 > 0 \ni y(t) > 0 \forall t \in (0, T_1)$. If this were not true then we could form a sequence of time instants $t_k \rightarrow 0 \ni y(t_k) \leq 0$. Then

$$\lim_{t_k \rightarrow 0} \frac{y(t_k) - y(0)}{t_k - 0} = \lim_{t_k \rightarrow 0} \frac{y(t_k) - 0}{t_k} \leq 0$$

which contradicts $\dot{y}(0) > 0$.

Let T_1 denote the largest such time instant such that $y(t) > 0 \forall t \in (0, T_1)$. Suppose $T_1 < T$. Then $y(T_1) = 0$ by continuity of $y(\cdot)$. As $y(t) \geq y_1(t) \forall t, y_1(T_1) \leq 0$. At $t = T_1, x_3 = 1$ by (38) and hence $x_4(T_1) = 0$ by (39). Therefore

$$\dot{y}(T_1) = \frac{\frac{M_s}{a} \frac{k}{\mu_0} \left(\frac{\partial \mathcal{L}}{\partial z}(\zeta) - c \frac{\partial \mathcal{L}}{\partial z}(z) \right) + (\bar{\alpha} - \tilde{\alpha}(T_1)) \frac{M_s}{a} \frac{\partial \mathcal{L}}{\partial z}(\zeta) \left(\frac{k}{\mu_0} \frac{c M_s}{a} \frac{\partial \mathcal{L}}{\partial z}(z) \right)}{\frac{k}{\mu_0} - \tilde{\alpha}(T_1) \left(\frac{k}{\mu_0} \frac{c M_s}{a} \frac{\partial \mathcal{L}}{\partial z}(z) \right)} u(T_1).$$

Arguing exactly as in the case of $t = 0$ before, we show using (54) that

$$\dot{y}(T_1) > 0.$$

Therefore for some $\epsilon > 0$ sufficiently small (with $\epsilon < T_1$),

$$\begin{aligned}
y(T_1 - \epsilon) &= y(T_1) - \epsilon \dot{y}(T_1) + o(\epsilon^2) \\
&= 0 - \epsilon \dot{y}(T_1) + o(\epsilon^2) \\
&< 0,
\end{aligned}$$

which is a contradiction of the fact that $y(t) > 0 \forall t \in (0, T_1)$.

Hence $y(t) > 0 \forall t \in (0, T)$.

2. We now verify that $y(t) \leq \frac{\frac{k}{\mu_0} \frac{M_s(1-c)}{3a} + \frac{k}{\mu_0} \frac{M_s}{3a} \frac{2GM_s}{3a} (c+9C_1)}{1 - \frac{2GM_s}{3a}} + \frac{2GM_s^2}{3a} \triangleq y_{max}$.

As $u(t) > 0$ for $t \in (0, T)$, $x_3(t) = 1$ by (38). We proved that $y(t) > 0$ for $t \in (0, T)$ implying that $x_4(t) = 1$. The maximum value of y is achieved when $\dot{y}(t^*) = 0$ for some $t^* \geq 0$. The numerator of $\dot{y}(t^*)$ must be zero. Solving for $y_1(t^*)$ we get

$$y_1(t^*) = \frac{\frac{k}{\mu_0} \frac{M_s}{a} \left(\frac{\partial \mathcal{L}}{\partial z}(\zeta) - c \frac{\partial \mathcal{L}}{\partial z}(z) \right) + (\bar{\alpha} - \tilde{\alpha}(t^*)) \frac{M_s}{a} \frac{\partial \mathcal{L}}{\partial z}(\zeta) \frac{k}{\mu_0} \frac{cM_s}{a} \frac{\partial \mathcal{L}}{\partial z}(z)}{1 - (\bar{\alpha} - \tilde{\alpha}(t^*)) \frac{M_s}{a} \frac{\partial \mathcal{L}}{\partial z}(\zeta)}$$

As $\frac{\partial \mathcal{L}}{\partial z}(\zeta)$ is smooth, by Theorem B.3.1 we have

$$\begin{aligned}
\left| \frac{\partial \mathcal{L}}{\partial z}(\zeta) - \frac{\partial \mathcal{L}}{\partial z}(z) \right| &\leq C_1 |\zeta - z| \\
&= C_1 |\zeta - z| \\
&= C_1 2G \sup_{(t, \zeta, y) \in D} \left| \frac{x_2}{a} \right|, \tag{55}
\end{aligned}$$

$$\leq C_1 \frac{2GM_s}{a}. \tag{56}$$

(56) is obtained by noticing that $x_2 \leq M_s$ because $y \geq 0$. Hence

$$y_1(t^*) \leq \frac{\frac{k}{\mu_0} \frac{M_s}{a} \left(C_1 \frac{2GM_s}{a} + \frac{(1-c)}{3} \right) + \frac{2GM_s}{3a} \frac{k}{\mu_0} \frac{cM_s}{3a}}{1 - \frac{2GM_s}{3a}}$$

where we have made use of the following inequalities: $|\bar{\alpha} - \tilde{\alpha}| \leq 2G$; $|\frac{\partial \mathcal{L}}{\partial z}(z)| \leq \frac{1}{3}$; and $|\frac{\partial \mathcal{L}}{\partial z}(\zeta)| \leq \frac{1}{3}$. By (46),

$$y(t^*) \leq y_1(t^*) + M_s \sup_{(t, \zeta, y) \in D} |\mathcal{L}(\zeta) - \mathcal{L}(z)|.$$

As $\mathcal{L}(\zeta)$ is smooth, by Theorem B.3.1 we have

$$\begin{aligned} |\frac{\partial \mathcal{L}}{\partial z}(\zeta) - \frac{\partial \mathcal{L}}{\partial z}(z)| &\leq \left(\sup_{\zeta} |\frac{\partial \mathcal{L}}{\partial z}(\zeta)| \right) |\zeta - z| \\ &= \frac{1}{3} |\zeta - z| \\ &= \frac{1}{3} 2G \sup_{(t, \zeta, y) \in D} \left| \frac{x_2}{a} \right|, \end{aligned} \tag{57}$$

$$\leq \frac{1}{3} \frac{2GM_s}{a}. \tag{58}$$

Therefore,

$$\begin{aligned} y(t^*) &\leq y_1(t^*) + \frac{2GM_s^2}{3a} \\ &= \frac{\frac{k}{\mu_0} \frac{M_s(1-c)}{3a} + \frac{k}{\mu_0} \frac{M_s}{3a} \frac{2GM_s}{3a} (c + 9C_1)}{1 - \frac{2GM_s}{3a}} + \frac{2GM_s^2}{3a} \\ &= y_{max} \end{aligned}$$

Therefore the solution can be extended in time to the boundary of $[0, T)$. In the course of continuing the solutions, we also proved that $(M_s \mathcal{L}(\zeta(t)) - x_2(t)) > 0 \forall t \in (0, T)$.

• **Uniqueness**(We show the uniqueness of the solution.)

At each $t \geq 0$, $u(t) > 0$ implying $x_3 = 1$. As $y > 0$ for $t > 0$, $x_4 = 1$ for $t > 0$.

We concentrate on this case below. At $t = 0$, $x_4 = 0$ and the Lipschitz constants obtained in the following analysis can again be used to show uniqueness.

A defined by (50) is a lower bound for the denominator of $f_1(t, w)$. Let $w_a = (\zeta_a, y_a)$ and $w_b = (z_b, y_b)$, be any two points. As y_1 and z are functions of (t, ζ, y) , denote $y_1(t, \zeta_i, y_i) = y_{1_i}$ and $z(t, \zeta_i, y_i) = z_i$ $i = a, b$.

$$f_1(t, w_1) - f_1(t, w_2) = \frac{u(t) \frac{k}{\mu_0}}{\text{Den}(f_2(t, w_1)) \text{Den}(f_2(t, w_2))} (\bar{\alpha}(y_{1_a} - y_{1_b}) + \frac{k}{\mu_0} \frac{\bar{\alpha} c M_s}{a} \left(\frac{\partial \mathcal{L}}{\partial z}(z_a) - \frac{\partial \mathcal{L}}{\partial z}(z_b) \right))$$

Now we use the fact that y_1 and z are continuously differentiable functions of (t, ζ, w) to assert the existence of constants $K_1(t), K_2(t)$ (by Theorem B.3.1) such that

$$|y_{1_a} - y_{1_b}| \leq K_1(t) \|w_a - w_b\|, \quad (59)$$

$$|z_a - z_b| \leq K_2(t) \|w_a - w_b\|. \quad (60)$$

As $\frac{\partial \mathcal{L}}{\partial z}(z)$ is a smooth function of z and $|\frac{\partial \mathcal{L}}{\partial z}(z)| \leq \frac{1}{3}$ we have

$$|f_1(t, w_1) - f_1(t, w_2)| \leq \frac{u(t) \frac{k}{\mu_0}}{A^2} (\bar{\alpha} K_1(t) \|w_a - w_b\| \quad (61)$$

$$+ \frac{k}{\mu_0} \frac{\bar{\alpha} c M_s}{3a} K_2(t) \|w_a - w_b\|) = \bar{K}_1(t) \|w_a - w_b\| \quad (62)$$

where $\bar{K}_1(t)$ is only a function of time. For the vectorfield f_2 we have (after some simplification)

$$\begin{aligned}
f_2(t, w_1) - f_2(t, w_2) &= \frac{u(t)}{D(f_2(t, w_1))D(f_2(t, w_2))} \frac{k}{\mu_0} \left(\frac{M_s}{a} \left(\frac{k}{\mu_0} + \tilde{\alpha}(\bar{\alpha} - \tilde{\alpha})y_{1_a}y_{1_b} - \tilde{\alpha}y_{1_a} \right. \right. \\
&\quad \left. \left. + (\bar{\alpha} - \tilde{\alpha})y_{1_b} - \frac{\tilde{\alpha}(\bar{\alpha} - \tilde{\alpha})cM_s}{a} \left(\frac{k}{\mu_0} \frac{\partial \mathcal{L}}{\partial z}(z_a) \frac{\partial \mathcal{L}}{\partial z}(z_b) + y_{1_a} \frac{\partial \mathcal{L}}{\partial z}(z_b) + y_{1_b} \frac{\partial \mathcal{L}}{\partial z}(z_a) \right) \right. \right. \\
&\quad \left. \left. + \frac{kcM_s}{\mu_0 a} \left((\bar{\alpha} - \tilde{\alpha}) \frac{\partial \mathcal{L}}{\partial z}(z_a) - \tilde{\alpha} \frac{\partial \mathcal{L}}{\partial z}(z_b) \right) \right) \left(\frac{\partial \mathcal{L}}{\partial z}(\zeta_a) - \frac{\partial \mathcal{L}}{\partial z}(\zeta_b) \right) \\
&\quad - \frac{k}{\mu_0} \frac{cM_s}{a} \left(1 - \frac{\bar{\alpha}M_s}{a} \frac{\partial \mathcal{L}}{\partial z}(\zeta_b) \right) \left(\frac{\partial \mathcal{L}}{\partial z}(z_a) - \frac{\partial \mathcal{L}}{\partial z}(z_b) \right) - \left(1 - \frac{\bar{\alpha}M_s}{a} \frac{\partial \mathcal{L}}{\partial z}(\zeta_a) \right) (y_{1_a} - y_{1_b})
\end{aligned}$$

where $D(f_2(\cdot, \cdot))$ is the denominator of $f_2(\cdot, \cdot)$. We make use of the following bounds on some of the terms in the above equation

$$\frac{\partial \mathcal{L}}{\partial z}(\zeta) \leq \frac{1}{3}, \quad (63\text{-a})$$

$$\frac{\partial \mathcal{L}}{\partial z}(z) \leq \frac{1}{3}, \quad (63\text{-b})$$

$$y_{1_i} \leq y_{max} \quad i = a, b. \quad (63\text{-c})$$

As $\frac{\partial \mathcal{L}}{\partial z}(\zeta)$ is a smooth function of ζ , there exists a positive number C_1 (by Theorem B.3.1) such that

$$\left| \frac{\partial \mathcal{L}}{\partial z}(\zeta_a) - \frac{\partial \mathcal{L}}{\partial z}(\zeta_b) \right| \leq C_1 |\zeta_a - \zeta_b| \quad (64)$$

As $\frac{\partial \mathcal{L}}{\partial z}(z)$ is a smooth function of (\cdot, ζ, w) for each t , there exists a function $C_2(t)$ (by Theorem B.3.1) such that

$$\left| \frac{\partial \mathcal{L}}{\partial z}(z_a) - \frac{\partial \mathcal{L}}{\partial z}(z_b) \right| \leq C_2(t) \|w_a - w_b\| \quad (65)$$

Using the bounds (63-a - 63-c) and the Lipschitz inequalities (59), (60), (64) and (65), we get

$$\begin{aligned}
|f_2(t, w_1) - f_2(t, w_2)| &\leq \frac{u(t)}{A^2} \left(\left(\left(\frac{k}{\mu_0} \right)^2 \frac{M_s}{a} + \frac{(\alpha+G)2GM_s}{a} y_{max}^2 + \frac{k}{\mu_0} \frac{(\alpha+3G)M_s}{a} y_{max} \right. \right. \\
&\quad \left. \left. + \frac{(\alpha+G)2Gck}{\mu_0} \left(\frac{M_s}{a} \right)^2 \left(\frac{k}{\mu_0} \frac{1}{9} + \frac{2y_{max}}{3} \right) + \left(\frac{k}{\mu_0} \right)^2 \left(\frac{M_s}{a} \right)^2 c \left(\frac{\alpha+3G}{3} \right) \right) C_1 |\zeta_a - \zeta_b| \\
&+ \left(\frac{k}{\mu_0} \right)^2 \frac{cM_s}{a} \left(1 + \frac{(\alpha+G)M_s}{3a} \right) C_2(t) \|w_a - w_b\| + \frac{k}{\mu_0} \left(1 + \frac{(\alpha+G)M_s}{3a} \right) K_1(t) \|w_a - w_b\|
\end{aligned} \tag{66}$$

As $|\zeta_a - \zeta_b| \leq \|w_a - w_b\|$ we have

$$|f_2(t, w_1) - f_2(t, w_2)| \leq \frac{u(t)}{A^2} D(t) \|w_a - w_b\|. \tag{67}$$

where the function of time $D(t)$ is defined using (66). Hence by Theorem B.3.2, there exists atmost one solution in D .

For inputs $u(\cdot)$ with $u(t) < 0$ for $t \in (0, T)$, the same proof can be repeated to arrive at the conclusion that $(M_s \mathcal{L}(\zeta(t)) - x_2(t)) < 0 \forall t \in (0, T)$.

□

Suppose that an input $u(t) > 0$ for $t \in [0, T)$ has been applied to the system (21 - 24). Let

$$x_0 = (x_{10}, x_{20}) = \lim_{t \rightarrow T} (x_1, x_2)(t). \tag{68}$$

x_0 is well-defined because of Theorem B.2.1. Define (Figure 3.2).

$$u(T) = \lim_{t \rightarrow T} u(t) \tag{69}$$

$$u_1(T) = -u(T - t) \quad \text{for } t \in [0, T]. \tag{70}$$

Let the initial condition be x_0 as defined in (68). Then the next theorem claims that there exists a time $0 < T_1 < T$ such that $x_2(T_1) = M_s \mathcal{L} \left(\frac{x_1(T_1) + (\alpha+G)x_2(T_1)}{a} \right)$.

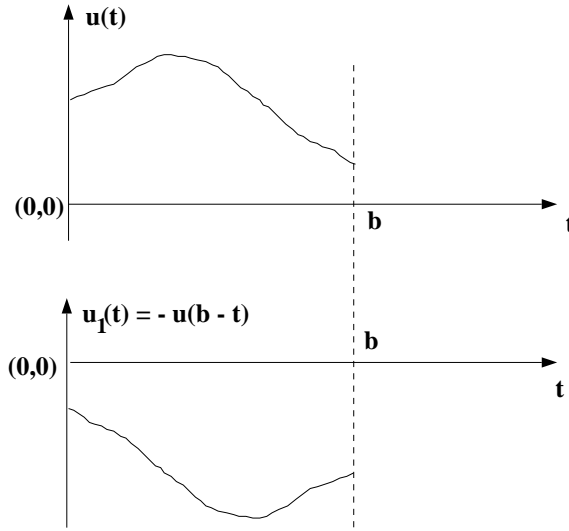


Figure 3.2: Sample signals $u(\cdot)$ and $u_1(\cdot)$.

In other words, the solution trajectory intersects with the anhyseretic curve in the (x_1, x_2) -plane at time $T_1 < T$.

Theorem 3.2.2 *Consider the system of equations (21 - 24). Let the initial condition $(x_1, x_2)(t = 0) = (x_{10}, x_{20})$ where (x_{10}, x_{20}) is defined by (68). Let the parameters satisfy (31 - 32) and the continuously differentiable function of time $g(\cdot) : [0, T) \rightarrow \mathbb{R}$ satisfy (27 - 30). Let $u(t)$ be a continuous function of t with $u(t) > 0$ for $t \in [0, T)$, and $u_1(t)$ be defined by (69 - 70). If $u_1(t)$ is the input to the system (21 - 24) for $t \in [0, T]$, then $\exists T_1 > 0$ such that $T_1 < T$ and $x_2(T_1) = M_s \mathcal{L}(\frac{x_1(T_1) + (\alpha + G)x_2(T_1)}{a})$.*

The proof of this theorem utilizes the same ideas as Theorem 2.2.2 that was proved in Chapter 2. It will be more complicated because of presence of the perturbation $g(\cdot)$ but as the proof of Theorem 3.2.1 showed, the ideas of the proofs in the unperturbed case essentially carry over to the perturbed case. The

only difference between Theorem 2.2.2 and Theorem 3.2.2 is that the parameters now have to satisfy the condition (30).

From this point until the end of this subsection, it is assumed that the parameters and $g(\cdot)$ satisfy conditions (27-32).

Claim 3.2.1 *If $u(t)$ does not change its sign $\forall t \in [l, m]$ and if $\tilde{x}(l), \check{x}(l)$ are two initial states of the system with $\tilde{x}_2(l) \geq \check{x}_2(l)$, then $\tilde{x}_2(t) \geq \check{x}_2(t) \forall t \in [l, m]$.*

Proof

Suppose for some $t \in [l, m]$, $\tilde{x}_2(t) < \check{x}_2(t)$. Then by continuity of the solution trajectories, $\exists t^* \in (l, t), \exists \tilde{x}_2(t^*) = \check{x}_2(t^*)$. Now $\dot{\tilde{x}}(t^*) = \dot{\check{x}}(t^*)$ by Equation (22). Hence $\forall t \geq t^*$, $\tilde{x}_2(t) = \check{x}_2(t)$. This contradicts our initial assumption.

□

Theorems 3.2.1 - 3.2.2 and Claim 3.2.1 lead to the following theorem.

Theorem 3.2.3 *Consider the system given by Equations (21-24), with input given by Equation (26) and $b \neq 0$. Suppose the $\frac{2\pi}{\omega}$ -periodic continuously differentiable function of time $g(\cdot) : \mathbb{R} \rightarrow \mathbb{R}$ and the parameters satisfy conditions (27-32).*

If $(x_1, x_2)(0) = (0, 0)$, then the Ω -limit set of the system is a periodic orbit with period $\frac{2\pi}{\omega}$.

Proof

The proof is identical to the one with $b = 0$ (Theorem 2.2.3 in Chapter 2).

□

The conclusion of the above theorem can be strengthened without changing the proof much by noticing that Theorems 3.2.1 - 3.2.2 and Claim 3.2.1 do not

need the input $u(\cdot)$ to be co-sinusoidal. In fact, any periodic input will do. Thus we have

Theorem 3.2.4 *Consider the system given by Equations (21–24) with $b \neq 0$. Suppose the T -periodic continuously differentiable function of time $g(\cdot) : \mathbb{R} \rightarrow \mathbb{R}$ and the parameters satisfy conditions (27 - 32). Let the input $u(\cdot) : \mathbb{R} \rightarrow \mathbb{R}$ be a continuous, T periodic function of time.*

If $(x_1, x_2)(0) = (0, 0)$, then the Ω -limit set of the system is a periodic orbit with period T .

Proof

The proof is identical to that of Theorem 3.2.3.

□

Denote the periodic solution of the perturbed magnetic system (21 - 24) with perturbation $g(\cdot)$ and input $u(\cdot)$ as $\bar{x}(\cdot)$. It is a two dimensional vector and a $T = \frac{2\pi}{\omega}$ periodic function. As in the method of proof outlined in the introduction define the sets $B = \{\phi \in \mathcal{C}([0, T], \mathbb{R}) : |\phi| \leq \beta_1; |\phi(t) - \phi(\bar{t})| \leq M_1|t - \bar{t}| \ \forall t, \bar{t} \in [0, T]\}$, $D = \{\psi \in \mathcal{C}([0, T], \mathbb{R}) : |\psi| \leq \beta_2; |\psi(t) - \psi(\bar{t})| \leq M_2|t - \bar{t}| \ \forall t, \bar{t} \in [0, T]\}$, where $\beta_1, \beta_2, M_1, M_2$ are positive constants. Let $\mathcal{P}_1, \mathcal{P}_2 : \mathcal{C}([0, T], \mathbb{R}^2) \rightarrow \mathcal{C}([0, T], \mathbb{R})$ denote the projection operators defined by $\mathcal{P}_1(f, g) = f$ and $\mathcal{P}_2(f, g) = g$.

Consider the mappings $\mathcal{G} : B \rightarrow \mathcal{C}([0, T], \mathbb{R}^2); g(\cdot) \mapsto \bar{x}(\cdot)$ and $\mathcal{H} : D \rightarrow \mathcal{C}([0, T], \mathbb{R}^2); h(\cdot) \mapsto \bar{y}(\cdot)$. We first show \mathcal{G} to be continuous.

Theorem 3.2.5 *\mathcal{G} is a continuous map.*

Proof Let the system (21 - 24) be represented by

$$\dot{x} = f(t, x, \tilde{\alpha}) ; \quad (t, x) \in D \subset \mathbb{R}^3$$

where $\tilde{\alpha} = \alpha - \frac{2bg(t)}{\mu_0}$, and D is an open set. The state x is 2-dimensional because the discrete states x_3 and x_4 are functions of x_1, x_2 and $u = U \cos(\omega t)$. Let the initial condition be $(x_1, x_2)(0) = (0, 0)$.

If $g_n \rightarrow g$ in the uniform norm over $[0, T]$ where T is the period of f , then $\tilde{\alpha}_n \rightarrow \tilde{\alpha}$. Consider the sequence of systems $\dot{x} = f_n(t, x) = f(t, x, \tilde{\alpha}_n)$. As f is continuous in $\tilde{\alpha}$, $f_n \rightarrow f(t, x, \tilde{\alpha})$ in the uniform norm if $\tilde{\alpha}_n \rightarrow \tilde{\alpha}$ (Theorem B.4.1). The solutions of each of the systems $\{f_n\}$ and f exist and is unique for $t \in [0, T]$. Then by Theorem B.4.2, the solutions $\phi_n(t)$ of $\dot{x} = f_n(t, x)$ converge uniformly to $\phi(t)$ the solution of $\dot{x} = f(t, x, \tilde{\alpha})$ for $t \in [0, T]$.

Consider the time interval $[T, 2T]$. We have shown that $\phi_n(T) \rightarrow \phi(T)$. Then again by Theorem B.4.2, $\phi_n(t) \rightarrow \phi(t)$ for $t \in [T, 2T]$. Thus we can keep extending the solutions $\phi_n(t)$ and $\phi(t)$ and obtain uniform convergence over any interval $[mT, (m+1)T]$ where $m > 0$. Therefore, for each m and $\epsilon > 0$, there exists $N(m) > 0$ such that $|\phi_n - \phi| < \frac{\epsilon}{3} \quad \forall n \geq N(m)$.

By Theorem 3.2.4 there exist Ω limit sets that are periodic orbits \bar{x}_n of the systems $\dot{x} = f_n(t, x)$ and \bar{x} of the system $\dot{x} = f(t, x, \tilde{\alpha})$. Hence for each n and $\epsilon > 0$, there exists $M \geq 0$ such that $|\bar{x}_n - \phi_n| < \frac{\epsilon}{3}$ and $|\bar{x} - \phi| < \frac{\epsilon}{3} \quad \forall m \geq M$ and $t \in [mT, (m+1)T]$.

Hence for all $n \geq N(M)$ and $t \in [mT, (m+1)T]$ where $m \geq M$, we have $|\bar{x}_n - \bar{x}| \leq |\bar{x}_n - \phi_n| + |\phi_n - \phi| + |\bar{x} - \phi| < \epsilon$. Hence \mathcal{G} is a continuous map.

□

Analysis of the uncoupled mechanical system

In this subsection, we consider the mechanical system with periodic perturbation given by Equation (25). We assume the homogenous system (that is, (25) with $h(t) = 0$) to be asymptotically stable. The relevant results are collected in the appendix.

Theorem 3.2.6 *Consider the system (25). If the eigenvalues of A have negative real parts, the initial state is at the origin and $h(\cdot)$ is an T periodic function, then (25) has an T periodic solution that is asymptotically orbitally stable.*

Proof This follows from Lemma D.0.1 and Theorem D.0.3 in the appendix.

□

Theorem 3.2.7 *If the eigenvalues of A have negative real parts, then \mathcal{H} is a continuous map.*

Proof This again follows from Lemma D.0.1 and Theorem D.0.3.

□

3.2.2 Analysis of the magnetostriction model

We now prove the existence of an Ω -limit set that is a periodic orbit for the magnetostriction model.

Let D_1 denote the range of $\mathcal{P}_2 \circ \mathcal{G}$ and B_1 denote the range of $\mathcal{P}_1 \circ \mathcal{H}$. Thus $\mathcal{P}_2 \circ \mathcal{G} : B \mapsto D_1$ and $\mathcal{P}_1 \circ \mathcal{H} : D \mapsto B_1$.

Lemma 3.2.2 *Suppose the parameters of the magnetic system satisfy*

$$\frac{\alpha M_s}{3a} < 1, \quad (71)$$

$$0 < c < 1, \quad (72)$$

$$k > 0. \quad (73)$$

There exists a $\bar{b} > 0$ such that if $|b| \leq \bar{b}$ then $\mathcal{P}_2 \circ \mathcal{G} : B_1 \mapsto D_1$ and $\mathcal{P}_1 \circ \mathcal{H} : D_1 \mapsto B_1$.

Proof First we show that the sets B_1 and D_1 have the same structure as that of B and D respectively. Then we choose \bar{b} so that the domains and ranges of \mathcal{G} and \mathcal{H} are suitably adjusted. Choose $\beta_1 = M_s$ and $M_1 = \frac{M_s}{3a}U$ in the definition of the set D .

By Claim 3.2.1, the elements of D_1 are uniformly bounded by M_s . Let $\bar{x} = \mathcal{G}g$. Therefore $\mathcal{P}_2 \circ \mathcal{G}g = \bar{x}_2$. Now $\bar{x}_2(t_2) - \bar{x}_2(t_1) = \int_0^1 \dot{\bar{x}}_2(t_1 + s(t_2 - t_1))(t_2 - t_1) ds$ by the Mean Value Theorem. As the parameters of the system (21 - 24) satisfy the conditions (27 - 31), the vector field $f(t, x)u(t)$ is uniformly bounded. Therefore $|\bar{x}_2(t_1) - \bar{x}_2(t_2)| \leq M_1|t_2 - t_1|$. Thus D_1 has the same structure of D .

Let $\bar{y} = \mathcal{H}h$. Therefore $\bar{y}_1 = \mathcal{P}_1 \circ \mathcal{H}h$. The elements of B_1 are uniformly bounded because \mathcal{H} is linear in h^2 and the functions $h \in D$ are uniformly bounded. $|\bar{y}_1| \leq |\bar{y}| \leq |\mathcal{P}_1 \circ \mathcal{H}|M_s^2 = \beta_2$. We need to choose \bar{b} so that $G = \alpha - \frac{2\bar{b}g_{max}}{\mu_0}$ (with $g_{max} = \sup_t |g(t)|$) defined in Theorem 3.2.1 satisfies (29) and (30). This is possible by Lemma 3.2.1.

Now $\bar{y}_1(t_2) - \bar{y}_1(t_1) = \int_0^1 \dot{\bar{y}}_1(t_1 + s(t_2 - t_1))(t_2 - t_1) ds$ by the Mean Value Theorem. $|\dot{\bar{y}}| \leq |A|\beta_2 + b\mathcal{V}\beta_1^2 = M_2$. Therefore $|\bar{y}_1(t_2) - \bar{y}_1(t_1)| \leq M_2|t_2 - t_1|$. Thus B_1 has the same structure of B .

Our choice of $\bar{b} > 0$ ensures that if $b \leq \bar{b}$ then $\mathcal{P}_2 \circ \mathcal{G} : B_1 \mapsto D_1$ and $\mathcal{P}_1 \circ \mathcal{H} : D_1 \mapsto B_1$.

□

We now prove the main theorem of this Section. The system rewritten in terms of the state variable form is

$$\dot{x}_1 = u, \quad (74)$$

$$\dot{x}_2 = \left(\frac{\frac{kx_3}{\mu_0} \frac{cM_s}{a} \frac{\partial \mathcal{L}}{\partial z}(z) + x_4 M_s \left(\mathcal{L}(z) - \frac{x_2}{M_s} \right)}{\frac{kx_3}{\mu_0} - x_4 M_s \left(\mathcal{L}(z) - \frac{x_2}{M_s} \right) \tilde{\alpha}(t) - \frac{kx_3}{\mu_0} \tilde{\alpha}(t) \frac{cM_s}{a} \frac{\partial \mathcal{L}}{\partial z}(z)} \right) u, \quad (75)$$

$$z = \frac{x_1 + \tilde{\alpha}x_2}{a}, \quad (76)$$

$$x_3 = \text{sign}(u), \quad (77)$$

$$x_4 = \begin{cases} 0 & : x_3 < 0 \text{ and } \coth(z) - \frac{1}{z} - \frac{x_2}{M_s} > 0, \\ 0 & : x_3 > 0 \text{ and } \coth(z) - \frac{1}{z} - \frac{x_2}{M_s} < 0, \\ 1 & : \text{otherwise,} \end{cases} \quad (78)$$

$$\dot{y} = Ay - \frac{b\mathcal{V}}{m_{eff}} x_2^2, \quad (79)$$

where $\tilde{\alpha} = \alpha - \frac{2by_1}{\mu_0}$; $y = \begin{bmatrix} y_1 & y_2 \end{bmatrix}^T$; $A = \begin{bmatrix} 0 & 1 \\ -d & -c_1 \end{bmatrix}$.

Theorem 3.2.8 *Consider the model for magnetostriction given by Equations (74 - 79). Suppose the input $u(\cdot) : \mathbb{R} \rightarrow \mathbb{R}$ is a continuous and T periodic function of time. Suppose the matrix A has eigenvalues with negative real parts*

and the parameters satisfy conditions (71-73). If the initial condition is at the origin, then there exists $\bar{b} > 0$ such that $\forall b$ with $|b| \leq \bar{b}$, the Ω limit set of the solution trajectory is a periodic orbit with period T .

Proof We choose \bar{b} as in Lemma 3.2.2. The sets B_1 and D_1 are compact and convex by Lemma A.0.1. Then $B_1 \times D_1$ is compact in the uniform product norm by Theorem A.0.3. Obviously it is also convex.

Let Ψ be defined as, $\Psi : B_1 \times D_1 \rightarrow B_1 \times D_1; \Psi(x_2, y_1) = (\mathcal{P}_1 \circ \mathcal{H}(x_2), \mathcal{P}_2 \circ \mathcal{G}(y_1))$. Then Ψ is continuous because $\mathcal{P}_2 \circ \mathcal{G}$ and $\mathcal{P}_1 \circ \mathcal{H}$ are continuous by Theorems 3.2.5 and 3.2.7, and the continuity of the projection operator.

Then by the Schauder Fixed Point Theorem A.0.8, there exists a limit point of the mapping Ψ in the set $B_1 \times D_1$. Since the elements of the sets B_1, D_1 are projections of Ω -limit sets of trajectories starting at the origin, it follows that the limit point of the mapping Ψ in the set $B_1 \times D_1$, is the projection of the Ω limit set of the trajectory starting at the origin.

Thus the Ω -limit sets of the state variables x_2 and y_1 are periodic with period T . But $(y_1, y_2) = \mathcal{G}x_2$ and hence by Theorem 3.2.6, the Ω -limit set of (y_1, y_2) is a periodic orbit with period T . Also $(x_1, x_2) = \mathcal{H}y_1$ and by Theorem 3.2.4, the Ω -limit set of (x_1, x_2) is a periodic orbit with period T .

□

3.3 The magnetostrictive actuator in an electrical network

In the previous section, we proved that the solution trajectory of the magnetostriction model has a periodic orbit with period T as its Ω limit set when the

input $\dot{H}(\cdot)$ is periodic in time with period T . In a practical situation, usually a voltage source is used to provide the energy input. We now show that the conclusions of the last section hold with voltage input.

By Maxwell's laws of electromagnetism, the *induced electro-motive force* in a coil wound on the magnetostrictive rod is given by

$$E_{emf} = \oint \mathbf{E}(x) \cdot d\mathbf{l} = \int_S -\frac{d\mathbf{B}}{dt}(y) \cdot d\mathbf{s},$$

where $\mathbf{E}(x)$ is the electric field at any point x , $d\mathbf{l}$ is a length element, and S is the total surface area of the magnetostrictive rod bounded by the coil. $\mathbf{B}(y)$ is the magnetic flux density at any point y in the magnetostrictive rod. As we have assumed the magnetic flux density to be uniform in the rod (equal to B) and directed along the axis of the rod, we have

$$E_{emf} = -\frac{dB}{dt}NA$$

where N is the number of turns of the coil, and A is the area of cross-section of the magnetostrictive rod. If $V(t)$ is the voltage applied to the coil at time t , then we have

$$V(t) = \frac{dB}{dt}(t)NA$$

The other Maxwell's laws do not yield anything interesting mainly because of our simplifying assumptions. We have assumed the magnetic field at any point x in the rod – $\mathbf{H}(x)$ to be uniform ($= H$) and directed along the axis which implies

$$\nabla \times \mathbf{H}(x) = 0.$$

There are no true charges in the rod implying

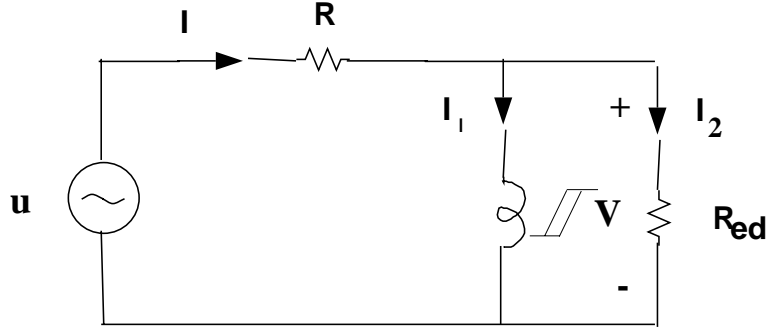


Figure 3.3: Schematic diagram of a thin magnetostrictive actuator in a resistive circuit.

$$\nabla \cdot \mathbf{D}(x) = 0,$$

where $\mathbf{D}(x)$ is the electric displacement vector at a point x in the rod. As eddy currents are assumed to be present in the rod due to its finite resistivity, then we have to incorporate a resistor R_{eddy} in parallel with the magnetostrictive element as seen in Section 3.1. If R_{lead} is the resistance of the coil winding, then the full circuit will be as shown in Figure 3.3.

Though physically it is impossible to separate the resistor representing the eddy current losses from the magnetostrictive element and the coil resistance in Figure 3.3, lets first assume that they are not present for ease of analysis. Thus we set $R_{eddy} = \infty$ and $R_{lead} = 0$. Let the state variables be defined as in the last section. In addition, define $r = B$. Hence

$$r = \frac{x_1 + x_2}{\mu_0}. \quad (80)$$

We can now rewrite the state equations with the state variables $(r, x_2, y, \dot{y}$ as

$$\dot{r} = \frac{V}{NA}, \quad (81)$$

$$\dot{x}_2 = \left(\frac{\frac{kx_3}{\mu_0} \frac{cM_s}{a} \frac{\partial \mathcal{L}}{\partial z}(z) + x_4 M_s \left(\mathcal{L}(z) - \frac{x_2}{M_s} \right)}{\frac{kx_3}{\mu_0} - x_4 M_s \left(\mathcal{L}(z) - \frac{x_2}{M_s} \right) \tilde{\alpha}(t) - \frac{kx_3}{\mu_0} \tilde{\alpha}(t) \frac{cM_s}{a} \frac{\partial \mathcal{L}}{\partial z}(z)} \right) u, \quad (82)$$

$$z = \frac{r}{\mu_0} + \frac{(\tilde{\alpha} - 1)x_2}{a}, \quad (83)$$

$$x_3 = \text{sign}\left(\frac{\dot{r}}{\mu_0} - \dot{x}_2\right), \quad (84)$$

$$x_4 = \begin{cases} 0 & : x_3 < 0 \text{ and } \coth(z) - \frac{1}{z} - \frac{x_2}{M_s} > 0, \\ 0 & : x_3 > 0 \text{ and } \coth(z) - \frac{1}{z} - \frac{x_2}{M_s} < 0, \\ 1 & : \text{otherwise,} \end{cases} \quad (85)$$

$$\dot{y} = Ay - \frac{b\mathcal{V}}{m_{eff}} x_2^2, \quad (86)$$

where $\tilde{\alpha} = \alpha - \frac{2by_1}{\mu_0}$; $y = \begin{bmatrix} y_1 & y_2 \end{bmatrix}^T$; $A = \begin{bmatrix} 0 & 1 \\ -d & -c_1 \end{bmatrix}$.

Theorem 3.2.8 can now be written as:

Theorem 3.3.1 *Consider the model for magnetostriction given by Equations (74 - 79). Suppose the input $V(\cdot) : \mathbb{R} \rightarrow \mathbb{R}$ is a continuous and T periodic function of time. Suppose the matrix A has eigenvalues with negative real parts and the parameters satisfy conditions (71-73). If the initial state is at the origin then there exists $\bar{b} > 0$ such that $\forall b$ with $|b| \leq \bar{b}$, the Ω limit set of the solution trajectory is a periodic orbit with period T .*

Proof

The mapping $\psi : \mathbb{R}^2 \rightarrow \mathbb{R}^2$ defined by

$$\psi(r, x_2) = (x_1, x_2)$$

is a diffeomorphism because

$$\frac{\partial \psi}{\partial (r, x_2)}(r, x_2) = \begin{bmatrix} \frac{1}{\mu_0} & -1 \\ 0 & 1 \end{bmatrix}$$

and hence Determinant $\left(\frac{\partial \psi}{\partial (r, x_2)}(r, x_2)\right) = \frac{1}{\mu_0}$. As $(r, x_2)(t = 0) = (0, 0)$, we have $x_1(t = 0) = 0$. Thus in the transformed co-ordinates, the initial state is at the origin which is on the anhyseretic curve. The existence, extension and uniqueness of trajectories is shown exactly as in Theorem 3.2.1 and 3.2.2. We choose the set D as in Theorem 3.2.1 and 3.2.2 to prove the existence of a solution at the origin. As the denominator of \dot{x}_2 is positive for all points in D , we have $\text{sign}(\dot{x}_2) = \text{sign}(\dot{x}_1)$. This implies $\text{sign}(\dot{r}) = \text{sign}(\dot{x}_1)$. Thus we can replace the condition (84) with

$$x_3 = \text{sign}(V). \tag{87}$$

With this modification, the proof of the Ω -limit set of the solution trajectory being a periodic orbit with period T is exactly the same as that of Theorem 3.2.8.

□

3.3.1 The magnetostrictive actuator in an electrical network

In this subsection, we consider the magnetostrictive actuator to be part of an R-L-C network as shown in Figure 3.4. The eddy current and lead resistors in Figure 3.3 can be thought of as part of this network. Our aim is to show that if a periodic input voltage signal is applied to the whole system, then the solution trajectory of the system with the initial state at the origin tends towards a periodic orbit. The methodology of the proof follows the same scheme as in the previous section.

1. We consider the output of the network to be a voltage signal which is applied to the magnetostrictive actuator. First consider the voltage signal to be T -periodic in time. Then the solution of the magnetostrictive actuator model has an Ω limit that is a T -periodic signal as was shown in Theorem 3.3.1. The output of the magnetostrictive actuator model is the current through the actuator (which we can assume to be a state variable in the actuator model).
2. Next we consider the network as being applied an external periodic voltage input and the output of the magnetostrictive actuator system which is the current through the actuator as mentioned before. If the output of the magnetostrictive actuator model is a T -periodic signal in time, then the network (with some conditions on the parameters defining it) has an Ω -limit set that is a T -periodic orbit by Theorem D.0.3.
3. Finally, we consider the combined actuator plus network system with voltage input. We show via the Schauder fixed point theorem, that there is a

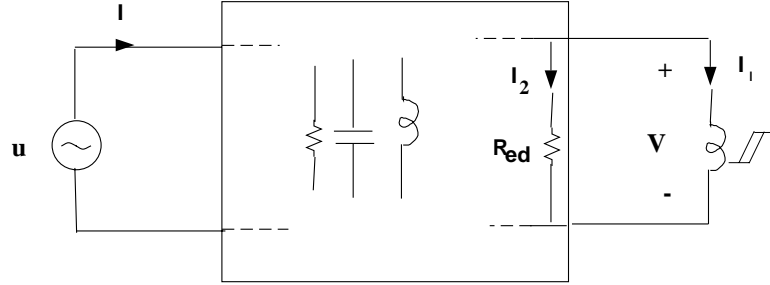


Figure 3.4: Schematic diagram of an magnetostrictive element as a part of a R-L-C network.

periodic solution for the interconnected system.

Consider the magnetostriction model to be described by the equation

$$\dot{x} = f(t, x, w_1). \quad (88)$$

where $x = (x_1, x_2, y_1, y_2)$. w_1 denotes the voltage across the magnetostrictive element. Assume $x(t = 0) = (0, 0, 0, 0)$. The external R-L-C circuit can be described by the following linear equation

$$\dot{w} = Cw + Eu + Fx_1 \quad w(0) = 0. \quad (89)$$

where, $w \in \mathbb{R}^m$, $u \in \mathbb{R}$, w_1 is the voltage across the magnetostrictive element. As the current thorough the magnetostrictive element I_1 is related to the magnetic field x_1 via a constant, that is

$$x_1 = KI_1,$$

where K is called the coil factor, we consider x_1 as an input to the network. The input voltage to the network is assumed to be

$$u(t) = U \cos(\omega t). \quad (90)$$

As mentioned earlier, we consider the uncoupled circuits with periodic perturbation, $g(\cdot), h(\cdot)$ with period $\frac{2\pi}{\omega}$. The uncoupled systems are

$$\dot{x} = f(t, x, g); \quad x(t=0) = (0, 0, 0, 0) \quad (91)$$

$$\dot{w} = Cw + Eu + Fh \quad w(t=0) = (0, \dots, 0) \quad (92)$$

Denote the Ω limit set of the uncoupled magnetostrictive system (91) as $\bar{x}(\cdot)$. Theorem 3.2.4 shows that it exists and is a $T = \frac{2\pi}{\omega}$ -periodic function of time. For the network we have the following theorem.

Theorem 3.3.2 *Suppose the matrix E has eigenvalues with negative real parts. If $u(\cdot), h(\cdot) : \mathbb{R} \rightarrow \mathbb{R}$ are continuous and T -periodic functions of time, then the solution of (92) has a periodic orbit of period T as its Ω limit set.*

Proof The proof follows from Theorem D.0.3.

□

Define the sets $B = \{\phi \in \mathcal{C}([0, T], \mathbb{R}) : |\phi| \leq \beta_1; |\phi(t) - \phi(\bar{t})| \leq M_1|t - \bar{t}| \quad \forall t, \bar{t} \in [0, T]\}$, $D = \{\psi \in \mathcal{C}([0, T], \mathbb{R}) : |\psi| \leq \beta_2; |\psi(t) - \psi(\bar{t})| \leq M_2|t - \bar{t}| \quad \forall t, \bar{t} \in [0, T]\}$, where $\beta_1, \beta_2, M_1, M_2$ are positive constants. Let $\mathcal{P}_1 : \mathcal{C}([0, T], \mathbb{R}^4) \rightarrow \mathcal{C}([0, T], \mathbb{R})$ and $\mathcal{P}_2 : \mathcal{C}([0, T], \mathbb{R}^m) \rightarrow \mathcal{C}([0, T], \mathbb{R})$ denote the projection operators defined by $\mathcal{P}_1(f) = f_1$ and $\mathcal{P}_2(g) = g_1$.

Consider the mappings $\mathcal{G} : B \rightarrow \mathcal{C}([0, T], \mathbb{R}^4); g(\cdot) \mapsto \bar{x}(\cdot)$ and $\mathcal{H} : D \rightarrow \mathcal{C}([0, T], \mathbb{R}^m); h(\cdot) \mapsto \bar{y}(\cdot)$. We first show \mathcal{G} and \mathcal{H} to be continuous.

Theorem 3.3.3 *Suppose the parameters of the magnetic system satisfy conditions (71 - 73). If $y_{max} = \sup_t |y(t)|$, and $G = \frac{2by_{max}}{\mu_0}$, then assume that G satisfies (29) and (30). Further assume that E has eigenvalues with negative real parts. Then \mathcal{G} and \mathcal{H} are continuous.*

Proof Consider the magnetostrictive system given by Equation (91).

Suppose $g_n \rightarrow g$ in the uniform norm over $[0, T]$ where T is the period of u . Consider the sequence of systems $\dot{x} = f_n(t, x) = f(t, x, g_n)$. As f is continuous in g , $f_n \rightarrow f$ in the uniform norm if $g_n \rightarrow g$ (Theorem B.4.1). The solutions of each of the systems $\{f_n\}$ and f exist and is unique for $t \in [0, T]$. Then by Theorem B.4.2, the solutions $\phi_n(t)$ of $\dot{x} = f_n(t, x)$ converge uniformly to $\phi(t)$ the solution of $\dot{x} = f(t, x, g)$ for $t \in [0, T]$.

Consider the time interval $[T, 2T]$. We have shown that $\phi_n(T) \rightarrow \phi(T)$. Then again by Theorem B.4.2, $\phi_n(t) \rightarrow \phi(t)$ for $t \in [T, 2T]$. Thus we can keep extending the solutions $\phi_n(t)$ and $\phi(t)$ and obtain uniform convergence over any interval $[mT, (m+1)T]$ where $m > 0$. Therefore, for each m and $\epsilon > 0$, there exists $N(m) > 0$ such that $|\phi_n - \phi| < \frac{\epsilon}{3} \quad \forall n \geq N(m)$.

By Theorem 3.3.1 there exist asymptotically orbitally stable periodic orbits \bar{x}_n of the systems $\dot{x} = f_n(t, x)$ and \bar{x} of the system $\dot{x} = f(t, x, g)$. Hence for each $\epsilon > 0$, there exists $M \geq 0$ such that $|\bar{x}_n - \phi_n| < \frac{\epsilon}{3}$ and $|\bar{x} - \phi| < \frac{\epsilon}{3} \quad \forall m \geq M$ and $t \in [mT, (m+1)T]$.

Therefore for all $n \geq N(M)$ and $t \in [mT, (m+1)T]$ where $m \geq M$, we have $|\bar{x}_n - \bar{x}| \leq |\bar{x}_n - \phi_n| + |\phi_n - \phi| + |\bar{x} - \phi| < \epsilon$. Hence \mathcal{G} is a continuous map.

As E has eigenvalues with negative real parts, the fact that \mathcal{H} is continuous follows from Lemma D.0.1 and Theorem D.0.3.

□

Let D_1 denote the range of $\mathcal{P}_1 \circ \mathcal{G}$ and B_1 denote the range of $\mathcal{P}_2 \circ \mathcal{H}$. Thus $\mathcal{P}_1 \circ \mathcal{G} : B \mapsto D_1$ and $\mathcal{P}_2 \circ \mathcal{H} : D \mapsto B_1$.

Lemma 3.3.1 $\mathcal{P}_1 \circ \mathcal{G} : B_1 \mapsto D_1$ and $\mathcal{P}_2 \circ \mathcal{H} : D_1 \mapsto B_1$.

Proof The proof is similar to that of Lemma 3.2.2.

□

Theorem 3.3.4 *Consider the systems (88) and (89) with input given by Equation (90). Suppose the matrix E has no eigenvalues that are purely imaginary with value $\frac{2\pi}{\omega}i$. Suppose the parameters satisfy conditions (71-73) with the magnetostriction constant $b \leq \bar{b}$ chosen so that $G = \frac{2by_{max}}{\mu_0}$ (where $y_{max} = \sup_t y(t)$) satisfies (29) and (30). Then the solution trajectory has an Ω limit set that is a periodic orbit.*

Proof The sets B_1 and D_1 are compact and convex by Lemma A.0.1. Then $B_1 \times D_1$ is compact in the uniform product norm by Theorem A.0.3. Obviously it is also convex.

Let Ψ be defined as, $\Psi : B_1 \times D_1 \rightarrow B_1 \times D_1; \Psi(x_1, w_1) = (\mathcal{P}_2 \circ \mathcal{H}(x_1), \mathcal{P}_1 \circ \mathcal{G}(w_1))$. Then Ψ is continuous because $\mathcal{P}_1 \circ \mathcal{G}$ and $\mathcal{P}_2 \circ \mathcal{H}$ are continuous by Theorem 3.3.3 and the continuity of the projection operator.

Then by the Schauder Fixed Point Theorem A.0.8, there exists a limit point of the mapping Ψ in the set $B_1 \times D_1$. This gives us the periodicity of the two state variables x_1 and w_1 . Now since $w = \mathcal{H}x_1$ and $x = \mathcal{G}w_1$, by Theorem 3.3.1 (x, w) is a periodic orbit. Thus the solution trajectory of the system has an Ω limit set that is a periodic orbit.

□

Chapter 4

Parameter Estimation

The magnetostrictive actuator model developed in the last Chapter has several parameters that need to be identified before the model can be used for simulation purposes. A schematic of the circuit used for the identification purpose is shown in Figure (4.1). Essentially, it is the magnetostrictive actuator connected to a power source. The parameters to be found are:

- R_{lead} – lead resistance parameter.
- R_{eddy} – eddy current parameter.
- α, b, a, M_s – non-hysteretic magnetic parameters.
- c, k – hysteretic magnetic parameters.
- c_1 – mechanical dynamic losses parameter.
- m_{eff} – inertia parameter.
- d – elasticity parameter.
- F – prestress parameter.

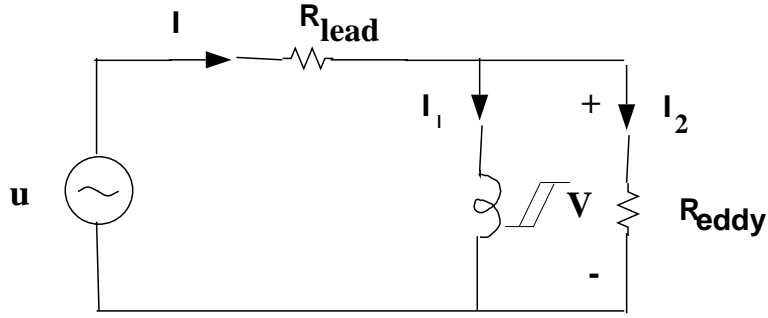


Figure 4.1: Schematic diagram of the circuit used for the identification of parameters.

As each of the parameters have different origin, we can systematically identify each of them by doing specific experiments. First, R_{lead} can be measured using an ohmmeter. The value of the saturation magnetization M_s can be obtained from the manufacturer. To estimate the rest of the parameters, the two proposed experiments are as follows.

1) We apply a sinusoidal current input of a very low frequency (say 0.5 Hz) to the actuator, and measure the voltage, displacement of the actuator as a function of time. With the same set up, we repeat the same experiment, keeping the maximum amplitude of the input current constant for atleast two different frequencies. We also repeat the 0.5 Hz experiment with a known mechanical load applied to the actuator. This experiment leads to the evaluation of c , k , m_{eff} , c_1 , R_{eddy} as explained in the next section.

2) In this experiment, we would like to obtain the anhysteretic displacement vs current curve for the actuator. To obtain the anhysteretic displacement for a particular current I , we apply a decaying alternating current with a D.C bias of I to the actuator. Further processing of the experimental data as described in the next section leads to the evaluation of F , d , b , a , α .

4.1 Algorithm for parameter estimation from experimental data

First, we measure R_{lead} that accounts for the lead resistance using an ohm-meter. Another quantity that needs to be evaluated separately by another experiment is the saturation magnetization M_s for the rod actuator. The manufacturer usually publishes this data or it could also be determined using Graham's method [36]. Once this has been accomplished, then the procedure for evaluating the rest of the parameters is as follows.

Step 1: R_{eddy} needs to be found first as it is critical to the rest of the identification scheme. In one cycle, the energy supplied by the source is given by

$$\mathcal{E} = \oint u(t) I(t) dt. \quad (1)$$

The losses in the resistor R_{lead} are

$$E_1 = \oint I^2 R_{lead} dt. \quad (2)$$

The losses due to mechanical damping is given by

$$E_2 = \oint c_1 \dot{x}^2 dt. \quad (3)$$

The eddy current losses are given by

$$E_3 = \oint \frac{(u(t) - I(t) R_{lead})^2}{R_{eddy}} dt. \quad (4)$$

Let \mathcal{H} be the loss due to magnetic hysteresis in one cycle. Then by (14)

$$\mathcal{E} = E_1 + E_2 + E_3 + \mathcal{H}. \quad (5)$$

In the above equation, the unknowns are R_{eddy} , c_1 and \mathcal{H} . A straight forward approach to estimating the constants would be to take several measurements and then use a *least squares* approach. By a *measurement*, we mean the determination of the quantities $u(t)$, $I(t)$, and $\dot{x}(t)$ for one cycle.

Obviously, we need to keep \mathcal{H} a constant in each measurement because it is not known apriori how it varies with the input current/voltage. Now \mathcal{H} is determined by the maximum and minimum values of the (applied) magnetic field H . As H is directly proportional to I_1 , we need to maintain I_1 a constant for each measurement. It can be seen by a simple calculation that even if the inductor in Figure 3.1) is linear, it is impossible to maintain I_1 between the same limits if the measurements are done at different frequencies. Thus we can obtain c_1 and R_{eddy} for each frequency by the calculations described below.

If a large number of measurements is made then we can determine the unknown quantities as follows. After the n th measurement, compute the quantities: $x_1(n) = \oint \dot{x}^2 dt$ and $x_2(n) = \oint (u(t) - I(t) R_{lead})^2 dt$. Let

$$\begin{aligned} \kappa &= \begin{bmatrix} c_1 \\ \frac{1}{R_{eddy}} \\ \mathcal{H} \end{bmatrix}, \\ Z(n) &= \mathcal{E}(n) - E_1(n), \\ X^T(n) &= [x_1(n), x_2(n), 1]. \end{aligned}$$

Define

$$Z = \begin{bmatrix} Z(1) \\ \vdots \\ Z(k) \end{bmatrix}; \quad X = \begin{bmatrix} X^T(1) \\ \vdots \\ X^T(k) \end{bmatrix}.$$

Therefore

$$Z = X \kappa. \quad (6)$$

If $X^T X$ is non-singular, then by the least-squares theorem E.0.4 the best estimate for the parameter vector κ is given by

$$\hat{\kappa} = (X^T X)^{-1} X^T Z. \quad (7)$$

If it is too difficult to maintain $u-I R$ between the same maximum and minimum values for each measurement, then another way of determining R_{eddy} is from theory. It is shown in Appendix F that if the resistivity of the material is ρ , then we can calculate the theoretical value of the eddy current resistance using the following formula:

$$R_{eddy} = \frac{N^2 8\pi\rho}{l_m} \frac{b^2 - a^2}{b^2 + a^2}, \quad (8)$$

where a, b are the inner and the outer radii of the rod, l_m is its length, N is the number of turns of coil on the rod. Once R_{eddy} has been calculated, then we use same method outlined above to calculate c_1 .

Step 2: The next step is the identification of the anhysteretic parameters $\alpha, b, a, M_s, c_2, F$. We can obtain the anhysteretic displacement curve for the magnetostrictive actuator (Figure 4.2) by a method as described in Chikazumi [27]. Essentially to obtain the anhysteretic strain/displacement for a certain value of input current I , an decaying alternating current with the D.C. bias of I is applied to the actuator. By repeating the experiment for differing values of I , we obtain the anhysteretic displacement/strain curve. In Figure 4.2, we can see

that the strains obtained for both the increasing and decreasing currents almost coincide showing no hysteresis.

Coming back to the identification scheme, we can write the equations satisfied by the magnetostrictive actuator following the anhysteretic curve in a quasi-static manner as follows:

$$dx + b M^2 \mathcal{V} = F, \quad (9)$$

$$\begin{aligned} M_{an}(H_e) &= M_s \mathcal{L}\left(\frac{H_e}{a}\right) \\ &= M_s \left(\coth\left(\frac{H_e}{a}\right) - \frac{a}{H_e} \right), \end{aligned} \quad (10)$$

$$H_e = H + \alpha M - \frac{2 b M x}{\mu_0}. \quad (11)$$

The parameters relating to dynamics do not appear in Equation 9 because the anhysteretic displacement x is measured after the actuator has reached steady state (after the decaying alternating current has sufficiently died down).

Step 2a: We note in Equation 9 that the minimum value of the anhysteretic displacement corresponds to $M = 0$. Thus

$$x_{min} = \frac{F}{d}. \quad (12)$$

In the above equation, F is a prestress load that is already present in the actuator. For the ETREMA MP50/6 magnetostrictive actuator it is not possible to know the value of this parameter. But by repeating the experiment - specifically finding the minimum value of the anhysteretic displacement at a known load F_1 , we can find the values of F and d . The equation would be

$$x_{min_2} = \frac{F + F_1}{d}. \quad (13)$$

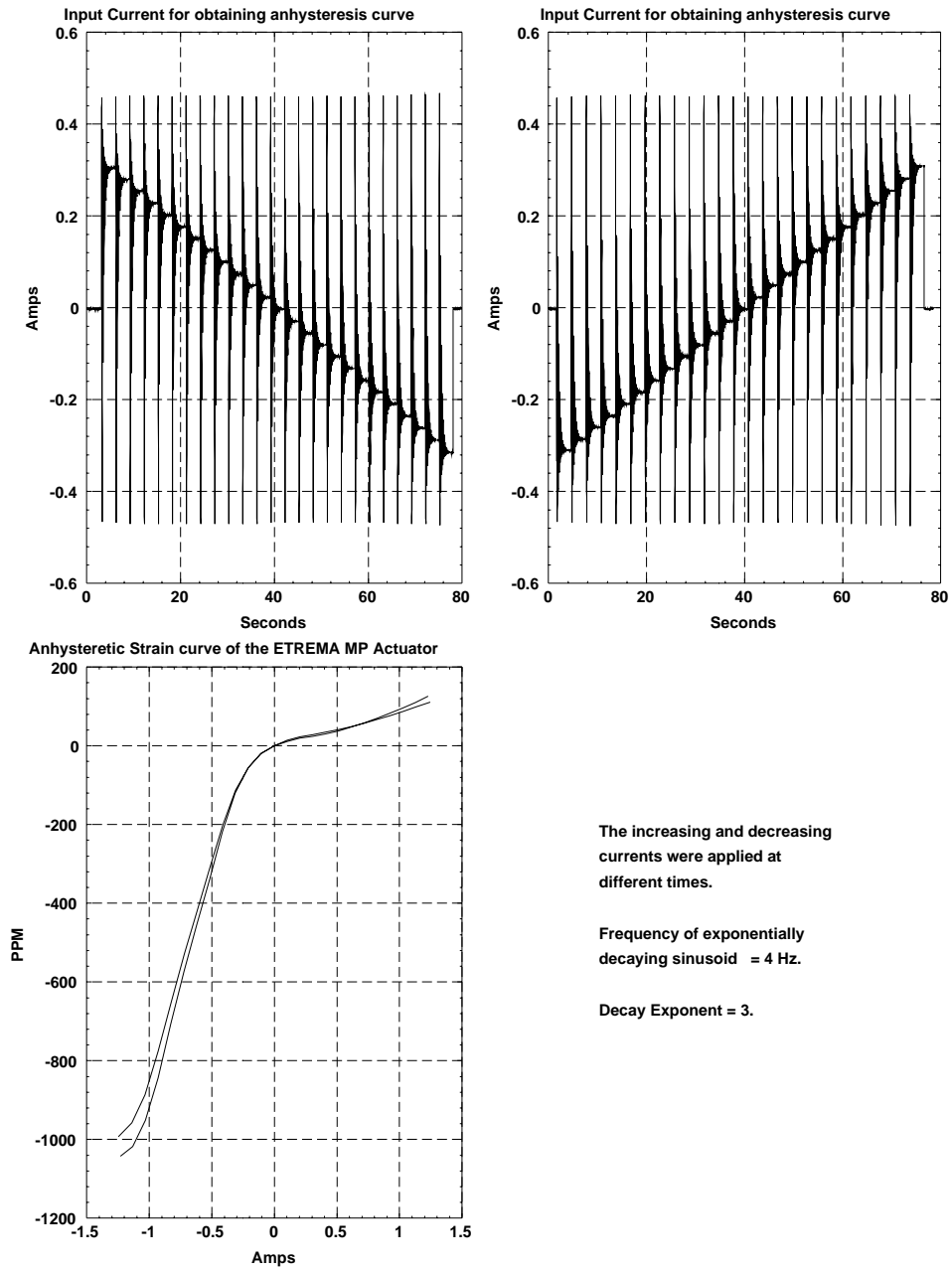


Figure 4.2: The anhyseretic displacement curve for a thin magnetostrictive actuator.

Equation 9 further says that

$$x_{sat} = -b M_s^2 \mathcal{V} + x_{min}. \quad (14)$$

Step 2b: At this point we make the assumption that we know the value of M_s through some other measurements. Then by Equation (14) we can calculate the parameter b . We can now determine the rest of the magnetic parameters that do not pertain to hysteresis, using Equations 9 - 11. The relation between the inductor current I_1 which is a known quantity and the magnetic field intensity H is as follows:

$$H = K I_1 + H_{bias}. \quad (15)$$

where K is a constant called the *coil factor* and H_{bias} is the permanent magnetic biasing field. If we assume no leakage flux and then the theoretical value of K is given by

$$K = \frac{N_m}{l_m}.$$

In the above equation, N_m is the number of turns of the coil which is known, and l_m is the average length of the magnetic path in the actuator which is also a known quantity. For the Terfenol-D actuator MP50/6, ETREMA Inc. (the manufacturer) has empirically determined the constant K to be 194 Oe/Amp .

We can now rewrite Equations 9 - 11 as follows:

$$\begin{aligned} I_1 &= \frac{1}{K} \left(H_e - H_{bias} - \left(\alpha - \frac{2bx}{\mu_0} \right) M \right) \\ &= \frac{1}{K} \left(H_e - H_{bias} - \alpha M_s \mathcal{L} \left(\frac{H_e}{a} \right) + \frac{2bM}{\mu_0} \left(\frac{-bM^2\mathcal{V}}{d} + \frac{F}{d} \right) \right) \end{aligned}$$

$$= \frac{1}{K} \left(H_e - H_{bias} + \left(-\alpha M_s + \frac{2bFM_s}{\mu_0 d} \right) \mathcal{L}\left(\frac{H_e}{a}\right) - \frac{2b^2 M_s^3 \mathcal{V}}{\mu_0 d} \mathcal{L}^3\left(\frac{H_e}{a}\right) \right).$$

Define new parameters η, ν and β by

$$\eta = \frac{1}{K} a, \quad (16)$$

$$\nu = \frac{1}{K} \left(-\alpha M_s + \frac{2bFM_s}{\mu_0 d} \right), \quad (17)$$

$$\beta = -\frac{1}{K} \frac{2b^2 M_s^3 \mathcal{V}}{\mu_0 d}. \quad (18)$$

$\beta < 0$ is known, while $\eta > 0$ and $\nu < 0$ are unknown. Define a new variable \widehat{H}_e by

$$\widehat{H}_e = \frac{H_e}{a}. \quad (19)$$

Then

$$I_1 + \frac{H_{bias}}{K} = \eta \widehat{H}_e + \nu \mathcal{L}(\widehat{H}_e) + \beta \mathcal{L}^3(\widehat{H}_e). \quad (20)$$

Thus $I_1 + \frac{H_{bias}}{K}$ is linear in the new parameters. The identification algorithm for the parameters η and ν is simple.

- *Step a:* Compute the value of \widehat{H}_e from the anhysteretic displacement using Equations (9) and (10). For example, $M = \sqrt{\frac{F-dx}{b\mathcal{V}}}$. The square root is well defined because the actuator has a permanent magnet bias. Note that at some data points M should manually made negative. These points can be identified by looking at a plot of I_1 versus M . By Equation (10) $\widehat{H}_e = \mathcal{L}^{-1}(\widehat{H}_e)$. The inverse of the monotonous function $\mathcal{L}(\widehat{H}_e)$ may be computed by a bisection algorithm.

- *Step b:* If n denotes the n th data point, then let $y(n) = I_1(n) - \beta \mathcal{L}^3(\widehat{H}_e)(n)$, $\theta = [\eta \ \nu]^T$ and $w(n) = [\widehat{H}_e(n) \ \mathcal{L}(\widehat{H}_e)(n)]^T$. We now form the vectors of data points, $W = [w(1) \ w(2) \ \dots]^T$; $Y = [y(1) \ y(2) \ \dots]^T$ so that $Y = W \theta$. The problem is to find the vector $\widehat{\theta}$ that is the “best fit” for the data points. If $W^T W$ is nonsingular then by Theorem E.0.4

$$\widehat{\theta} = (W^T W)^{-1} W^T Y.$$

Step 3: At this point, the only unknown parameters are the magnetic ones related to hysteresis c, k , and effective mass m_{eff} . We first focus on the magnetic hysteretic parameters. One approach that works for sufficiently low frequency of cycling, so that the dynamic effects are negligible is as follows. As the system satisfies Equation 9 we can evaluate $M(t)$ from $x(t)$. Now, to a first approximation

$$M(t + t_0) = M(t_0) + \frac{dM}{dH}(t_0) (H(t + t_0) - H(t_0)). \quad (21)$$

The above equation gives us the value of $\frac{dM}{dH}(t_0)$. We now know the values of $x, H, M, \frac{dM}{dH}$ at every time step. δ is known at every time step t_0 by comparing $H(t + t_0)$ with $H(t_0)$. As we also know \widehat{H}_e at every time step, we can compute δ_M by comparing M and $\mathcal{L}(\widehat{H}_e)$. We can now use Equation 12, to obtain the values of k and c as all the other values are known. The details are discussed next.

Rewriting Equation (12) we get

$$\frac{k \delta}{\mu_0} - \left(\delta_M (M_{an} - M) + \frac{k \delta}{\mu_0} c \frac{dM_{an}}{dH_e} \right) \left(\alpha - \frac{2 b M x}{\mu_0} \right) \frac{dM}{dH} = \frac{k \delta}{\mu_0} c \frac{dM_{an}}{dH_e} + \delta_M (M_{an} - M).$$

That is

$$\frac{k \delta}{\mu_0} \frac{dM}{dH} - \frac{k \delta}{\mu_0} c \frac{dM_{an}}{dH_e} \left(\bar{\alpha}(M, x) \frac{dM}{dH} + 1 \right) = \delta_M (M_{an} - M) \left(\bar{\alpha}(M, x) \frac{dM}{dH} + 1 \right),$$

where $\bar{\alpha}(M, x) = \alpha - \frac{2bMx}{\mu_0}$.

Define $\lambda = [k \ k c]^T$, $\bar{y}(n) = \delta_M (M_{an} - M) \left(\bar{\alpha}(M, x) \frac{dM}{dH} + 1 \right) (n)$, and

$$\bar{w}(n) = \left[\frac{k \delta}{\mu_0} (n) \frac{dM}{dH} - \frac{\delta}{\mu_0} \frac{dM_{an}}{dH_e} \left(\bar{\alpha}(M, x) \frac{dM}{dH} + 1 \right) (n) \right]^T. n \text{ denotes the time-step.}$$

Define

$$\bar{W} = [\bar{w}(1), \bar{w}(2), \dots, \bar{w}(t)]^T; \text{ and } \bar{Y} = [\bar{y}(1), \bar{y}(2), \dots, \bar{y}(t)]^T. \text{ Then}$$

$$\bar{Y} = \bar{W} \lambda.$$

If $\bar{W}^T \bar{W}$ is non-singular, then by the Least-squares theorem E.0.4, the best estimate for the parameter vector λ is given by

$$\hat{\lambda} = (\bar{W}^T \bar{W})^{-1} \bar{W}^T \bar{Y}.$$

Thus k and c can be identified.

Step 4: Finally, we can perform one last experiment to obtain the unknown parameter m_{eff} . This parameter is one of the most crucial in the model. We apply sinusoidal current signals of constant magnitude to the actuator and measure the maximum displacement obtained at each frequency. The lowest frequency corresponding to a peak in the response can then be used to find m_{eff} . Suppose ω_0 is this frequency in *rad/sec*, then

$$m_{eff} = \frac{\omega_0^2}{d}.$$

gives the effective mass.

A_m	\triangleq	Area of the magnetostrictive rod face = $2.8274 \times 10^{-1} \text{ sq.cm}$
l_m	\triangleq	Length of the magnetostrictive rod = 5.13 cm
N_m	\triangleq	Number of turns of wire on the magnetostrictive rod = 1300,
R_{lead}	\triangleq	Lead resistance = 6.0Ω

Table 4.1: Factory specifications for the magnetostrictive actuator

4.2 Experimental validation

The above algorithm was used to find the parameters of a test Terfenol-D magnetostrictive actuator manufactured by ETREMA Products, Inc. Figure 1.10 represents a cut away section of this actuator. The basic parameters of the actuator are presented in Table 4.1. The magnetostrictive rod itself is made by the free stand zone melt (FSZM) technique. The factory identification number for the type of rod in the actuator is FSZM 96-11B. The quasi-static strain in parts per million vs. applied magnetic field for such a rod is shown in Figure 4.3.

Factory measurements of the saturation magnetization for the above rod yielded M_s to be approximately 9000 Oe . The application handbook published by ETREMA [23] mentions that the Young's modulus of the material to be in the range $25 - 35 \text{ GPa}$. The factory set prestress on the rod actuator was set to be 6.9 MPa . As the experimental apparatus used to the measure the strain (the LVDT strain sensor plus the signal conditioner unit) had some drift associated with the measurement, it was extremely difficult to measure the strains from one experiment to the next with respect to some fixed reference. Of course, the hysteresis and after-effect of the rod contributed to the drift. Therefore it was extremely difficult to calculate the elastic constant d as outlined in Step 2 in the previous section. To overcome this difficulty, we used the Young's modulus of

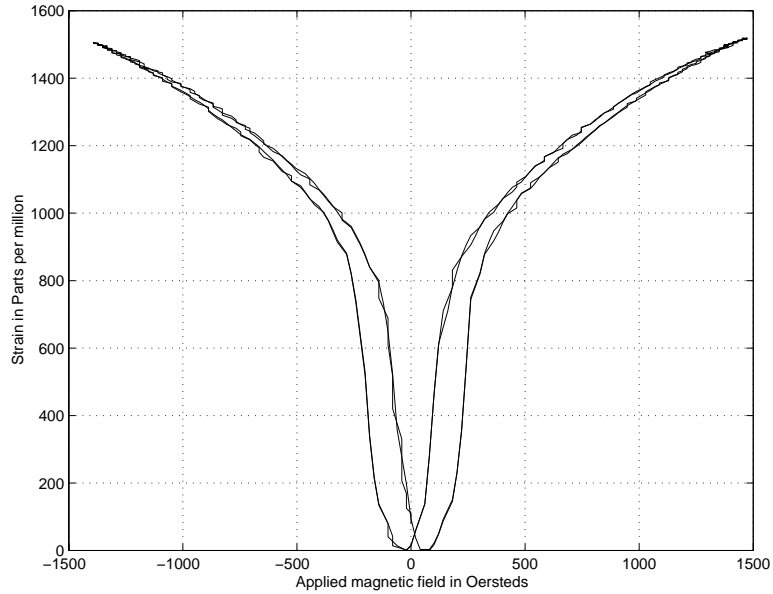


Figure 4.3: Quasi-static strain vs applied magnetic field for an ETREMA FSZM 96-11B Terfenol-D rod (Courtesy ETREMA Products, Inc.).

the rod to calculate d approximately as

$$d = \frac{\gamma^H A_m}{l_m} = 1.9288 \times 10^{10} \text{ dynes/cm.}$$

Please note that all the parameters are expressed in their C.G.S. units. This is because these units are usually employed by workers in the magnetism area, and also because the numbers are then not too big or too small. This helps in avoiding bad conditioning in the numerical method. The lead resistance in the circuit was measured to be 7.5 Ohms . This value needs to be multiplied by 10^7 in the simulation because otherwise $I^2 R$ will give us power in Joules/sec when I is in Amperes . Table 4.2 lists the factors for converting the S.I units to the C.G.S equivalents used in the simulation.

In addition, the permeability μ_0 in the SI units = $4\pi \times 10^{-7} \text{ H/m}$ while it is dimensionless and equal to 1.0 in the CGS units. Note that true CGS units

Quantity	S.I unit	multiply to get	CGS unit
Current	<i>Amperes (A)</i>	1.0	<i>A (CGS)</i>
Voltage	<i>Volts (V)</i>	10^7	<i>V (CGS)</i>
Resistance	<i>Ohms (Ω)</i>	10^7	Ω (CGS)
Energy	<i>Joules (J)</i>	10^7	<i>Ergs</i>
Force	<i>Newtons (N)</i>	10^5	<i>Dynes</i>
Pressure	<i>N/m^2 or Pascals</i>	10	<i>Dynes/cm²</i>
Mass	<i>Kilograms (Kg)</i>	10^3	<i>gm</i>
Distance	<i>Meters (m)</i>	10^3	<i>cm</i>
Magnetic field	<i>A/m</i>	$4\pi \times 10^{-3}$	<i>Oersteds (Oe)</i>
Magnetization	<i>A/m</i>	$4\pi \times 10^{-3}$	<i>G or Oe</i>
Magnetic Flux	<i>Weber/m² or Tesla</i>	10^{-4}	<i>Gauss (G)</i>
Density			

Table 4.2: Physical quantities in SI and CGS units

Frequency (Hz)	c_1	R_{eddy}	\mathcal{H}
50	5.09×10^3	26.35	-4.29×10^3
100	-825	24.9	-2.17×10^3
240	4.76×10^5	40.1	-1.0×10^3
480	2.62×10^5	41.48	-443.38

Table 4.3: Results of Step 1

of Voltage and Current have two different units called stat-Volts; ab-Volts and stat-Amps; ab-Amps respectively. Instead of defining Voltage and Current in the true CGS units, we simply multiply them by 10^7 and 1.0 respectively as a matter of convenience.

Step 1:

The first step of the identification process was carried out as mentioned in the last section. Signals of frequency 50, 100, 200, 500 Hz were applied and the displacement, coil current and voltage at the power supply output were measured. The current versus displacement curves are shown in Figure 4.4. One can see a drift in the curves which could be ascribed to the LVDT signal conditioning unit. Having measured the resistance of the coil and the leads (7.5 Ohms), the least squares method was then employed as described in the last subsection and the constants found are described in the Table 4.3. The tolerance for the least squares method was 10^{-3} .

The reason for the negative coefficients was that unconstrained least-squares minimization was sought. Matlab analysis of the data showed that the hysteresis loss per cycle \mathcal{H} was less than 1% of the total energy input. Most of the energy loss happened due to the lead resistance at low frequencies and at $480Hz$ the

$$a = 1.9 \times 10^2$$

$$\alpha = 1.9 \times 10^{-4}$$

$$b = -2.1$$

$$d = 1.9 \times 10^{10}$$

Table 4.4: Results of Step 2

losses due to the lead and the eddy current resistances became equal. This perhaps explains why the parameters due to the insignificant energy contributions came out to be negative. The value of R_{eddy} obtained at high frequency was the value used in the simulation.

Step 2: The determination of F and d were described before due to the difficulties in the eliminating drifts in the LVDT sensor. The saturation strain was determined using the ETREMA Terfenol-D application handbook [23] (Table 7), to be $3000ppm$. That is

$$\begin{aligned} x_{sat} &= 3 \times 10^{-3} \times 5.13 \text{ cm} \\ &= 1.54 \times 10^{-2}. \end{aligned}$$

The rest of the identification process was exactly as described in the last subsection and results are captured in Table 4.4. The anhysteretic strain curves obtained for an applied load of 340 grams are shown in Figure 4.5. The current applied to obtain this result has a shape as shown in Figure 4.2.

Step 3:

The method of Step 3 *could not* be followed as described in the last subsection. The main reason is that the least squares method did not yield plausible coefficients. This could be due to a number of reasons - the main one being the

$$k = 48.19$$

$$c = 0.3$$

Table 4.5: Results of Step 3

many differentiation of the data signals required to be done. The result of this step would have been the identification of the parameters c and k related to the magnetic hysteresis. As such they were found approximately by inputting some values into a simulation and comparing the result with the experimental curves. As the rest of the identification had been done (Step 4 was completed before Step3 due to this difficulty), the finding of the last two parameters was not very difficult. The result was

Step 4:

As mentioned before, this step was performed before Step 3, mainly so that all the known parameters are collected together before estimating the two unknown ones by heuristics. The resonance frequency ω_0 was approximately determined to be $432Hz$. This facilitated the determination of m_{eff} according to (22):

$$m_{eff} = \frac{\omega_0^2}{d}. \quad (22)$$

The simulation of magnetostrictive actuator using the above constants are shown in Figure 4.6 and 4.7. The trend in the peak current inputs and peak displacement outputs are shown in Table 4.6. It can be compared with experimental results on the Terfenol-D actuator shown in Figures 4.4 (experiment performed on 11/29/98) and in Figures 4.8, 4.9 (experiments performed on 6/17/98). The peak current and peak displacement output for the latter experiment are collected in Table 4.7.

Frequency Hz	Peak - Peak Current input Amps	Peak - Peak Displacement Microns
1	2.13	71
10	2.26	71
50	2.17	63
100	2.22	54
150	2.19	50
200	2.28	42
350	2.11	54
500	2.39	45

Table 4.6: Simulation results

Frequency Hz	Peak - Peak Current input Amps	Peak - Peak Displacement Microns
0.25	2.5	53
1	2.5	53
10	2.5	54
50	2.5	54
100	2.5	51
200	2.5	58
350	2.5	66
500	2.3	44

Table 4.7: Experimental results

Discussion of results

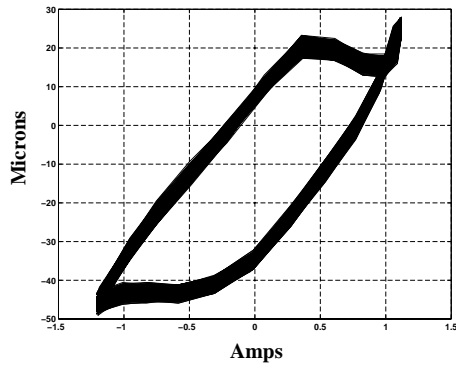
The goal of this chapter, was to provide a method to an application engineer to perform identification experiments on a magnetostrictive rod actuator, and then evaluate its performance in a smart structure via simulation studies. The major problem that we encountered in implementing the algorithm proposed in this Chapter was that the measured characteristics varied each time an experiment was performed. The results of the experiments performed on 10/21/1996 on the same actuator is shown in Figure 5.8. Figures 4.8 and 4.9 show the results of experiments performed on 6/17/98, while Figure 4.4 shows the results of experiments performed on 11/29/98). It is actually difficult to compare them because Figure 4.4 has many more cycles than the previous ones.

Some of these variations could be the result of a drift in the LVDT sensor apparatus. Whether this is the case or there is an inherent drift in the material characteristics depending on the method of storage, loading etc. needs to be examined more closely in the future. In this connection, it might be mentioned here that there was a statistical study done on 50 different rods at the same time with respect to variations of low-signal parameters based on a linear model of the rod and a linear model of the magneto-elastic transduction effect [37]. But we have not come across a study of the properties of the same actuator done at different points in time.

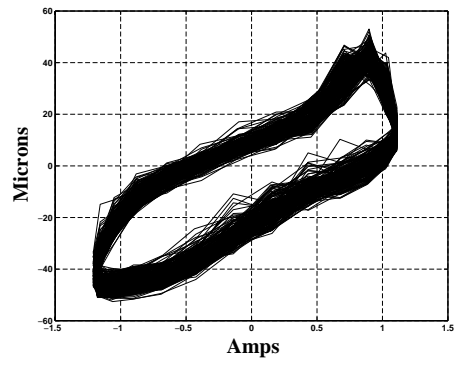
Lets verify whether these parameters satisfy the conditions that were obtained in Chapter 3. As G is the bound on the perturbation of the parameter α , its value is (by (27))

$$\begin{aligned} G &= \left| \frac{2b x_{sat}}{\mu_0} \right| \\ &= 6.46 \times 10^{-2}. \end{aligned}$$

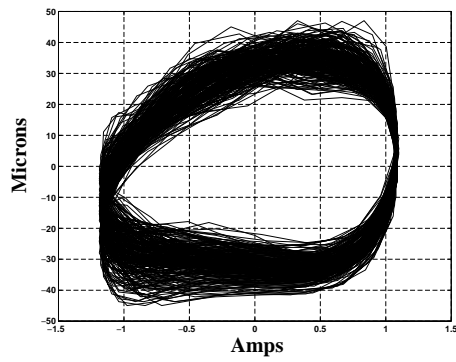
Then it can be seen that the sufficient conditions (29 - 30) are not satisfied, but the necessary condition (33) is satisfied by the parameters.



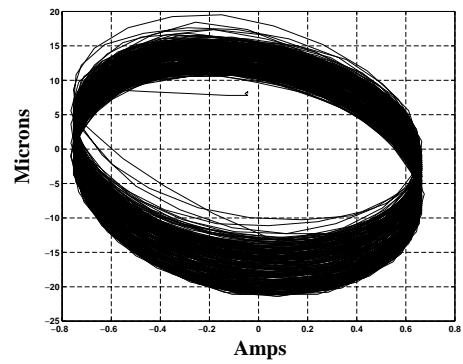
(a) 50 Hz.



(b) 100 Hz.



(c) 240 Hz.



(d) 480 Hz.

Figure 4.4: Displacement versus current data obtained from experiment.

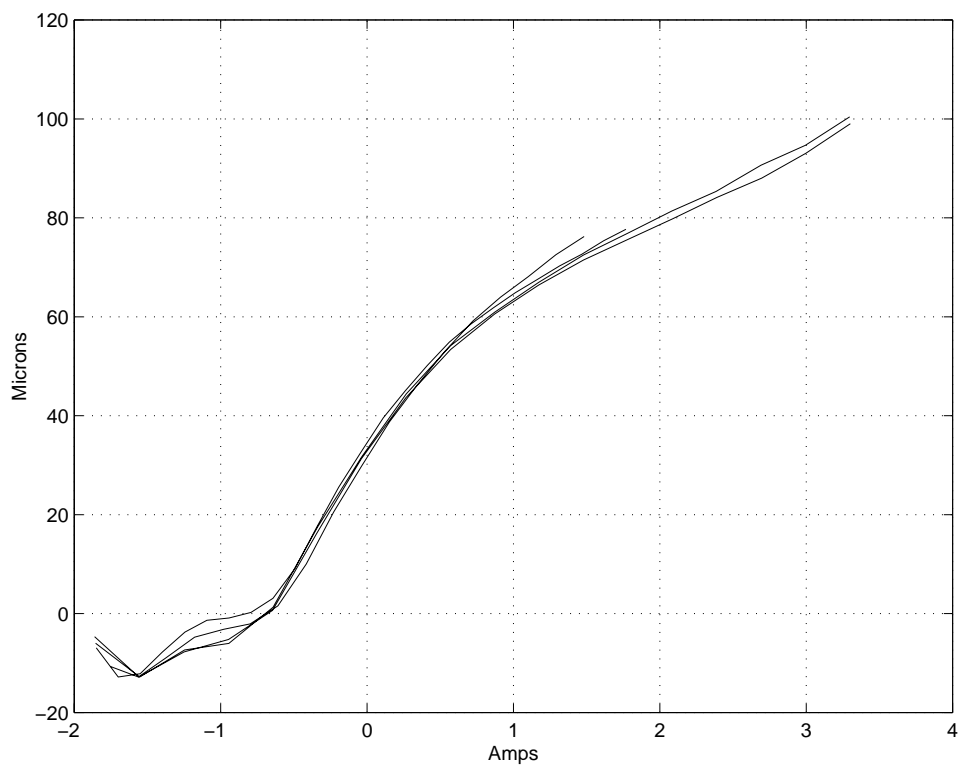
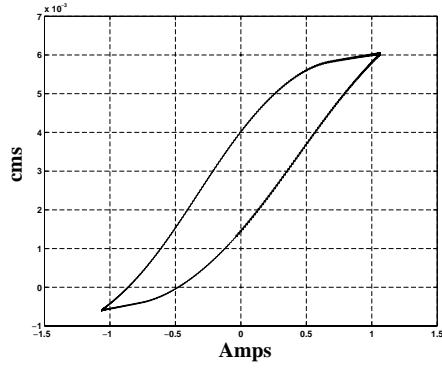
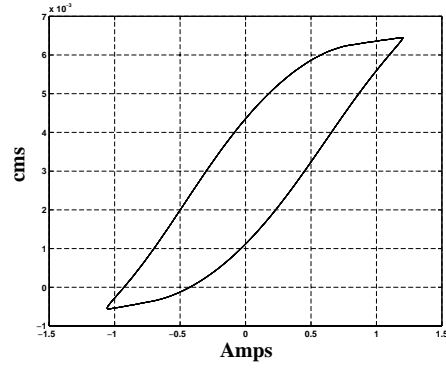


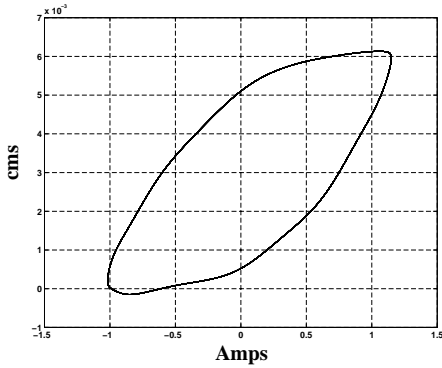
Figure 4.5: Experimental results.



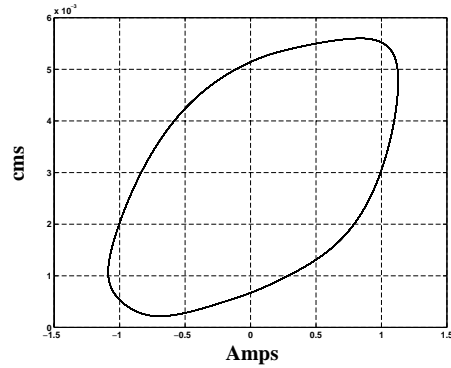
(a) 1 Hz.



(b) 10 Hz.

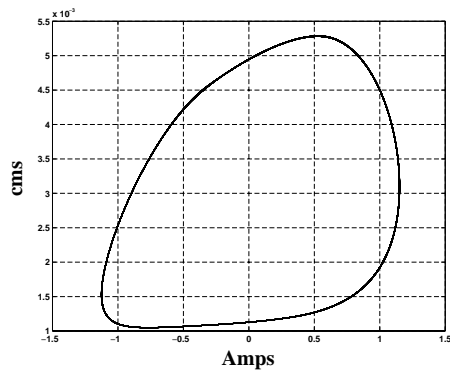


(c) 50 Hz.

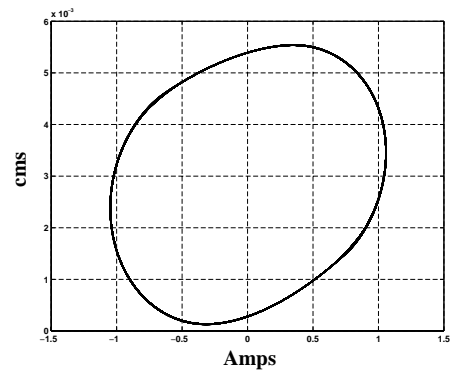


(d) 100 Hz.

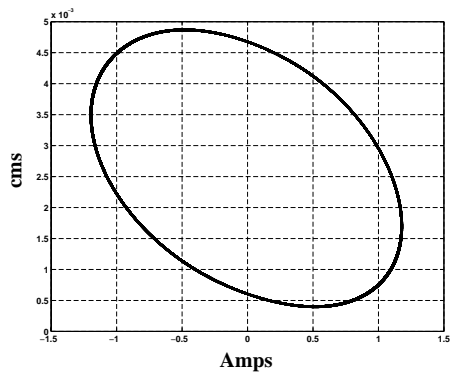
Figure 4.6: Simulation results for sinusoidal voltage inputs of frequencies 1 - 100 Hz.



(a) 200 Hz.



(b) 350 Hz.



(c) 500 Hz.

Figure 4.7: Simulation results for sinusoidal voltage inputs of frequencies 200 - 500 Hz.

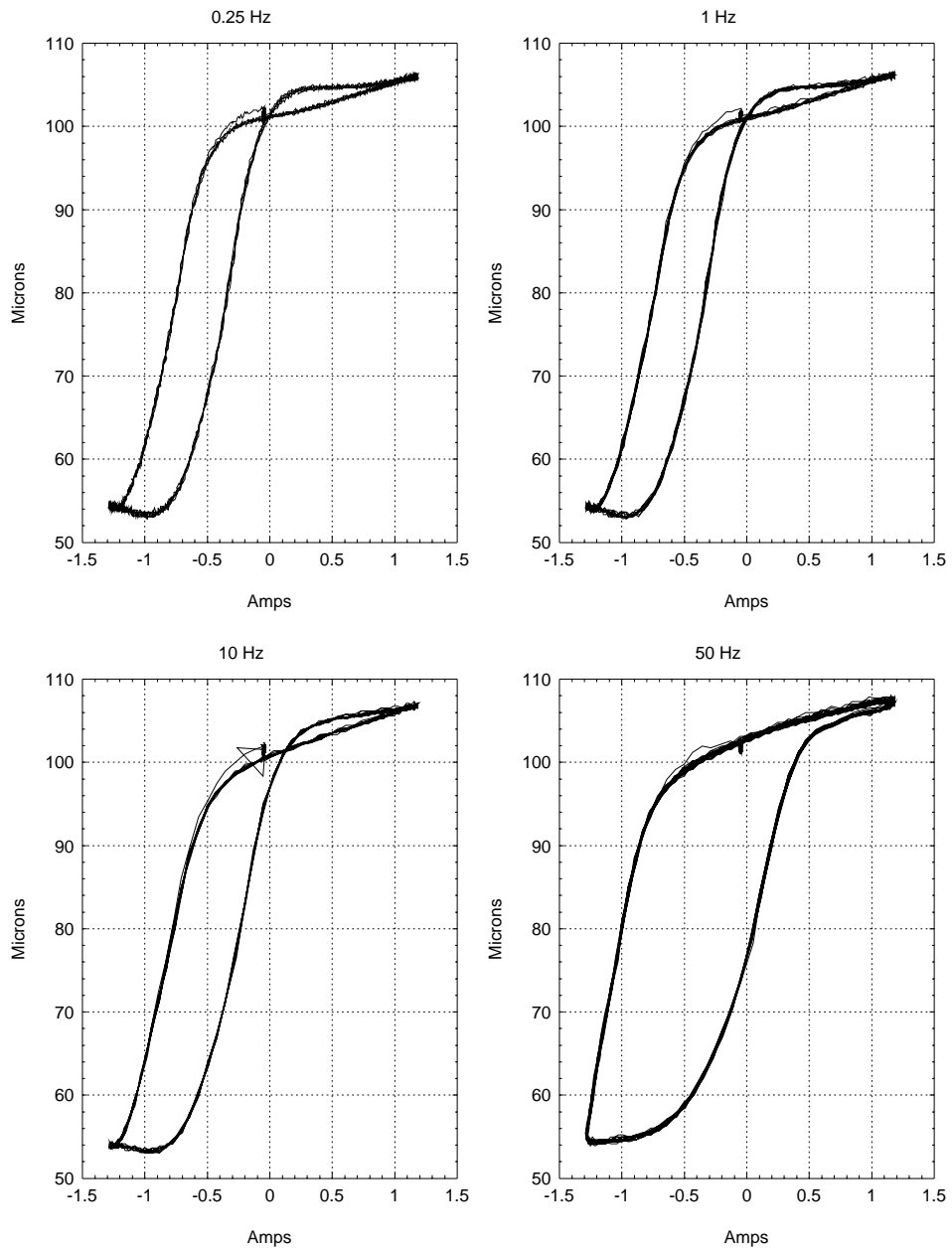


Figure 4.8: Experimental results.

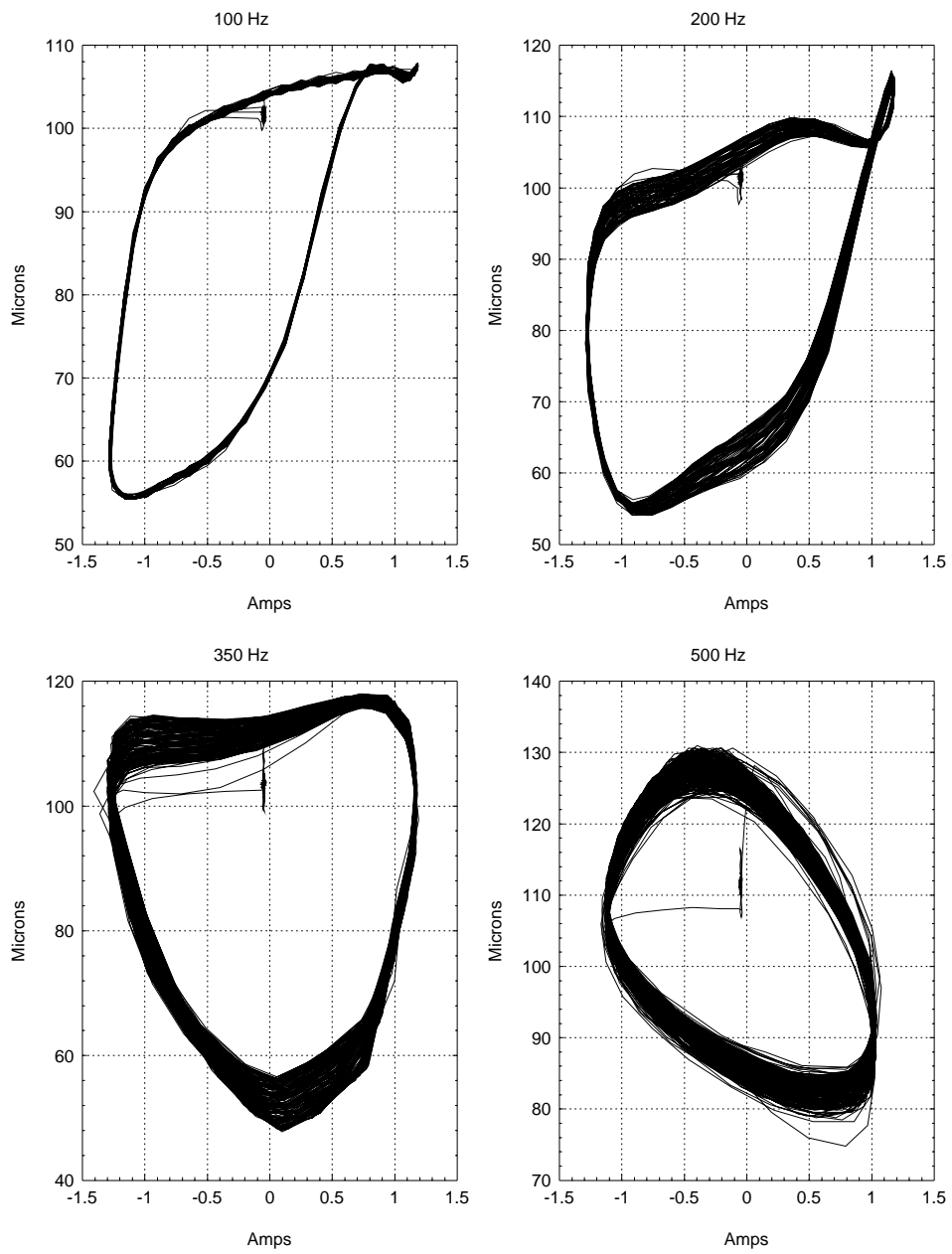


Figure 4.9: Experimental results.

Chapter 5

Trajectory tracking controller design

In this chapter, we design a non-identifier based adaptive controller for trajectory tracking. We consider the magnetostrictive actuator as a single input, single output system with voltage input and displacement output. It is desired that the output track a reference trajectory which belongs to a certain class of signals. The reason for using non-identifier based adaptive controller design instead of a model based controller design is that the model described in the previous chapter yields the correct output response only if the input is sinusoidal. The reason for this was discussed in the last chapter. Besides, it is known that the performance of Terfenol-D actuators is strongly temperature dependent [38]. We could incorporate temperature effects into the model in a straightforward way, but we will have one more parameter to estimate.

In the approach taken in this chapter, we do away with the estimation of parameters and design a direct adaptive controller. There are obvious advantages to this approach, but there are some disadvantages as well that are not so obvious. We will go into this topic later in the chapter. In the following section, the basic idea of a high gain adaptive controller for relative degree one linear

systems is presented. The extension of this idea for controlling relative degree one linear systems with a set valued input nonlinearity is also presented in this section. The second section deals with adaptive controller design for the relative degree two systems with set valued input nonlinearity. The last section of this chapter deals with results of experiments where a controller of the type discussed in Section 5.3 is used to control a magnetostrictive actuator.

5.1 Universal adaptive stabilization and tracking for relative degree one linear systems

A wide range of control theory deals with the design of a feedback controller for a *known* plant so that certain control objectives are achieved [39]. The fundamental difference between this approach and that of adaptive control is that in adaptive control the plant is *not known* exactly, only structural information is available. This structural information may be minimality, minimum phase, known relative degree etc. The aim is therefore to design a *single* controller which achieves prespecified control objectives for every member of a given class. The controller has to learn from the output data and, based on this information, to adjust its parameters.

The area of *non-identifier* based adaptive control was initiated by Nussbaum (1983), Morse (1983), Willems and Byrnes (1984) etc. In their approach, the adaptive feedback strategy is not based on any identification or estimation of the process to be controlled. The class of systems under consideration were either minimum phase or more generally, only stabilizable and detectable [40]. Their seminal work was later extended by Achim Ilchmann, Eugene Ryan and others

to linear systems with relative degree two and set-valued input nonlinearities.

The problem definition is as follows. Suppose Σ denotes a certain class of linear, finite dimensional, time invariant systems of the form

$$\left. \begin{aligned} \dot{x}(t) &= Ax(t) + Bu(t), & x(0) &= x_0 \in \mathbb{R}^n, \\ y(t) &= Cx(t) + Du(t). \end{aligned} \right\} \quad (1)$$

where $(A, B, C, D) \in \mathbb{R}^{n \times n} \times \mathbb{R}^{n \times m} \times \mathbb{R}^{m \times n} \times \mathbb{R}^{m \times m}$, are unknown, m is usually fixed, the state dimension n is an arbitrary and unknown number. The aim is to design a single adaptive output feedback mechanism $u(t) = \mathcal{F}(y(\cdot)|[0, t])$ which is a universal stabilizer for the class Σ , that is, if $u(t) = \mathcal{F}(y(\cdot)|[0, t])$ is applied to any system (1) belonging to Σ , then the output $y(t)$ of the closed loop system tends to zero as t tends to infinity and the internal variables are bounded.

Most of the adaptive stabilizers found in the literature [39, 40] are of the following simple form: A tuning parameter $k(t)$ generated by an adaptation law

$$\dot{k}(t) = g(y(t)), \quad k(0) = k_0, \quad (2)$$

where $g : \mathbb{R}^m \rightarrow \mathbb{R}$ is continuous and locally lipschitz, is implemented into the feedback law via

$$u(t) = F(k(t), y(t), \dot{y}(t), \dots, y^p(t)), \quad (3)$$

where $F : \mathbb{R}^{p+1} \rightarrow \mathbb{R}^m$ is piecewise continuous and locally Lipschitz where p is the relative degree (to be defined later) of the system.

Definition 5.1.1 [39] *A controller, consisting of the adaptation law (2) and the feedback rule (3), is called a universal adaptive stabilizer for the class of systems*

Σ , if for arbitrary initial condition $x_0 \in \mathbb{R}^n$ and any system (1) belonging to Σ , the closed loop system (1)-(3) has a solution with the properties

1. there exists a unique solution $(x(\cdot), y(\cdot)) : [0, \infty) \rightarrow \mathbb{R}^{n+1}$,
2. $x(\cdot), y(\cdot), u(\cdot), k(\cdot)$ are bounded,
3. $\lim_{t \rightarrow \infty} y(t) = 0$,
4. $\lim_{t \rightarrow \infty} k(t) = k_\infty \in \mathbb{R}$ exists.

The concept of adaptive tracking is similar. Suppose a class \mathcal{Y}_{ref} of reference signals is given. It is desired that the error between the output $y(t)$ of (1) and the reference signal $y_{ref}(t)$

$$e(t) \triangleq y(t) - y_{ref}(t)$$

is forced, via a simple adaptive feedback mechanism, either to zero or towards a ball around zero of arbitrary small prespecified radius $\lambda > 0$. The latter is called λ -tracking. λ -tracking does not involve an internal model – usually referred to as *universal adaptive tracking with internal model*. In this dissertation, λ tracking is used for achieving trajectory tracking in magnetostrictive actuators and hence adaptive tracking with an internal model is not discussed further. A good description on this subject can be found in Ilchmann [39].

Definition 5.1.2 [39] *For prespecified $\lambda > 0$, a controller consisting of an adaptation law (2) and a feedback law (3) is called a universal adaptive λ -tracking controller for the class of systems Σ and reference signals \mathcal{Y}_{ref} , if for every $y_{ref}(\cdot) \in \mathcal{Y}_{ref}$, $x_0 \in \mathbb{R}^n$ and every system (1) belonging to Σ , the closed loop system (1)-(3) satisfies*

1. *there exists a unique solution $x(\cdot), y(\cdot) : [0, \infty) \rightarrow \mathbb{R}^{n+1}$,*
2. *the variables $x(t), y(t), u(t)$ diverge to ∞ or $-\infty$ no faster than $y_{ref}(t)$,*
3. *$e(t) = (y(t) - y_{ref}(t)) \rightarrow \bar{\mathcal{B}}_\lambda(0)$ as $t \rightarrow \infty$,*
4. *$\lim_{t \rightarrow \infty} k(t) = k_\infty \in \mathbb{R}$ exists.*

Many results found in the literature fit into the framework described above. Results can also be found for linear systems subjected to nonlinear perturbations in the state, input and output, corrupted input and output noise [39, 24]. In this dissertation, we are particularly interested in systems with input nonlinearity and hence the discussion is developed in this direction.

5.1.1 Basic Idea

The basic idea of universal adaptive stabilization can be explained by considering a scalar system. Consider the system to be stabilized to belong to the class of scalar systems described by

$$\dot{x} = ax + bu(t); \quad x(0) = x_0, \quad (4\text{-a})$$

$$y(t) = cx(t), \quad (4\text{-b})$$

where $a, b, c, x_0 \in \mathbb{R}$ are unknown and the only structural assumption is $cb > 0$. If we apply the feedback law $u(t) = -ky(t)$ to the above system, then the closed loop system has the form

$$\dot{x}(t) = (a - kcb)x(t); \quad x(0) = x_0. \quad (5)$$

Clearly, if $\frac{a}{|cb|} < |k|$ and $\text{sign}(k) = \text{sign}(cb)$, then Equation 5 is exponentially stable. However a, b, c are not known and thus the problem is to find adaptively an appropriate k so that the motion of the feedback system tends to zero. Now a *time varying* feedback is built into the feedback law

$$u(t) = -k(t)y(t),$$

where $k(t)$ has to be adjusted so that it gets large enough to ensure stability but also remains bounded. This can be achieved by the adaptation rule,

$$\dot{k}(t) = y^2(t), \quad k(0) \in \mathbb{R}.$$

The nonlinear closed loop system is therefore

$$\dot{x}(t) = (a - kcb)x(t),$$

where

$$k(t) = \int_0^t x(s)^2 ds + k(0); \quad (k(0), x(0)) \in \mathbb{R}^2$$

has at least a solution on a small interval $[0, \omega)$, and the non-trivial solution

$$x(t) = \exp \int_0^t (a - k(s)cb) ds x(0)$$

is monotonically increasing as long as $a - k(t)cb > 0$. Hence $k(t) \geq t(cx(0))^2 + k(0)$ increases as well. Therefore, there exists a $t^* \geq 0$ such that $a - k^*cb = 0$ and $a - k(t)cb < 0$ for all $t > t^*$. Hence the solution $x(t)$ decays exponentially and $\lim_{t \rightarrow \infty} k(t) = k_\infty \in \mathbb{R}$ exists.

□

The above analysis can be done in a more instructive way if we rewrite the system given by (4-a - 4-b) in the following form [25]:

$$\dot{y} = \bar{a} y + g u, \quad (6)$$

where $\bar{a} = c a$ and $g = c b$ with $g \neq 0$. If $\sigma_g = \text{sign}(g)$ is known, stabilization can be achieved with the adaptive controller $u = -\sigma_g k y$ with the evolution of k in time given by $\dot{k} = y^2$. To prove this fact, choose the indicator function

$$V(t) = \frac{y^2(t)}{2}. \quad (7)$$

The time derivative of $V(y, k)$ is given by

$$\dot{V}(t) = (\bar{a} - |g| k) \dot{k}.$$

This equation can be integrated to yield

$$V(t) = \bar{a} k(t) - |g| \frac{k^2(t)}{2} + C, \quad (8)$$

where C is a constant. Examination of the above equation reveals that $k \in L^\infty$, the space of essentially bounded functions on $(0, \infty)$. This is so because, if it were not true, then for $|k|$ sufficiently large, V would become negative which by Equation (7) would be impossible. Hence by Equation (8), $V \in L^\infty$, and by Equation (7) $y \in L^\infty$ as well.

The closed loop system is given by

$$\dot{y} = (\bar{a} - |g| k) y, \quad (9\text{-a})$$

$$\dot{k} = y^2. \quad (9\text{-b})$$

Equation (9-a) implies that $\dot{y} \in L^\infty$ while Equation (9-b) implies that $y \in L^2$, the space of square integrable functions on $(0, \infty)$; it follows that $y(t) \rightarrow 0$ as $t \rightarrow \infty$.

The above *non-classical analysis* approach is very useful in the theory of *universal adaptive stablization*. Consider the adaptive stablization of (6), but now with σ_g unknown. In this situation, consider the control law

$$u = N(k)ky, \quad (10)$$

where $N(\cdot)$ is a *Nussbaum function* defined as below.

Definition 5.1.3 *Let $k' \in \mathbb{R}$. A piecewise right continuous and locally Lipschitz function $N(\cdot) : [k', \infty) \rightarrow \mathbb{R}$ is called a Nussbaum function if it satisfies*

$$\begin{aligned} \sup_{k > k_0} \frac{1}{k - k_0} \int_{k_0}^k N(\mu) \mu d\mu &= \infty, \\ \inf_{k > k_0} \frac{1}{k - k_0} \int_{k_0}^k N(\mu) \mu d\mu &= -\infty, \end{aligned} \quad (11)$$

for some $k_0 \in (k', \infty)$. A Nussbaum function is called *scaling-invariant* if, for arbitrary $\alpha, \beta > 0$,

$$\tilde{N}(t) \triangleq \begin{cases} \alpha N(t) & \text{if } N(t) \geq 0 \\ \beta N(t) & \text{if } N(t) < 0 \end{cases} \quad (12)$$

is a Nussbaum function as well.

To prove that the resulting closed loop system

$$\dot{y} = (\bar{a} + g N(k) k) y, \quad (13\text{-a})$$

$$\dot{k} = y^2, \quad (13\text{-b})$$

is stable, we proceed just as before by evaluating the rate of change of the indicator function $V = \frac{y^2}{2}$ along solutions to (13-a - 13-b). Thus $\dot{V} = (\bar{a} + gN(k)k)y^2 = (\bar{a} + gN(k)k)\dot{k}$. Therefore by integrating \dot{V} we get:

$$V(t) = ak(t) + g \int_0^{k(t)} N(\mu) \mu d\mu + C. \quad (14)$$

The definition of $N(\cdot)$ clearly implies that for some number $k^* \geq k(0)$,

$$\bar{a}k^* + g \int_0^{k^*} N(\mu) \mu d\mu + C < 0.$$

Since by definition $V \geq 0$, $k(t)$ cannot attain this value. It follows that $k(0) \leq k(t) < k^*$ or that $k \in L^\infty$. The definition of V together with Equation (14) thus imply that $y \in L^\infty$ as well. With $(y, k) \in L^\infty$, we prove $y \rightarrow 0$ by using (13-a - 13-b) just as before.

□

Before we conclude this subsection, we present some examples of Nussbaum functions.

Example 5.1.1 [39]

The following functions are Nussbaum:

$$\begin{aligned} N_1(k) &= k^2 \cos(k), \quad k \in \mathbb{R}, \\ N_2(k) &= k \cos(\sqrt{|k|}), \quad k \in \mathbb{R}, \\ N_3(k) &= \ln(k) \cos(\sqrt{\ln(k)}), \quad k > 1, \\ N_4(k) &= \begin{cases} k & \text{if } n^2 \leq |k| < (n+1)^2, \quad n \text{ even,} \\ -k & \text{if } n^2 \leq |k| < (n+1)^2, \quad n \text{ odd,} \end{cases} \quad k \in \mathbb{R}, \end{aligned}$$

$$N_5(k) = \begin{cases} k & \text{if } 0 \leq |k| < \tau_0, \\ k & \text{if } \tau_n \leq |k| < \tau_{n+1}, \quad n \text{ even}, \\ -k & \text{if } \tau_n \leq |k| < \tau_{n+1}, \quad n \text{ odd}, \\ \text{with } \tau_0 > 1, \tau_{n+1} \triangleq \tau_n^2, \end{cases} \quad k \in \mathbb{R},$$

$$N_6(k) = \cos\left(\frac{\pi}{2}k\right) \exp k^2, \quad k \in \mathbb{R}.$$

5.1.2 Extension to relative degree one, minimum phase, linear systems

The analysis in the previous subsection can be generalized to relative degree one systems of higher order. It will be seen that they also have to be minimum phase. The definition of the above terms are presented next.

Definition 5.1.4 (Zeros, Poles and Relative degree) *Let $G(\cdot) \in \mathbb{R}(s)^{m \times m}$ be a rational matrix with Smith-McMillan form*

$$\text{diag} \left\{ \frac{\epsilon_1(s)}{\psi_1(s)}, \dots, \frac{\epsilon_r(s)}{\psi_r(s)}, 0, \dots, 0 \right\} = U(s)^{-1}G(s)V(s)^{-1},$$

where $U(\cdot), V(\cdot) \in \mathbb{R}(s)^{m \times m}$ are unimodular, $\text{rank}G(\cdot) = r$, $\epsilon_i(\cdot), \psi_i(\cdot) \in \mathbb{R}(s)$ are monic and coprime and satisfy $\epsilon_i(\cdot) | \epsilon_{i+1}(\cdot), \psi_i(\cdot) | \psi_{i+1}(\cdot)$ for $i = 1, \dots, r$. Set

$$\epsilon(s) = \prod_{i=1}^r \epsilon_i(s), \quad \psi(s) = \prod_{i=1}^r \psi_i(s).$$

s_0 is a (transmission) zero of $G(\cdot)$, if $\epsilon(s_0) = 0$, and a pole of $G(\cdot)$, if $\psi(s_0) = 0$. If $G(\cdot) = g(\cdot) \in \mathbb{R}(s)$, then $\text{deg}\psi(\cdot) - \text{deg}\epsilon(\cdot)$ is called the relative degree of $g(\cdot)$.

Definition 5.1.5 (Proper, Strictly proper) $G(\cdot)$ is proper resp. strictly proper if $\text{deg}\psi(\cdot) \geq \text{deg}\epsilon(\cdot)$ resp. if $\text{deg}\psi(\cdot) > \text{deg}\epsilon(\cdot)$.

Definition 5.1.6 (Minimum realization, Minimum phase) *The system*

$$\begin{aligned}\dot{x}(t) &= Ax(t) + Bu(t), \\ y(t) &= Cx(t) + Du(t),\end{aligned}$$

with $(A, B, C, D) \in \mathbb{R}^{n \times n} \times \mathbb{R}^{n \times m} \times \mathbb{R}^{m \times n} \times \mathbb{R}^{m \times m}$, is called a minimum realization of $G(\cdot) \in \mathbb{R}^{m \times m}$, if (A, B) is controllable and (A, C) is observable and $G(s) = C(sI_n - A)^{-1}B + D$.

$G(\cdot)$ is said to be minimum phase, if

$$\epsilon(s) \neq 0 \quad \forall s \in \bar{\mathbb{C}}_+.$$

A state space system $(A, B, C, D) \in \mathbb{R}^{n \times n} \times \mathbb{R}^{n \times m} \times \mathbb{R}^{m \times n} \times \mathbb{R}^{m \times m}$, is called minimum phase, if it is stabilizable and detectable and $G(s)$ has no zeros in $\bar{\mathbb{C}}_+$.

A characterization of the minimum phase condition for the state space system is given in the following proposition [39]:

Proposition 5.1.1 $(A, B, C, D) \in \mathbb{R}^{n \times n} \times \mathbb{R}^{n \times m} \times \mathbb{R}^{m \times n} \times \mathbb{R}^{m \times m}$, satisfies

$$\det \begin{bmatrix} sI_n - A & -B \\ -C & -D \end{bmatrix} \neq 0 \quad \forall s \in \bar{\mathbb{C}}_+$$

if and only if, the following three conditions are satisfied

- $\text{rank}[sI_n - A, B] = n$ for all $s \in \bar{\mathbb{C}}_+$, i.e. (A, B) is stabilizable by state feedback,
- $\text{rank} \begin{bmatrix} sI_n - A \\ C \end{bmatrix} = n$ for all $s \in \bar{\mathbb{C}}_+$, i.e. (A, C) is detectable,

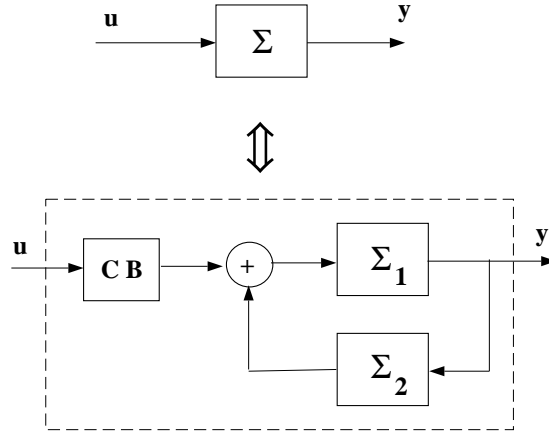


Figure 5.1: Equivalent realization for a linear system.

- $G(s)$ has no zeros in $s \in \bar{\mathbb{C}}_+$.

The key lemma that enables us to apply the analysis presented in the last subsection to higher order linear systems is presented next. It enables us separate the inputs and the outputs from the rest of the system states as shown in Figure 5.1. The main point that is brought out in the equivalent realization is that the system Σ_2 shown in figure is Hurwitz because of the minimum phase property of Σ .

Lemma 5.1.1 (Equivalent Realization) [39] *Consider the system*

$$\left. \begin{aligned} \dot{x}(t) &= Ax(t) + Bu(t), & x(0) &= x_0 \in \mathbb{R}^n, \\ y(t) &= Cx(t), \end{aligned} \right\} \quad (15)$$

with $\det(CB) \neq 0$. Then there exists an invertible state space transformation S that converts (15) into

$$\left. \begin{aligned} \dot{y}(t) &= A_1 y(t) + A_2 z(t) + CBu(t), \\ \dot{z}(t) &= A_3 y(t) + A_4 z(t), \end{aligned} \right\} \left(\begin{array}{c} y(0) \\ z(0) \end{array} \right) = S^{-1}x_0. \quad (16)$$

If (A, B, C) is minimum phase, then A_4 in (16) is asymptotically stable.

The following theorem is the main result of this subsection and is presented as in Ilchmann[39].

Theorem 5.1.1 *Suppose the system (15) is minimum phase. Let $p \geq 1$, and $N(\cdot) : \mathbb{R} \rightarrow \mathbb{R}$ be a Nussbaum function, scaling-invariant if $m > 1$ or $p \neq 2$. If the adaptation law*

$$\dot{k} = \|y(t)\|^p, \quad k(0) = k_0, \quad (17)$$

together with one of the feedback laws

$$u(t) = -k(t)y(t), \quad \text{if } \sigma(CB) \subset \mathbb{C}_+, \quad (18\text{-a})$$

$$u(t) = -N(k(t))y(t), \quad \text{if } \sigma(CB) \subset \mathbb{C}_+, \text{ or } \mathbb{C}_- \quad (18\text{-b})$$

$$(18\text{-c})$$

and arbitrary $k_0 \in \mathbb{R}$, $x_0 \in \mathbb{R}^n$, is applied to (15), then the closed loop system has the properties

- the unique solution $(x(\cdot), k(\cdot)) : [0, \infty) \rightarrow \mathbb{R}^{n+1}$ exists,
- $\lim_{t \rightarrow \infty} k(t) = k_\infty$ exists and is finite,
- $x(\cdot) \in L^p(0, \infty) \cap L^\infty(0, \infty)$ and $\lim_{t \rightarrow \infty} x(t) = 0$.

5.2 λ tracking

In this section, the results of the previous section on universal adaptive stabilization is extended to solve the λ -tracking problem for various classes of linear,

minimum phase systems of the form

$$\left. \begin{aligned} \dot{x}(t) &= Ax(t) + bu(t), & x(0) &= x_0 \in \mathbb{R}^n, \\ y(t) &= cx(t), \end{aligned} \right\} \quad (19)$$

with $(A, b, c) \in \mathbb{R}^{n \times n} \times \mathbb{R}^n \times \mathbb{R}^{1 \times n}$ and minimum phase. The class of reference signals is the *Sobolev space*

$$\mathcal{Y}_{ref} = \mathcal{W}^{1,\infty}(\mathbb{R}, \mathbb{R}). \quad (20)$$

The following theorem solves the λ -tracking problem for the class of single-input, single-output (SISO), minimum phase systems with high-frequency gain $cb > 0$ or $cb \neq 0$. The statement of the theorem follows Ilchmann. Though Ilchmann extends the result to multi-input, multi-output (SMIMO) systems, only the SISO case is presented here.

Theorem 5.2.1 [39] *Let $\lambda > 0$, $N(\cdot) : \mathbb{R} \rightarrow \mathbb{R}$ a Nussbaum function and $y_{ref}(\cdot) \in \mathcal{Y}_{ref}$. If the adaptation law*

$$\dot{k} = \begin{cases} (|e(t)| - \lambda)|e(t)|, & \text{if } |e(t)| \geq \lambda; \\ 0, & \text{if } |e(t)| < \lambda; \end{cases} \quad , k(0) = k_0, \quad (21)$$

together with one of the feedback laws

$$u(t) = -k(t)e(t); \quad \text{if } cb > 0, \quad (22\text{-a})$$

$$u(t) = -N(k(t))e(t); \quad \text{if } cb \neq 0, \quad (22\text{-b})$$

where $e(t) = y(t) - y_{ref}(t)$, is applied to (19), for arbitrary $x_0 \in \mathbb{R}^n$, $k_0 \in \mathbb{R}$, then the closed-loop system has the properties

1. *there exists a unique solution $(x(\cdot), k(\cdot)) : [0, \infty) \rightarrow \mathbb{R}^{n+1}$,*
2. *$\lim_{t \rightarrow \infty} k(t) = k_\infty$ exists and is finite,*
3. *$x(\cdot), k(\cdot) \in L^\infty(0, \infty)$,*
4. *the error $e(t)$ approaches the interval $[-\lambda, \lambda]$ as $t \rightarrow \infty$.*

Ilchmann proves that the above theorem with slight modifications in the gain update and control law is also true for linear systems with nonlinear perturbations of the state equation and presence of noise at the output. This is a very nice result, but as it is not used in this dissertation, it is not presented.

5.2.1 Extensions to systems with input non-linearity

In this subsection, we present a theorem that shows that we can still have λ -tracking even in the presence of input and output nonlinearities. We consider classes of systems of the form

$$\left. \begin{aligned} \dot{x}(t) &= Ax(t) + b\xi(t, u(t)); & x(0) &= x_0 \in \mathbb{R}^n, \\ y(t) &= cx(t) + n(t), \end{aligned} \right\} \quad (23)$$

with $(A, b, c) \in \mathbb{R}^{n \times n} \times \mathbb{R}^n \times \mathbb{R}^{1 \times n}$ and minimum phase (see Figure 5.2). $\xi(t, u(t))$ represents a time-varying actuator nonlinearity and the output may also be not directly available but via $\eta(t, y(t))$, a time varying sensor nonlinearity. The noise input is also assumed to belong to \mathcal{Y}_{ref} . We assume that $\xi(\cdot, \cdot)$ and $\eta(\cdot, \cdot)$ are Carathéodory functions and they are sector bounded with bounds given by

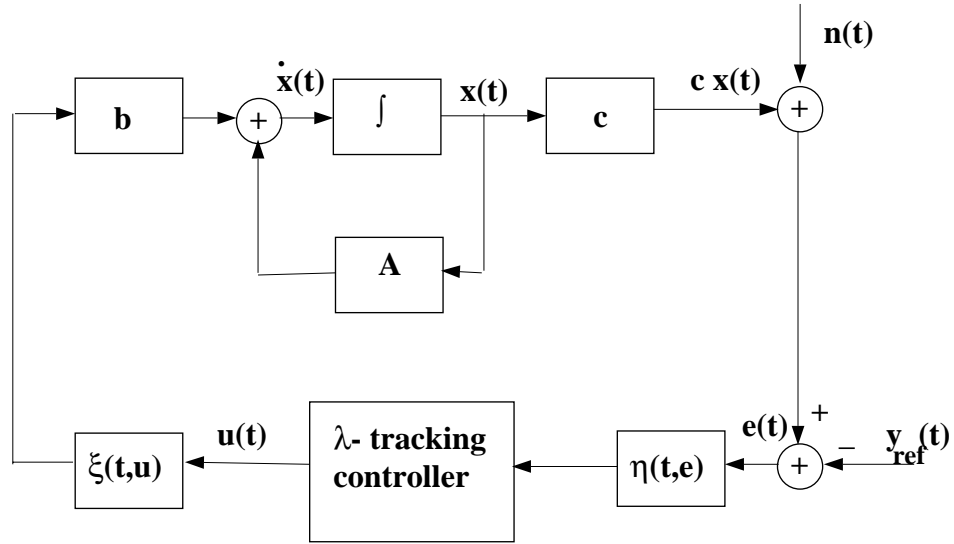


Figure 5.2: Adaptive λ -tracking for linear systems with input, output nonlinearity in the presence of noise.

$$\left. \begin{aligned} \xi(\cdot, \cdot) : \mathbb{R} \times \mathbb{R} &\rightarrow \mathbb{R} \quad , \xi_1 u^2 \leq \xi(t, u) u \leq \xi_2 u^2 \\ \eta(\cdot, \cdot) : \mathbb{R} \times \mathbb{R} &\rightarrow \mathbb{R} \quad , \eta_1 y^2 \leq \eta(t, y) y \leq \eta_2 y^2 \end{aligned} \right\}. \quad (24)$$

The inequalities in (24) are assumed to hold for some (unknown) $0 < \xi_1 < \xi_2$, $0 < \eta_1 < \eta_2$, for almost all $t \in \mathbb{R}$ and for all $u, y \in \mathbb{R}$.

Theorem 5.2.2 *Consider system (23) with sector bounded input and output nonlinearities $\xi(\cdot, \cdot)$ and $\eta(\cdot, \cdot)$ given by (24). Suppose $cb > 0$. If $\lambda > 0$, and the adaptive feedback mechanism*

$$\left. \begin{aligned} e(t) &= y(t) - y_{ref}(t), \\ u(t) &= -k(t) \eta(t, e(t)), \\ \dot{k}(t) &= d_\lambda(\eta(t, e(t))) |\eta(t, e(t))|; \quad k(0) = k_0, \end{aligned} \right\}. \quad (25)$$

is applied to (23), for arbitrary $x_0 \in \mathbb{R}^n$, $k_0 \in \mathbb{R}$, $n(\cdot)$, $y_{ref}(\cdot) \in \mathcal{Y}_{ref}$, then there exists a solution $x(\cdot), k(\cdot) : [0, \omega) \rightarrow \mathbb{R}^{n+1}$ of the closed-loop system for

some $\omega > 0$ and every solution has on its maximal interval of existence $[0, \omega)$ the properties

- $\omega = \infty$,
- $\lim_{t \rightarrow \infty} k(t) = k_\infty$ exists and is finite,
- $x(\cdot), k(\cdot) \in L^\infty(0, \infty)$,
- the error $e(t)$ approaches the interval $[-\lambda, \lambda]$ as $t \rightarrow \infty$.

Ilchmann in his book [39], also presents a variant of the above theorem where at the expense of allowing only sector bounded *input* nonlinearities, a nonlinear perturbation of the state equation is tolerated and the sign of the high-frequency gain cb is not necessary to be known. The next theorem due to Eugene Ryan shows that the λ -tracking problem is solvable even for systems with certain set-valued input nonlinearities [24].

Ryan considers a class of nonlinearly perturbed, SISO linear systems $\Sigma = (A, b, c, d, f, g)$ with nonlinear actuator characteristics:

$$\left. \begin{aligned} \dot{x}(t) &= Ax(t) + b(f(t, x(t) + v(t)) + d(t, x(t))), \\ x(t_0) &= x_0, \\ v(t) &= g(t, u(t), u_t(\cdot)), \\ y(t) &= cx(t). \end{aligned} \right\} \quad (26)$$

$x(\cdot) \in \mathbb{R}^n$ and the output $y(t)$ is available for feedback. The control signal drives an actuator modeled by g . The actuator may be a device with memory, that is, it may depend on the history $u_t(\cdot) : s \mapsto u(s), s \leq t$, of the control signal, as is the case with hysteresis. The class of reference signals is $\mathcal{Y}_{ref} = \mathcal{W}^{1,\infty}(\mathbb{R})$. The assumptions on the class Σ is as follows.

1. $cb \neq 0$.
2. The linear system (A, b, c) has the minimum phase property.
3. $d : \mathbb{R} \times \mathbb{R}^n \rightarrow \mathbb{R}^n$ is a Carathéodory function and has the property that, for some scalar δ , $\|d(t, x)\| \leq \delta(1 + |cx|)$ for almost all t and all x .
4. $f : \mathbb{R} \times \mathbb{R}^n \rightarrow \mathbb{R}^n$ is a Carathéodory function and has the property that, for some scalar α and known continuous function $\phi : \mathbb{R} \rightarrow [0, \infty)$

$$|f(t, x)| \leq \alpha(\|x\| + \phi(cx)),$$

for almost all t and x .

5. There exists a non-empty set valued map $G : \mathbb{R} \rightarrow 2^{\mathbb{R}}$, $u \mapsto G(u) \subset \mathbb{R}$ such that every actuator characteristic is contained in the graph of G in the following sense: for all $(t, \xi) \in \mathbb{R}^2$ and every $u(\cdot) : \mathbb{R} \rightarrow \mathbb{R}$ with $u(t) = \xi$, $g(t, \xi, u_t(\cdot)) \in G(\xi)$. Furthermore, G is an upper semicontinuous map from \mathbb{R} to the compact intervals of \mathbb{R} with the property that, for some scalars $\Gamma > 0$ and $\gamma_2 \geq \gamma_1 > 0$

$$\text{sign}(\xi) G(\xi) \subset [\gamma_1 |\xi|, \gamma_2 |\xi|] \subset \mathbb{R} \quad \forall \xi \in \mathbb{R} [-\Gamma, \Gamma].$$

For example, Figure 5.3 shows an illustration of the set valued input non-linearity [24].

For some $\lambda > 0$, define $s_\lambda : \mathbb{R} \rightarrow \mathbb{R}$ be any continuous function with the property

$$|\xi| \geq \lambda \Rightarrow s_\lambda(\xi) = \text{sign}(\xi).$$

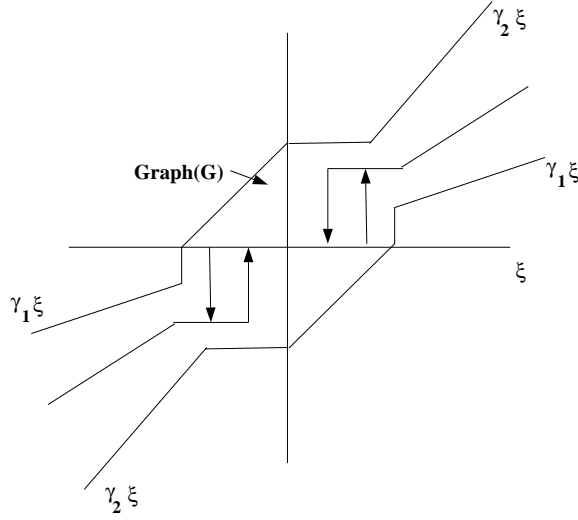


Figure 5.3: Set valued input nonlinearity allowed by Ryan

An example of s_λ could be (following the suggestion of Ryan)

$$s_\lambda : \xi \mapsto \begin{cases} \text{sign}(\xi), & |\xi| \geq \lambda \\ \lambda^{-1} \xi, & |\xi| < \lambda \end{cases} \quad (27)$$

Define $d_\lambda : \mathbb{R} \rightarrow [0, \infty)$ by

$$d_\lambda \triangleq \begin{cases} |\xi| - \lambda, & |\xi| \geq \lambda \\ 0 & |\xi| < \lambda \end{cases} \quad (28)$$

Ryan's also defines a particular kind of scaling invariant Nussbaum function as follows. Let $N(\cdot) : \mathbb{R} \rightarrow \mathbb{R}$ be any continuous function with the property that, for all $\gamma = (\gamma_0, \gamma_a, \gamma_b) \in \mathbb{R}^3$ with $\gamma_0 \geq 0, \gamma_a, \gamma_b > 0$, the associated function

$$N_\gamma : \mathbb{R} \rightarrow \mathbb{R}, \quad \xi \mapsto \begin{cases} \gamma_a N(\xi), & N(\xi) \geq \gamma_0 \\ 0, & N(\xi) \in (-\gamma_0, \gamma_0) \\ \gamma_b N(\xi), & -N(\xi) \leq \gamma_0 \end{cases}$$

has the property

$$\limsup_{\kappa \rightarrow \infty} \frac{1}{\kappa} \int_0^{\kappa} N_{\gamma} = \infty$$

$$\liminf_{\kappa \rightarrow \infty} \frac{1}{\kappa} \int_0^{\kappa} N_{\gamma} = -\infty.$$

The control strategy proposed by Ryan is

$$u(t) = N(k) (y - y_{ref} + \phi(y) s_{\lambda}(y - y_{ref})), \quad (29-a)$$

$$\dot{k} = d_{\lambda}(y - y_{ref}) (|y - y_{ref}| + \phi(y)). \quad (29-b)$$

Theorem 5.2.3 [24] *Consider the system (26) belonging to class Σ , and the control strategy given by (29-a) - (29-b). If $(x(\cdot), k(\cdot)) : [t_0, \omega) \rightarrow \mathbb{R}^{n+1}$ is the solution of the closed loop system then*

1. $\omega = \infty$,
2. $(x(\cdot), k(\cdot))$ is bounded,
3. $\lim_{t \rightarrow \infty} k(t) = k_{\infty}$ exists and is finite,
4. $d_{\lambda}(e(t)) \rightarrow 0$ as $t \rightarrow \infty$, that is, $e(\cdot) = y(\cdot) - y_{ref}(\cdot)$ approaches the compact interval $[-\lambda, \lambda] \subset \mathbb{R}$.

5.3 Relative degree two systems

It is well known from root-locus considerations that minimum phase, relative degree one systems can always be stabilized (in a non-adaptive context) with high gain control laws of the form $u = ky$ provided gain k is of the appropriate sign and sufficiently large in magnitude. Root locus arguments can also be used

to identify those relative degree two, minimum phase systems which can be similarly stabilized. In particular, if $\beta(s) = s^2 + a s + b$ is the denominator of the transfer function of the quotient system of Σ , then Σ can be stabilized with a high gain feedback $u = k y$ provided the *damping coefficient* $a > 0$.

Morse has shown that when the sign of the high frequency gain σ_g is known, an adaptive strategy $u = \sigma_g k y$ with gain update law $\dot{k} = y^2$ stabilizes the system [25]. But, for systems with input nonlinearity this law does not stabilize (this fact can be checked with a simple simulation example). Therefore, we consider controllers of a different type. Morse has shown that the following controller stabilizes any second order system.

Theorem 5.3.1 [25] *The controller given by*

$$\begin{aligned} u &= -k_2 \theta - k_1 k_2 y, \\ \dot{\theta} &= -\lambda \theta + u, \end{aligned}$$

where λ is a positive constant, stabilizes any second order system for sufficiently large $k_1, k_2 \in \mathbb{R}$.

Proof Suppose the above controller is applied to a relative degree two, minimum phase system Σ with transfer function $g \frac{\alpha}{\beta}$, with $\alpha(s)$ and $\beta(s)$ monic polynomials, then for sufficiently large values of parameter constants k_1 and k_2 stability will result, because the closed loop system characteristic polynomial

$$\pi(s) = (s + \lambda) \beta(s) + k_2 (\beta(s) + k_1 g \alpha(s) (s + \lambda)),$$

has roots in the left half plane of $\mathbb{C}(s)$. This is so because, $\frac{\alpha(s)(s+\lambda)}{\beta(s)}$ is a minimum phase, relative degree one transfer function. Hence, for $k_1 g$ sufficiently

large, $\beta(s) + k_1 g \alpha(s) (s + \lambda)$ will be stable. With k_1 fixed at such a value, $\frac{\beta(s) + k_1 g \alpha(s) (s + \lambda)}{(s + \lambda) \beta(s)}$ is also a minimum phase, relative degree one transfer function.

So for k_2 sufficiently large $\pi(s)$ will be a stable polynomial.

□

And adaptive version of the above result for unknown g can be found in [41].

The tuning formulas for this controller are

$$k_2 = -N((k_\theta^2 + k_y^2)^{\frac{1}{2}}) k_\theta,$$

$$k_1 = -N((k_\theta^2 + k_y^2)^{\frac{1}{2}}) k_y,$$

$$k_\theta = \theta y + z_\theta,$$

$$k_y = \frac{1}{2} y^2 + z_y,$$

$$\dot{z}_\theta = (\lambda + \lambda_1) \theta y - u y,$$

$$\dot{z}_y = \lambda_1 y^2,$$

where λ_1 is a positive constant, and $N(\cdot)$ is a Nussbaum gain. In particular, if we assume $sign(g)$ to be known then, setting $k_1 = sign(g) k$ and $k_2 = k$ and adjust k according to the rule $\dot{k} = y^2$. The resulting controller is thus described by the equations

$$u = -k \theta - sign(g) k^2 y, \tag{30}$$

$$\dot{\theta} = -\lambda \theta + u, \tag{31}$$

$$\dot{k} = y^2. \tag{32}$$

The proof that the above controller indeed stabilizes a relative degree two, minimum phase, linear system can be found in Morse [25]. Similar results for even

higher relative degree systems can be found in Ilchmann [40].

Remarks : The results of adaptive stabilization for systems with relative degree three or more, using high gain type adaptive tuning appears to be a result of theoretical importance only. Even for stable, minimum phase, high order (≥ 3) relative degree systems, the closed loop system can become *unstable* before it gets stabilized. This can be checked by writing a simple program in Matlab or some other software to plot the closed loop system poles for each value of the parameter k . Such a plot for a stable system show the poles move into the right half plane of $\mathbb{C}(s)$ before moving back into the left half plane of $\mathbb{C}(s)$ as k continues to increase.

When such a controller is implemented in practice, the system will diverge and then *never recover* because of limitations like actuator saturation which then come into play.

5.3.1 Linear systems with input nonlinearity

For a relative degree two, minimum phase linear system with set-valued input nonlinearity and known high frequency gain, we sought to find a tracking controller by combining the ideas of Morse and Ryan. In particular, the scheme as shown in Figure 5.4 was tried.

The idea behind the scheme is that for k large compared to $|s|$, $\frac{k(s+\lambda)}{(s+\lambda+k)}$ is approximately $(s+\lambda)$. Thus the system

$$\Sigma_1(s) = g \frac{\alpha(s)}{\beta(s)} \frac{k(s+\lambda)}{(s+\lambda+k)}$$

is approximately of relative degree one. Therefore, $\Sigma_1(s)$ with a set valued input nonlinearity can be stabilized by Ryan's method.

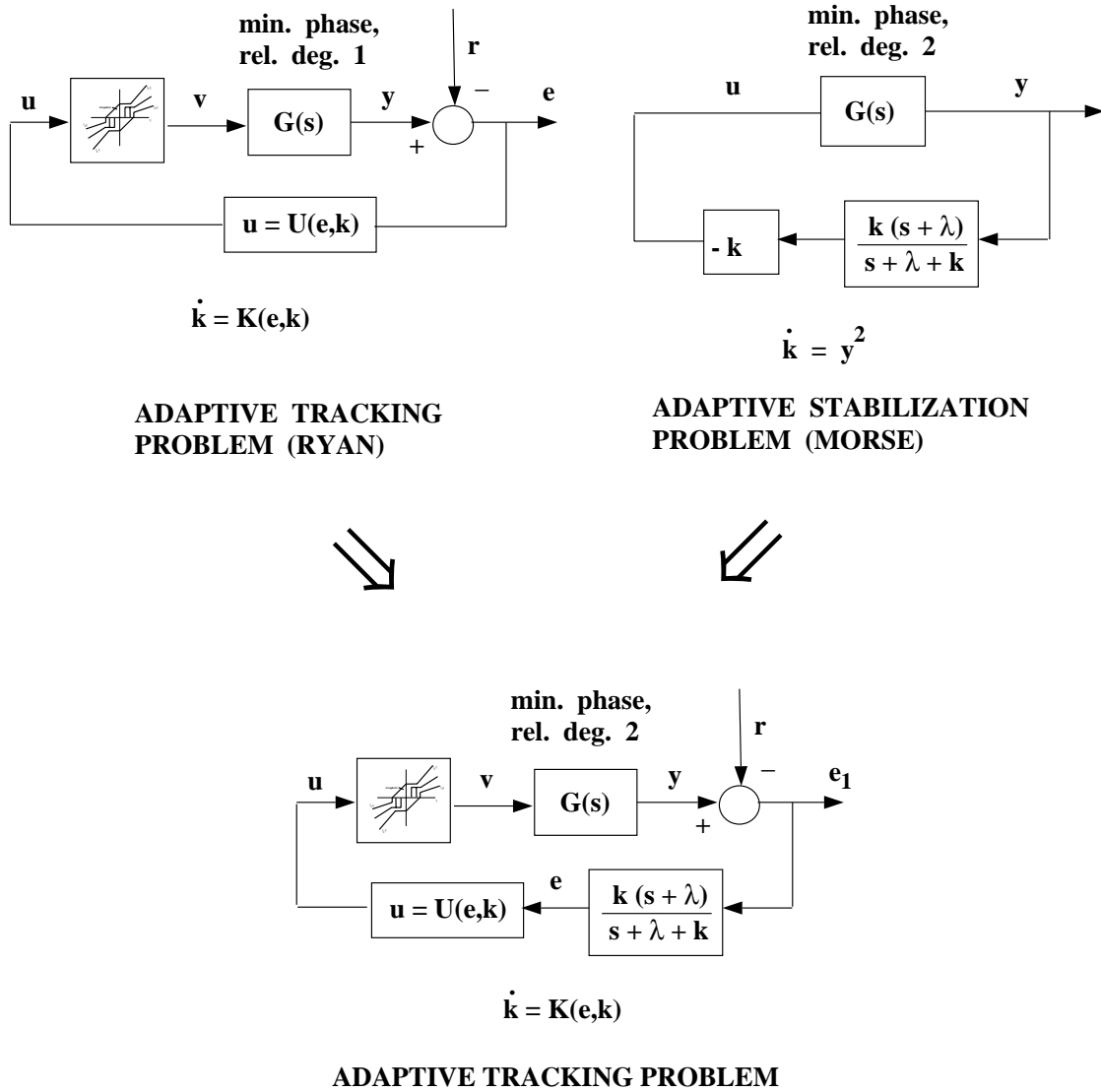


Figure 5.4: Adaptive tracking controller idea for relative degree two, minimum phase systems with input non-linearity.

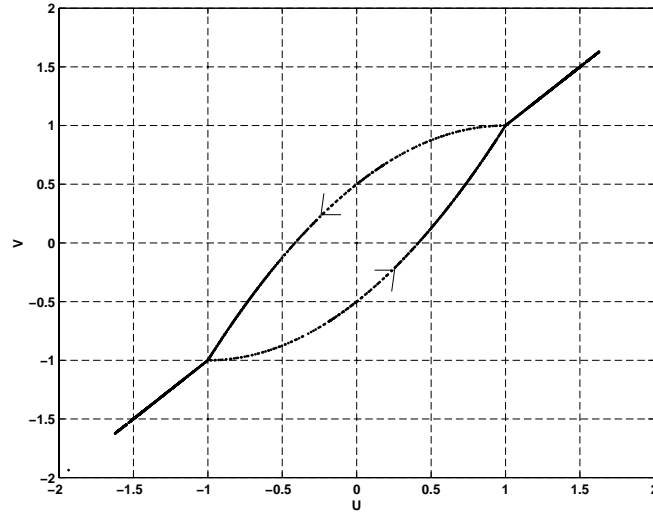


Figure 5.5: Set valued input nonlinearity for example 1.

Example

The plant Σ was chosen to be the linear system $\frac{4 \times 10^4}{s^2 + 400s + 4 \times 10^4}$, with a set valued input map $F : u \mapsto v$ as shown in Figure 5.5.

If $y(t)$ is the output of Σ and $y_{ref}(t)$ is the desired output, then applying the following Morse - Ryan λ tracking controller

$$\epsilon_1(t) = y(t) - y_{ref}(t), \quad (33-a)$$

$$\dot{\theta}(t) = -\alpha \theta(t) + \epsilon(t), \quad (33-b)$$

$$\epsilon(t) = -k \theta + k \epsilon_1(t), \quad (33-c)$$

$$u(t) = -k (\epsilon(t) + s_\lambda(\epsilon)(t)), \quad (33-d)$$

with the adpatation law given by

$$\dot{k}(t) = d_\lambda(\epsilon(t)) (|\epsilon(t)|), \quad (33-e)$$

we find the output trajectory to be as in Figure 5.6(a), if the desired trajectory is a sine wave of frequency $25Hz$ and $\lambda = 0.05$. The initial states for the plant were $x_1(0) = 1$ and $x_2(0) = -20$, and the initial state for the controllers were chosen to be $\theta(0) = 0$ and $k(0) = 1$. The gain evolution for this system is shown in Figure 5.6(b).

□

Similar results were obtained for other set valued nonlinearities satisfying assumption 5, and other bounded and differentiable reference trajectories.

5.3.2 Experimental results

The ETREMA Terfenol-D MP series actuators come with a permanent magnet bias, so that we can get both positive and negative motion by applying positive and negative current respectively. Thus for zero external current, the strain is not zero but has some residual value depending on the biasing field. This fact is very desirable from the control perspective, because if there was no biasing field, then the same positive strain can be obtained by applying a positive or a negative current. With the biasing field applied, the current - strain relationship is as shown in Figure 5.7. If the desired trajectory is of bounded amplitude so that any increase in the trajectory corresponds to an increase in the current, then the mapping $F : I_1 \mapsto x$ is a set valued mapping with a graph that satisfies assumption 5.

The simulation results of the last subsection encouraged us to try out the controller (33-a - 33-e) on a magnetostrictive actuator. We did not pursue a theoretical result in the form of a theorem proving that the controller proposed above achieves λ tracking for a relative degree 2, minimum phase, linear sys-

tem with set valued input nonlinearity satisfying assumption 5, because of time constraints.

The magnetostrictive actuator on which the experiment was performed was an MP 50/6 actuator manufactured by ETREMA Products, Inc. We had earlier performed experiments to see its behaviour at different frequencies [14]. The results are shown in Figure 5.8. The control law was implemented on a TMS320C31 digital signal processor card manufactured by DSP Tools, Inc. Figure 5.9 shows the schematic diagram of the experimental set up.

λ was chosen to be 0.07 Volts. The reference trajectory was a sinusoidal voltage signal, whose amplitude and frequency could be adjusted.

The control law implemented on the DSP board also took into account the effective eddy current resistance and the lead resistance. Suppose $u(t) = I_1(t)$ is the output of the direct adaptive controller. Then the actual current that needs to be applied is given by (refer to Figure 3.1)

$$I(t) = \frac{V(t) - I_1(t) R_{ed}}{R}, \quad (34)$$

where R_{ed} is the eddy current resistance, R is the resistance of the actuator coil, and V is the voltage measured across the amplifier terminals. *It must be noted that if this compensation is not done and $u(t)$ is applied to the actuator directly, then the output trajectory diverges even for reference trajectory frequencies as low as 10 Hz.*

Figure 5.10(a) shows the position output of the magnetostrictive actuator with the frequency of the reference trajectory approximately 1Hz. The initial state for the controller was chosen to be $\theta(0) = 0$, and the initial gain was chosen to be $k(0) = 0.3$. For higher initial gains, unstable behaviour was observed. The

parameters for the controller were $\lambda = 0.07\text{Volts}$, and $\alpha = 1$. As can be seen from the figure, the system is affected by a considerable amount of noise. The output trajectory follows the sum of the reference and the disturbance signal and hence, λ must be chosen to be greater than the size of the disturbance. When λ was chosen to be smaller than $0.07V$, again unstable behaviour was observed. The noise affecting the displacement output trajectory was found to be approximately 60Hz . It was very difficult to get rid of, because the signals were approximately of the same frequency.

The current waveform (Figure 5.10(a)) which is the input to the actuator can be seen to be a 1Hz signal with some disturbance component.

Figures 5.11(a), 5.12(a), 5.13(a), 5.14(a), 5.15(a) show the position output of the magnetostrictive actuator with the frequency of the reference trajectory approximately 10, 50, 200, 500, and 750Hz respectively. The initial states and the parameters for the controller were identical to the last case. Again, because of the noise, we were unable to reduce the parameter λ .

As the frequency increases it is harder to tell the correspondence between the reference and the output trajectories. This is because the output trajectory tries to follow the reference signal plus the noise. However, Figures 5.11(b), 5.12(b), 5.13(b), 5.14(b), 5.15(b) show that the current signal to the actuator in each case has the frequency component of the reference trajectory plus some noise components.

Discussion of the experimental results

Negative :

The experiments show that the proposed Morse-Ryan controller does not

work very well in the experiments that were performed. This is mainly due to the fact that disturbances are not rejected very well by the controller. Low pass filters to get rid of the offending frequencies could not be added because of the strict relative degree condition on the plant. This brings us to the major disadvantage of the universal adaptive stabilization scheme that is not obvious when one is carrying out a theoretical study. It is that for relative degrees greater than two, the controllers may initially destabilize even a stable plant and as the gain continues to grow, eventually stabilize it. This fact can be checked using root locus plots.

For example, Figure 5.16 shows the schematic of a closed loop system where the plant output is being filtered by a second order butterworth filter and the universal adaptive stabilizer takes account of the relative degree (4) of the open loop system. The plant transfer function is given by $P(s) = \frac{\omega_n^2}{s^2 + 0.75\omega_n s + \omega_n^2}$, where $\omega_n = 1000\pi \text{ rad/s}$. The filter has a cutoff frequency of 5000 Hz . The universal stabilizer is given by the transfer function, $C(s) = \frac{k(s+\alpha)^3}{(s+k+\alpha)^3}$ with $\alpha = 0.1$. Figure 5.17 shows how the poles of the closed loop system vary if k is increased from 0 to 2×10^5 . It can be seen that the closed loop system would be initially destabilized if we used an adaptive strategy like $\dot{k} = \epsilon^2$, though later it is stabilized again.

The above discussion shows that if the adaptive universal controller is used in a practical situation, then the performance is likely to be extremely poor. Thus the two main limitations of the universal stabilizer/controller that makes it a poor candidate for control design are :

- The relative degree of the system must be not greater than 2.
- Very poor noise rejection. The system output follows the noise + the

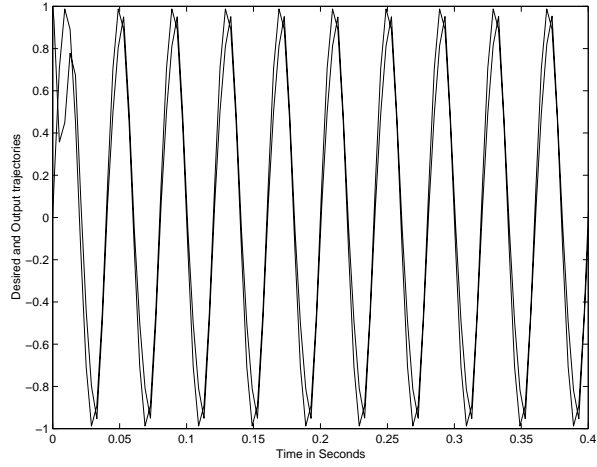
reference trajectory.

Positive :

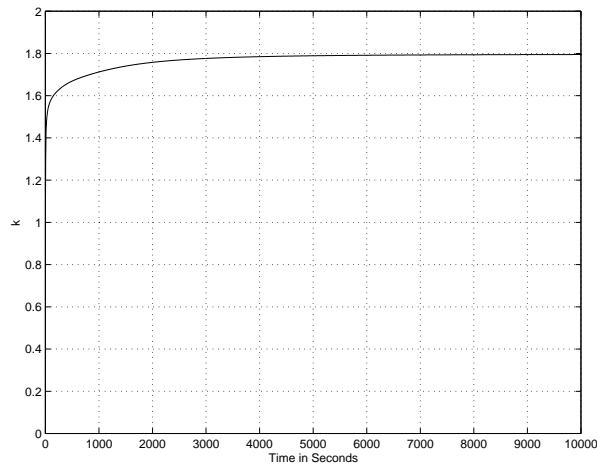
In spite of the negative results of the tracking experiment, some positive results can be gained from the experiments. The Morse - Ryan controller has a very strict relative degree requirement, and this implies that if the relative degree of the system is greater than two, then the closed loop system will be unstable. An experiment with the Ryan controller (which is designed for relative degree one systems with input nonlinearity) showed the closed loop system to be unstable. Therefore, we can deduce that our system has relative degree two. This experimentally established fact corroborates our modeling effort. Thus it is correct to look at the magnetostrictive actuator system as shown in Figure 5.7 is correct for low frequencies. The reason for this is that at high frequencies, we may have to add zeros to the transfer function to reproduce the actuator trajectories, keeping the relative degree of the system two. This is a very significant insight into the actuator dynamics. Even though the actuator trajectories for sinusoidal inputs of various frequencies look like those in Figure 5.8, we can separate out the contributions due to eddy current effects, and view the rest of the model as shown in Figure 5.7. The main simplification is that in Figure 5.7, the input nonlinearity can be found by doing quasi-static experiments only.

Elaborating on the comment about the need to add zeros at high frequencies, please consider Figure 5.18. The force F_{mag} in the figure, is equal to $|b M^2 \mathcal{V}|$ as in Chapter 3. The transfer function $\frac{x(s)}{F_{mag}(s)}$ in each of the cases in the figure can be verified to have relative degree two. In Figure 5.18(a), $\frac{x(s)}{F_{mag}(s)}$ has no zeros and has two poles; in case (b), $\frac{x(s)}{F_{mag}(s)}$ has two zeros and four poles; while in case (c), $\frac{x(s)}{F_{mag}(s)}$ has $2n - 2$ zeros and $2n$ poles. Case (a) corresponds to the model

derived in Chapter 3, where only one mass, spring, and dashpot were considered. If we wish to model higher frequencies, the model becomes more complex but still retains the relative degree two property. Interestingly, Marcelo Dapino et al. [42] have a similar idea in their paper where they model the rod to be a continuum and then discretize it. But, they were only interested in quasi-static matching of the model and the actuator trajectories, while according to our arguments, such model is appropriate for modeling high frequency behaviour.



(a) System output and desired trajectories



(b) Gain evolution

Figure 5.6: Morse - Ryan controller applied to the system of example 1

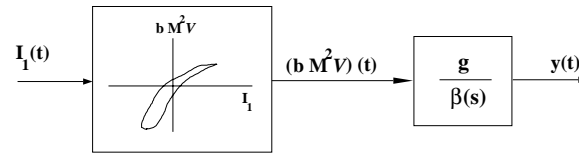


Figure 5.7: The magnetostrictive actuator model.

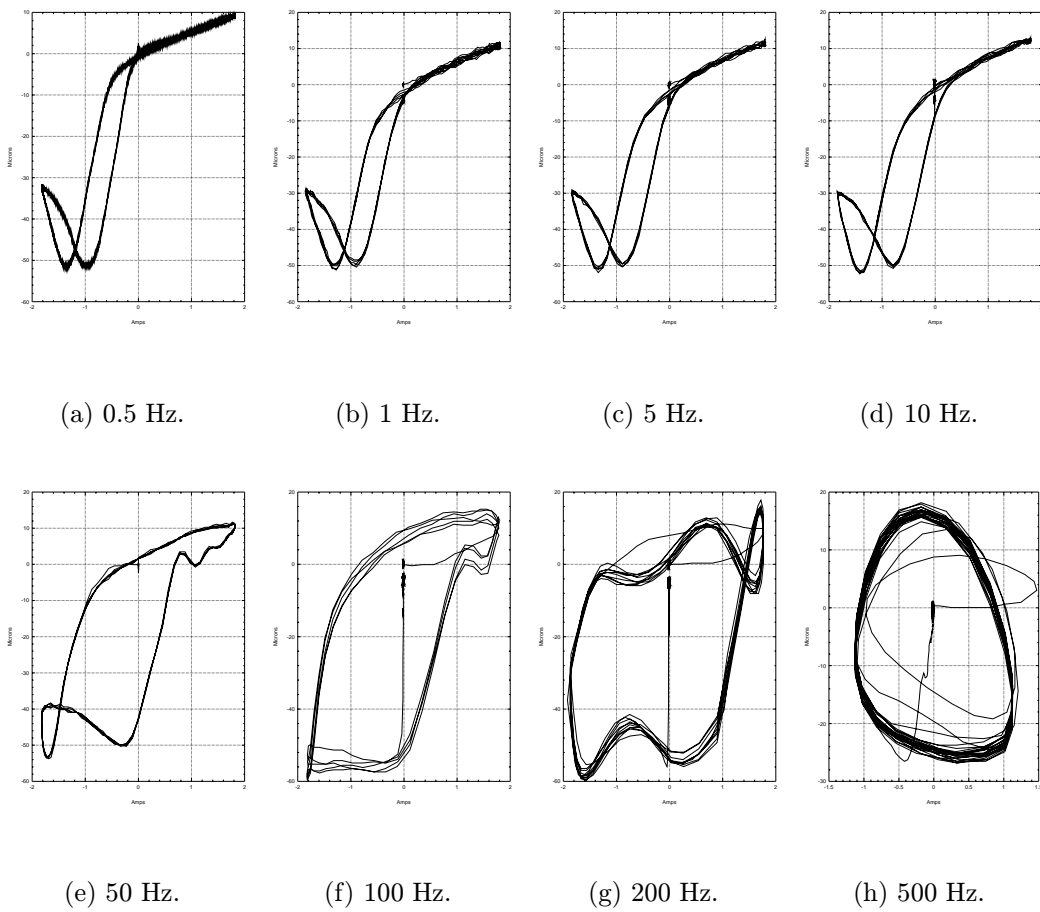


Figure 5.8: ETREMA MP 50/6 Actuator characteristic at different driving frequencies.

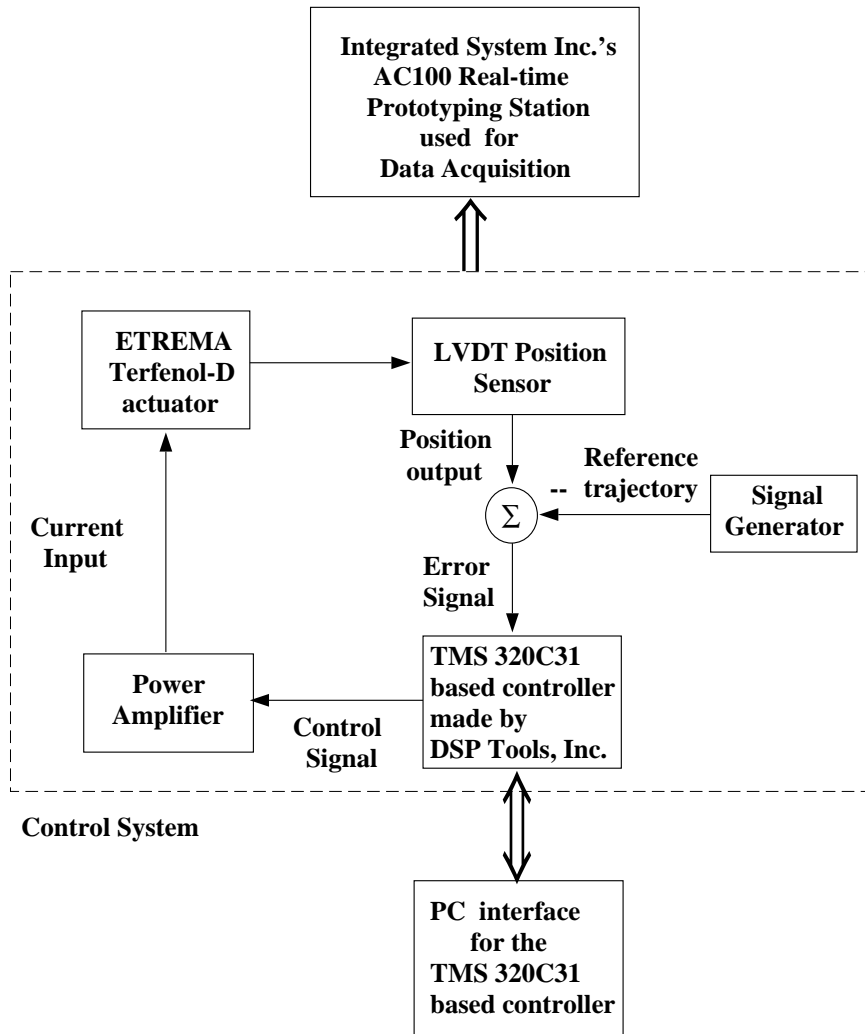
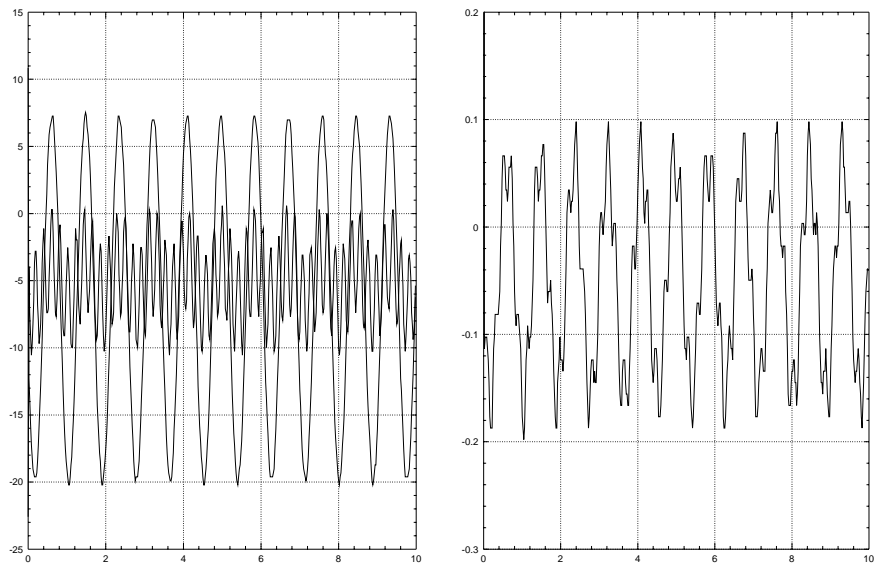


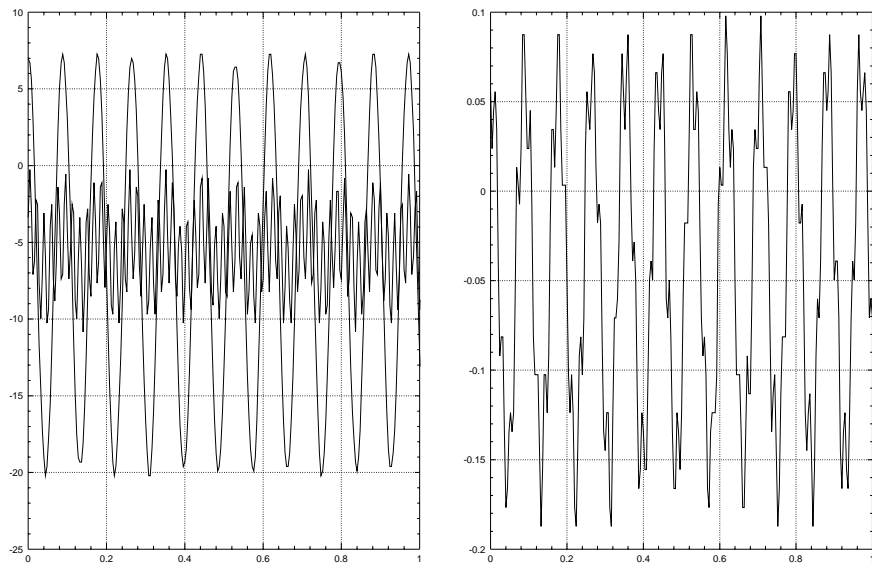
Figure 5.9: Schematic diagram of the experimental setup.



(a) Reference and actuator trajectories.

(b) Current input to the actuator

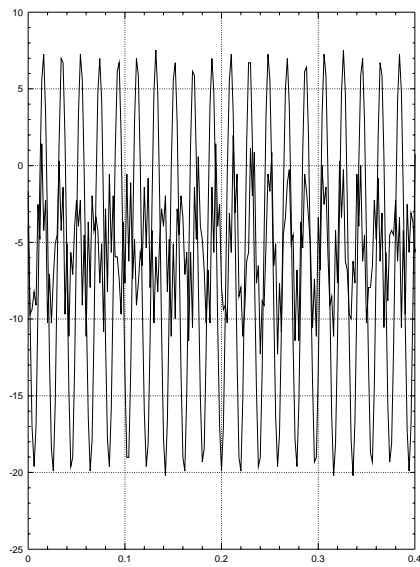
Figure 5.10: Reference trajectory frequency approximately 1 Hz



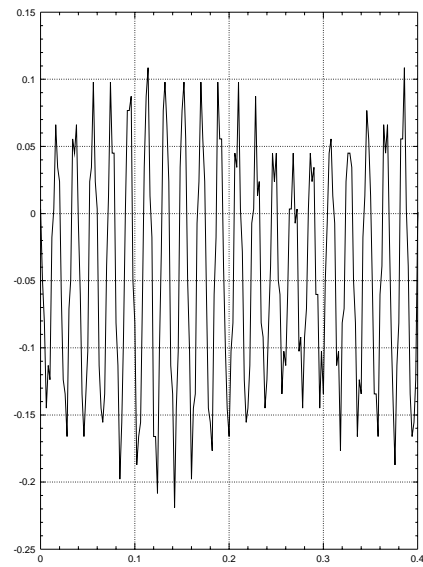
(a) Reference and actuator trajectories.

(b) Current input to the actuator

Figure 5.11: Reference trajectory frequency approximately 10 Hz

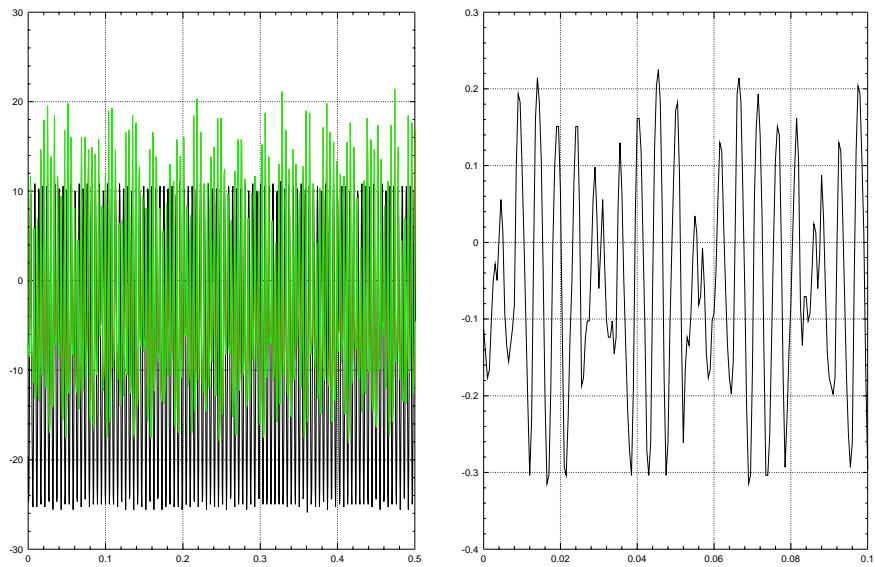


(a) Reference and actuator trajectories.



(b) Current input to the actuator

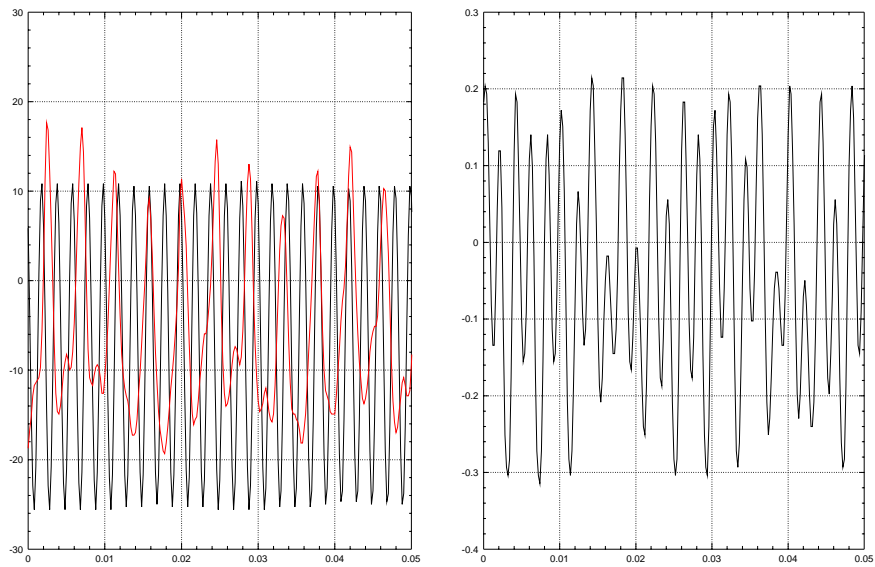
Figure 5.12: Reference trajectory frequency approximately 50 Hz



(a) Reference and actuator trajectories.

(b) Current input to the actuator

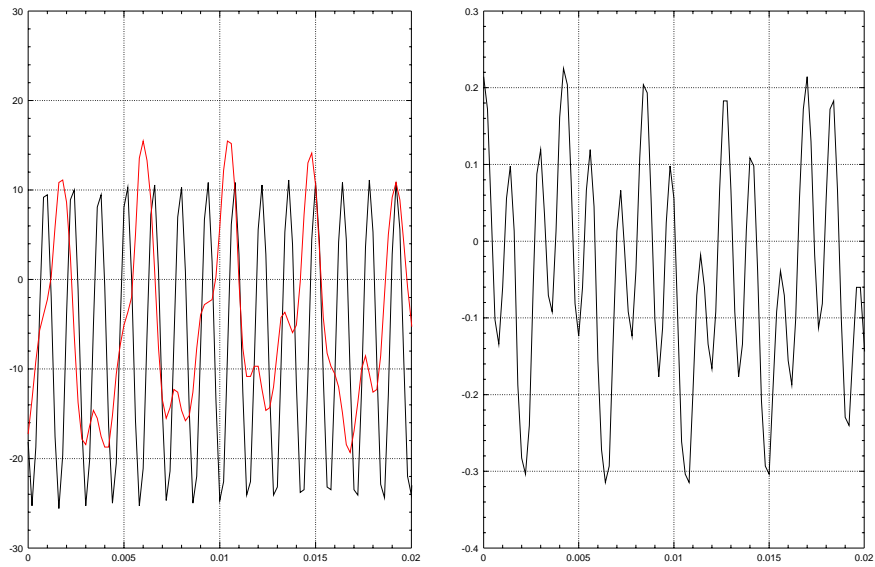
Figure 5.13: Reference trajectory frequency approximately 200 Hz



(a) Reference and actuator trajectories.

(b) Current input to the actuator

Figure 5.14: Reference trajectory frequency approximately 500 Hz



(a) Reference and actuator trajectories. (b) Current input to the actuator

Figure 5.15: Reference trajectory frequency approximately 750 Hz

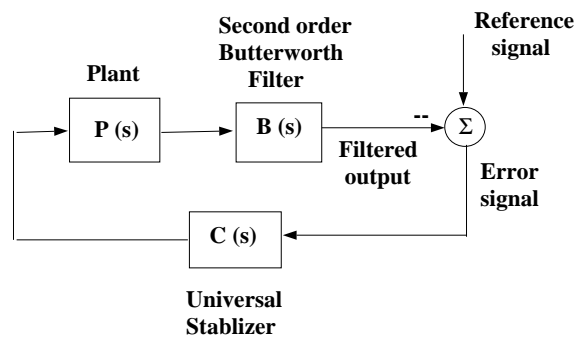


Figure 5.16: Example system for discussion of root locus properties.

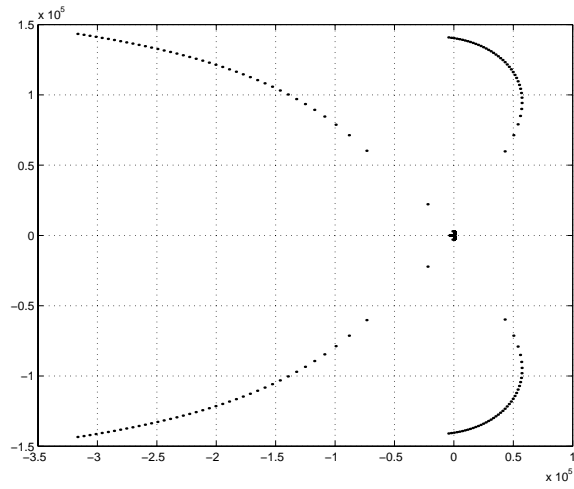


Figure 5.17: Root locus of example system.

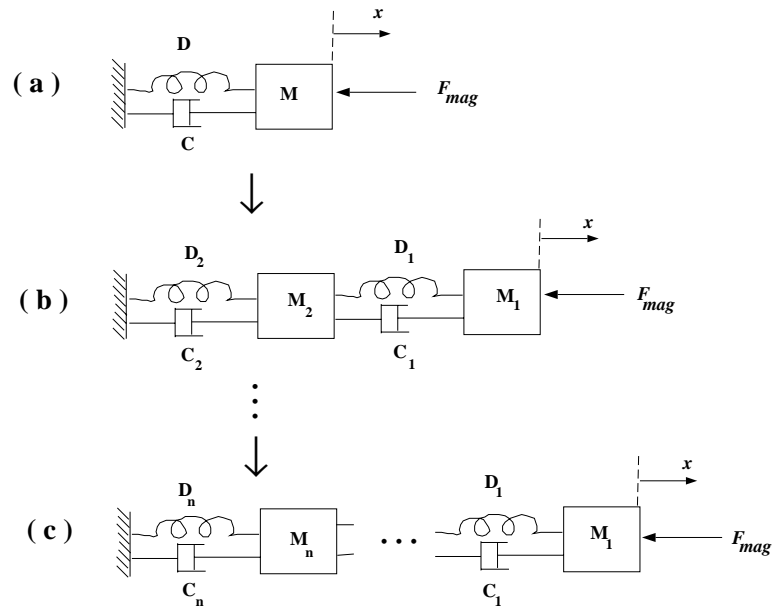


Figure 5.18: Mechanical system model at high frequencies.

Chapter 6

Conclusions and Future Work

The main contribution of this dissertation is a model for bulk magnetostriction for a thin rod actuator. This model is phenomenology based and covers magneto-elastic effects; eddy current effects; ferromagnetic hysteresis; inertial effects; and losses due to mechanical motion. The model has 12 parameters and tries to explain the magnetostrictive by means of coupled differential equations that represent the evolution of the mechanical and magnetic subsystems. We also showed rigorously that the model is well-posed inspite of its strong nonlinearity, by proving that trajectories starting at the origin have a periodic orbit as its Ω limit set.

It is envisaged that this model will be of use to a SMART structures application design engineer and enable her/him to conduct simulation studies of systems with magnetostrictive actuators. For this purpose, we have also developed an algorithm for parameter identification that is simple and intuitive.

As our system of equations do not model transient effects, they do not model the minor-loop closure property. This implies that a controller to achieve trajectory tracking cannot use our model for prediction. Another reason to use

model free approaches to control design is that magnetostrictive actuators seem to have slight variations in their behaviour with time. The strong non-linearity of the model makes these changes very difficult to handle for a design engineer. Therefore, we tried to use a direct adaptive control methodology that uses features of the model. The system is now looked at as a relative degree two linear system with set-valued input nonlinearity. Extensions of Eugene Ryan's work on universal tracking for a relative degree one linear system and Morse's work on stabilization for relative degree two linear systems were sought. Experimental verification of our method confirmed our intuition about the model structure. Though the tracking results were not very satisfactory due to the presence of sensor noise, the experimental results nevertheless validate our modeling effort in a sense.

Refining the experimental methodology to improve tracking and the development of controllers perhaps based on linear H_∞ control theory could be possible future work for researchers.

Appendix A

Banach Spaces

Much of the material in this section is a reproduction from Hale [43].

Definition A.0.1 (Vector Space) *An abstract vector space (or linear space) \mathcal{X} over the field \mathcal{R} is a collection elements $\{x, y, \dots\}$ such that for each x, y in \mathcal{X} , the sum $x + y$ is defined; for $a, b \in \mathbb{R}$, scalar multiplication $a x$ is defined and*

1. $x + y \in \mathcal{X}$;
2. $x + y = y + x$;
3. *there is an element 0 in \mathcal{X} such that $x + 0 = x$ for all $x \in \mathcal{X}$;*
4. $a x \in \mathcal{X}$ and $1 x = x$;
5. $(a b) x = a (b x) = b (a x)$;
6. $(a + b) x = a x + b x$;

Definition A.0.2 (Normed Linear Space) *A linear space \mathcal{X} is called a normed linear space if to each $x \in \mathcal{X}$, there corresponds a real number $|x|$ called the norm of x which satisfies*

1. $|x| > 0$ for $x \neq 0$, $|0| = 0$;
2. $|x + y| \leq |x| + |y|$ (*triangle inequality*);
3. $|ax| = |a| \cdot |x|$ for all a in \mathcal{R} and x in \mathcal{X} .

Definition A.0.3 The mapping f of a normed linear space \mathcal{X} into itself is said to be continuous at a point x_0 in \mathcal{X} if for any $\epsilon > 0$ there is a $\delta > 0$ such that $|x - x_0| < \delta$ implies $|f(x) - f(x_0)| < \epsilon$.

A sequence x_n of points in a normed linear space \mathcal{X} converges to x in \mathcal{X} if $\lim_{n \rightarrow \infty} |x_n - x| = 0$. We then write $\lim_{n \rightarrow \infty} x_n = x$. A sequence x_n of points in a normed linear space \mathcal{X} is called a *Cauchy sequence* if for every $\epsilon > 0$ there exists an $N(\epsilon) > 0$ such that $|x_n - x_m| < \epsilon$ if $n, m \geq N(\epsilon)$. A normed linear space \mathcal{X} is called *complete* if every Cauchy sequence converges to an element in \mathcal{X} . A complete normed linear space is called a *Banach space*. The ϵ -neighbourhood of an element x of a normed linear space \mathcal{X} is $\{y \in \mathcal{X} : |y - x| < \epsilon\}$. A set S in \mathcal{X} is *open* if for every $x \in S$, an ϵ -neighbourhood of x is also contained in S . An element x is a *limit point* of a set S if each ϵ -neighbourhood of x contains points of S . A set S is *closed* if it contains its limit points. The *closure* of a set S is the union of S and its limit points. If S is a subset of \mathcal{X} , A is a subset of \mathcal{R} and V_a ; $a \in A$ is a collection of open sets of \mathcal{X} such that $S \subset \bigcup_{a \in A} V_a$, then the collection V_a is called an *open covering* of S . A set S in \mathcal{X} is *compact* if every open covering of S contains a finite number of open sets which also cover S . A set S is *sequentially compact* if every sequence $\{x_n\}$, $x_n \in S$, contains a subsequence which converges to an element of S . For Banach spaces a set S is compact if and only if it is sequential compact. A set S in \mathcal{X} is bounded if there exists an $r > 0$ such that $S \subset \{x \in \mathcal{X} : |x| < r\}$.

The definition of continuity of a function given before in terms of norms, is equivalent to the topological definition given in terms of open sets. The latter definition is as follows. The mapping f of a normed linear space \mathcal{X} into itself is said to be *continuous at a point* x_0 in \mathcal{X} if for any neighbourhood \mathcal{V} of $f(x_0)$, there exists a neighbourhood \mathcal{U} of x_0 such that $f(\mathcal{U}) \subset \mathcal{V}$.

A mapping A of a vector space X into a vector space Y is called a *linear mapping*, if $A(\alpha_1 x_1 + \alpha_2 x_2) = \alpha_1 A x_1 + \alpha_2 A x_2$ for all x_1, x_2 in X and all real α_1, α_2 . If X and Y are normed vector spaces, we call a linear operator A *bounded* if there is a constant M such that for all x we have $|Ax| \leq M|x|$. We call the least such M the *norm* of A and denote it by $|A|$.

Theorem A.0.2 [44] *A bounded linear operator is uniformly continuous. If a linear operator is continuous at one point, it is bounded.*

Let $(X, |\cdot|_1)$ and $(Y, |\cdot|_2)$ be normed linear spaces. Then two *standard* norms for the product space $X \times Y$ are

$$\begin{aligned}\|(x, y), (\acute{x}, \acute{y})\|_1 &= |x - \acute{x}|_1 + |y - \acute{y}|_2 \\ \|(x, y), (\acute{x}, \acute{y})\|_2 &= \max(|x - \acute{x}|_1, |y - \acute{y}|_2)\end{aligned}$$

Theorem A.0.3 [45] *Let A, B be compact subsets of $(X, |\cdot|_1)$ and $(Y, |\cdot|_2)$ respectively. Then $A \times B$ is compact (under either of the standard metrics).*

Let D be a compact subset of \mathbb{R}^m and $\mathcal{C}(D, \mathbb{R}^n)$ be the linear space of continuous functions which take D into \mathbb{R}^n . A sequence of functions $\{\phi_n, n = 1, 2, \dots\}$ in $\mathcal{C}(D, \mathbb{R}^n)$ is said to *converge uniformly* on D if there exists a function ϕ taking D into \mathbb{R}^n such that for every $\epsilon > 0$ there is an $N(\epsilon)$ (independent of

n) such that $|\phi_n(x) - \phi(x)| < \epsilon$ for all $n \geq N(\epsilon)$ and $x \in D$. A sequence $\{\phi_n\}$ is said to be uniformly bounded if there exists an $M > 0$ such that $|\phi_n(x)| < M$ for all $x \in D$ and all $n = 1, 2, \dots$. A sequence $\{\phi_n\}$ is said to be *equicontinuous* if for every $\epsilon > 0$, there is a $\delta > 0$ such that

$$|\phi_n(x) - \phi_n(y)| < \epsilon, \quad n = 1, 2, \dots$$

if $|x - y| < \delta$, $x, y \in D$. A function f in $\mathcal{C}(D, \mathbb{R}^n)$ is said to be Lipschitzian in D if there is a constant K such that $|f(x) - f(y)| \leq K|x - y|$ for all $x, y \in D$. The most frequently encountered equicontinuous sequences in $\mathcal{C}(D, \mathbb{R}^n)$ are sequences $\{\phi_n\}$ which are Lipschitzian with a Lipschitz constant independent of n .

Theorem A.0.4 (*Arzelà-Ascoli*) [43] *Any uniformly bounded equicontinuous sequence of functions in $\mathcal{C}(D, \mathbb{R}^n)$ has a subsequence which converges uniformly on D .*

Theorem A.0.5 [43] *If a sequence in $\mathcal{C}(D, \mathbb{R}^n)$ converges uniformly on D , then the limit function is in $\mathcal{C}(D, \mathbb{R}^n)$.*

It is easy to verify that $\mathcal{C}(D, \mathbb{R}^n)$ is a vector space. If we define

$$|\phi| = \max_{x \in D} |\phi(x)|, \tag{1}$$

then we can verify that $|\cdot|$ is a norm on $\mathcal{C}(D, \mathbb{R}^n)$. The next theorem shows that $\mathcal{C}(D, \mathbb{R}^n)$ is complete and hence a Banach space.

Theorem A.0.6 *$\mathcal{C}(D, \mathbb{R}^n)$ is a Banach space*

Proof We have already seen that $\mathcal{C}(D, \mathbb{R}^n)$ is a normed linear space with the norm defined as in Equation (1). Suppose $\{\phi_n\}$ is a Cauchy sequence in $\mathcal{C}(D, \mathbb{R}^n)$. Then given $\epsilon > 0$, there exists an $N > 0$ such that

$$|\phi_m(x) - \phi_n(x)| < \frac{\epsilon}{3}. \quad (2)$$

uniformly in x if $m, n \geq N$. By completeness of \mathcal{R} , for each x there exists a limit $\phi(x)$. It remains to be shown that $\phi(x) \in \mathcal{C}(D, \mathbb{R}^n)$. Holding n fixed in Equation (2) and taking the limit as $m \rightarrow \infty$ we get,

$$|\phi(x) - \phi_n(x)| < \frac{\epsilon}{3}.$$

uniformly in x if $m, n \geq N$. By completeness of \mathcal{R} , for each x there exists a limit $\phi(x)$. It remains to be shown that $\phi(x) \in \mathcal{C}(D, \mathbb{R}^n)$. Holding n fixed in Equation (2) and taking the limit as $m \rightarrow \infty$ we get,

$$|\phi(x) - \phi_n(x)| < \frac{\epsilon}{3}.$$

if $n \geq N$ and uniformly in x . Thus we have a uniform convergence of a sequence of continuous functions $\{\phi_n\}$ to a function $\phi(x)$. By continuity of each ϕ_n , given $\epsilon > 0$, there exists an $\delta > 0$ such that if $|x - y| < \delta$ then,

$$|\phi_n(x) - \phi_n(y)| < \frac{\epsilon}{3}$$

Hence if $|x - y| < \delta$ and by choosing $n \geq N$ we have,

$$|\phi(x) - \phi(y)| \leq |\phi(x) - \phi_n(x)| + |\phi_n(x) - \phi_n(y)| + |\phi_n(y) - \phi(y)| \quad (3)$$

$$< \frac{\epsilon}{3} + \frac{\epsilon}{3} + \frac{\epsilon}{3} \quad (4)$$

$$= \epsilon \quad (5)$$

Therefore $\phi(x) \in \mathcal{C}(D, \mathbb{R}^n)$ and $\mathcal{C}(D, \mathbb{R}^n)$ is a Banach space with the norm $|\cdot|$.

□

Theorem A.0.7 (Brouwer fixed point theorem) [43] *Any continuous mapping of the closed unit ball in \mathbb{R}^n into itself must have a fixed point.*

The Brouwer fixed point theorem has been generalized to Banach spaces by Schauder and to locally convex linear topological spaces by Tychonov. The result for Banach spaces is formulated below. A subset \mathcal{A} of a Banach space is *convex* if for $x, y \in \mathcal{A}$ it follows that $tx + (1 - t)y \in \mathcal{A}$ for $0 \leq t \leq 1$.

Theorem A.0.8 (Schauder fixed point theorem) [43] *If \mathcal{A} is a convex, compact subset of a Banach space \mathcal{X} and $f : \mathcal{A} \rightarrow \mathcal{A}$ is continuous, then f has a fixed point in \mathcal{A} .*

Lemma A.0.1 *Suppose D is a compact subset of \mathbb{R}^m ; M, β are positive constants and \mathcal{A} is the subset of $\mathcal{C}(D, \mathbb{R}^n)$ such that $\phi \in \mathcal{A}$ implies $|\phi| \leq \beta$; $|\phi(t) - \phi(\bar{t})| \leq M |t - \bar{t}|$ for $t, \bar{t} \in D$. Then the set \mathcal{A} is convex and compact.*

Proof [43] The set \mathcal{A} is obviously convex and closed. Furthermore, any sequence $\{\phi_n\}$ in \mathcal{A} is uniformly bounded and equicontinuous. By the Arzela-Ascoli Theorem, imply the existence of a ϕ in $\mathcal{C}(D, \mathbb{R}^n)$ such that $\lim_{n \rightarrow \infty} \phi_n = \phi$. But \mathcal{A} is closed so that ϕ belongs to \mathcal{A} . For Banach spaces sequential compactness is equivalent to compactness and hence \mathcal{A} is compact.

□

Theorem A.0.9 *Suppose $\mathcal{F}(\mathbb{R}, \mathbb{R}^n) = \{f \mid f(t + T); |f| \leq M |f(t) - f(\bar{t})| \leq K |t - \bar{t}|\}$ where T, M and K are positive real numbers. Then \mathcal{F} is compact.*

Proof The functions in \mathcal{F} can be restricted to one period, say $[0, T]$ and then we can define, $\mathcal{C}([0, T], \mathbb{R}^n) = \mathcal{F}$. Then by the previous theorem, \mathcal{F} is compact.

□

Appendix B

Solutions of Ordinary Differential Equations

In this section, we discuss the notion of a solution to an ordinary differential equation and present theorems for the existence and uniqueness of solutions. The material of this section can be found in greater detail in Chapter 1 of Hale [43].

B.1 Existence of solutions

Let t be a real scalar; let D be an open set in \mathbb{R}^{n+1} with an element of D written as (t, x) ; let $f : D \rightarrow \mathbb{R}^n$, be continuous and let $\dot{x} = \frac{dx}{dt}$. A differential equation is a relation of the form

$$\dot{x}(t) = f(t, x(t)). \tag{1}$$

A *solution* of Equation (1) on an interval $I \subset \mathbb{R}$ if $x(\cdot)$ is a continuously differentiable function defined on I , $(t, x(t)) \in D$, $t \in I$ and $x(\cdot)$ satisfies (1) on I . Suppose $(t_0, x_0) \in D$ is given. An *initial value problem for Equation (1)*

consists of finding an interval I containing t_0 and a solution of x of (1) satisfying $x(t_0) = x_0$. Symbolically the problem is stated as

$$\dot{x}(t) = f(t, x(t)), \quad x(t_0) = x_0, \quad t \in I. \quad (2)$$

If there exists an interval I containing t_0 and an x satisfying (2), we refer to this as a solution of (1) passing through (t_0, x_0) .

Lemma B.1.1 [43] *Problem (2) is equivalent to*

$$x(t) = x_0 + \int_{t_0}^t f(\tau, x(\tau)) \, d\tau \quad (3)$$

provided $f(t, x)$ is continuous.

If $f(t, x)$ is continuous, any solution of (3) automatically possesses a continuous first derivative. On the other hand, (3) will be meaningful for a more general class of functions f if it is not required that x have a continuous first derivative. We now make these notions precise for a class of functions f .

Suppose D is an open set in \mathbb{R}^{n+1} and $f : D \rightarrow \mathbb{R}^n$, is not necessarily continuous. The problem is to find an absolutely continuous function $x(\cdot)$ defined on a real interval I such that $(t, x(t)) \in D$ for $t \in I$ and

$$\dot{x}(t) = f(t, x(t)) \quad (4)$$

for all $t \in I$ except on a set of Lebesgue measure zero. If such a function $x(\cdot)$ and interval I exist, we say $x(\cdot)$ is a *Carathéodory solution* of (4). A solution of (4) through (t_0, x_0) is a Carathéodory solution $x(\cdot)$ of (4) with $x(t_0) = x_0$. Having made precise the notion of solution for a more general class of functions f not necessarily continuous, we now make precise the class of functions next.

Carathéodory Conditions:

Suppose D is an open set in \mathbb{R}^{n+1} . Let $f : D \rightarrow \mathbb{R}^n$, and let

1. the function $f(t, x)$ be defined and continuous in x for almost all t ;
2. the function $f(t, x)$ be measurable in t for each x ;
3. on each compact set U of D , $|f(t, x)| \leq m_U(t)$, where the function $m_U(t)$ is integrable .

The equation $\dot{x} = f(t, x)$, where x is a scalar or a vector and the function f satisfies the above conditions is called the *Carathéodory equation*[46].

Theorem B.1.1 [43] (*Existence of solutions*) *If D is an open set in \mathbb{R}^{n+1} and f satisfies the Carathéodory conditions on D , then, for any (t_0, x_0) in D , there is a solution of $\dot{x} = f(t, x)$, through (t_0, x_0) .*

B.2 Extension of solutions

If $\phi(\cdot)$ is a solution of a differential equation on an interval I , we say $\widehat{\phi}(\cdot)$ is a *continuation or extension* of $\phi(\cdot)$ if $\widehat{\phi}(\cdot)$ is defined on an interval \widehat{I} which properly contains I , $\widehat{\phi}(\cdot)$ coincides with $\phi(\cdot)$ on I and $\widehat{\phi}(\cdot)$ satisfies the differential equation on \widehat{I} . A solution $\phi(\cdot)$ is *noncontinuable* if no such continuation exists; that is, the interval I is the *maximal interval of existence of the solution* $\phi(\cdot)$.

Before we can discuss extending a solution to a maximal interval of existence, we first need to discuss the existence of a solution on an *interval of existence*. Theorem B.1.1 asserts the existence of a solution through each point (t_0, x_0) in D . The following lemma is a corollary of Theorem B.1.1, and shows the existence of a solution on a interval of time containing t_0 .

Lemma B.2.1 *If U is a compact set of D , $U \subset V$, an open set in D with the closure \bar{V} of V in D , then there is an $\alpha > 0$ such that, for any initial value $(t_0, x_0) \in U$, there is a solution of $\dot{x} = f(t, x)$, through (t_0, x_0) which exists at least on the interval $t_0 - \alpha \leq t \leq t_0 + \alpha$.*

Theorem B.2.1 [43] *(Extension of solutions to a maximal set) If D is an open set in \mathbb{R}^{n+1} , f satisfies the Carathéodory conditions on D , and ϕ is a solution of $\dot{x} = f(t, x)$ on some interval, then there is a continuation of ϕ to a maximal interval of existence. Furthermore, if (a, b) is a maximal interval of existence of $\dot{x} = f(t, x)$, then $x(t)$ tends to the boundary of D as $t \rightarrow a$ and $t \rightarrow b$.*

The above continuation theorem can be used (utilizing a technique in Hale [43]) in specific examples to verify that a solution is defined on a large time interval. For example, if it is desired to show that a solution is defined on an interval $[0, \infty)$, it is sufficient to proceed as follows. If the function $f(t, x)$ is continuous for t in (t_1, ∞) , $t_1 < t_0$, $|x| < \alpha$, and one can by some means ascertain that a certain solution $x(t)$ must always satisfy $|x(t)| \leq \beta < \alpha$ for all values of $t \geq 0$ for which $x(t)$ is defined, then necessarily $x(t)$ is defined on $[t_0, \infty)$. To show this, choose any $T \geq t_0$ and γ such that $\beta < \gamma < \alpha$ and define the rectangle D_1 as $D_1 = \{(t, x) : t_0 \leq t \leq T, |x| \leq \gamma\}$. Then $f(t, x)$ is bounded on D_1 and the continuation theorem implies that the solution $x(t)$ can be continued to the boundary of D_1 . But $\gamma > \beta$ implies that $x(t)$ must reach this boundary by reaching the face of the rectangle defined by $t = T$. Therefore $x(t)$ exists for $t_0 \leq t \leq T$. Since T is arbitrary, this proves the assertion.

B.3 Uniqueness of solutions

The discussion in the Sections B.1 and B.2 was about the existence and extension of solutions through a point (t_0, x_0) in an open set $D \subset \mathbb{R}^n$. In this section, we discuss conditions on $f(\cdot, \cdot)$ so that there is only *one* solution through (t_0, x_0) .

A function $f(t, x)$ defined on a domain D in \mathbb{R}^{n+1} is said to be *locally Lipschitzian* in x if for any closed bounded set U in D there is a $k = k_U$ such that $|f(t, x) - f(t, y)| \leq k|x - y|$ for $(t, x), (t, y)$ in U . If $f(t, x)$ has continuous first partial derivatives with respect to x in D , then $f(t, x)$ is locally Lipschitzian in x .

Theorem B.3.1 [47] (*Sufficient condition for local Lipschitzness*) Let $f(t, x)$ be continuous on $[a, b] \times \mathcal{O}$, for some domain $\mathcal{O} \subset \mathbb{R}^n$. If $[\partial f / \partial x]$ exists and is continuous on $[a, b] \times \mathcal{O}$, then f is locally Lipschitz in x on $[a, b] \times \mathcal{O}$.

The basic existence and uniqueness theorem under the hypothesis that $f(t, x)$ is locally Lipschitzian in x is usually referred to as the *Picard-Lindelöf theorem*.

Theorem B.3.2 [43] (*Uniqueness of solutions*) If D is an open set in \mathbb{R}^{n+1} , f satisfies the Carathéodory conditions on D , and for each compact set U in D , there is an integrable function $k_U(t)$ such that

$$\|f(t, x) - f(t, y)\| \leq k_U(t) \|x - y\|, \quad (t, x) \in U, \quad (t, y) \in U.$$

Then for any (t_0, x_0) in U , there exists a unique solution $x(t, t_0, x_0)$ of the problem

$$\dot{x} = f(t, x), \quad x(t_0) = x_0.$$

The domain E in \mathbb{R}^{n+2} of definition of the function $x(t, t_0, x_0)$ is open and $x(t, t_0, x_0)$ is continuous in E .

B.4 Continuous dependence on parameters

The following theorem characterizes the notion of continuity of a function in terms of convergence of sequences for normed linear spaces. It is also true for metric spaces and false for general topological spaces [48].

Theorem B.4.1 *If X and Y are normed linear spaces and f is a mapping from X to Y , then f is continuous at x if and only if for each sequence $\{x_n\}$ in X converging to x we have $\{f(x_n)\}$ converging to $f(x)$ in Y .*

Proof (if) Suppose $\{x_n\}$ is a sequence in X and $x_n \rightarrow x_0$. Then $f(x_n) \rightarrow f(x_0)$. Hence, given $\epsilon > 0$ we can choose $N > 0$ such that $|f(x_n) - f(x)| < \epsilon$. Then choosing $\delta = |x_N - x_0|$ we can see that f is continuous.

(only if) Suppose f is continuous, $\{x_n\}$ is a sequence in X and $x_n \rightarrow x_0$. Suppose $f(x_n)$ does not converge to $f(x_0)$. Then there exists $\epsilon > 0$ such that $|f(x_n) - f(x)| > \epsilon \quad \forall n$. Let $\mathcal{V} = \{y : |y - f(x_0)| < \frac{\epsilon}{2}\}$. Then by continuity of f , there exists a neighbourhood \mathcal{U} of x_0 , such that $f(\mathcal{U}) \subset \mathcal{V}$. Since $x_n \rightarrow x_0$, there exists $N > 0$ such that $x_n \in \mathcal{U} \quad \forall n \geq N$. This is a contradiction because then $f(x_n) \in \mathcal{V} \quad \forall n \geq N$.

□

The following theorem can be used to prove the continuity of solutions with respect to parameters. The assumption of a uniform bound on the sequence of functions allows to relax the condition of continuity that is used in Hale [43]. Further, the functions of the sequence are assumed to satisfy the Carathéodory conditions so that the solution exists for each of them. Going over to the integral formulation of a solution,

$$Tx(t) = x_0 + \int_{t_0}^t f(s, x(s)) ds$$

and applying the Lebesgue Convergence Theorem [44] for integrals we get the required continuity of solutions.

Theorem B.4.2 *Suppose $\{f_n\}$, $n = 1, 2, \dots$, is a sequence of uniformly bounded functions defined and satisfying the Carathéodory conditions on an open set D in \mathbb{R}^{n+1} with $\lim_{n \rightarrow \infty} f_n = f_0$ uniformly on compact subsets of D . Suppose (t_n, x_n) is a sequence of points in D converging to (t_0, x_0) in D as $n \rightarrow \infty$ and let $\phi_n(t)$, $n = 1, 2, \dots$, be a solution of the equation $\dot{x} = f_n(t, x)$ passing through the point (t_n, x_n) . If $\phi_0(t)$ is defined on $[a, b]$ and is unique, then there is an integer n_0 such that each $\phi_n(t)$, $n \geq n_0$, can be defined on $[a, b]$ and converges uniformly to $\phi_0(t)$ uniformly on $[a, b]$.*

Proof The proof is identical to that of Lemma I.3.1 in Hale [43].

□

Appendix C

Stability of Periodic Solutions

Consider the autonomous system of differential equations [47, 43, 49]

$$\dot{x} = f(x) \tag{1}$$

where $f : D \rightarrow \mathbb{R}^n$ is a Lipschitz continuous map and $D \subset \mathbb{R}^n$ is an open and connected subset. Let $\psi : \mathbb{R}_+ \rightarrow D$ be a solution of Equation (1) and denote its path by

$$\gamma = \{x \in D : x = \psi(t), t \in \mathbb{R}_+\}. \tag{2}$$

Definition C.0.1 (Orbital Stability) *The solution $\psi : \mathbb{R}_+ \rightarrow D$ of Equation (1) is said to be orbitally stable if for every $\epsilon > 0$ there exists a $\delta > 0$ such that if $\text{dist}(x(0), \gamma) < \delta$, then $\text{dist}(\phi(t, x(0)), \gamma) < \epsilon$.*

Definition C.0.2 (Asymptotic Orbital Stability) *The solution $\psi : \mathbb{R}_+ \rightarrow D$ of Equation (1) is said to be asymptotically orbitally stable if it is orbitally stable and there exists a $\delta > 0$ such that if $\text{dist}(x(0), \gamma) < \delta$, then $\text{dist}(\phi(t, x(0)), \gamma) \rightarrow 0$, as $t \rightarrow \infty$.*

Definition C.0.3 (Asymptotic Phase Property) *The solution $\psi : \mathbb{R}_+ \rightarrow D$ of Equation (1) is said to have the asymptotic phase property if a $\delta > 0$ exists such that to each initial value $x(0)$ satisfying $\text{dist}(x(0), \gamma) < \delta$ there corresponds an $\alpha(x(0)) \in \mathbb{R}$ with the property*

$$\lim_{t \rightarrow \infty} |\phi(t + \alpha(x(0))), x(0)) - \psi(t)| = 0. \quad (3)$$

The requirement in Equation (3) is equivalent to

$$\lim_{t \rightarrow \infty} |\phi(t, x(0)) - \psi(t - \alpha(x(0)))| = 0. \quad (4)$$

C.1 Poincaré Map

The following discussion on the Poincaré map closely follows the presentation in Khalil [47]. Let γ be a periodic orbit of the n th order system given by Equation (1). Let p be a point on γ and H be an $(n-1)$ dimensional at p that is transversal to γ at p . That is H is a surface $a^T(x - p) = 0$ for some $a \in \mathbb{R}^n$ and $a^T f(p) \neq 0$. Let $S \subset H$ be a local section such that $p \in S$ and $a^T f(x) \neq 0$ for all $x \in S$. The trajectory starting from p will hit p in T seconds, where T is the period of the periodic orbit. Due to continuity of solutions with respect to initial states, the trajectories starting on S in a sufficiently small neighbourhood of p will in approximately T seconds, intersect S in the vicinity of p . The Poincaré map $g : U \rightarrow S$ is defined for a point $x \in U$ by

$$g(x) = \phi(\tau, x) \quad (5)$$

where $\phi(t, x)$ is the solution of Equation (1) that starts at x at time $t = 0$, and

$\tau = \tau(x)$ is the time taken for the trajectory starting at x to first return to S . Note that τ depends on x and need not be equal to T , the period of γ . The Poincaré map is defined on locally; that is, it need not be defined for all $x \in S$. Suppose that U in the foregoing definition is chosen such that the map is defined for all $x \in U$. Starting with $x_0 \in U$, let $x_1 = g(x_0)$. If $x_1 \in U$, the Poincaré map will be defined at x_1 ; then set $x_2 = g(x_1)$. As long as $x_k \in U$, $x_{k+1} = g(x_k)$ will be defined. The sequence $\{x_k\}$ is the solution of the discrete-time system

$$x_{k+1} = g(x_k) \tag{6}$$

It is clear that p is an equilibrium point of Equation (6) since $p = g(p)$. Although the vector x is n -dimensional, the solution generated by Equation (6) is restricted to the $(n - 1)$ -dimensional hyperplane H . Hence it is equivalent to the solution of an $(n - 1)$ -dimensional system,

$$y_{k+1} = h(y_k) \tag{7}$$

There is an intimate relationship between the stability properties fo the periodic orbit γ and stability properties of q as an equilibrium point for the discrete-time system given by Equation (7).

Theorem C.1.1 *Let γ be a periodic orbit of Equation (1). Define the Poincaré map and the discrete-time system given by Equation (7) as explained above. If q is an asymptotically stable equilibrium point of Equation (7), then γ is asymptotically stable.*

Appendix D

Perturbations of Linear Systems

We first present the major results of the Floquet theory for linear periodic systems. Then we consider periodic perturbations of non-critical linear systems. The material closely follows the presentation in Hale [43].

Consider the homogenous linear periodic system

$$\dot{x} = A(t)x \tag{1}$$

where $A(t + T) = A(t)$, $T > 0$ and $A(t)$ is a continuous $n \times n$ real or complex matrix function of t .

Theorem D.0.2 [43] (*Floquet*) *Every fundamental matrix solution $X(t)$ of Equation (1) has the form*

$$X(t) = P(t) \exp B t$$

where $P(t)$, B are $n \times n$ matrices, $P(t + T) = P(t)$ for all t , and B is a constant.

Therefore every homogenous system given by Equation (1) can be transformed

to a system with constant coefficients by defining the transformation $x = P(t)y$. Then the equation for y is given by

$$\dot{y} = By \tag{2}$$

A *monodromy matrix* of system (1) is a nonsingular matrix C associated with a fundamental matrix solution $X(t)$ of (1) through the relation $X(t+T) = X(t)C$. The eigenvalues ρ of a monodromy matrix are called the *characteristic multipliers* of (1) and any λ such that $\rho = \exp \lambda T$ is called a *characteristic exponent* of (1). Note that the characteristic exponents are not uniquely defined by characteristic multipliers are.

Definition D.0.1 *If $A(t)$ is an $n \times n$ continuous matrix function on $(-\infty, \infty)$ and \mathcal{D} is a given class of functions which contains the zero function, the homogenous system $\dot{x} = A(t)x$ is said to be noncritical with respect to \mathcal{D} if the only solution of Equation (1) which belongs to \mathcal{D} is the solution $x = 0$. Otherwise, system (1) is said to be critical with respect to \mathcal{D} .*

The set \mathcal{P}_T denoting the set of T -periodic continuous functions is a Banach space with the sup-norm. That is, $\|f\| = \sup_{-\infty < t < \infty} |f(t)|$; $f \in \mathcal{P}_T$. Let \mathcal{B} denote the set of continuous bounded functions from \mathcal{R} to \mathbb{R}^n .

Lemma D.0.1 [43] (a) *System (1) with $A(t) \in \mathcal{P}_T$ is noncritical with respect to \mathcal{B} if and only if the characteristic exponents of (1) have nonzero real parts.*

(b) *System (1) with $A \in \mathcal{P}_T$ is noncritical with respect to \mathcal{P}_T if and only if $I - X(T)$ is nonsingular, when $X(t)$, $X(0) = I$, is a fundamental matrix solution of (1).*

Remark If A in equation (1) is a constant, then (1) is noncritical with respect to \mathcal{P}_T if and only if all eigenvalues λ of A satisfy $\lambda T \neq 0 \pmod{2\pi i}$.

Lemma D.0.2 (*Fredholm's alternative*) If A is in \mathcal{P}_T and f is a given element of \mathcal{P}_T , then the equation

$$\dot{x} = A(t)x + f(t) \tag{3}$$

has a solution in \mathcal{P}_T if and only if

$$\int_0^T y(t)f(t) dt = 0 \tag{4}$$

for all solutions y of the adjoint equation

$$\dot{y} = -yA(t)$$

such that y' is in \mathcal{P}_T ($'$ denotes the transpose of a matrix). If Equation (4) is satisfied, then system (3) has an r -parameter family of solutions in \mathcal{P}_T , where r is the number of linearly independent solutions of (1) in \mathcal{P}_T .

Theorem D.0.3 Suppose A is in \mathcal{P}_T . Then the nonhomogenous equation (3) has a solution $\mathcal{K}f$ in \mathcal{P}_T , if and only if system (1) is noncritical with respect to \mathcal{P}_T . Furthermore, if system (1) is noncritical with respect to \mathcal{P}_T , then $\mathcal{K}f$ is the only solution of (3) in \mathcal{P}_T and is linear and continuous in f .

Appendix E

Principle of Least Squares

The material in this section is a selection from Astrom's book on adaptive control [50].

Least squares is a basic technique for parameter estimation problems in system identification. The method is particularly simple if the mathematical model can be written in the form

$$y(t) = w_1(t) \theta_1 + \cdots + w_n(t) \theta_n = w(t)^T \theta \quad (1)$$

where y is the observed variable, $\theta_1, \theta_2, \dots, \theta_n$ are unknown parameters, and w_1, w_2, \dots, w_n are known functions that may depend on other known variables. The model is indexed by t which often denotes time. We assume t to be a discrete set which could be the result of sampling in an experiment. The pairs $(y(i), w(i))$, $i = 1, 2, \dots, t$ are obtained from such an experiment. The problem is to determine the parameters in such a way that the outputs computed from the model in Equation (1) agree as closely as possible with the measured variables $y(i)$ in the sense of least squares. Let

$$Y(t) = [y(1) y(2) \cdots, y(t)]^T$$

$$W(t) = [w(1) w(2) \cdots, w(t)]^T$$

$$E(t) = [\epsilon(1) \epsilon(2) \cdots, \epsilon(t)]^T$$

where the residuals $\epsilon(i)$ are defined by

$$\epsilon(i) = y(i) - \hat{y}(i) = y(i) - w(t)^T \theta$$

The least square error is defined by

$$\begin{aligned} V(\theta, t) &= \frac{1}{2} \sum_{i=1}^t (y(i) - w(t)^T \theta)^2 \\ &= \frac{1}{2} E^T E \\ &= \frac{1}{2} \|E\|^2 \end{aligned} \tag{2}$$

where

$$E = Y - \hat{Y} = Y - W \theta$$

the solution to the least-squares problem is given by the following theorem [50].

Theorem E.0.4 *The function of Equation (2) is minimal for parameters $\hat{\theta}$ such that*

$$W^T W \hat{\theta} = W^T Y \tag{3}$$

If the matrix $W^T W$ is nonsingular, the minimum is unique and given by

$$\hat{\theta} = (W^T W)^{-1} W^T Y \tag{4}$$

Appendix F

Eddy Current Losses in a Magnetostrictive Actuator

The high frequency limitation of the magnetostrictive rod actuator is generally due to eddy current losses. In this section, we obtain an expression for the power lost due to eddy currents using Maxwell's equations. The shape of the actuator is a thin rod with a coil tightly wound around it (Please see Figure 1.10 in Chapter 1 for a cross-section of an ETREMA MP 50/6 actuator). We simplify the problem by assuming the magnetic flux density B to be uniform across the face of the rod. This is the case for a thin magnetostrictive rod actuator. We show that the expression for power loss due to eddy currents enable us to model the effect of the eddy currents by a resistor in parallel with the coil in an electrical circuit (See Figure F.2).

Let the resistivity of the magnetostrictive material be ρ , and the resistance of the coil be R . The flux density B is along the x -direction (figure F.1) and the electric field E in the material lies in the y - z plane with no radial component. Then,

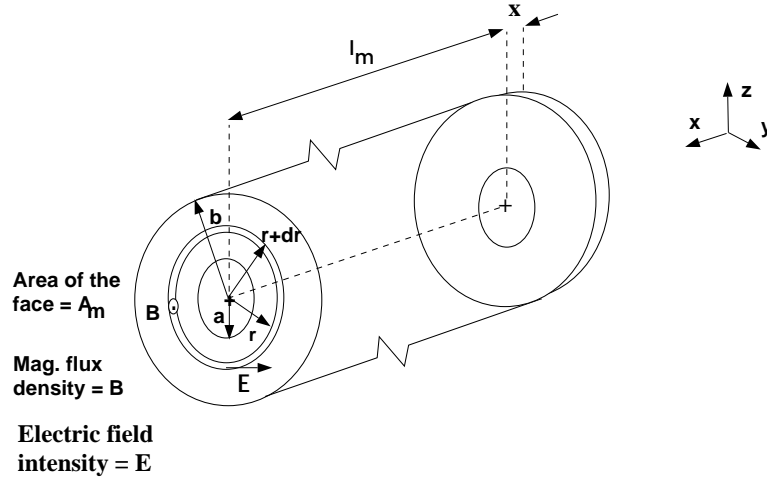


Figure F.1: Derivation of V-I-x relationship for the thin magnetostrictive rod.

$$|E_\phi| = \frac{|\dot{B}|r}{2}$$

$$|J| = \frac{|E|}{\rho} = \frac{|\dot{B}|r}{2\rho}$$

Therefore the current in an element of thickness dr and length l_m is

$$di = \frac{|\dot{B}|r l_m dr}{2\rho}$$

The voltage at a point on the element can be found from a contour integral around the element, and it is

$$V(r) = |E_\phi| 2\pi r = |\dot{B}| \pi r^2$$

The Power lost due to the eddy currents in the element is

$$dP(r) = V(r) di = \frac{|\dot{B}|^2 \pi l_m r^3 dr}{2\rho}$$

The total instantaneous power lost due to the eddy currents,

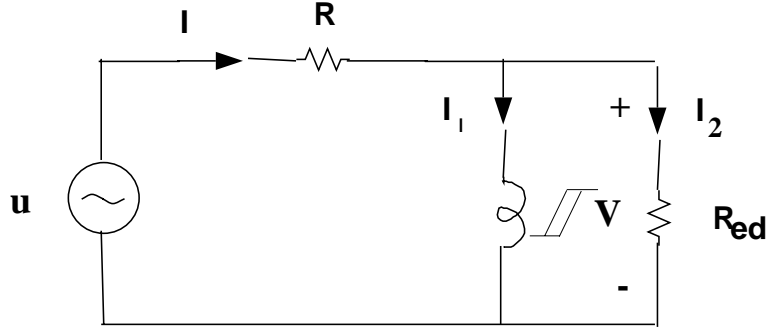


Figure F.2: Representation of eddy current effects as a resistor in parallel with the primary coil.

$$P = \int_a^b dP(r) = \frac{(V_m - IR)^2 l_m}{N^2 8\pi\rho} \frac{b^2 + a^2}{b^2 - a^2}$$

Therefore the resistance seen by the eddy current (Figure F.2) is,

$$R_{ed} = \frac{N^2 8\pi\rho}{l_m} \frac{b^2 - a^2}{b^2 + a^2}$$

The above equation may be seem a bit puzzling at first sight. For example, if $a = 0$, then it says that the eddy current resistance does not depend on the outer diameter of the rod! If a increases and approaches b , then R_{ed} decreases, and consequently P increases! This apparent inconsistencies can be understood if we realize that R_{ed} is the *effective resistance of the core reflected to the primary side of the transformer*. The primary coil of the transformer is the coil winding, and the secondary of the transformer is the core which carries a current. Essentially, the view point is that the applied electromotive force (emf) to the primary coil induces an emf that leads to the current in the core.

Let us obtain an expression for the power lost P in terms of the eddy current I_{eddy} .

$$\begin{aligned}
I_{eddy} &= \int_a^b di \\
&= \frac{|\dot{B}| l_m (b^2 - a^2)}{4 \rho}
\end{aligned}$$

Then,

$$\begin{aligned}
P &= \int_a^b dP(r) \\
&= \frac{|\dot{B}|^2 \pi l_m}{2 \rho} \frac{b^4 - a^4}{4} \\
&= I_{eddy}^2 \frac{2 \rho \pi}{l_m} \frac{b^2 + a^2}{b^2 - a^2} \tag{1}
\end{aligned}$$

The above equation expresses P as $I_{eddy}^2 R_{effective}$. According to Equation 1, if $a = 0$, then P is proportional to the square of I_{eddy} which in turn is proportional to b^2 . Thus the eddy current losses increase with b even if $a = 0$. Also P is proportional to $b^2 - a^2$ after substitutions, and hence decreases as a approaches b .

Bibliography

- [1] J. A. Ewing, *Magnetic Induction in Iron and Other Metals*. 1, 2, and 3, Salisbury Court, Fleet Street, London, E.C.: The Electrician Printing and Publishing Co., Ltd., 1894.
- [2] A. Andronov, A. Vitt, and S. Khaikin, *Theory of Oscillators*. Dover Publications, INC., 1966.
- [3] M. Brokate and J. Sprekels, *Hysteresis and Phase Transitions*. Applied Mathematical Sciences, Springer Verlag, 1996.
- [4] D. Kinderlehrer and L. Ma, “Computational hysteresis in modeling magnetic systems,” *IEEE Transactions on Magnetism*, vol. 30, no. 6, pp. 4380–4382, 1994.
- [5] J. E. Marsden and T. S. Ratiu, *Introduction to Mechanics and Symmetry*. Texts in Applied Mathematics, Springer–Verlag New York, Inc., 1992.
- [6] W. F. Brown Jr., *Micromagnetics*. Interscience Tracts on Physics and Astronomy, John Wiley & Sons, New York, 1963.
- [7] W. F. Brown Jr., *Magnetostatic Principles in Ferromagnetism*. Series of Monographs on Selected Topics in Solid State Physics, North–Holland Publishing Company, Amsterdam, 1962.

- [8] J. William Fuller Brown, *Magnetoelastic Interactions*. Springer Tracts in Natural Philosophy, Springer-Verlag, 1966.
- [9] E. Stoner and E. Wohlfarth, “A mechanism of magnetic hysteresis in heterogeneous alloys,” *Trans. R. Soc. London*, vol. 240, pp. 599–642, May 1948.
- [10] L. D. Landau and E. Lifshitz, “On the theory of the dispersion of magnetic permeability in ferromagnetic bodies,” *Phys. Z. Soviet Un.*, vol. 8, p. 135, 1935.
- [11] T. G. Shepherd, “A general method for finding extremal states of hamiltonian dynamical systems, with applications to perfect fluids,” *Journal of Fluid Mechanics*, vol. 213, pp. 573–587, 1990.
- [12] D. Kinderlehrer and L. Ma, “Simulation of hysteresis in nonlinear systems,” *Proc. SPIE, Math. and Control in Smart Structures*, vol. 21, pp. 78–87, 1992.
- [13] F. Jona and G. Shirane, *Ferroelectric Crystals*. Dover Publications, Inc., 1993.
- [14] R. Venkataraman and P. Krishnaprasad., “Characterization of the Etrema MP 50/6 magnetostrictive actuator,” Tech. Rep. TR 98-1, University of Maryland at College Park, 1998. Technical report of the Institute for Systems Research, UMCP.
- [15] I. Mayergoyz, *Mathematical models of Hysteresis*. Springer, 1991.
- [16] M. Krasnoselskii and A. Pokrovskii, *Systems with Hysteresis*. Springer-Verlag, 1989.

- [17] A. Visintin, *Differential Models of Hysteresis*. Applied Mathematical Sciences, Springer, 1994.
- [18] R. J. Zimmer, *Essential Results of Functional Analysis*. Chicago Lectures in Mathematics, The University of Chicago Press, 1990.
- [19] N. Ahmed, *Optimization and Identification of Systems Governed by Evolution Equations on Banach Space*. Pitman Research Notes in Mathematics Series, Longman Scientific & Technical, 1988.
- [20] E. D. Torre, "A Preisach model for accommodation," *IEEE Transactions on Magnetism*, vol. 30, pp. 2701–2707, September 1994.
- [21] D. Jiles and D. Atherton, "Ferromagnetic hysteresis," *IEEE Transactions on Magnetism*, vol. MAG-19, pp. 2183–2185, September 1983.
- [22] D. Philips, L. R. Dupre, and J. Melkebeek, "Comparison of Jiles and Preisach hysteresis models in magnetodynamics," *IEEE Trans. Magnetism*, vol. 31, pp. 3551–3553, November 1995.
- [23] J. L. Butler, *Application Manual for the Design of ETREMA Terfenol-D magnetostrictive transducers*. Edge Technologies Inc., ETREMA Division, 306 South 16th Street, Ames, Iowa 50010., 1998.
- [24] E. P. Ryan, "A nonlinear universal servomechanism," *IEEE Transactions on Automatic Control*, vol. 39, pp. 753–761, Apr. 1994.
- [25] A. S. Morse, *Simple algorithms for adaptive stabilization*, vol. 105 of *Lecture Notes in Control and Information Sciences*, pp. 254–264. Berlin: Springer Verlag, 1988.

- [26] J. McMillan, *Electron Paramagnetism*. Reinhold Book Corporation, 1968.
- [27] S. Chikazumi, *Physics of Magnetism*. John Wiley and Sons, Inc., 1966.
- [28] D. Jiles and D. Atherton, “Theory of ferromagnetic hysteresis,” *Journal of Magnetism and Magnetic Materials*, vol. 61, pp. 48–66, 1986.
- [29] R. M. Bozorth, *Ferromagnetism*. 120 Alexander St., Princeton, New Jersey.: D. Van Nostrand Company, Inc., 1964.
- [30] N. K. Sinha, *Control Systems*. Holt, Rinehart and Winston, 1986.
- [31] J. Deane, “Modelling of a chaotic circuit containing a saturating/hysteretic inductor,” *Electronics Letters*, vol. 29, pp. 957–958, May 1993.
- [32] J. Deane, “Modeling the dynamics of nonlinear inductor circuits,” *IEEE Trans. Magnetics*, vol. 30, pp. 2795–2801, September 1994.
- [33] D. Jiles, J. Thoelke, and M. Devine, “Numerical determination of hysteresis parameters for the modeling of magnetic properties using the theory of ferromagnetic hysteresis,” *IEEE Trans. Magnetics*, vol. 28, pp. 27–35, January 1992.
- [34] R. Venkataraman, “A hybrid actuator,” Master’s thesis, University of Maryland at College Park, May 1995. TR 95-4, Technical report of the Institute for Systems Research, UMCP.
- [35] R. Venkataraman, W. Dayawansa, and P. Krishnaprasad., “The hybrid motor prototype: Demonstration results,” Tech. Rep. TR 98-2, University of Maryland at College Park, 1998. Technical report of the Institute for Systems Research, UMCP.

- [36] H. Zijlstra, *Experimental methods in magnetism – 2. Measurement of magnetic quantities*. Selected topics in solid state physics, John Wiley and Sons, Inc. - New York, 1967.
- [37] M. J. Dapino, A. Flatau, and F. Calkins, “Statistical analysis of terfenol-d material properties,” in *Proceedings of SPIE’s 1997 Symposium on Smart Structures and Materials*, vol. 3041, pp. 256 – 267, 1997.
- [38] M. J. Dapino, F. T. Calkins, and A. B. Flatau, “On identification and analysis of fundamental issues in terfenol-d transducer modeling,” in *Proceedings of SPIE’s 5th Annual International Symposium on Smart Structures and Materials*, 1998.
- [39] A. Ilchmann, *Non-Identifier based High-Gain Adaptive Control*. Lecture Notes in Control and Information Sciences, Springer Verlag, 1993.
- [40] A. Ilchmann, “Non-Identifier-Based adaptive control of dynamical systems: A survey,” *IMA Journal of Mathematical Control and Information*, vol. 8, pp. 321–366, 1991.
- [41] A. S. Morse, “A three dimensional universal controller for the adaptive stabilization of any strictly proper, minimum phase system with relative degree not exceeding two.,” *IEEE Transactions on Automatic Control*, vol. AC - 30, pp. 1188 – 1191, Dec. 1985.
- [42] M. J. Dapino, R. C. Smith, and A. B. Flatau, “An active and structural strain model for magnetostrictive transducers,” in *SPIE’s 5th Annual International Symposium on Smart Structures and Materials*, Mar. 1998. Preprint.

- [43] J. Hale, *Ordinary Differential Equations*. Krieger Publishing Company, Malabar, Florida, 1980.
- [44] H. L. Royden, *Real Analysis*. Macmillan Publishing Company, 1989.
- [45] J. Pryce, *Basic Methods of Linear Functional Analysis*. Hutchinson University Library, London, 1973.
- [46] A. Filippov, *Differential Equations with Discontinuous Righthand Sides*. Mathematics and Its Applications, Kluwer Academic Publishers, 1988.
- [47] H. K. Khalil, *Nonlinear Systems*. Macmillan Publishing Company, New York, 1992.
- [48] K. D. Joshi, *Introduction to General Topology*. Wiley Eastern limited, 1988.
- [49] M. Farkas, *Periodic Motions*. Applied Mathematical Sciences, Springer, 1994.
- [50] K. J. Astrom and B. Wittenmark, *Adaptive Control*. Addison-Wesley Publishing Company, 1989.